A GENERALIZED PROCEDURE FOR THE OPTIMUM DESIGN OF LARGE-SCALE TRUSS STRUCTURES SUBJECTED TO HARMONIC EXCITATIONS

By

CHAO-WEI HSIAO

A DISSERTATION PRESENTED TO THE GRADUATE SCHOOL
OF THE UNIVERSITY OF FLORIDA IN PARTIAL FULFILLMENT
OF THE REQUIREMENTS FOR THE DEGREE OF
DOCTOR OF PHILOSOPHY

UNIVERSITY OF FLORIDA

2001

I dedicate this work to my family.

ACKNOWLEDGMENTS

The author wishes to express his gratitude to the members of his supervisory committee, Dr. Ali Seireg, Dr. Joseph Duffy, Dr. Carl Crane, Dr. John Schueller, and Dr. Jacob Hammer, for their interest and willingness to be a part of this effort. The author is especially grateful to his advisor, Dr. Ali Seireg, for his guidance, patient assistance, and many enlightening discussions during the preparation of his work. Finally, the author wishes to thank his parents for their unconditional support throughout this effort and his wife for her understanding and encouragement.

TABLE OF CONTENTS

page

ACKNOWLEDGMENTS iii

LIST OF TABLES vii

LIST OF FIGURES xi

ABSTRACT xvi

CHAPTERS

1 INTRODUCTION 1

- 1.1 Introduction 1
- 1.2 Literature Review 2
- 1.3 Objective 9
- 1.4 Outline of the Dissertation 10

2 MODELING, ANALYSIS, AND OPTIMIZATION PROBLEM FORMULATION 12

- 2.1 Modeling of the Structural Member 12
- 2.2 Structural Analysis 16
  - 2.2.1 Formulation of the Governing Differential Equations: . 16
  - 2.2.2 Solution of the Governing Differential Equations . . . 18
- 2.3 Optimization Problem Formulation 19

3 SOLUTION ALGORITHM BY THE SUCCESSIVE ITERATION APPROACH 31

- 3.1 The Essence of the Optimization Problem 31
- 3.2 Successive Iteration Approach 31
- 3.3 Illustrative Problems for the Successive Iteration Approach . 34
  - 3.3.1 Simple Three-Link Truss 34
  - 3.3.2 Forty-Seven-Member Tower 36
  - 3.3.3 Two-Hundred-Member Structure 37

4 SOLUTION ALGORITHM BY INCORPORATING LINEAR PROGRAMMING 81

- 4.1 Linear Programming and Simplex Techniques 81
- 4.2 Topology of the System Matrices 83

4.2.1 General Cases 83
4.2.2 Adding Discrete Masses at the Joints 88
4.3 Linear Program for This Study 90
4.4 Improvements in Previous Example Problems by Incorporating Linear Programming 90

5 SOLUTION ALGORITHM BY NONLINEAR PROGRAMMING APPROACH 97

5.1 Nonlinear Programming Techniques 97
5.2 Sequential Quadratic Programming 100
5.3 Illustrative Problems 103

6 RECOMMENDED APPROACH 123

6.1 General Remarks 123
6.2 A General Recommended Approach 124
6.3 An Alternative Search Process For Cases Where Convergence Difficulties May Be Encountered 126
6.4 Numerical Illustration of the Proposed Approach 129

7 SOME OBSERVATIONS ON THE EFFECT OF THE NUMBER OF LINKS AND THE LOADING CONDITIONS 139

8 DYNAMIC RESPONSE ANALYSIS 145

8.1 Introduction 145
8.2 The Constant Average Acceleration Method-An Implicit Algorithm 148

9 INTERACTIVE PROCEDURE 151

9.1 Introduction 151
9.2 The Interactive Program 152

10 SUMMARY, CONCLUSION, AND RECOMMENDATIONS 162

10.1 Summary 162
10.2 Conclusion 165
10.3 Recommendations 165

APPENDICES

A FORMULATION OF A CONSISTENT MASS MATRIX 167

B BASE EXCITATION 177

C IMPULSIVE LOADING 193

REFERENCES 207

BIOGRAPHICAL SKETCH 214

LIST OF TABLES

Table page

2.1 Natural frequencies calculated by both lumped and consistent mass matrix approaches for the length of 10 feet bar 24

3.1 Optimum volumes of the three-link truss for different lengths and excitation frequencies 39

3.2 Optimum results of the three-link truss for a wide range of frequencies for $L = 10'$ 40

3.3 Optimum results of the forty-seven-member tower for $\omega = 0$ 41

3.4 Optimum results of the forty-seven-member tower for $\omega = 10$ rad/sec . 42

3.5 Optimum results of the forty-seven-member tower for $\omega = 30$ rad/sec . 43

3.6 Optimum results of the forty-seven-member tower for $\omega = 50$ rad/sec . 44

3.7 Optimum results of the forty-seven-member tower for $\omega = 80$ rad/sec . 45

3.8 Optimum results of the forty-seven-member tower for $\omega = 100$ rad/sec 46

3.9 Optimum results of the forty-seven-member tower for $\omega = 140$ rad/sec 47

3.10 Optimum results of the forty-seven-member tower for $\omega = 190$ rad/sec 48

3.11 Optimum results of the forty-seven-member tower for $\omega = 200$ rad/sec 49

3.12 Optimum results of the forty-seven-member tower for $\omega = 220$ rad/sec 50

3.13 Optimum results of the two-hundred-member structure for $\omega = 0$ (I) . 51

3.14 Optimum results of the two-hundred-member structure for $\omega = 0$ (II) 52

3.15 Optimum results of the two-hundred-member structure for $\omega = 0$ (III) 53

3.16 Optimum results of the two-hundred-member structure for $\omega = 20$ rad/sec (I) 54

3.17 Optimum results of the two-hundred-member structure for $\omega = 20$ rad/sec (II) 55

3.18 Optimum results of the two-hundred-member structure for $\omega = 20$ rad/sec (III) 56

3.19 Optimum results of the two-hundred-member structure for $\omega = 50$ rad/sec (I) 57

3.20 Optimum results of the two-hundred-member structure for $\omega = 50$ rad/sec (II) 58

3.21 Optimum results of the two-hundred-member structure for $\omega = 50$ rad/sec (III) 59

3.22 Optimum results of the two-hundred-member structure for $\omega = 70$ rad/sec (I) 60

3.23 Optimum results of the two-hundred-member structure for $\omega = 70$ rad/sec (II) 61

3.24 Optimum results of the two-hundred-member structure for $\omega = 70$ rad/sec (III) 62

5.1 NLP results for the three-link truss 106

5.2 NLP results of the forty-seven-member tower for $\omega = 0$ 107

5.3 NLP results of the forty-seven-member tower for $\omega = 30$ rad/sec 108

5.4 NLP results of the forty-seven-member tower for $\omega = 50$ rad/sec 109

5.5 NLP results of the forty-seven-member tower for $\omega = 80$ rad/sec 110

5.6 NLP results of the forty-seven-member tower for $\omega = 100$ rad/sec 111

5.7 NLP results of the forty-seven-member tower for $\omega = 140$ rad/sec 112

5.8 NLP results of the forty-seven-member tower for $\omega = 190$ rad/sec 113

5.9 NLP results of the forty-seven-member tower for $\omega = 200$ rad/sec 114

5.10 NLP results of the two-hundred-member structure for $\omega = 20$ rad/sec (I) 115

5.11 NLP results of the two-hundred-member structure for $\omega = 20$ rad/sec (II) 116

5.12 NLP results of the two-hundred-member structure for $\omega = 20$ rad/sec (III) 117

5.13 NLP results of the two-hundred-member structure for $\omega = 50$ rad/sec (I) 118

5.14 NLP results of the two-hundred-member structure for $\omega = 50$ rad/sec (II) 119

5.15 NLP results of the two-hundred-member structure for $\omega = 50$ rad/sec (III) 120

5.16 Comparisons between the proposed approach and NLP approach for the forty-seven-member tower 121

5.17 Comparisons between the proposed approach and NLP approach for the two-hundred-member structure 122

6.1 Natural frequencies at different excitation frequencies (rad/sec) 131

A.1 Optimum results of the three-link truss for both the discrete mass model and consistent mass model 173

A.2 Comparison of optimum results for the three-link truss between the discrete mass model and consistent mass model 173

A.3 Optimum results of the forty-seven-member tower by using the discrete mass model 174

A.4 Optimum results of the forty-seven-member tower by using the consistent mass model 175

A.5 Comparison of optimum results for the forty-seven-member tower between the discrete mass model and consistent mass model 175

B.1 Optimum results of the two-hundred-member structure for static case (I) 179

B.2 Optimum results of the two-hundred-member structure for static case (II) 180

B.3 Optimum results of the two-hundred-member structure for static case (III) 181

B.4 Optimum results of the two-hundred-member structure under base excitation for $\omega = 5$ rad/sec (I) 182

B.5 Optimum results of the two-hundred-member structure under base excitation for $\omega = 5$ rad/sec (II) 183

B.6 Optimum results of the two-hundred-member structure under base excitation for $\omega = 5$ rad/sec (III) 184

B.7 Optimum results of the two-hundred-member structure under base excitation for $\omega = 15$ rad/sec (I) 185

B.8 Optimum results of the two-hundred-member structure under base excitation for $\omega = 15$ rad/sec (II) 186

B.9 Optimum results of the two-hundred-member structure under base excitation for $\omega = 15$ rad/sec (III) 187

B.10 Optimum results of the two-hundred-member structure under base excitation for $\omega = 30$ rad/sec (I) 188

B.11 Optimum results of the two-hundred-member structure under base excitation for $\omega = 30$ rad/sec (II) 189

B.12 Optimum results of the two-hundred-member structure under base excitation for $\omega = 30$ rad/sec (III) 190

C.1 Five modes approximation for the forty-seven-member tower under impulsive loading (I) 199

C.2 Fifteen modes approximation for the forty-seven-member tower under impulsive loading (I) 200

C.3 All modes (forty) expansion for the forty-seven-member tower under impulsive loading (I) 201

C.4 Forty-seven-member tower under Impulse = 50 lb-sec 202

C.5 Forty-seven-member tower under Impulse = 80 lb-sec 203

C.6 Forty-seven-member tower under Impulse = 150 lb-sec 204

LIST OF FIGURES

Figure page

2.1 Typical members of a truss 25

2.2 A simple half-half mass model 25

2.3 Consistent mass model 26

2.4 Axially oscillating bar fixed at one end 26

2.5 Comparison of the fundamental frequency between consistent and lumped mass models 27

2.6 Comparison of the second natural frequency between consistent and lumped mass models 27

2.7 Comparison of the third natural frequency between consistent and lumped mass models 28

2.8 Typical truss member and discrete mass model 28

2.9 A single particle suspended by N springs 29

2.10 Elastically connected system of masses 29

2.11 Local coordinates for a generic link 30

2.12 Global coordinates for a generic link 30

3.1 Flowchart of solution algorithm by the successive iteration approach . 63

3.2 Simple three-link truss 64

3.3 Convergent performance for $\omega = 0\,\mathrm{rad/sec}$ 65

3.4 Convergent performance for $\omega = 300\,\mathrm{rad/sec}$ 65

3.5 Convergent performance for $\omega = 700\,\mathrm{rad/sec}$ 66

3.6 Convergent performance for $\omega = 1000\,\mathrm{rad/sec}$ 66

3.7 Dependency on initial values for arbitrarily chosen cross sectional areas 67

3.8 Dependency on initial values for cross sectional areas obtained for $\omega = 1200\,\mathrm{rad/sec}$ 67

3.9 Dependency on initial values for cross sectional areas obtained for $\omega = 1250\,\mathrm{rad/sec}$ 68

3.10 Dependency on initial values for cross sectional areas obtained for $\omega = 1270\,\mathrm{rad/sec}$ 68

3.11 Dependency on initial values for cross sectional areas obtained for $\omega = 1290\,\mathrm{rad/sec}$ 69

3.12 Dependency on initial values for cross sectional areas obtained for $\omega = 1295\,\mathrm{rad/sec}$ 69

3.13 Displacements at top node for $\omega = 1000\,\mathrm{rad/sec}$ 70

3.14 Stresses in each link for $\omega = 1000\,\mathrm{rad/sec}$ 70

3.15 Displacements at top node for $\omega = 1100\,\mathrm{rad/sec}$ 71

3.16 Stresses in each link for $\omega = 1100\,\mathrm{rad/sec}$ 71

3.17 Displacements at top node for $\omega = 1200\,\mathrm{rad/sec}$ 72

3.18 Stresses in each link for $\omega = 1200\,\mathrm{rad/sec}$ 72

3.19 Displacements at top node for $\omega = 1300\,\mathrm{rad/sec}$ 73

3.20 Stresses in each link for $\omega = 1300\,\mathrm{rad/sec}$ 73

3.21 Optimum volume ratios of the three-link truss for a wide range of forcing frequencies (I) 74

3.22 Optimum volume ratios vs. discrete values of added mass for resonant situation of the three-link truss 74

3.23 Forty-seven-member tower 75

3.24 Optimum design of forty-seven-member tower for $\omega = 50$ rad/sec . . . 76

3.25 Optimum design of forty-seven-member tower for $\omega = 200$ rad/sec . . 76

3.26 Optimum volume ratios of the forty-seven-member tower for a wide range of forcing frequencies (I) 77

3.27 Two-hundred-member structure 78

3.28 Optimum design of two–hundred-member structure for $\omega = 20$ rad/sec 79

3.29 Optimum design of two–hundred-member structure for $\omega = 80$ rad/sec 79

3.30 Optimum volume ratios of the two-hundred-member structure for a wide range of forcing frequencies (I) 80

4.1 Flowchart of solution algorithm by incorporating linear programming 93

4.2 Optimum volume ratios of the three-link truss for a wide range of forcing frequencies (II) 94

4.3 The first mode shape of the three-link truss 94

4.4 The second mode shape of the three-link truss 95

4.5 Optimum volume ratios of the three-link truss for added mass case . . 95

4.6 Optimum volume ratios of the forty-seven-member tower for a wide range of forcing frequencies (II) 96

4.7 Optimum volume ratios of the two-hundred-member structure for a wide range of forcing frequencies (II) 96

6.1 A typical non-convergence case of iteration history at a specific excitation frequency 132

6.2 Candidates of optimum volume ratio for $\omega = 50\,\mathrm{rad/sec}$ 132

6.3 Candidates of optimum volume ratio for $\omega = 100\,\mathrm{rad/sec}$ 133

6.4 Candidates of optimum volume ratio for $\omega = 150\,\mathrm{rad/sec}$ 133

6.5 Candidates of optimum volume ratio for $\omega = 200\,\mathrm{rad/sec}$ 134

6.6 Candidates of optimum volume ratio for $\omega = 250\,\mathrm{rad/sec}$ 134

6.7 Candidates of optimum volume ratio for $\omega = 300\,\mathrm{rad/sec}$ 135

6.8 Candidates of optimum volume ratio for $\omega = 350\,\mathrm{rad/sec}$ 135

6.9 Candidates of optimum volume ratio for $\omega = 400\,\mathrm{rad/sec}$ 136

6.10 Candidates of optimum volume ratio for $\omega = 450\,\mathrm{rad/sec}$ 136

6.11 Candidates of optimum volume ratio for $\omega = 500\,\mathrm{rad/sec}$ 137

6.12 Optimum volume ratios of the two-hundred-member structure for a wide range of forcing frequencies (III) 137

6.13 Natural frequencies of the optimized structure at different excitation frequencies 138

7.1 Three-link truss 141

7.2 Five-link truss 141

7.3 Six-link truss 142

7.4 Ten-link truss (four-loads) 142

7.5 Ten-link truss (two loads) 143

7.6 Forty-seven-member tower 143

7.7 Two-hundred-member structure 144

9.1 Main window of the interactive program 155

9.2 The structural model creation program 155

9.3 Interactive input of geometric information through the structural model creation program 156

9.4 Interactive input of material information through the structural model creation program 156

9.5 A new generated structural model through the structural model creation program 157

9.6 Automatically generated input data sheet through the structural model creation program 157

9.7 Automatically loaded structural model into the main window 158

9.8 Numerical result data sheet for optimum design 158

9.9 The relative area distribution drawn in the main window 159

9.10 Iteration history at a specific excitation frequency 159

9.11 A plot of optimum volume ratio for a range of frequencies 160

9.12 Sample results for the time history analysis 160

9.13 Display of the movement of the forty-seven-member tower under harmonic loading 161

A.1 Coordinate transformation 176

B.1 Optimum weights of the two-hundred-member structure under base excitation for a range of frequencies 191

B.2 Ratios of the optimum weight to frequency square of the two-hundred-member structure under base excitation for a range of frequencies . 191

B.3 Optimum volume ratios of the two-hundred-member structure under base excitation for a range of frequencies 192

C.1 Five modes approximation for the forty-seven-member tower under impulsive loading (II) 205

C.2 Fifteen modes approximation for the forty-seven-member tower under impulsive loading (II) 205

C.3 All modes (forty) expansion for the forty-seven-member tower under impulsive loading (II) 206

C.4 All modes (forty) expansion for the forty-seven-member tower under impulsive loading (The areas of links 23 and 25 not represented in order to show all other elements to scale) (II) 206

Abstract of Dissertation Presented to the Graduate School
of the University of Florida in Partial Fulfillment of the
Requirements for the Degree of Doctor of Philosophy

A GENERALIZED PROCEDURE FOR THE OPTIMUM DESIGN OF LARGE-SCALE TRUSS STRUCTURES SUBJECTED TO HARMONIC EXCITATIONS

By

Chao-Wei Hsiao

May 2001

Chairman: Dr. Ali A. Seireg
Major Department: Mechanical Engineering

The study presented in this dissertation investigates the development of an efficient and user friendly computer based procedure for the optimum design of large-scale truss structures subjected to sinusoidal loadings. The procedure utilizes a scheme for automated formulation of the system equations and applies successive iteration and linear programming algorithms for the optimization.

The developed procedure proved to be orders of magnitudes computationally faster than nonlinear programming for large-scale truss structures. It also guarantees convergence to the optimum solution from any arbitrary initial guess, contrary to nonlinear programming which will not generally converge without a good initial guess. Harmonic forces, impulsive loading, and ground disturbances are considered in this investigation.

CHAPTER 1
INTRODUCTION

1.1 Introduction

Structural optimization is an important issue in many applications. Overwhelming efforts of research in the field of optimal design of structures have dealt with solving optimum structural problems for various static loading conditions. Relatively little attention has been focused on the optimal design under dynamic loading due to the complexities associated with dynamic loads. Although there has been a growing interest in this field, published papers are still limited both in number and scope, especially for large-scale structures. The problems of optimizing such structures are considered as large-scale since the number of design variables and constraints are high. This dissertation deals with the problem of minimum weight design of large-scale truss structures under dynamic loading with a stress constraint. The problem is nonlinear in essence.

Solving large-scale problems directly can involve many numerical difficulties and sometimes the problems become intractable. Therefore, decomposition techniques have been used by many researchers. A two level decomposition technique will be applied to the large-scale structural optimization problems considered in this study in order to overcome the difficulties of using nonlinear programming to solve the problem directly.

Optimum design of systems subjected to dynamic loads is a challenging problem, and it is important to use an efficient and effective method in finding the solution. To solve the dynamically loaded large-scale structures efficiently and effectively, a successive iteration approach is presented in this study. It is desirable to obtain the volume distribution of a dynamically loaded structure such that its total volume reaches a minimum and the maximum value of stress in each member should be as close as possible to a specified allowable value without exceeding this value. The iterative process can be stated as follows: an initial structure is first analyzed and, as a result of the analysis, an improved structure is obtained. The process is repeated until no significant gains can be made. The process proved to be very efficient. Linear programming can also be incorporated for high frequencies.

The successive iteration procedure is used to develop a general algorithm for the optimum designs of large-scale truss structures under harmonic excitations for a wide range of frequency spectrum. The general algorithm developed herein is applied to several examples to illustrate its superiority to the nonlinear programming approach.

1.2 Literature Review

Formulations for structural analysis involving modeling of the mass matrix exist extensively in the literature. Archer [1] is generally known as the first author who proposed the consistent mass matrix. In his paper the basic equation for computing the mass matrix coefficients is given a physical interpretation. In an attempt to improve the accuracy of the dynamic analysis as it is affected by the mass matrix, a consistent mass matrix construction is investigated that accounts for the actual distribution of mass throughout the structure in a manner similar to the Rayleigh-Ritz formulation. It is shown that the natural frequencies obtained by the use of the consistent mass matrix are upper bounds to the exact solution. However, diagonal or lumped mass matrices are often used due to their simplicity and economy. There are several ways of constructing lumped mass matrices as shown in the book by Hughes [2]. Recently, Haug and Pan [3] presented an optimal inertia lumping formulation using modal mass matrices, rather than a consistent mass matrix, obtained from structural analysis. The method is applicable even for situations in which substructuring is employed and the consistent mass matrix is lost during the model reduction process. In this study, after reviewing the above works, a consistent mass matrix and a lumped mass matrix will be used to derive a new formulation of effective mass matrix which is an equivalent mass matrix to the first mode of the truss member.

Optimization techniques in mechanical elements and structures design have been reviewed by several authors. A comprehensive review of the literature on optimal structural design from Galileo to the end of 1962 was reported by Wasiutynski and Brandt [4]. Sheu and Prager [5] reviewed this field from 1962 to 1968. Seireg [6] presented an extensive review of some illustrative examples of the use of optimization techniques in the design of mechanical elements and systems. The cases cited include gears, bearings, dynamic systems, rotating discs, pressure vessels, shafts under bending and torsion, beams subjected to longitudinal impact, and problems of elastic contact and load distribution. Belegundu and Arora [7,8] presented a comprehensive review of various mathematical programming techniques used for structural optimization. The aim of this paper is twofold: (a) to discuss the applicability of modern optimization techniques to structural design problems, and (b) to present mathematical programming methods from a unified and design engineer's viewpoint. Theoretical aspects are considered in this paper, while numerical results of test problems are discussed in a companion paper. From the test problems in this companion paper, two types of the structures are used in this study for dynamic loadings, although they were originally used for static loads. In Papalambros's review [9], large-scale system design and topology or configuration design are identified as the most important areas of future design optimization research. Some new approaches for partitioning large design problems and for topology optimization of multi-component structural systems are introduced.

Structural optimization problems are considered as large-scale because of the dimensionality of the number of design variables and/or the large number of constraints. Solving large-scale structural optimization problems can encounter many numerical difficulties, and sometimes the problem becomes intractable as stated in

Sobieszczanski-Sobieski [10]. In order to overcome these difficulties, decomposition techniques are usually adopted as in the work of Khorshid and Seireg (see Khorshid [11]). Decomposition in large-scale structures is classified into different categories as follows: First, methods based on dynamic programming [12–18]; second, hierarchical multilevel methods [19–26]; third, optimality criteria methods [27–29].

Optimum design problems of structures subjected to dynamic excitations exist in numerous places in the literature. Icerman [30] investigated the optimal design of structures of various types that are excited by a single harmonic load. The amplitude and frequency of this load are prescribed as well as the "dynamic response" of the structure, which is defined by the virtual work of the load on the displacement of its point of application. This paper is the earliest paper dealing with dynamic response constraint according to Icerman. Icerman considered only concentrated masses at the joints with negligible body masses of the truss. However, as the body weight becomes higher, for large-scale structures, the masses of the structures become more and more important and should not be neglected. Therefore, in this study since large-scale structures are considered, the body masses should be included in the formulation. Fox and Kapoor [31] considered the planar truss-frame with both distributed and concentrated mass as the model, subjected to shock loads, with limitations on the maximum dynamic stresses and displacements as well as on the natural frequencies of the structure. They employed a feasible direction technique of optimization. In a study by Mróz [32], optimal design of elastic structures subjected to one or several dynamic, harmonically-varying load systems is discussed assuming the notion of dynamic stiffness as the design criterion. A generalized variational principle is used in deriving the necessary and sufficient conditions of optimal design. A method of solving infinite dimensional optimal design problems including minimum weight design of structures with constraints on strength and natural frequency was presented by McCart, Haug, and Streeter [33]. A steepest-descent boundary-value method is developed for a three-member frame design problem. Rubin [34] introduced an analytical procedure for the determination of the least weight structure which satisfies a specific frequency requirement. The approach is to modify an existing structure by varying the cross-sectional properties of its member. This is accomplished by using separate gradient equations to first obtain the correct structural frequency and then, while the frequency is held constant, to minimize the weight. According to Rubin, the method of analysis presented in the paper represents the first published procedure for redesigning a complex structure to achieve the least weight configuration which must have its fundamental frequency equal to some specified value. A literature survey of optimal structural design under dynamic constraints was presented by Pierson [35]. In this review, dynamic constraints are classified as constraints on structural frequencies and on transient dynamic response. Levy [36] provided fully stressed designs of a rod and beam subjected to impulsive loads. He determined the maximum stress by setting the derivative of stress with respect to time equal to zero and checking the total energy of the system at the time grid points. Cassis and Schmit [37] treated dynamic response constraints parametrically in time. Approximation concepts, previously studied in static optimization problems, are extended and used in the dynamic response regime. The approximations employed are the following: (1) design variable linking; (2) time parametric constraint deletion; and (3) use of first-order Taylor series expansions to approximate the dynamic response functions in explicit form with respect to the design variables. Feng, Arora, and Haug [38] developed an algorithm for optimal design of elastic structures subjected to dynamic loads. Finite element, modal analysis and a generalized steepest descent method are employed in developing the computational algorithm. Structural weight is minimized subjected to constraints on dynamic response (stress and displacement), natural frequencies, and design parameters (member size). Hsieh and Arora [39, 40] presented and analyzed methods for design sensitivity analysis of both static and dynamic responses for structural systems when general boundary conditions are used during the analysis phase. Zacharopoulos, Willmert, and Khan [41] presented a procedure, based on optimality criterion methods, for minimum weight design of structures subjected to stress, displacement and natural frequency constraints. No approximate analyses or determination of large numbers of Lagrange multipliers is involved. Kramer and Grierson [42] developed a method for the minimum weight design of planar frameworks subjected to dynamic loading. Their method can account for combined axial and bending stresses, and is capable of designing minimum weight structures under simultaneous static and dynamic loading. The examples they used were for relatively small structures. Truman and Petruska [43] presented an optimization algorithm using a time history analysis for plane frame building systems subjected to time history loading. The optimality criteria method is used with the objective function being the weight of the structure. Possible constraints are displacement, story drift, stress, frequency, and side constraints. Chahande and Arora [44] investigated the multiplier method for optimization of large-scale mechanical and structural systems subjected to dynamic loads. They found that the multiplier algorithm is more efficient than the primal method, that is, the sequential quadratic programming algorithm, for dynamic response optimization of large-scale problems. Their model is a simple fifty masses mass-spring shear elastic system. Bensalem, Sibbald, and Fairfield [45] presented the use of modal characteristics for the optimal design of arches. Natural frequency and dynamic direct implicit time integration analyses were performed to determine the resonant frequencies and analyze the responses to impact loading. A relationship was found between the resonant frequencies and the load carrying capacities of such arches. Dutta and Ramakrishnan [46] provided a computational method of design sensitivities for structures under transient dynamic loads using time marching scheme. In their paper, they handled the problem by systematically achieving an adaptive mesh for a reasonably fine but constant time step. Min, Kikuchi, Park, Kim, and Chang [47] utilized the homogenization design method to generate the optimal topology for structures and employed an explicit direct integration scheme to solve the linear transient problems. The optimization problem is formulated to find the best configuration of structures that minimizes the dynamic compliance within a specified time interval. An optimization procedure for the minimum weight optimization with discrete design variables for truss structures subjected to constraints on stresses, natural frequencies and frequency response was presented by Tong and Liu [48]. A binary number combinatorial algorithm is employed to perform the zero-one programming.

Structural optimization for earthquake resistant design is growing in volume, but is still limited. Bhatti and Pister [49] presented a dual criteria approach for optimal design of earthquake-resistant structural systems. In the work of Balling, Pister, and Ciampi [50], nonlinear step-by-step integration is used as the analysis technique within the design process itself rather than as a check at the end of the design process. Objective functions include the minimization of structural volume as well as the minimization of response quantities such as story drifts and inelastically dissipated energy. Cheng and Truman [51] have studied optimization of structures utilizing modal response spectrum analyses. Cheng and Juang [52,53], and Truman and Cheng [54] studied two- and three-dimensional building structures with respect to various code provisions and cost functions. Truman and Petruska [43] have applied optimality criteria techniques for optimization of two-dimensional structures using time history analysis procedures coupled with actual seismic accelerogram base excitation.

Several investigators dealt with the issue of fully stressed design versus minimum weight design. Schmidt [55] derived the conditions for the minimum weight design of redundant elastic pin-jointed trusses under several alternative load systems. It was shown that these require the determination of all fully stressed designs. The minimum of these will be the least weight design. A systematic method is given which enables such designs to be found if the process is carried far enough. Razani [56] provided the necessary condition for the equivalence of the fully stressed design to minimum weight design by using the Kuhn-Tucker optimality condition of nonlinear programming. A computationally practical method for verification of the optimality of fully stressed design is obtained. Although the Kuhn-Tucker approach is a perfectly valid criterion for optimality, it does not help with the selection of improved designs for non-optimal cases. It was also observed by Razani that the faster the rate of convergence of the iterative fully stressed design, the more likely the optimality of the design. Therefore, it was concluded by Razani that the fully stressed design of the structures with normal action is more likely to be optimum. Kicher [57] also discussed the issue of minimum weight versus fully stressed optimum design. Dayaratnam and Patnaik [58] showed that the fully stressed design is feasible under certain conditions associated with the number and nature of load conditions, order of indeterminancy, and topology of the structure. All of the above papers dealt with static loads only. A more detailed discussion on fully stressed design for static loads is shown in the book by Gallagher and Zienkiewicz [59]. Levy and Wolf [60] considered fully stressed dynamically loaded structures. In the case of static loading of statically determinate structures, it is well known that fully stressed designs are, in fact, optimal designs. In their work, which considered statically determinate structures under dynamic loading, the existence of a fully stressed design had been demonstrated, and since, unlike the static case, these designs may not be optimal, a method of determining whether the design is a local optimum has been illustrated. As discussed in their work, even if the fully stressed design is not optimum, it is expected that it will be more convenient to obtain an optimum design using an iterative procedure by starting from the fully stressed structure than by starting from some arbitrarily selected structure. Mathias and Röhrle [61] presented an optimal structural design of dynamically excited systems using the finite element method by both the fully stressed design and the gradient method. In this way, the advantages of the rapid initial convergence of the fully stressed design are combined with the mathematically exact optimization according to the gradient method. The task consisted of designing harmonically excited structures with viscous damping that are optimal with respect to weight. One example of optimization calculations is carried out for the satellite AEROS with only eight and eighteen degrees of freedom models.

All the above investigations on dynamic design dealt with relatively small-scale structures when non-linear optimization approaches can be relied upon to converge to a solution. None of these studies tested the methods on large-scale systems to evaluate their applicability for such systems and the computational efficiency.

1.3 Objective

It can be seen from the literature review that there is a need for a computationally efficient method capable of optimizing very large-scale structures subjected to dynamic loading. Because of the inherent nonlinearity of the problem and the large number of decision variables, current approaches would require extensive computational efforts and a good initial guess for starting the search. There would be no guarantee that a convergent solution can be reached from an arbitrary initial guess. If convergence occurs, the solution may only represent the best local optimum attainable from the selected starting point, and tremendous computational effort may be needed.

This study was, therefore, initiated to investigate the possibility of developing an efficient general procedure for determining the cross sectional areas of the links in very large-scale truss designs which make the structures as fully stressed as possible when subjected to harmonic excitations at any frequency. The analytical formulation assumes small displacements at the joints such that the geometric shape does not undergo any appreciable changes and linear elasticity conditions can be considered. The algorithm presented in this study is, therefore, developed with the objective of efficiently guaranteeing a convergent solution from any arbitrary initial guess for "fully stressed" large-scale trusses subjected to harmonic forcing functions at any excitation frequency. A two-hundred member truss is used for illustration. Using nonlinear programming in such case was found to require a good initial guess and orders of magnitude larger computing effort.

1.4 Outline of the Dissertation

The contents of the individual chapters are described below.

- In this chapter, a literature review is presented covering the following topics: lumped mass versus consistent mass formulation, application of optimization techniques in mechanical elements and structures design, large-scale structural optimization and decomposition, optimum design of structures subjected to dynamic excitations, and structural optimization for earthquake resistant design.
- Problem formulation for analysis and optimization is presented in Chapter 2 which includes the construction of the proposed effective mass model of the truss member.
- The solution algorithm by successive iteration approach is introduced in Chapter 3 with several illustrative problems. Decomposition of large-scale structures is also described.
- The solution algorithm by incorporating linear programming as an extension of the successive iteration approach is presented in Chapter 4. The topology of the system matrices is formulated in detail for the general truss case with and without additional masses at the joints. The benefits of incorporating linear programming are illustrated.
- Nonlinear programming is applied to the example problems in Chapter 5 in order to illustrate the advantages of the proposed approach.

- In Chapter 6, a general recommended procedure is developed for design of trusses subjected to a wide range of excitation frequencies. A search procedure is presented for cases where convergence can not be quickly achieved by the general procedure.
- In Chapter 7, some observations on the effect of the number of links and the loading conditions on the obtained solutions are given.
- One of the commonly used implicit time integration methods is discussed in Chapter 8. This method can be used as an analysis tool for the interactive program which is discussed in Chapter 9.
- In Chapter 9, an interactive program combining the proposed algorithms with an interactive model generation scheme via graphical user interfaces is developed as an aid to the total design process.
- The final chapter gives a summary and conclusion of the work presented in this dissertation as well as several recommendations for future research.

CHAPTER 2
MODELING, ANALYSIS, AND OPTIMIZATION PROBLEM FORMULATION

This chapter will address modeling of the truss member used in this study first. Then, analysis of the truss structures will be introduced, and finally, the optimization problem will be formulated.

2.1 Modeling of the Structural Member

In design of dynamically loaded structures, damping effect will be ignored, for simplification and as a safety factor. In actual structures, the responses will be damped out due to the dissipation of energy in materials during dynamic loads; therefore, treating systems as undamped is a safe way for design. Before conducting a full analysis of a structure as a discrete parameter system, modeling of the equivalent mass and stiffness of a generic member of the structure should be considered first. Since each member is hinged at both ends and is straight in shape, it is only subjected to axial loads. An illustration of a typical member of the truss is shown in Figure 2.1. The model of a truss member used in this study is treated as massless axial spring with equivalent discrete masses at the joints. For linear elastic materials, stiffness can be expressed as $k = AE/L$, where A is the cross sectional area, E is the modulus of elasticity, and L is the length of the truss member, as long as the displacements are small.

An approximate and simple way to account for the effect of inertia force is to model the massless link as a two degrees of freedom system as shown in Figure 2.2. The simplest lumped mass matrix $(\mathbf{m})$ can be expressed as follows:

$$\mathbf{m} = \frac{\rho A L}{2} \begin{bmatrix} 1 & 0 \\ 0 & 1 \end{bmatrix} \tag{2.1}$$

where

$\rho \equiv$ mass density of the link

$A \equiv$ cross sectional area of the link

$L \equiv$ length of the link

Another approach, which is more reasonable, is to utilize a consistent mass matrix as originally proposed by Archer [1]. The idea is using the same shape functions as used in integration for the stiffness matrix to integrate for the mass matrix as shown in Figure 2.3. A consistent mass matrix ($\mathbf{m}$), therefore, has the same pattern of entries as the corresponding stiffness matrix ($\mathbf{k}$). Besides, a consistent damping matrix ($\mathbf{c}$) and a consistent force matrix ($\mathbf{f}$) can be constructed in a similar fashion as in constructing a consistent mass matrix ($\mathbf{m}$). For an axially loaded member and linear interpolation of displacements, the consistent mass matrix can be expressed as

$$\mathbf{m} = \frac{\rho A L}{6} \begin{bmatrix} 2 & 1 \\ 1 & 2 \end{bmatrix} \tag{2.2}$$

This mass matrix can be derived from the following shape function and integral form of mass matrix

$$\mathbf{N} = \left(1 - \frac{x}{L}, \frac{x}{L}\right) \tag{2.3}$$

$$\mathbf{m} = \int_V \rho \mathbf{N}^T \mathbf{N} \, dV \tag{2.4}$$

where

$\mathbf{N} \equiv$ shape function matrix

$\mathbf{m} \equiv$ consistent mass matrix

Detailed description of the derivation can be found in Appendix A.

In this study, a new mass matrix of a truss member is developed as follows: First, find the natural frequencies of an axially oscillating bar constrained at one end (shown in Figure 2.4). More accurate results can be obtained by refining the mesh, for example, one hundred elements, and using the above two approaches, lumped mass matrix and consistent mass matrix, to calculate the natural frequencies. The test results are given in Table 2.1 by using $\rho = 15.2\,\mathrm{slug/ft^3}$, $E = 30,000,000\,\mathrm{psi}$, $L = 10\,\mathrm{ft}$, and an arbitrary value of the cross-sectional areas. Furthermore, the comparison between these two approaches is shown in Figure 2.5 to Figure 2.7 for the first three frequencies. It is seen that for this problem, the lumped mass solution for natural frequencies converges from lower values toward the upper-bound solution while the consistent mass solution converges from higher values toward the lower-bound solution. Both solutions give about the same level of accuracy with mesh refinement. From Table 2.1, the prediction of the fundamental natural frequency is about 2648.16 rad/sec for the consistent mass solution and 2648.11 rad/sec for the lumped mass solution.

This result can also be proved by solving the wave equation for the same boundary conditions using separation of variables,

$$\frac{\partial^2 u}{\partial x^2} = \frac{1}{a^2}\frac{\partial^2 u}{\partial t^2} \tag{2.5}$$

where

$$a = \sqrt{\frac{E}{\rho}} \tag{2.6}$$

Let $u = x(A\cos\omega t + B\sin\omega t)$, and use the boundary conditions:

$$u = 0 \quad \text{at } x = 0 \tag{2.7}$$

$$\frac{\partial u}{\partial x} = 0 \quad \text{at } x = 1 \tag{2.8}$$

Therefore, a series of natural frequencies can be solved by substituting u into the wave equation and satisfying the above boundary conditions,

$$(\omega_n)_i = \frac{i\pi a}{2L} = \frac{i\pi}{2L}\sqrt{\frac{E}{\rho}},\ i = 1, 3, 5, \cdots, \infty \tag{2.9}$$

For the same problem above, when $\rho = 15.2\,\text{slug/ft}^3$, $E = 30,000,000\,\text{psi}$, and $L = 10\,\text{ft}$, the fundamental natural frequency can be obtained as 2648.13 rad/sec by setting $i = 1$. As would be expected, both lumped and consistent mass numerical solutions in this case give a result of the same order of accuracy as the continuous theoretical solution.

In order to achieve better accuracy by using the simple lumped mass model, an effective mass is derived based on the relations among stiffness, mass, and natural frequency,

$$\omega_n = \sqrt{\frac{k}{m}} \tag{2.10}$$

Assume k is a constant since stiffness is invariant. The natural frequency (ω_n) is inversely proportional to the square root of the mass (m) according to Equation (2.10); thus,

$$\frac{\omega_n}{(\omega_n)_e} = \frac{\sqrt{m_e}}{\sqrt{m}} \tag{2.11}$$

where

$\omega_n \equiv$ fundamental frequency calculated by one lumped mass model

$(\omega_n)_e \equiv$ "exact" fundamental frequency

$m \equiv$ lumped mass

$m_e \equiv$ effective mass

Therefore,

$$m_e = \left(\frac{\omega_n}{(\omega_n)_e}\right)^2 \times m \tag{2.12}$$

The effective mass at each end can be calculated to be approximately 0.40528 of the total mass of the link according to Table 2.1 when $\omega_n = 2384.16\,\mathrm{rad/sec}$, $(\omega_n)_e = 2648.16\,\mathrm{rad/sec}$, and m = half of the total mass of the link. The result is also independent of the length of the link, which is tested using different values of lengths. This result greatly simplifies the analysis and design processes.

In summary, the model to be used in this study is a discrete mass model with 0.40528 of the total link mass lumped at each end connected by a massless link as shown in Figure 2.8.

2.2 Structural Analysis

In the solution of the structural optimization problem, a structural analysis would be required to find the internal forces in the links and the nodal displacements in each iteration.

2.2.1 Formulation of the Governing Differential Equations:

There are several means to formulate the governing differential equations. One is using the approach by Seireg [62] for small displacements. Suppose a particle suspended by N springs, shown in Figure 2.9, and take the elastic constant for each spring as k_i and its directional cosines as l_i, m_i, n_i, where i is $1, 2, \cdots, N$; the equations of motion for a small displacement x, y, z will be

$$m\ddot{x} = \sum F_x = -\left[\sum_{i=1}^{N} l_i^2 k_i\right] x - \left[\sum_{i=1}^{N} l_i m_i k_i\right] y - \left[\sum_{i=1}^{N} l_i n_i k_i\right] z \tag{2.13}$$

$$m\ddot{y} = \sum F_y = -\left[\sum_{i=1}^{N} m_i l_i k_i\right] x - \left[\sum_{i=1}^{N} m_i^2 k_i\right] y - \left[\sum_{i=1}^{N} m_i n_i k_i\right] z \tag{2.14}$$

$$m\ddot{z} = \sum F_z = -\left[\sum_{i=1}^{N} n_i l_i k_i\right] x - \left[\sum_{i=1}^{N} n_i m_i k_i\right] y - \left[\sum_{i=1}^{N} n_i^2 k_i\right] z \tag{2.15}$$

These equations of motion can easily be extended to an elastically connected system of particles, which is shown in Figure 2.10, by considering relative displacements for x, y, z in the equations. This approach is much more physically descriptive and is easier to implement than other methods, especially in the formulation for the linear programming approach. Detailed formulation will be stated in Chapter 4.

Another approach is the matrix methods of analysis. In general, there are two basic methods commonly used: the displacement (or stiffness) method and the force (or flexibility) method. The displacement method considers equilibrium of forces or moments. Such a formulation yields nodal displacements. The force method is formulated from the consideration of geometrical compatibility, and this formulation yields forces at the node points. Because the displacement method is based on equilibrium, it is easier than the force method in computer programming implementation. The displacement method can be used in both determinate and indeterminate structural analysis. A brief explanation of the displacement (or stiffness) method is as follows. For one link, as shown in Figure 2.11, the equations of motion can be expressed in terms of local coordinates as

$$\begin{bmatrix} m_1 & 0 \\ 0 & m_2 \end{bmatrix} \begin{Bmatrix} \ddot{x}_1 \\ \ddot{x}_2 \end{Bmatrix} + k \begin{bmatrix} 1 & -1 \\ -1 & 1 \end{bmatrix} \begin{Bmatrix} x_1 \\ x_2 \end{Bmatrix} = \begin{Bmatrix} f_1 \\ f_2 \end{Bmatrix} \tag{2.16}$$

Representing the link in terms of global coordinates, as shown in Figure 2.12, the equation of motion is described by

$$\begin{bmatrix} m_1 & 0 & 0 & 0 \\ 0 & m_1 & 0 & 0 \\ 0 & 0 & m_2 & 0 \\ 0 & 0 & 0 & m_2 \end{bmatrix} \begin{Bmatrix} \ddot{x}_1 \\ \ddot{y}_1 \\ \ddot{x}_2 \\ \ddot{y}_2 \end{Bmatrix} + k \begin{bmatrix} c^2 & cs & -c^2 & -cs \\ cs & s^2 & -cs & -s^2 \\ -c^2 & -cs & c^2 & cs \\ -cs & -s^2 & cs & s^2 \end{bmatrix} \begin{Bmatrix} x_1 \\ y_1 \\ x_2 \\ y_2 \end{Bmatrix} = \begin{Bmatrix} f_{1x} \\ f_{1y} \\ f_{2x} \\ f_{2y} \end{Bmatrix} \tag{2.17}$$

where

$$c = \cos\theta \tag{2.18}$$

$$s = \sin\theta \tag{2.19}$$

Both Equation (2.16) and Equation (2.17) can also be represented in the matrix form:

$$\mathbf{m}\ddot{\mathbf{x}} + \mathbf{k}\mathbf{x} = \mathbf{f} \tag{2.20}$$

where the stiffness matrix ($\mathbf{k}$) in Equation (2.17) is obtained by the coordinate transformation. The transformation process can also be found in Appendix A.

After constructing equations of motion for each link, these matrix equations of motion can be expanded to full size. Then, they are assembled to form the structural equations of motion in the matrix form as

$$\mathbf{M}\ddot{\mathbf{X}} + \mathbf{K}\mathbf{X} = \mathbf{F} \tag{2.21}$$

The mass matrix ($\mathbf{M}$) is diagonal in this case. The stiffness matrix ($\mathbf{K}$) is symmetric and singular. In order to obtain a unique solution, the support boundary conditions need to be imposed on the free structure. In other words, if unsupported, the structure can have rigid body motions.

2.2.2 Solution of the Governing Differential Equations

Assume that sinusoidal external forces $\mathbf{F} = \mathbf{F}_1 \sin \omega t$ are exerted on the structure and the steady state response is of the form $\mathbf{X} = \mathbf{X}_1 \sin \omega t$, the matrix equations of motion or dynamic equilibrium equations become

$$\left(\mathbf{K} - \omega^2 \mathbf{M}\right) \mathbf{X}_1 = \mathbf{F}_1 \quad \text{or} \quad \mathbf{X}_1 = \left(\mathbf{K} - \omega^2 \mathbf{M}\right)^{-1} \mathbf{F}_1 \tag{2.22}$$

Instead of solving the inverse of a matrix, which is too expensive for large systems, the Gauss elimination method can be employed to solve the nodal displacements ($\mathbf{X}_1$) efficiently. Then, the internal force (f) for each link can be calculated by means of Hooke's law. For example, consider a typical link as shown in Figure 2.12, the equation can be written as

$$\left[(x_2 \cos\theta + y_2 \sin\theta) - (x_1 \cos\theta + y_1 \sin\theta)\right]\ k = f \tag{2.23}$$

In matrix form,

$$f = k \begin{pmatrix} \cos\theta & \sin\theta \end{pmatrix} \begin{pmatrix} x_2 - x_1 \\ y_2 - y_1 \end{pmatrix} \tag{2.24}$$

Finally, the strain and stress in each link will be obtained in a usual way as follows:

$$\epsilon = \frac{[(x_2\cos\theta + y_2\sin\theta) - (x_1\cos\theta + y_1\sin\theta)]}{L} \tag{2.25}$$

$$\sigma = E\epsilon \tag{2.26}$$

Moreover, frequencies and mode shapes can be calculated by solving the eigenproblem $\mathbf{K}\mathbf{X}_1 = \omega^2\mathbf{M}\mathbf{X}_1$.

2.3 Optimization Problem Formulation

A general problem of optimal structural design can be stated as one of choosing design variables subjected to certain design related constraints so that the objective function is minimized. The general form of the optimization problem is

$$\begin{array}{ll} \text{Find} & \mathbf{x} \\ \text{To minimize} & f(\mathbf{x}) \\ \text{Subject to} & \begin{cases} \mathbf{g}(\mathbf{x}) \leq \mathbf{0} \\ \mathbf{h}(\mathbf{x}) = \mathbf{0} \end{cases} \end{array} \tag{2.27}$$

where

$$\mathbf{x} = (x_1, x_2, \cdots, x_n)^T \tag{2.28}$$

$$\mathbf{g} = (g_1, g_2, \cdots, g_m)^T \tag{2.29}$$

$$\mathbf{h} = (h_1, h_2, \cdots, h_k)^T \tag{2.30}$$

The design variables $(\mathbf{x})$ may represent the member sizes, topology of the structure, geometric layout of the structure, or physical properties of the materials from a physical point of view. From a mathematical point of view, they can be continuous or discrete design variables. The objective (or merit) function (f) is a scalar function of the design variables $(\mathbf{x})$. Several objective functions have been used in the literature: for instance, the weight of the structure, the cost of the structure, energy expenditure, or any other criterion where some possible designs are preferred to others. In general, the objective function may represent the most important single property of a design, or it may represent a weighted sum of all important objective functions. In the latter case, it is called a multiobjective function. Weight is the most frequently used objective function in structural design for the reason that it is a readily quantifiable measure of merit. Although cost is more practically important than weight, it is often difficult to obtain sufficient data for the creation of a real cost objective function. Any set of values for the design variables represents a design of the structure.

The requirements that must be met in order to produce a feasible design are either inequality constraints $(\mathbf{g} \leq \mathbf{0})$ or equality constraints $(\mathbf{h} = \mathbf{0})$ from a mathematical point of view. Limitations on maximum (or allowable) stresses, displacements, or upper or lower bound on cross sectional areas are some examples of inequality constraints. On the other hand, examples of equality constraints include structural equilibrium equations, symmetry of nodes, and so on. From a physical point of view, constraints can be categorized into design (or side) constraints and behavior constraints. A design constraint is a specified limitation (upper or lower bound) on a design variable or a relationship which fixes the relative value of a group of design variables. Such constraints are explicit in form. Examples of design constraints include upper or lower bound on cross sectional areas, minimum thickness of a plate, or maximum height of a shell structure. Constraints imposed on behavior requirements are called behavior constraints. Limitations on maximum (or allowable) stresses, displacements, vibrational frequency, or buckling strength in structural design are all typical examples of behavior constraints. Behavior constraints could be either explicit or implicit in form. One of the examples for implicit behavior constraints is the limitations on maximum (or allowable) stresses if cross sectional areas are chosen to be the only design variables. Stresses depend on displacements which comes from the equilibrium equations, and displacements depend on the inverse stiffness matrix ($\mathbf{K}^{-1}$) which is a nonlinear and implicit function of the design variables. Consequently, stresses are also implicit function of the design variables in this case.

The optimization problem in this study can be formulated as follows

$$\begin{array}{ll} \text{Find} & \mathbf{A} \\ \text{To minimize} & W = \sum_{i=1}^{n} \rho_i A_i L_i \\ \text{Subject to} & \left\{ \begin{array}{c} \left(\mathbf{K} - \omega^2 \mathbf{M}\right) \mathbf{X} = \mathbf{F} \\ \boldsymbol{\sigma} \leq \boldsymbol{\sigma}_{allow} \\ \mathbf{A}_{lower} \leq \mathbf{A} \end{array} \right. \end{array} \tag{2.31}$$

where

$$\mathbf{A} = \left(A_1, A_2, \cdots, A_n\right)^T \tag{2.32}$$

$$\mathbf{X} = \left(d_1, d_2, \cdots, d_m\right)^T \tag{2.33}$$

$$\mathbf{F} = \left(F_1, F_2, \cdots, F_m\right)^T \tag{2.34}$$

$n \equiv$ number of links

$m \equiv$ number of equations

Cross sectional areas ($\mathbf{A}$) are chosen to be the design variables. Displacements ($\mathbf{X}$), which depend on the value of the design variables, are behavior variables. The weight (W) of the structure which depends on mass densities (ρ_i), lengths (L_i), and cross sectional areas (A_i) is used as the objective function. Dynamic equilibrium equations which consist of stiffness matrix ($\mathbf{K}$), mass matrix ($\mathbf{M}$), force vector ($\mathbf{F}$), and forcing frequency (ω) are the equality constraints. Inequality behavior constraints are imposed on stress in which calculated stresses ($\boldsymbol{\sigma}$) are not allowed to be greater than the allowable stresses $(\boldsymbol{\sigma}_{allow})$. The other inequality constraints which are design constraints are the lower bound $(\mathbf{A}_{lower})$ on the cross sectional areas $(\mathbf{A})$. The problem is a nonlinear optimization problem since stiffness matrix $(\mathbf{K})$ and mass matrix $(\mathbf{M})$, which multiplied by displacements and accelerations, respectively, are both functions of the cross sectional areas $(\mathbf{A})$.

The problem can be transformed into a simpler form "symbolically" in order that the only variables are the cross sectional areas. The displacements can be found symbolically by dynamic equilibrium equations as follows:

$$\mathbf{X} = \left(\mathbf{K} - \omega^2\mathbf{M}\right)^{-1}\mathbf{F} \tag{2.35}$$

Then, combined with the relations between stresses $(\boldsymbol{\sigma})$ and displacements $(\mathbf{X})$:

$$\boldsymbol{\sigma} = \mathbf{S}\mathbf{X} \tag{2.36}$$

where

$$\mathbf{S} \equiv \text{stress matrix}$$

The stresses can be obtained in the form

$$\boldsymbol{\sigma} = \mathbf{S}\left(\mathbf{K} - \omega^2\mathbf{M}\right)^{-1}\mathbf{F} \tag{2.37}$$

Consequently, the optimization problem formulation can be "symbolically" transformed into the following:

$$\begin{array}{ll} \text{Find} & \mathbf{A} \\ \text{To minimize} & W = \sum\limits_{i=1}^{n} \rho_i A_i L_i \\ \text{Subject to} & \left\{ \begin{array}{c} \mathbf{S}\left(\mathbf{K} - \omega^2\mathbf{M}\right)^{-1}\mathbf{F} \leq \boldsymbol{\sigma}_{allow} \\ \mathbf{A}_{lower} \leq \mathbf{A} \end{array} \right. \end{array} \tag{2.38}$$

As for large-scale problems, it is not practical to construct the inequality constraints in this fashion, although the equality constraints are eliminated in the transformation and it results in fewer variables than the previous form. Furthermore, the transformed formulation is still a nonlinear programming problem.

In summary, the equality constraints should not be eliminated in the problem formulation, and the first formulation will be used throughout this study. In addition, the first formulation can be easily expressed and implemented by using the decomposition technique which will be presented in the next chapter.

Table 2.1: Natural frequencies calculated by both lumped and consistent mass matrix approaches for the length of 10 feet bar

Lumped Mass				Consistent Mass			
Element	$(\omega_n)_1$	$(\omega_n)_2$	$(\omega_n)_3$	Element	$(\omega_n)_1$	$(\omega_n)_2$	$(\omega_n)_3$
1	2384.16	****	****	1	2919.99	****	****
2	2580.59	6230.11	****	2	2716.61	9490.19	****
3	2617.99	7152.47	9770.46	3	2678.48	8759.96	15891.84
4	2631.15	7492.88	11213.89	4	2665.18	8407.69	15272.83
5	2637.26	7653.62	11920.79	5	2659.04	8240.69	14599.93
10	2645.41	7871.10	12902.97	10	2650.86	8018.10	13583.06
15	2646.92	7911.77	13089.94	15	2649.34	7977.11	13392.39
20	2647.45	7926.04	13155.76	20	2648.81	7962.79	13325.90
25	2647.70	7932.65	13186.29	25	2648.57	7956.17	13295.19
30	2647.83	7936.24	13202.89	30	2648.44	7952.57	13278.51
35	2647.91	7938.40	13212.91	35	2648.36	7950.40	13268.47
40	2647.96	7939.81	13219.41	40	2648.30	7949.00	13261.95
45	2648.00	7940.77	13223.87	45	2648.27	7948.03	13257.48
50	2648.03	7941.46	13227.06	50	2648.24	7947.34	13254.29
55	2648.04	7941.97	13229.42	55	2648.22	7946.83	13251.92
60	2648.06	7942.36	13231.22	60	2648.21	7946.44	13250.13
65	2648.07	7942.66	13232.62	65	2648.20	7946.14	13248.73
70	2648.08	7942.90	13233.73	70	2648.19	7945.90	13247.62
75	2648.09	7943.10	13234.62	75	2648.18	7945.71	13246.72
80	2648.09	7943.25	13235.35	80	2648.18	7945.55	13245.99
85	2648.10	7943.38	13235.96	85	2648.17	7945.42	13245.38
90	2648.10	7943.49	13236.47	90	2648.17	7945.31	13244.87
95	2648.10	7943.59	13236.90	95	2648.16	7945.22	13244.44
100	2648.11	7943.67	13237.27	100	2648.16	7945.14	13244.07

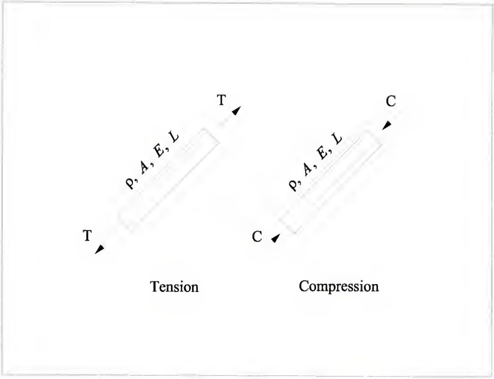

Figure 2.1: Typical members of a truss

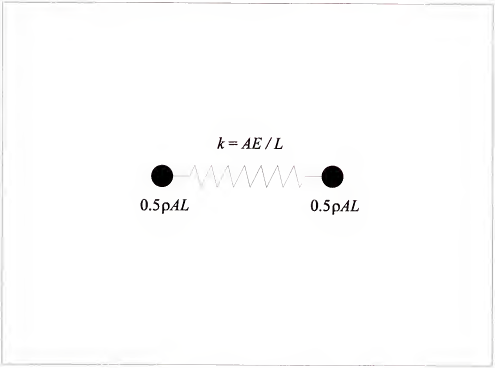

Figure 2.2: A simple half-half mass model

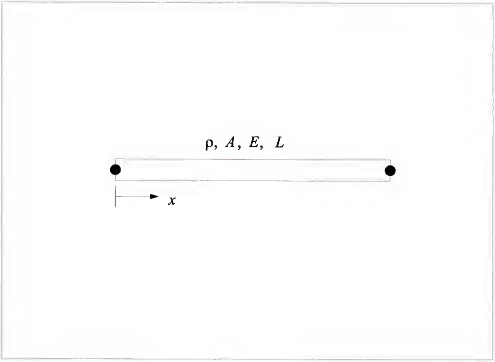

Figure 2.3: Consistent mass model

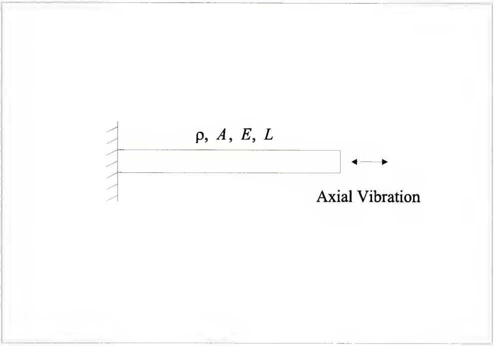

Figure 2.4: Axially oscillating bar fixed at one end

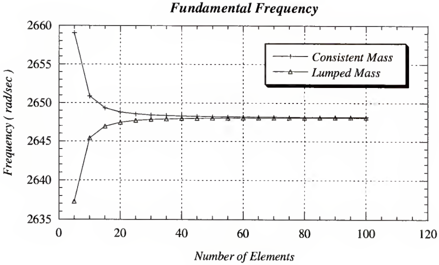

Figure 2.5: Comparison of the fundamental frequency between consistent and lumped mass models

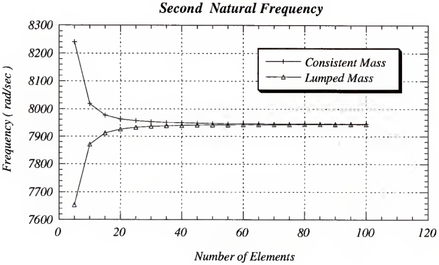

Figure 2.6: Comparison of the second natural frequency between consistent and lumped mass models

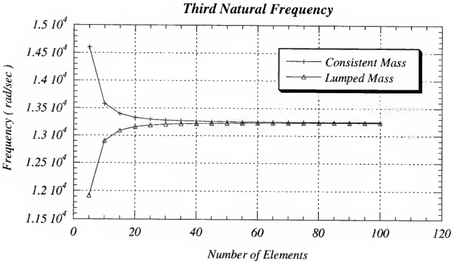

Figure 2.7: Comparison of the third natural frequency between consistent and lumped mass models

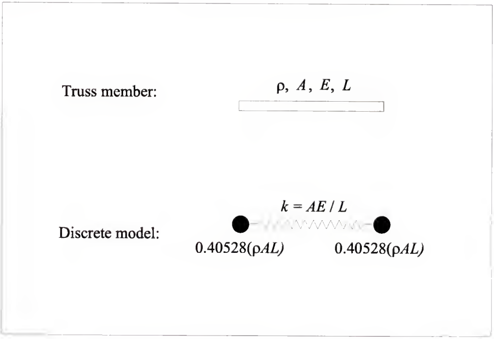

Figure 2.8: Typical truss member and discrete mass model

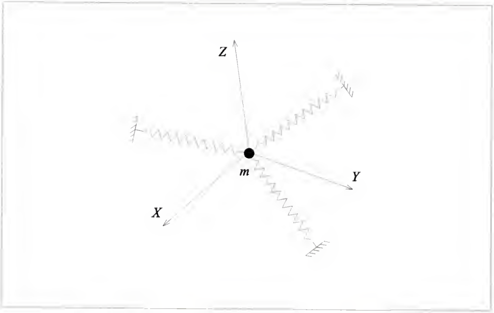

Figure 2.9: A single particle suspended by N springs

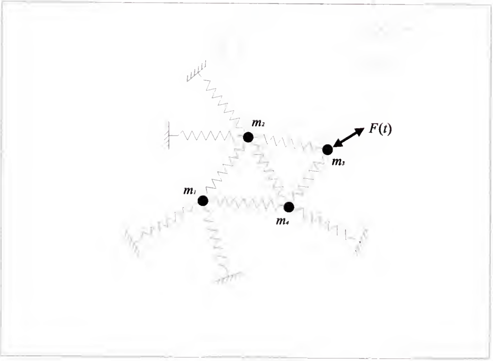

Figure 2.10: Elastically connected system of masses

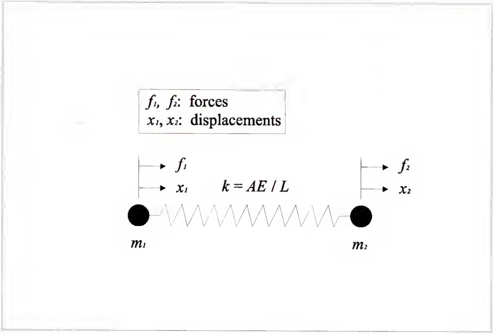

Figure 2.11: Local coordinates for a generic link

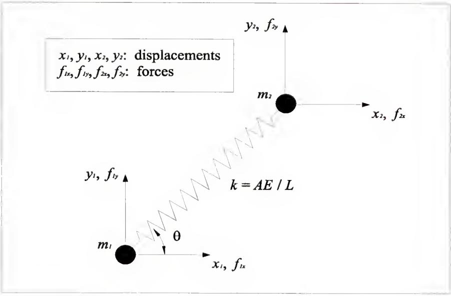

Figure 2.12: Global coordinates for a generic link

CHAPTER 3
SOLUTION ALGORITHM BY THE SUCCESSIVE ITERATION APPROACH

In this chapter, the successive iteration approach will be introduced first. Following that, the solution algorithm by using this approach will be stated and flowcharted. Finally, several example problems which have been tested will be illustrated.

3.1 The Essence of the Optimization Problem

The optimization problem formulation in the previous chapter is classified as nonlinear programming (NLP) problem on account of the nonlinearity of the structural dynamic equilibrium equations. The mass and stiffness matrices ($\mathbf{M}$ and $\mathbf{K}$, respectively) are both functions of the cross sectional areas of the links. Being multiplied by the acceleration vector ($\ddot{\mathbf{X}}$) and the displacement vector ($\mathbf{X}$), respectively, makes this equality constraint nonlinear in essence.

However, the problem can be decomposed into a set of linear problems by the successive iteration approach. This chapter proposes a simple and efficient solution algorithm by the successive iteration approach which overcomes the difficulties of using a nonlinear programming approach to solve the problem directly. The solution algorithm by the nonlinear programming approach will be addressed in Chapter 5 for comparison.

3.2 Successive Iteration Approach

The basic idea of the successive iteration approach is to transform a nonlinear programming (NLP) problem into a set of linear optimization problems. The problem can be decomposed into a linear problem by assuming the cross sectional areas, solving for the displacements, and then calculating new areas based on the allowable stresses including the buckling critical stresses. The process is iterated until convergence occurs.

The minimization problem is defined mathematically in the previous chapter and restated as follows:

$$
\begin{array}{ll}
\text{Find} & \mathbf{A} \\
\text{To minimize} & W = \sum_{i=1}^{n} \rho_i A_i L_i \\
\text{Subject to} & \left\{ \begin{array}{c} \left(\mathbf{K} - \omega^2 \mathbf{M}\right) \mathbf{X} = \mathbf{F} \\ \boldsymbol{\sigma} \leq \boldsymbol{\sigma}_{allow} \\ \mathbf{A}_{lower} \leq \mathbf{A} \end{array} \right.
\end{array}
\tag{3.1}
$$

where

$$\mathbf{A} = (A_1, A_2, \cdots, A_n)^T \tag{3.2}$$

$$\mathbf{X} = (d_1, d_2, \cdots, d_m)^T \tag{3.3}$$

$$\mathbf{F} = (F_1, F_2, \cdots, F_m)^T \tag{3.4}$$

$n \equiv$ number of links

$m \equiv$ number of equations

The decomposition is done by separating the constraints into two categories. The equality constraints are solved separately from the inequality constraints. Equality constraints of equilibrium are solved first; then, the cross sectional areas are minimized by scaling the areas of the links to be "fully stressed." After scaling to obtain the new cross sectional areas, called $\mathbf{A}_{new}$, the mass matrix $(\mathbf{M})$ and stiffness matrix $(\mathbf{K})$ are formulated. Subsequently, the equality constraints of equilibrium are solved again for the nodal displacements $(\mathbf{X})$ and the internal forces $(\mathbf{f})$.

In the first level, the equality constraints of equilibrium are solved by the Gauss elimination method. This technique is itself essentially a decomposition technique and described in the book by Chvátal [63]. In the second level, the cross sectional areas are scaled to their allowable stresses, which can be the compression including buckling or the tension limit. The internal forces $(\mathbf{f})$ of the links, solved in the first level, are used to decompose the links by the sign of the internal forces into two types, compressed and tensioned links. This is the second decomposition, and this partitioning of the links according to their state is used to scale the cross sectional areas as follows:

$$(A_i)_{new} = \frac{f_i}{\sigma_{allow}} \tag{3.5}$$

The process of analysis and scaling is repeated until either the stress reaches the allowable values in all links or no further weight reduction is possible. The decomposition combined with solving the problem in two levels converts the problem from nonlinear to two linear problems. This is the main feature of decomposition in this type of structural optimization that allows very large problem to be solved efficiently and easily.

To summarize, the solution algorithm by the successive iteration approach can be stated and flowcharted as follows:

(1) Assume initial cross sectional areas $(\mathbf{A}_0)$.

(2) Formulate the mass matrix $(\mathbf{M})$ and stiffness matrix $(\mathbf{K})$ automatically by displacement (or stiffness) method.

(3) Calculate nodal displacements $(\mathbf{X})$ by the Gauss elimination method, then find the internal forces $(\mathbf{f})$ and stresses $(\boldsymbol{\sigma})$.

(4) Find new cross sectional areas $(\mathbf{A}_{new})$ from the internal forces $(\mathbf{f})$, allowable stresses $(\boldsymbol{\sigma}_{allow})$, and buckling critical stresses $(\boldsymbol{\sigma}_b)$ for the compressioned members.

(5) Repeat from step (1) until either the structure is fully stressed or no further weight reduction is possible.

A flowchart of the solution algorithm by the successive iteration approach showing the basic steps of the process can be found in Figure 3.1.

3.3 Illustrative Problems for the Successive Iteration Approach

The program used is implemented in both Fortran language and MATLAB* environment, and it is designed for a 3-D model. Therefore, the actual CPU time of a 2-D version should be even shorter than those given here.

3.3.1 Simple Three-Link Truss

The simple three-link truss, shown in Figure 3.2, is disturbed by a nodal sinusoidal external force with the amplitude (F) and forcing frequency (ω). Each link has a cross sectional area (A_i), modulus of elasticity (E_i), and specific weight (γ_i). Each link has length (L) since this is an equilateral triangle. Each node will be displaced (x_i, y_i) due to the disturbance exerted on the structure. The numerical data used are as follows:

$$\gamma = \gamma_1 = \gamma_2 = \gamma_3 = 0.283241\,\mathrm{lb/in^3} \tag{3.6}$$

$$E = E_1 = E_2 = E_3 = 30,000\,\mathrm{ksi} \tag{3.7}$$

$$A_{lower} = 0.1\,\mathrm{in^2} \quad \text{(lower bound)} \tag{3.8}$$

$$\sigma^t_{allow} = 20\,\mathrm{ksi} \tag{3.9}$$

$$\sigma^c_{allow} = -20\,\mathrm{ksi} \tag{3.10}$$

$$F = 50\,\mathrm{ksi} \tag{3.11}$$

$$L = 5', 6', \cdots, 10' \tag{3.12}$$

$$\omega = 0, 100, 200, \cdots\ \mathrm{rad/sec} \tag{3.13}$$

By the successive iteration approach, optimum volumes for different length and forcing frequency cases are shown in Table 3.1. The table also gives an approximate indication of the fundamental natural frequency of the structure for the different lengths. The fundamental frequency (ω_n) for each case is also calculated by solving the eigenproblem and listed in Table 3.1. A more detailed result of 10 ft length is shown in Table 3.2 where the natural frequencies (by solving the eigenproblem), displacements at the top node, stresses in each link, and optimum volume for different forcing frequencies are tabulated. It is observed that the stress in each link reaches the allowable stress level, that is, fully stressed, for most cases. The required cross sectional area for each link versus the number of iterations for some typical forcing frequencies for the case of 10 ft length can be found in Figure 3.3 to Figure 3.6, showing the fast convergence. An interesting point worth mentioning is that in observing Figure 3.7 to Figure 3.12, the number of iterations is found to be dependent on the initial values of cross sectional areas. As would be expected, the closer the values chosen for the initial cross sectional areas to the solution, the faster the convergence is. This result proves that the convergence rate will be improved by appropriately choosing initial values of cross sectional areas.

---

* MATLAB is a registered trademark of The MathWorks, Inc.

The displacements at the top node and stress in each link versus the number of iterations for some typical forcing frequencies for the case of 10 ft length are shown in Figure 3.13 to Figure 3.20. The fast convergence rate by using the successive iteration approach is also demonstrated.

The optimum volume ratios between the static and dynamic loading for a wide range of forcing frequencies are shown in Figure 3.21. It can be observed that the resonant frequency is approximately at 1184.29 rad/sec. For the cases of forcing frequencies higher than 1400 rad/sec, using the successive iteration approach alone seemingly could not find convergent results; however, this situation can be well remedied by incorporating the linear programming approach, which will be discussed in the next chapter. The non-convergent situations exhibit oscillatory behavior of the weight during iteration when using successive iteration approach alone. A reasonable explanation is the alternatively increasing and decreasing nature of the stresses ($\boldsymbol{\sigma}$)

and cross sectional areas (**A**) during each successive iteration for a specific higher forcing frequency, since the forces (**F**) are invariant.

Another design variable can also be shown to improve the performance. Figure 3.22 shows the optimum volume ratios versus discrete values of added mass for the condition where forcing frequency (ω) equals the natural frequency of the original structure. The discrete mass ratio can be defined as a multiplier of the joint mass of the structure itself. It can be seen that if masses are added at each joint, the optimum volume can be significantly reduced at the point of resonant frequency.

3.3.2 Forty-Seven-Member Tower

Figure 3.23 shows the considered structure and its dimension with the external oscillatory forces applied on its nodes 17 and 22. This example of forty-seven-member tower has been used in many publications for the case of static loadings [8,11,64,65]. The numerical data used are as follows:

$$\gamma = 0.3\,\mathrm{lb/in}^3 \tag{3.14}$$

$$E = 30 \times 10^4\,\mathrm{ksi} \tag{3.15}$$

$$A_{lower} = 0.1\,\mathrm{in}^2 \quad \text{(lower bound)} \tag{3.16}$$

$$\sigma^t_{allow} = 20\,\mathrm{ksi} \tag{3.17}$$

$$\sigma^c_{allow} = -15\,\mathrm{ksi} \tag{3.18}$$

$$|F_x| = 6\,\mathrm{kips} \tag{3.19}$$

$$|F_y| = 14\,\mathrm{kips} \tag{3.20}$$

Results of minimum weight, CPU time, cross sectional area and stress in each link, and displacements in x and y directions of each node are shown in Table 3.3 to Table 3.12 for several forcing frequencies. As stated in the previous example that the convergence rate will be improved by appropriately choosing initial values of design variables, the initial cross sectional areas of each frequency case here are chosen to be the calculated cross sectional areas from the previous lower frequency case. As would be expected, the results show faster convergence rate if the calculated cross sectional areas from the previous lower frequency are used as an initial guess. From Table 3.3 to Table 3.12, it is shown that the allowable stresses have been reached for most of the cases except for some low stressed members. The stresses in these members is further addressed in Chapter 5 when nonlinear programming approach is discussed. Two optimum designs for $\omega = 50$ rad/sec and $\omega = 200$ rad/sec are shown in Figure 3.24 and Figure 3.25, respectively. Figure 3.26 represents the optimum volume ratio for a range of forcing frequencies. It is found that for forcing frequencies higher than 220 rad/sec, some convergence problem still exists if the successive iteration approach alone is used. This situation which is similar to the three-link truss will also be discussed in the next chapter. Otherwise for the lower frequency cases, the convergence is rapidly achieved. Using Pentium II 333 MH_z personal computer, the CPU time is approximately 0.065 sec per iteration, which is fast for a relatively large structure such as the one considered in this example.

3.3.3 Two-Hundred-Member Structure

The two-hundred-member large structure and its dimension with applied loadings is shown in Figure 3.27. This example has been presented by several authors [8, 11, 66, 67] and is one of the largest scale problems found in the literature regarding the number of design variables. However, all of these publications were dealing with static loadings. The numerical data used are as follows:

$$\gamma = 0.283\,\mathrm{lb/in^3} \tag{3.21}$$

$$E = 30 \times 10^4\,\mathrm{ksi} \tag{3.22}$$

$$A_{lower} = 0.1\,\mathrm{in^2} \quad \text{(lower bound)} \tag{3.23}$$

$$\sigma^t_{allow} = 30\,\mathrm{ksi} \tag{3.24}$$

$$\sigma^c_{allow} = -30\,\mathrm{ksi} \tag{3.25}$$

$$|F_x| = 1\,\mathrm{kip} \tag{3.26}$$

$$|F_y| = 10\,\mathrm{kips} \tag{3.27}$$

Detailed results of cross sectional area and stress in each link, displacements in x and y directions of each node, minimum weight, and CPU time are shown in Table 3.13 to Table 3.24 for several forcing frequencies. It is also shown that the allowable stresses have been reached for most of the cases except for some low stressed members. The stresses of these members need to be further addressed in Chapter 5 when nonlinear programming approach is discussed. Two optimum designs for ω = 20 rad/sec and ω = 80 rad/sec are shown in Figure 3.28 and Figure 3.29, respectively. Figure 3.30 represents the optimum volume ratio of the two-hundred-member structure for a range of forcing frequencies. It is found that for forcing frequencies higher than 80 rad/sec, some convergence problems still exist if the successive iteration approach alone is used. This situation which is similar to previous cases will also be discussed in Chapter 4. Otherwise for the lower frequency cases, the convergence is rapidly achieved. Using Pentium II 333 $\mathrm{MH_z}$ personal computer, the CPU time is approximately 0.33 sec per iteration, which is reasonably fast for a relatively large structure as the one considered in this example.

Table 3.1: Optimum volumes of the three-link truss for different lengths and excitation frequencies

ω	$L = 5$’	$L = 6$’	$L = 7$’	$L = 8$’	$L = 9$’	$L = 10$’
0	375.00	450.00	525.00	600.00	675.00	750.00
100	375.76	451.31	527.09	603.12	679.44	756.11
200	378.05	455.29	533.44	612.65	693.10	774.97
300	381.93	462.07	544.33	629.16	717.00	808.39
400	387.49	471.87	560.28	653.67	753.09	859.81
500	394.85	485.03	582.08	687.85	804.63	935.34
600	404.20	502.06	610.91	734.30	877.03	1045.75
700	415.77	523.64	648.51	797.12	979.48	1211.25
800	429.91	550.73	697.48	882.96	1128.59	1473.51
900	447.02	584.68	761.82	1003.20	1357.20	1933.35
1000	467.67	627.45	847.88	1178.81	1740.02	2911.13
1100	492.61	681.90	966.40	1453.02	2490.54	6248.76
1200	522.88	752.40	1136.90	1930.86	4559.97	33124.28
1300	559.88	845.95	1398.94	2950.61	32862.93	4471.36
1400	605.63	974.49	1846.37	6534.76	6159.25	2402.27
1500	663.09	1160.01	2768.85	26499.42	2809.51	****
1600	736.76	1448.14	5717.92	4327.08	1829.07	****
1700	833.85	1951.19	63870.84	2355.67	****	****
1800	966.68	3039.98	4790.53	1625.79	****	****
1900	1158.05	7094.90	2484.73	****	****	****
2000	1455.56	19874.57	1681.59	****	****	****
2100	1977.75	4106.17	****	****	****	****
2200	3124.38	2286.78	****	****	****	****
2300	7626.94	1587.18	****	****	****	****
2400	16562.14	1219.34	****	****	****	****
2500	3944.67	****	****	****	****	****
2600	2235.68	****	****	****	****	****
2700	1560.84	****	****	****	****	****
2800	1201.13	****	****	****	****	****
2900	978.78	****	****	****	****	****
3000	****	****	****	****	****	****
ω_n	2368.59	1973.82	1691.85	1480.37	1315.88	1184.29

Table 3.2: Optimum results of the three-link truss for a wide range of frequencies for $L = 10$'

ω (rad/sec)	$(\omega_n)_1$ (rad/sec)	X_3 (in)	Y_3 (in)	σ_1 (psi)	σ_2 (psi)	σ_3 (psi)	A_1 (in^2)	A_2 (in^2)	A_3 (in^2)	Mini. Vol. (in^3)
0.00	1061.53	0.2000	-0.0231	20000.00	-20000.00	20000.00	1.2500	2.5000	2.5000	750.00
100.00	1062.68	0.2000	-0.0231	20000.00	-20000.00	20000.00	1.2650	2.5191	2.5168	756.11
200.00	1066.09	0.2000	-0.0231	20000.00	-20000.00	20000.00	1.3113	2.5783	2.5685	774.97
300.00	1071.69	0.2000	-0.0231	20000.00	-20000.00	20000.00	1.3937	2.6829	2.6600	808.39
400.00	1079.37	0.2000	-0.0231	20000.01	-20000.00	20000.00	1.5213	2.8434	2.8005	859.82
500.00	1088.94	0.2000	-0.0231	20000.06	-20000.04	20000.01	1.7099	3.0784	3.0061	935.33
600.00	1100.19	0.2000	-0.0231	20000.34	-20000.22	20000.04	1.9880	3.4208	3.3057	1045.74
700.00	1112.88	0.2000	-0.0231	20001.57	-20001.10	20000.25	2.4088	3.9317	3.7529	1211.21
800.00	1126.71	0.2000	-0.0231	20006.32	-20004.69	20001.31	3.0820	4.7372	4.4581	1473.28
900.00	1141.35	0.2001	-0.0231	20023.60	-20018.72	20006.62	4.2724	6.1407	5.6881	1932.14
1000.00	1156.46	0.2006	-0.0233	20089.09	-20075.94	20035.73	6.8157	9.0987	8.2851	2903.94
1100.00	1171.67	0.2000	-0.0231	20000.00	-20000.00	20000.00	15.6523	19.2577	17.1630	6248.76
1150.00	1179.19	0.2013	-0.0233	20147.22	-20142.27	20119.93	39.3115	46.3321	40.8815	15183.01
1180.00	1183.66	0.2143	-0.0248	21444.99	-21438.27	21404.99	306.5834	351.8209	308.4507	116022.60
1184.29	1184.29	-0.4324	0.0500	-43264.17	43257.81	-43222.22	13380.1118	15293.1954	13388.6661	5047436.80
1190.00	1185.13	-0.1888	0.0219	-18896.28	18889.86	-18857.07	252.3322	286.9605	251.0447	94840.49
1200.00	1186.61	-0.1955	0.0227	-19571.18	19563.98	-19526.00	90.0738	101.5065	88.6103	33622.87
1250.00	1193.86	-0.1983	0.0231	-19869.33	19858.54	-19791.01	21.9933	23.6569	20.4281	7929.40
1270.00	1196.70	-0.1985	0.0232	-19892.53	19879.95	-19795.27	17.0720	18.0155	15.4893	6069.22
1290.00	1199.51	-0.1985	0.0232	-19908.49	19893.87	-19787.62	14.0241	14.5146	12.4256	4915.72
1300.00	1200.90	-0.1985	0.0233	-19915.22	19899.46	-19780.41	12.8985	13.2192	11.2926	4489.24
1350.00	1207.69	-0.1984	0.0235	-19947.33	19924.59	-19713.26	9.3293	9.0934	7.6887	3133.37
1400.00	1214.20	-0.1982	0.0240	-19993.96	19961.50	-19581.86	7.4398	6.8840	5.7682	2411.04
1450.00	1220.37	-0.1979	0.0246	-20071.88	20025.89	-19401.52	6.2816	5.5070	4.5768	1963.85

Table 3.3: Optimum results of the forty-seven-member tower for $\omega = 0$

Forty-Seven-Member Tower (Force Excitation)								
Static case ($\omega = 0$)			No mass added and No L.P.					
$A_0 = 0.1\,\text{in}^2$			Modify C.S.A. of all members					
Link	Area (in^2)	Stress (psi)	Link	Area (in^2)	Stress (psi)	Displacements (in)		
						node	x-dir	y-dir
1	0.8979	20000.00	26	1.7000	20000.00	1	0.0000	0.0000
2	2.8028	-15000.00	27	1.3728	20000.00	2	0.0000	0.0000
3	0.4293	20000.00	28	0.1000	-14999.99	3	0.0200	0.0080
4	1.8276	-15000.00	29	0.9934	20000.00	4	0.0220	-0.0060
5	0.2858	20000.00	30	3.1476	-15000.00	5	0.0560	0.0160
6	0.7503	-15000.00	31	0.9340	-15000.00	6	0.0539	-0.0120
7	0.3272	20000.00	32	0.3812	20000.00	7	0.0980	0.0240
8	0.1000	20000.00	33	0.1742	19999.99	8	0.1060	-0.0180
9	0.9980	-15000.00	34	0.5357	20000.00	9	0.1210	0.0175
10	1.5972	-15000.00	35	3.2858	-15000.00	10	0.1180	-0.0158
11	2.0870	-15000.00	36	0.7981	20000.00	11	0.1613	0.0215
12	2.0870	-15000.00	37	0.1000	-10088.88	12	0.1653	-0.0188
13	0.2728	20000.00	38	0.1000	-5177.75	13	0.2155	0.0255
14	0.4362	-15000.00	39	1.6384	20000.00	14	0.2125	-0.0218
15	0.4627	20000.00	40	3.4154	-15000.00	15	0.2455	0.0780
16	0.5144	-15000.00	41	0.1000	17411.32	16	0.2420	-0.0882
17	2.0870	-15000.00	42	1.0153	-15000.01	17	0.2618	0.1030
18	2.0870	-15000.00	43	0.1000	5000.38	18	0.2658	0.0780
19	0.1000	0.00	44	1.7866	19999.99	19	0.2698	0.0295
20	0.1000	0.00	45	4.8179	-15000.00	20	0.2738	-0.0248
21	0.1000	0.00	46	0.7261	20000.03	21	0.2778	-0.0882
22	0.1000	0.00	47	0.1632	-14999.85	22	0.2818	-0.1752
23	1.1000	20000.00						
24	1.7000	20000.00						
25	1.1000	20000.00						

	ω_n (rad/sec)		
1	193.30		
2	485.42	Minimum Weight	1379.51 lb
3	872.47	CPU Time	3.064 sec

Table 3.4: Optimum results of the forty-seven-member tower for $\omega = 10$ rad/sec

Forty-Seven-Member Tower (Force Excitation)								
$\omega = 10$ rad/sec			No mass added and No L.P.					
$A_0 = (A)_{\omega=0}$			Modify C.S.A. of all members					
Link	Area (in^2)	Stress (psi)	Link	Area (in^2)	Stress (psi)	Displacements (in)		
						node	x-dir	y-dir
1	0.9004	20000.00	26	1.7003	20000.00	1	0.0000	0.0000
2	2.8068	-15000.00	27	1.3729	20000.00	2	0.0000	0.0000
3	0.4312	20000.00	28	0.1000	-14999.99	3	0.0200	0.0080
4	1.8294	-15000.00	29	0.9967	20000.00	4	0.0220	-0.0060
5	0.2869	20000.00	30	3.1517	-15000.00	5	0.0560	0.0160
6	0.7511	-15000.00	31	0.9354	-15000.00	6	0.0539	-0.0120
7	0.3273	20000.00	32	0.3820	20000.00	7	0.0980	0.0240
8	0.1003	20000.00	33	0.1736	19999.99	8	0.1060	-0.0180
9	0.9996	-15000.00	34	0.5380	20000.00	9	0.1210	0.0175
10	1.5969	-15000.00	35	3.2910	-15000.00	10	0.1180	-0.0158
11	2.0869	-15000.00	36	0.8002	20000.00	11	0.1613	0.0215
12	2.0872	-15000.00	37	0.1000	-10084.65	12	0.1653	-0.0188
13	0.2733	20000.00	38	0.1000	-5169.28	13	0.2155	0.0255
14	0.4370	-15000.00	39	1.6439	20000.00	14	0.2125	-0.0218
15	0.4634	20000.00	40	3.4207	-15000.00	15	0.2455	0.0780
16	0.5153	-15000.00	41	0.1000	17415.54	16	0.2420	-0.0883
17	2.0869	-15000.00	42	1.0183	-15000.01	17	0.2618	0.1030
18	2.0872	-15000.00	43	0.1000	5000.35	18	0.2658	0.0780
19	0.1000	-24.16	44	1.7921	19999.99	19	0.2698	0.0295
20	0.1000	27.76	45	4.8275	-15000.00	20	0.2738	-0.0248
21	0.1000	3.31	46	0.7285	20000.03	21	0.2778	-0.0883
22	0.1000	-5.75	47	0.1633	-14999.86	22	0.2818	-0.1752
23	1.0998	20000.00						
24	1.7002	20000.00						
25	1.0998	20000.00						

	ω_n (rad/sec)		
1	193.51		
2	485.80	Minimum Weight	1381.65 lb
3	872.61	CPU Time	0.981 sec

Table 3.5: Optimum results of the forty-seven-member tower for $\omega = 30$ rad/sec

Forty-Seven-Member Tower (Force Excitation)								
$\omega = 30$ rad/sec			No mass added and No L.P.					
$A_0 = (A)_{\omega=20}$			Modify C.S.A. of all members					
Link	Area (in^2)	Stress (psi)	Link	Area (in^2)	Stress (psi)	Displacements (in)		
						node	x-dir	y-dir
1	0.9209	20000.00	26	1.7030	20000.00	1	0.0000	0.0000
2	2.8384	-15000.00	27	1.3732	20000.00	2	0.0000	0.0000
3	0.4464	20000.00	28	0.1000	-14999.99	3	0.0200	0.0080
4	1.8440	-15000.00	29	1.0227	20000.00	4	0.0220	-0.0060
5	0.2956	20000.00	30	3.1853	-15000.00	5	0.0560	0.0160
6	0.7575	-15000.00	31	0.9467	-15000.00	6	0.0540	-0.0120
7	0.3285	20000.00	32	0.3882	20000.00	7	0.0980	0.0240
8	0.1030	20000.00	33	0.1685	19999.99	8	0.1060	-0.0180
9	1.0118	-15000.00	34	0.5565	20000.00	9	0.1210	0.0175
10	1.5946	-15000.00	35	3.3330	-15000.00	10	0.1180	-0.0158
11	2.0862	-15000.00	36	0.8175	20000.00	11	0.1613	0.0215
12	2.0890	-15000.00	37	0.1000	-10050.32	12	0.1653	-0.0188
13	0.2775	20000.00	38	0.1000	-5100.64	13	0.2155	0.0255
14	0.4434	-15000.00	39	1.6878	20000.00	14	0.2125	-0.0218
15	0.4693	20000.00	40	3.4628	-15000.00	15	0.2455	0.0781
16	0.5221	-15000.00	41	0.1000	17449.87	16	0.2420	-0.0883
17	2.0861	-15000.00	42	1.0429	-15000.01	17	0.2618	0.1030
18	2.0888	-15000.00	43	0.1000	5000.37	18	0.2658	0.0781
19	0.1000	-217.45	44	1.8364	19999.99	19	0.2698	0.0295
20	0.1000	250.15	45	4.9050	-15000.00	20	0.2738	-0.0248
21	0.1000	29.80	46	0.7474	20000.03	21	0.2778	-0.0883
22	0.1000	-51.85	47	0.1637	-14999.85	22	0.2818	-0.1752
23	1.0986	20000.00						
24	1.7022	20000.00						
25	1.0981	20000.00						

	ω_n (rad/sec)		
1	195.22		
2	488.80	Minimum Weight	1398.81 lb
3	873.62	CPU Time	1.282 sec

Table 3.6: Optimum results of the forty-seven-member tower for $\omega = 50$ rad/sec

Forty-Seven-Member Tower (Force Excitation)								
$\omega = 50$ rad/sec			No mass added and No L.P.					
$A_0 = (A)_{\omega=40}$			Modify C.S.A. of all members					
Link	Area (in^2)	Stress (psi)	Link	Area (in^2)	Stress (psi)	Displacements (in)		
						node	x-dir	y-dir
1	0.9619	20000.00	26	1.7083	20000.00	1	0.0000	0.0000
2	2.9023	-15000.00	27	1.3740	20000.00	2	0.0000	0.0000
3	0.4769	20000.00	28	0.1000	-14999.99	3	0.0200	0.0080
4	1.8733	-15000.00	29	1.0753	20000.00	4	0.0220	-0.0060
5	0.3136	20000.00	30	3.2528	-15000.00	5	0.0560	0.0160
6	0.7699	-15000.00	31	0.9696	-15000.00	6	0.0540	-0.0120
7	0.3307	20000.00	32	0.4004	20000.00	7	0.0980	0.0240
8	0.1082	20000.00	33	0.1584	19999.99	8	0.1060	-0.0180
9	1.0365	-15000.00	34	0.5939	20000.00	9	0.1210	0.0175
10	1.5899	-15000.00	35	3.4181	-15000.00	10	0.1180	-0.0158
11	2.0847	-15000.00	36	0.8528	20000.00	11	0.1613	0.0215
12	2.0925	-15000.00	37	0.1000	-9979.15	12	0.1653	-0.0188
13	0.2858	20000.00	38	0.1000	-4958.28	13	0.2155	0.0255
14	0.4561	-15000.00	39	1.7769	20000.00	14	0.2125	-0.0218
15	0.4812	20000.00	40	3.5483	-15000.00	15	0.2456	0.0782
16	0.5358	-15000.00	41	0.1000	17521.17	16	0.2421	-0.0884
17	2.0845	-15000.00	42	1.0929	-15000.01	17	0.2618	0.1030
18	2.0920	-15000.00	43	0.1000	5000.60	18	0.2658	0.0782
19	0.1000	-603.84	44	1.9264	19999.99	19	0.2698	0.0295
20	0.1000	696.69	45	5.0626	-15000.01	20	0.2738	-0.0248
21	0.1000	82.67	46	0.7860	20000.05	21	0.2778	-0.0884
22	0.1000	-144.61	47	0.1647	-14999.76	22	0.2818	-0.1752
23	1.0962	20000.00						
24	1.7060	20000.00						
25	1.0948	20000.00						

	ω_n (rad/sec)		
1	198.56		
2	494.59	Minimum Weight	1433.61 lb
3	874.98	CPU Time	1.272 sec

Table 3.7: Optimum results of the forty-seven-member tower for ω = 80 rad/sec

Forty-Seven-Member Tower (Force Excitation)								
ω = 80 rad/sec			No mass added and No L.P.					
$A_0 = (A)_{\omega=70}$			Modify C.S.A. of all members					
Link	Area (in^2)	Stress (psi)	Link	Area (in^2)	Stress (psi)	Displacements (in)		
						node	x-dir	y-dir
1	1.0617	20000.00	26	1.7214	20000.00	1	0.0000	0.0000
2	3.0628	-15000.00	27	1.3759	20000.00	2	0.0000	0.0000
3	0.5524	20000.00	28	0.1000	-14999.98	3	0.0200	0.0080
4	1.9450	-15000.00	29	1.2068	20000.00	4	0.0220	-0.0060
5	0.3608	20000.00	30	3.4193	-15000.00	5	0.0560	0.0160
6	0.7982	-15000.00	31	1.0279	-15000.00	6	0.0542	-0.0120
7	0.3346	20000.00	32	0.4288	20000.00	7	0.0980	0.0240
8	0.1209	20000.00	33	0.1333	19999.98	8	0.1060	-0.0180
9	1.0982	-15000.00	34	0.6871	19999.99	9	0.1210	0.0175
10	1.5781	-15000.00	35	3.6317	-15000.00	10	0.1180	-0.0158
11	2.0810	-15000.00	36	0.9422	20000.00	11	0.1613	0.0215
12	2.1012	-15000.00	37	0.1000	-9790.79	12	0.1653	-0.0188
13	0.3061	20000.00	38	0.1000	-4581.53	13	0.2155	0.0255
14	0.4873	-15000.00	39	2.0017	20000.01	14	0.2125	-0.0218
15	0.5103	20000.00	40	3.7628	-15000.00	15	0.2457	0.0784
16	0.5695	-15000.00	41	0.1000	17709.79	16	0.2422	-0.0887
17	2.0807	-15000.00	42	1.2205	-15000.01	17	0.2618	0.1030
18	2.0998	-15000.00	43	0.1000	5001.07	18	0.2658	0.0784
19	0.1000	-1544.76	44	2.1535	19999.98	19	0.2698	0.0295
20	0.1000	1795.11	45	5.4611	-15000.01	20	0.2738	-0.0248
21	0.1000	210.99	46	0.8846	20000.08	21	0.2778	-0.0887
22	0.1000	-373.86	47	0.1673	-14999.56	22	0.2818	-0.1752
23	1.0903	20000.00						
24	1.7155	20000.00						
25	1.0868	20000.00						

	ω_n (rad/sec)		
1	206.27		
2	507.54	Minimum Weight	1521.01 lb
3	874.79	CPU Time	1.221 sec

Table 3.8: Optimum results of the forty-seven-member tower for $\omega = 100$ rad/sec

Forty-Seven-Member Tower (Force Excitation)								
$\omega = 100$ rad/sec			No mass added and No L.P.					
$A_0 = (A)_{\omega=90}$			Modify C.S.A. of all members					
Link	Area (in^2)	Stress (psi)	Link	Area (in^2)	Stress (psi)	Displacements (in)		
						node	x-dir	y-dir
1	1.1532	19999.93	26	1.7335	20000.00	1	0.0000	0.0000
2	3.2175	-15000.02	27	1.3777	20000.00	2	0.0000	0.0000
3	0.6235	20000.00	28	0.1000	-14999.10	3	0.0200	0.0080
4	2.0118	-14999.99	29	1.3327	19999.99	4	0.0220	-0.0060
5	0.4093	20000.21	30	3.5753	-15000.00	5	0.0560	0.0160
6	0.8207	-14999.88	31	1.0854	-15000.00	6	0.0543	-0.0120
7	0.3362	19999.82	32	0.4530	20000.00	7	0.0980	0.0240
8	0.1326	19999.92	33	0.1102	19999.10	8	0.1060	-0.0180
9	1.1568	-15000.00	34	0.7757	19999.85	9	0.1210	0.0175
10	1.5667	-15000.00	35	3.8367	-15000.02	10	0.1180	-0.0157
11	2.0777	-15000.00	36	1.0292	20000.12	11	0.1613	0.0215
12	2.1093	-15000.00	37	0.1000	-9600.50	12	0.1653	-0.0187
13	0.3251	19999.99	38	0.1000	-4199.68	13	0.2155	0.0255
14	0.5166	-15000.00	39	2.2190	20000.13	14	0.2125	-0.0217
15	0.5375	20000.00	40	3.9689	-14999.91	15	0.2458	0.0786
16	0.6009	-15000.00	41	0.1000	17915.01	16	0.2424	-0.0890
17	2.0771	-15000.00	42	1.3455	-15000.33	17	0.2618	0.1030
18	2.1071	-15000.00	43	0.1000	5028.83	18	0.2658	0.0786
19	0.1000	-2412.13	44	2.3736	19999.38	19	0.2698	0.0295
20	0.1000	2821.79	45	5.8475	-15000.24	20	0.2738	-0.0247
21	0.1000	328.74	46	0.9813	20002.06	21	0.2778	-0.0890
22	0.1000	-589.52	47	0.1706	-14988.07	22	0.2818	-0.1752
23	1.0850	20000.00						
24	1.7244	20000.00						
25	1.0794	20000.00						

	ω_n(rad/sec)		
1	212.90		
2	518.15	Minimum Weight	1605.06 lb
3	869.78	CPU Time	0.611 sec

Table 3.9: Optimum results of the forty-seven-member tower for ω = 140 rad/sec

Forty-Seven-Member Tower (Force Excitation)								
ω = 140 rad/sec			No mass added and No L.P.					
$A_0 = (A)_{\omega=130}$			Modify C.S.A. of all members					
Link	Area (in^2)	Stress (psi)	Link	Area (in^2)	Stress (psi)	Displacements (in)		
						node	x-dir	y-dir
1	1.2885	19999.99	26	1.7666	20000.00	1	0.0000	0.0000
2	3.8009	-15000.00	27	1.3826	20000.00	2	0.0000	0.0000
3	0.8338	20000.00	28	0.1000	-14999.90	3	0.0200	0.0080
4	2.1735	-15000.00	29	1.7483	20000.00	4	0.0220	-0.0060
5	0.7104	20000.02	30	3.9223	-15000.00	5	0.0560	0.0160
6	0.6642	-14999.98	31	1.3826	-15000.00	6	0.0548	-0.0120
7	0.2407	19999.97	32	0.4124	19999.99	7	0.0980	0.0240
8	0.1430	19999.99	33	0.1000	19999.87	8	0.1060	-0.0180
9	1.3484	-15000.00	34	1.0234	20000.00	9	0.1210	0.0175
10	1.5158	-15000.00	35	4.4209	-15000.00	10	0.1180	-0.0157
11	2.0688	-15000.00	36	1.2832	20000.00	11	0.1613	0.0215
12	2.1314	-15000.00	37	0.1000	-8976.69	12	0.1653	-0.0187
13	0.3759	20000.00	38	0.1000	-2953.26	13	0.2155	0.0255
14	0.5970	-15000.00	39	2.8452	20000.00	14	0.2125	-0.0217
15	0.6124	20000.00	40	4.5561	-15000.00	15	0.2461	0.0792
16	0.6849	-15000.00	41	0.1000	18523.37	16	0.2427	-0.0897
17	2.0678	-15000.00	42	1.7151	-15000.00	17	0.2618	0.1030
18	2.1269	-15000.00	43	0.1000	5000.01	18	0.2658	0.0792
19	0.1000	-4719.61	44	3.0077	20000.00	19	0.2698	0.0295
20	0.1000	5621.39	45	6.9702	-15000.00	20	0.2738	-0.0247
21	0.1000	639.46	46	1.2692	20000.00	21	0.2778	-0.0898
22	0.1000	-1184.23	47	0.1795	-15000.00	22	0.2818	-0.1752
23	1.0707	20000.00						
24	1.7483	20000.00						
25	1.0600	20000.00						

	ω_n (rad/sec)		
1	230.57		
2	538.31	Minimum Weight	1845.32 lb
3	872.68	CPU Time	3.555 sec

Table 3.10: Optimum results of the forty-seven-member tower for ω = 190 rad/sec

Forty-Seven-Member Tower (Force Excitation)								
ω = 190 rad/sec			No mass added and No L.P.					
$A_0 = (A)_{\omega=180}$			Modify C.S.A. of all members					
Link	Area (in^2)	Stress (psi)	Link	Area (in^2)	Stress (psi)	Displacements (in)		
						node	x-dir	y-dir
1	1.5078	20000.00	26	1.8253	20000.00	1	0.0000	0.0000
2	4.9170	-15000.00	27	1.3900	20000.00	2	0.0000	0.0000
3	1.2647	20000.00	28	0.1000	-12645.26	3	0.0200	0.0080
4	2.3991	-15000.00	29	2.5477	20000.00	4	0.0220	-0.0060
5	1.3148	20000.00	30	4.5452	-15000.00	5	0.0560	0.0160
6	0.3280	-15000.00	31	1.9714	-15000.00	6	0.0560	-0.0120
7	0.1000	17645.28	32	0.2939	19999.99	7	0.0989	0.0240
8	0.1000	18822.64	33	0.1000	17645.25	8	0.1060	-0.0180
9	1.7939	-15000.00	34	1.4973	20000.00	9	0.1212	0.0179
10	1.3642	-15000.00	35	5.5610	-15000.00	10	0.1187	-0.0154
11	2.0536	-15000.00	36	1.7978	20000.00	11	0.1620	0.0219
12	2.1707	-15000.00	37	0.1000	-8677.50	12	0.1655	-0.0184
13	0.4634	20000.00	38	0.1000	-0.25	13	0.2157	0.0259
14	0.7452	-15000.00	39	4.0974	20000.00	14	0.2127	-0.0214
15	0.7507	20000.00	40	5.7149	-15000.00	15	0.2468	0.0805
16	0.8292	-15000.00	41	0.1064	19999.93	16	0.2436	-0.0906
17	2.0519	-15000.00	42	2.4816	-15000.00	17	0.2620	0.1034
18	2.1618	-15000.00	43	0.1000	5000.11	18	0.2660	0.0806
19	0.1000	-8689.55	44	4.2899	20000.00	19	0.2700	0.0299
20	0.1000	10635.13	45	9.2451	-15000.00	20	0.2740	-0.0244
21	0.1000	1167.41	46	1.8708	20000.01	21	0.2780	-0.0908
22	0.1000	-2268.19	47	0.2119	-14999.95	22	0.2820	-0.1749
23	1.0466	20000.00						
24	1.7906	20000.00						
25	1.0274	20000.00						
	ω_n (rad/sec)							
1	257.46							
2	554.91		Minimum Weight			2320.90 lb		
3	853.91		CPU Time			2.975 sec		

Table 3.11: Optimum results of the forty-seven-member tower for ω = 200 rad/sec

Forty-Seven-Member Tower (Force Excitation)	
$\omega = 200$ rad/sec	No mass added and No L.P.
$A_0 = (A)_{\omega=190}$	Modify C.S.A. of all members

Link	Area	Stress	Link	Area	Stress	Displacements (in)		
	(in^2)	(psi)		(in^2)	(psi)	node	x-dir	y-dir
1	1.5933	20000.00	26	1.8395	20000.00	1	0.0000	0.0000
2	5.1581	-15000.00	27	1.3921	20000.00	2	0.0000	0.0000
3	1.3682	20000.00	28	0.1000	-10125.98	3	0.0200	0.0080
4	2.4593	-15000.00	29	2.7406	20000.00	4	0.0220	-0.0060
5	1.4268	20000.00	30	4.7200	-15000.00	5	0.0560	0.0160
6	0.3017	-15000.00	31	2.0929	-15000.00	6	0.0560	-0.0120
7	0.1000	15125.98	32	0.2812	20000.00	7	0.0999	0.0240
8	0.1000	17562.99	33	0.1000	15125.98	8	0.1060	-0.0180
9	1.8985	-15000.00	34	1.6253	20000.00	9	0.1215	0.0182
10	1.3312	-15000.00	35	5.8564	-15000.00	10	0.1195	-0.0150
11	2.0498	-15000.00	36	1.9322	20000.00	11	0.1627	0.0222
12	2.1800	-15000.00	37	0.1000	-9937.01	12	0.1657	-0.0180
13	0.4851	20000.00	38	0.1000	0.00	13	0.2160	0.0262
14	0.7811	-15000.00	39	4.4267	20000.00	14	0.2130	-0.0210
15	0.7843	20000.00	40	6.0344	-15000.00	15	0.2472	0.0811
16	0.8650	-15000.00	41	0.1233	20000.00	16	0.2440	-0.0905
17	2.0481	-15000.00	42	2.6773	-15000.00	17	0.2622	0.1037
18	2.1700	-15000.00	43	0.1000	5000.00	18	0.2662	0.0813
19	0.1000	-9647.97	44	4.6466	20000.00	19	0.2702	0.0302
20	0.1000	11841.65	45	9.8512	-15000.00	20	0.2742	-0.0240
21	0.1000	1295.41	46	2.0258	20000.00	21	0.2782	-0.0907
22	0.1000	-2528.55	47	0.2391	-15000.00	22	0.2822	-0.1745
23	1.0409	20000.00						
24	1.8008	20000.00						
25	1.0197	20000.00						

	ω_n (rad/sec)		
1	263.28		
2	558.76	Minimum Weight	2448.34 lb
3	848.93	CPU Time	4.276 sec

Table 3.12: Optimum results of the forty-seven-member tower for $\omega = 220$ rad/sec

Forty-Seven-Member Tower (Force Excitation)	
$\omega = 220$ rad/sec	No mass added and No L.P.
$A_0 = (A)_{\omega=210}$	Modify C.S.A. of all members

Link	Area (in^2)	Stress (psi)	Link	Area (in^2)	Stress (psi)	Displacements (in)		
						node	x-dir	y-dir
1	1.7813	20001.82	26	1.8706	20000.22	1	0.0000	0.0000
2	5.7022	-15000.84	27	1.4035	19999.97	2	0.0000	0.0000
3	1.5993	20001.87	28	0.1000	-4059.04	3	0.0200	0.0080
4	2.5902	-15000.68	29	3.1791	20001.68	4	0.0220	-0.0060
5	1.6849	20001.41	30	5.1104	-15000.78	5	0.0560	0.0160
6	0.2384	-15000.40	31	2.3684	-15000.97	6	0.0560	-0.0120
7	0.1000	9060.08	32	0.2459	20001.33	7	0.1024	0.0240
8	0.1000	14531.73	33	0.1000	9059.06	8	0.1060	-0.0180
9	2.1343	-15000.89	34	1.9173	20001.94	9	0.1221	0.0191
10	1.2473	-14999.59	35	6.5361	-15000.84	10	0.1213	-0.0141
11	2.0414	-14999.91	36	2.2473	20001.31	11	0.1645	0.0231
12	2.1999	-15000.07	37	0.1000	-12970.92	12	0.1664	-0.0171
13	0.5398	20001.37	38	0.1000	0.63	13	0.2166	0.0271
14	0.8509	-15001.02	39	5.1930	20001.57	14	0.2136	-0.0201
15	0.8486	20001.30	40	6.7725	-15000.87	15	0.2481	0.0826
16	0.9566	-15000.93	41	0.1646	20001.72	16	0.2449	-0.0902
17	2.0398	-14999.92	42	3.1394	-15001.04	17	0.2629	0.1047
18	2.1879	-15000.07	43	0.1000	5000.02	18	0.2669	0.0827
19	0.1000	-11733.28	44	5.4800	20001.57	19	0.2709	0.0311
20	0.1000	14474.15	45	11.2676	-15000.94	20	0.2749	-0.0231
21	0.1000	1573.98	46	2.3930	20001.41	21	0.2789	-0.0905
22	0.1000	-3097.13	47	0.3060	-15001.08	22	0.2829	-0.1736
23	1.0286	19999.73						
24	1.8229	20000.16						
25	1.0032	19999.64						

	ω_n (rad/sec)		
1	275.30		
2	563.29	Minimum Weight	2743.16 lb
3	835.72	CPU Time	12.217 sec

Table 3.13: Optimum results of the two-hundred-member structure for $\omega = 0$ (I)

Two-Hundred-Member Structure (Force Excitation)	
$\omega = 0$	No mass added and No L.P.
$A_0 = 0.1\,\mathrm{in}^2$	Modify C.S.A. of all members

Displacements (in)			Displacements (in)			Displacements (in)		
node	x-dir	y-dir	node	x-dir	y-dir	node	x-dir	y-dir
1	0.0188	-0.2127	27	0.0660	-0.1578	53	0.0324	-0.0871
2	0.0353	-0.1800	28	0.0660	-0.1848	54	0.0397	-0.0792
3	0.0543	-0.1960	29	0.0013	-0.1551	55	0.0469	-0.1003
4	0.0759	-0.1800	30	0.0253	-0.1224	56	0.0469	-0.1272
5	0.0960	-0.2280	31	0.0392	-0.1384	57	-0.0163	-0.0975
6	0.0338	-0.1983	32	0.0528	-0.1224	58	0.0077	-0.0648
7	0.0298	-0.1791	33	0.0768	-0.1704	59	0.0211	-0.0808
8	0.0369	-0.1656	34	0.0181	-0.1407	60	0.0336	-0.0648
9	0.0439	-0.1726	35	0.0141	-0.1200	61	0.0576	-0.1128
10	0.0520	-0.1816	36	0.0209	-0.1080	62	0.0000	-0.0831
11	0.0602	-0.1721	37	0.0278	-0.1159	63	-0.0040	-0.0628
12	0.0682	-0.1656	38	0.0348	-0.1240	64	0.0019	-0.0504
13	0.0763	-0.1872	39	0.0417	-0.1159	65	0.0077	-0.0558
14	0.0763	-0.2136	40	0.0491	-0.1080	66	0.0143	-0.0664
15	0.0100	-0.1839	41	0.0565	-0.1291	67	0.0210	-0.0608
16	0.0340	-0.1512	42	0.0565	-0.1560	68	0.0290	-0.0504
17	0.0482	-0.1672	43	-0.0075	-0.1263	69	0.0370	-0.0712
18	0.0624	-0.1512	44	0.0165	-0.0936	70	0.0370	-0.0984
19	0.0864	-0.1992	45	0.0300	-0.1096	71	-0.0250	-0.0687
20	0.0269	-0.1695	46	0.0432	-0.0936	72	-0.0010	-0.0360
21	0.0229	-0.1488	47	0.0672	-0.1416	73	0.0000	-0.0520
22	0.0298	-0.1368	48	0.0093	-0.1119	74	0.0240	-0.0360
23	0.0368	-0.1448	49	0.0053	-0.0913	75	0.0480	-0.0840
24	0.0439	-0.1528	50	0.0120	-0.0792	76	0.0000	0.0000
25	0.0510	-0.1447	51	0.0188	-0.0872	77	0.0000	0.0000
26	0.0585	-0.1368	52	0.0256	-0.0952			

	ω_n (rad/sec)		
1	95.12		
2	334.57	Minimum Weight	6973.82 lb
3	524.80	CPU Time	29.342 sec

Table 3.14: Optimum results of the two-hundred-member structure for $\omega = 0$ (II)

Two-Hundred-Member Structure (Force Excitation)								
$\omega = 0$			No mass added and No L.P.					
$A_0 = 0.1\,\text{in}^2$			Modify C.S.A. of all members					
Link	Area (in^2)	Stress (psi)	Link	Area (in^2)	Stress (psi)	Link	Area (in^2)	Stress (psi)
1	0.1000	20622.20	35	0.7068	-30000.01	69	0.1000	-5362.14
2	0.1000	23695.78	36	0.1835	-30000.10	70	1.1122	-30000.00
3	0.1000	27023.47	37	0.1000	25078.92	71	0.1000	4398.43
4	0.1000	25139.79	38	0.5661	-29999.98	72	0.1000	-25553.60
5	0.2108	-29999.97	39	0.1436	30000.12	73	1.6138	-30000.01
6	0.1594	-30000.05	40	0.1000	17653.48	74	0.3033	-30000.15
7	0.1000	4538.78	41	0.1000	17791.34	75	0.1000	26505.06
8	0.3443	-30000.00	42	0.1094	30000.25	76	0.9731	-29999.95
9	0.1000	-262.30	43	0.5314	-29999.94	77	0.2733	30000.07
10	0.1000	-18201.12	44	0.3635	-30000.08	78	0.1000	17418.84
11	0.2268	-30000.01	45	0.1000	8477.00	79	0.1000	16990.06
12	0.1000	-23399.14	46	1.2388	-30000.00	80	0.1779	30000.16
13	0.1000	6356.01	47	0.1000	-5083.68	81	0.6771	-29999.93
14	0.3734	-30000.01	48	0.1000	-15952.25	82	0.5785	-30000.05
15	0.1000	9298.41	49	0.7789	-30000.00	83	0.1000	8563.17
16	0.1309	-30000.12	50	0.1000	-24780.08	84	2.2878	-30000.01
17	0.2328	-29999.95	51	0.1000	3624.91	85	0.1000	-5368.74
18	0.1000	-10000.00	52	1.2805	-30000.02	86	0.1000	-15981.58
19	0.1000	17651.59	53	0.1000	11856.32	87	1.3429	-29999.99
20	0.1000	17651.59	54	0.2545	-30000.18	88	0.1000	-25072.37
21	0.1000	20266.17	55	0.6397	-29999.92	89	0.1000	3382.23
22	0.1000	20266.17	56	0.1000	-10000.00	90	2.2849	-30000.03
23	0.1000	20204.88	57	0.1000	17408.87	91	0.1000	11973.07
24	0.1000	20204.88	58	0.1000	17408.87	92	0.3663	-30000.11
25	0.1000	0.00	59	0.1000	17765.41	93	0.9571	-29999.92
26	0.5442	-29999.99	60	0.1000	17765.41	94	0.1000	-10000.00
27	0.1000	26135.37	61	0.1000	18755.79	95	0.1000	17188.03
28	0.2314	-30000.04	62	0.1000	18755.79	96	0.1000	17188.03
29	0.6776	-30000.00	63	0.1000	0.00	97	0.1000	17373.19
30	0.1000	-16159.07	64	0.8647	-29999.96	98	0.1000	17373.19
31	0.1000	-2304.35	65	0.1000	29884.02	99	0.1000	18456.46
32	0.5601	-30000.01	66	0.4348	-30000.07	100	0.1000	18456.46
33	0.1000	6308.14	67	1.5721	-30000.00	101	0.1000	0.00
34	0.1000	-23351.26	68	0.1000	-15673.79	102	1.0104	-29999.95

Table 3.15: Optimum results of the two-hundred-member structure for $\omega = 0$ (III)

Two-Hundred-Member Structure (Force Excitation)								
$\omega = 0$			No mass added and No L.P.					
$A_0 = 0.1\,\text{in}^2$			Modify C.S.A. of all members					
Link	Area (in^2)	Stress (psi)	Link	Area (in^2)	Stress (psi)	Link	Area (in^2)	Stress (psi)
103	0.1000	29797.70	137	0.1000	18148.71	171	0.1000	14593.31
104	0.6493	-30000.04	138	0.1000	18148.71	172	0.1000	14593.31
105	2.6212	-30000.01	139	0.1000	0.00	173	0.1000	16588.09
106	0.1000	-15836.97	140	0.9949	-29999.95	174	0.1000	16588.09
107	0.1000	-5513.35	141	0.1000	29714.57	175	0.1000	20009.96
108	1.6763	-29999.99	142	0.8589	-30000.01	176	0.1000	20009.96
109	0.1000	4228.30	143	3.8352	-30000.01	177	0.1000	0.00
110	0.1000	-25918.44	144	0.1000	-16125.50	178	0.8369	-29999.95
111	2.6182	-30000.02	145	0.1000	-5516.22	179	0.1000	28784.31
112	0.4143	-30000.09	146	2.2403	-29999.99	180	1.0385	-29999.98
113	0.1000	26388.03	147	0.1000	3909.64	181	5.1992	-30000.01
114	1.2905	-29999.94	148	0.1000	-26158.26	182	0.1000	-15421.88
115	0.4080	30000.02	149	3.7082	-30000.03	183	0.1000	-12608.66
116	0.1000	16886.36	150	0.5187	-30000.03	184	2.8043	-29999.99
117	0.1000	16486.03	151	0.1000	26267.71	185	0.1000	10680.37
118	0.2455	30000.06	152	1.5274	-29999.94	186	0.1000	-27390.49
119	0.6616	-29999.92	153	0.5271	29999.98	187	4.8899	-30000.02
120	0.7886	-30000.01	154	0.1000	16707.86	188	0.6413	-29999.99
121	0.1000	8646.17	155	0.1000	15627.37	189	0.1000	26994.46
122	3.5019	-30000.01	156	0.3211	30000.00	190	1.6742	-29999.95
123	0.1000	-5511.97	157	0.5035	-29999.92	191	0.6362	29999.96
124	0.1000	-16129.74	158	0.9745	-29999.98	192	0.1000	1297.62
125	1.9069	-29999.99	159	0.1000	9576.32	193	0.8825	29999.95
126	0.1000	-25246.05	160	4.8659	-30000.01	194	1.2347	29999.96
127	0.1000	2997.43	161	0.1000	-11050.69	195	1.3178	-29999.97
128	3.3749	-30000.03	162	0.1000	-16979.85	196	6.3698	-30000.00
129	0.1000	12093.11	163	2.4709	-29999.99	197	1.0520	-30000.02
130	0.4714	-30000.04	164	0.1000	-24717.93	198	2.7248	-29999.99
131	1.1941	-29999.93	165	0.1000	8007.80	199	5.7861	-30000.02
132	0.1000	-10000.00	166	4.5566	-30000.02	200	2.3296	-29999.96
133	0.1000	16975.32	167	0.1000	11366.18			
134	0.1000	16975.32	168	0.5892	-29999.99			
135	0.1000	16980.75	169	1.3408	-29999.94			
136	0.1000	16980.75	170	0.1000	-10000.00			

Table 3.16: Optimum results of the two-hundred-member structure for $\omega = 20$ rad/sec (I)

Two-Hundred-Member Structure (Force Excitation)	
$\omega = 20\,\text{rad/sec}$	No mass added and No L.P.
$A_0 = 0.1\,\text{in}^2$	Modify C.S.A. of all members

Displacements (in)			Displacements (in)			Displacements (in)		
node	x-dir	y-dir	node	x-dir	y-dir	node	x-dir	y-dir
1	0.0189	-0.2127	27	0.0660	-0.1578	53	0.0324	-0.0871
2	0.0354	-0.1800	28	0.0660	-0.1848	54	0.0397	-0.0792
3	0.0543	-0.1960	29	0.0013	-0.1551	55	0.0470	-0.1003
4	0.0759	-0.1800	30	0.0253	-0.1224	56	0.0470	-0.1272
5	0.0960	-0.2280	31	0.0392	-0.1384	57	-0.0163	-0.0975
6	0.0339	-0.1983	32	0.0528	-0.1224	58	0.0077	-0.0648
7	0.0299	-0.1791	33	0.0768	-0.1704	59	0.0211	-0.0808
8	0.0369	-0.1656	34	0.0181	-0.1407	60	0.0336	-0.0648
9	0.0440	-0.1726	35	0.0141	-0.1200	61	0.0576	-0.1128
10	0.0521	-0.1816	36	0.0210	-0.1080	62	0.0000	-0.0831
11	0.0602	-0.1721	37	0.0278	-0.1159	63	-0.0040	-0.0628
12	0.0683	-0.1656	38	0.0348	-0.1240	64	0.0019	-0.0504
13	0.0763	-0.1872	39	0.0417	-0.1159	65	0.0077	-0.0558
14	0.0763	-0.2136	40	0.0491	-0.1080	66	0.0144	-0.0664
15	0.0101	-0.1839	41	0.0565	-0.1291	67	0.0210	-0.0608
16	0.0341	-0.1512	42	0.0565	-0.1560	68	0.0290	-0.0504
17	0.0482	-0.1672	43	-0.0075	-0.1263	69	0.0370	-0.0712
18	0.0624	-0.1512	44	0.0165	-0.0936	70	0.0370	-0.0984
19	0.0864	-0.1992	45	0.0300	-0.1096	71	-0.0250	-0.0687
20	0.0269	-0.1695	46	0.0432	-0.0936	72	-0.0010	-0.0360
21	0.0229	-0.1488	47	0.0672	-0.1416	73	0.0000	-0.0520
22	0.0299	-0.1368	48	0.0093	-0.1119	74	0.0240	-0.0360
23	0.0368	-0.1448	49	0.0053	-0.0913	75	0.0480	-0.0840
24	0.0439	-0.1528	50	0.0121	-0.0792	76	0.0000	0.0000
25	0.0510	-0.1447	51	0.0189	-0.0872	77	0.0000	0.0000
26	0.0585	-0.1368	52	0.0257	-0.0952			

	ω_n (rad/sec)		
1	95.10		
2	334.49	Minimum Weight	6979.15 lb
3	524.75	CPU Time	28.962 sec

Table 3.17: Optimum results of the two-hundred-member structure for $\omega = 20$ rad/sec (II)

Two-Hundred-Member Structure (Force Excitation)								
$\omega = 20\,\text{rad/sec}$			No mass added and No L.P.					
$A_0 = 0.1\,\text{in}^2$			Modify C.S.A. of all members					
Link	Area (in^2)	Stress (psi)	Link	Area (in^2)	Stress (psi)	Link	Area (in^2)	Stress (psi)
1	0.1000	20618.70	35	0.7070	-30000.01	69	0.1000	-5376.08
2	0.1000	23687.34	36	0.1832	-30000.10	70	1.1129	-30000.00
3	0.1000	27012.70	37	0.1000	25040.73	71	0.1000	4390.88
4	0.1000	25107.81	38	0.5665	-29999.98	72	0.1000	-25585.11
5	0.2109	-29999.97	39	0.1436	30000.13	73	1.6145	-30000.01
6	0.1594	-30000.05	40	0.1000	17643.54	74	0.3020	-30000.16
7	0.1000	4541.81	41	0.1000	17755.37	75	0.1000	26472.22
8	0.3444	-30000.00	42	0.1088	30000.26	76	0.9748	-29999.95
9	0.1000	-260.43	43	0.5317	-29999.94	77	0.2735	30000.07
10	0.1000	-18197.33	44	0.3636	-30000.09	78	0.1000	17414.04
11	0.2269	-30000.01	45	0.1000	8480.53	79	0.1000	16957.74
12	0.1000	-23403.60	46	1.2394	-30000.00	80	0.1767	30000.16
13	0.1000	6354.48	47	0.1000	-5080.88	81	0.6775	-29999.92
14	0.3735	-30000.01	48	0.1000	-15950.03	82	0.5788	-30000.05
15	0.1000	9310.40	49	0.7794	-30000.00	83	0.1000	8566.78
16	0.1307	-30000.12	50	0.1000	-24778.03	84	2.2892	-30000.01
17	0.2330	-29999.95	51	0.1000	3605.94	85	0.1000	-5363.79
18	0.1000	-10004.85	52	1.2809	-30000.02	86	0.1000	-15979.53
19	0.1000	17654.43	53	0.1000	11889.18	87	1.3439	-29999.99
20	0.1000	17646.93	54	0.2533	-30000.19	88	0.1000	-25068.42
21	0.1000	20260.19	55	0.6413	-29999.92	89	0.1000	3362.16
22	0.1000	20251.70	56	0.1000	-10006.81	90	2.2851	-30000.03
23	0.1000	20199.90	57	0.1000	17418.40	91	0.1000	12009.34
24	0.1000	20185.34	58	0.1000	17403.18	92	0.3640	-30000.11
25	0.1000	11.52	59	0.1000	17762.64	93	0.9610	-29999.92
26	0.5444	-29999.99	60	0.1000	17747.18	94	0.1000	-10005.48
27	0.1000	26129.48	61	0.1000	18760.36	95	0.1000	17203.09
28	0.2315	-30000.05	62	0.1000	18729.71	96	0.1000	17184.88
29	0.6778	-30000.00	63	0.1000	19.19	97	0.1000	17377.00
30	0.1000	-16165.47	64	0.8651	-29999.96	98	0.1000	17358.03
31	0.1000	-2318.69	65	0.1000	29880.51	99	0.1000	18469.08
32	0.5603	-30000.01	66	0.4351	-30000.07	100	0.1000	18426.49
33	0.1000	6306.39	67	1.5730	-30000.00	101	0.1000	22.60
34	0.1000	-23381.82	68	0.1000	-15676.97	102	1.0110	-29999.95

Table 3.18: Optimum results of the two-hundred-member structure for $\omega = 20$ rad/sec (III)

Two-Hundred-Member Structure (Force Excitation)								
$\omega = 20\,\text{rad/sec}$			No mass added and No L.P.					
$A_0 = 0.1\,\text{in}^2$			Modify C.S.A. of all members					
Link	Area (in^2)	Stress (psi)	Link	Area (in^2)	Stress (psi)	Link	Area (in^2)	Stress (psi)
103	0.1000	29794.10	137	0.1000	18166.82	171	0.1000	14601.13
104	0.6498	-30000.04	138	0.1000	18117.61	172	0.1000	14597.83
105	2.6229	-30000.01	139	0.1000	22.64	173	0.1000	16597.93
106	0.1000	-15835.79	140	0.9955	-29999.94	174	0.1000	16584.56
107	0.1000	-5525.26	141	0.1000	29709.81	175	0.1000	20032.85
108	1.6774	-29999.99	142	0.8596	-30000.01	176	0.1000	19985.20
109	0.1000	4224.88	143	3.8381	-30000.01	177	0.1000	19.75
110	0.1000	-25948.87	144	0.1000	-16121.30	178	0.8372	-29999.95
111	2.6187	-30000.02	145	0.1000	-5525.67	179	0.1000	28775.90
112	0.4120	-30000.09	146	2.2420	-29999.99	180	1.0393	-29999.98
113	0.1000	26351.76	147	0.1000	3909.69	181	5.2034	-30000.01
114	1.2945	-29999.94	148	0.1000	-26186.05	182	0.1000	-15416.70
115	0.4083	30000.02	149	3.7077	-30000.03	183	0.1000	-12621.28
116	0.1000	16886.64	150	0.5151	-30000.03	184	2.8065	-29999.99
117	0.1000	16457.38	151	0.1000	26231.84	185	0.1000	10689.33
118	0.2435	30000.06	152	1.5347	-29999.94	186	0.1000	-27413.45
119	0.6620	-29999.92	153	0.5276	29999.98	187	4.8875	-30000.02
120	0.7892	-30000.01	154	0.1000	16711.04	188	0.6367	-29999.99
121	0.1000	8650.93	155	0.1000	15604.57	189	0.1000	26964.10
122	3.5044	-30000.01	156	0.3185	29999.99	190	1.6854	-29999.95
123	0.1000	-5507.09	157	0.5038	-29999.92	191	0.6367	29999.96
124	0.1000	-16126.54	158	0.9752	-29999.98	192	0.1000	1286.71
125	1.9084	-29999.99	159	0.1000	9584.73	193	0.8941	29999.95
126	0.1000	-25241.75	160	4.8697	-30000.01	194	1.2429	29999.96
127	0.1000	2978.71	161	0.1000	-11054.17	195	1.3185	-29999.96
128	3.3741	-30000.03	162	0.1000	-16975.27	196	6.3751	-30000.00
129	0.1000	12128.97	163	2.4730	-29999.99	197	1.0431	-30000.02
130	0.4680	-30000.04	164	0.1000	-24713.67	198	2.7370	-29999.99
131	1.2011	-29999.93	165	0.1000	7998.85	199	5.7807	-30000.02
132	0.1000	-10002.76	166	4.5539	-30000.03	200	2.3439	-29999.96
133	0.1000	16991.51	167	0.1000	11396.53			
134	0.1000	16976.02	168	0.5847	-29999.99			
135	0.1000	16989.05	169	1.3519	-29999.94			
136	0.1000	16970.11	170	0.1000	-10000.01			

Table 3.19: Optimum results of the two-hundred-member structure for $\omega = 50$ rad/sec (I)

Two-Hundred-Member Structure (Force Excitation)								
ω = 50 rad/sec			No mass added and No L.P.					
$A_0 = 0.1\,\text{in}^2$			Modify C.S.A. of all members					
Displacements (in)			Displacements (in)			Displacements (in)		
node	x-dir	y-dir	node	x-dir	y-dir	node	x-dir	y-dir
1	0.0191	-0.2127	27	0.0661	-0.1579	53	0.0326	-0.0871
2	0.0356	-0.1800	28	0.0662	-0.1848	54	0.0399	-0.0792
3	0.0545	-0.1960	29	0.0015	-0.1551	55	0.0471	-0.1004
4	0.0760	-0.1800	30	0.0255	-0.1224	56	0.0471	-0.1272
5	0.0960	-0.2280	31	0.0394	-0.1384	57	-0.0162	-0.0975
6	0.0341	-0.1983	32	0.0528	-0.1224	58	0.0078	-0.0648
7	0.0301	-0.1791	33	0.0768	-0.1704	59	0.0212	-0.0808
8	0.0371	-0.1656	34	0.0182	-0.1407	60	0.0336	-0.0648
9	0.0442	-0.1726	35	0.0142	-0.1200	61	0.0576	-0.1128
10	0.0523	-0.1816	36	0.0211	-0.1080	62	0.0001	-0.0831
11	0.0603	-0.1721	37	0.0280	-0.1159	63	-0.0039	-0.0628
12	0.0684	-0.1656	38	0.0350	-0.1240	64	0.0019	-0.0504
13	0.0764	-0.1873	39	0.0419	-0.1159	65	0.0078	-0.0558
14	0.0765	-0.2136	40	0.0493	-0.1080	66	0.0145	-0.0664
15	0.0103	-0.1839	41	0.0566	-0.1292	67	0.0211	-0.0608
16	0.0343	-0.1512	42	0.0566	-0.1560	68	0.0291	-0.0504
17	0.0483	-0.1672	43	-0.0074	-0.1263	69	0.0371	-0.0713
18	0.0624	-0.1512	44	0.0166	-0.0936	70	0.0371	-0.0984
19	0.0864	-0.1992	45	0.0302	-0.1096	71	-0.0250	-0.0687
20	0.0271	-0.1695	46	0.0432	-0.0936	72	-0.0010	-0.0360
21	0.0231	-0.1488	47	0.0672	-0.1416	73	0.0000	-0.0520
22	0.0301	-0.1368	48	0.0094	-0.1119	74	0.0240	-0.0360
23	0.0370	-0.1448	49	0.0054	-0.0913	75	0.0480	-0.0840
24	0.0441	-0.1528	50	0.0122	-0.0792	76	0.0000	0.0000
25	0.0512	-0.1447	51	0.0190	-0.0872	77	0.0000	0.0000
26	0.0587	-0.1368	52	0.0258	-0.0952			

	ω_n (rad/sec)		
1	94.93		
2	334.07	Minimum Weight	7007.25 lb
3	524.43	CPU Time	27.540 sec

Table 3.20: Optimum results of the two-hundred-member structure for $\omega = 50$ rad/sec (II)

Two-Hundred-Member Structure (Force Excitation)								
ω = 50 rad/sec			No mass added and No L.P.					
A_0 = 0.1 in^2			Modify C.S.A. of all members					
Link	Area (in^2)	Stress (psi)	Link	Area (in^2)	Stress (psi)	Link	Area (in^2)	Stress (psi)
1	0.1000	20599.39	35	0.7083	-30000.01	69	0.1000	-5449.99
2	0.1000	23642.05	36	0.1818	-30000.12	70	1.1162	-30000.00
3	0.1000	26955.16	37	0.1000	24839.27	71	0.1000	4350.78
4	0.1000	24938.52	38	0.5683	-29999.98	72	0.1000	-25751.69
5	0.2113	-29999.96	39	0.1440	30000.16	73	1.6179	-30000.01
6	0.1594	-30000.07	40	0.1000	17589.85	74	0.2954	-30000.19
7	0.1000	4557.42	41	0.1000	17564.40	75	0.1000	26299.89
8	0.3450	-30000.00	42	0.1058	30000.31	76	0.9839	-29999.94
9	0.1000	-251.09	43	0.5333	-29999.92	77	0.2746	30000.08
10	0.1000	-18177.91	44	0.3641	-30000.11	78	0.1000	17387.82
11	0.2274	-30000.01	45	0.1000	8498.94	79	0.1000	16786.17
12	0.1000	-23427.82	46	1.2424	-30000.01	80	0.1701	30000.19
13	0.1000	6345.95	47	0.1000	-5066.78	81	0.6800	-29999.90
14	0.3742	-30000.01	48	0.1000	-15938.73	82	0.5805	-30000.06
15	0.1000	9373.19	49	0.7817	-29999.99	83	0.1000	8585.54
16	0.1295	-30000.14	50	0.1000	-24767.82	84	2.2966	-30000.01
17	0.2343	-29999.94	51	0.1000	3505.25	85	0.1000	-5338.09
18	0.1000	-10030.58	52	1.2830	-30000.02	86	0.1000	-15969.02
19	0.1000	17668.73	53	0.1000	12061.66	87	1.3489	-29999.99
20	0.1000	17621.49	54	0.2472	-30000.22	88	0.1000	-25048.10
21	0.1000	20227.75	55	0.6494	-29999.91	89	0.1000	3255.78
22	0.1000	20174.39	56	0.1000	-10042.97	90	2.2859	-30000.03
23	0.1000	20172.78	57	0.1000	17468.24	91	0.1000	12199.59
24	0.1000	20081.47	58	0.1000	17372.29	92	0.3521	-30000.13
25	0.1000	72.38	59	0.1000	17747.14	93	0.9811	-29999.91
26	0.5453	-29999.98	60	0.1000	17649.82	94	0.1000	-10034.64
27	0.1000	26098.11	61	0.1000	18783.38	95	0.1000	17282.45
28	0.2320	-30000.06	62	0.1000	18591.01	96	0.1000	17167.38
29	0.6790	-30000.00	63	0.1000	121.39	97	0.1000	17396.37
30	0.1000	-16199.54	64	0.8676	-29999.95	98	0.1000	17276.85
31	0.1000	-2394.50	65	0.1000	29862.18	99	0.1000	18534.42
32	0.5613	-30000.01	66	0.4363	-30000.09	100	0.1000	18267.20
33	0.1000	6297.05	67	1.5772	-30000.00	101	0.1000	144.08
34	0.1000	-23543.43	68	0.1000	-15693.95	102	1.0143	-29999.94

Table 3.21: Optimum results of the two-hundred-member structure for $\omega = 50$ rad/sec (III)

Two-Hundred-Member Structure (Force Excitation)								
$\omega = 50\,\mathrm{rad/sec}$			No mass added and No L.P.					
$A_0 = 0.1\,\mathrm{in}^2$			Modify C.S.A. of all members					
Link	Area (in^2)	Stress (psi)	Link	Area (in^2)	Stress (psi)	Link	Area (in^2)	Stress (psi)
103	0.1000	29775.39	137	0.1000	18261.17	171	0.1000	14642.48
104	0.6523	-30000.05	138	0.1000	17952.65	172	0.1000	14621.14
105	2.6319	-30000.01	139	0.1000	145.71	173	0.1000	16649.55
106	0.1000	-15829.53	140	0.9984	-29999.93	174	0.1000	16565.10
107	0.1000	-5588.42	141	0.1000	29685.02	175	0.1000	20152.59
108	1.6837	-29999.99	142	0.8633	-30000.01	176	0.1000	19854.28
109	0.1000	4206.56	143	3.8533	-30000.01	177	0.1000	128.50
110	0.1000	-26109.74	144	0.1000	-16098.96	178	0.8387	-29999.94
111	2.6212	-30000.03	145	0.1000	-5575.89	179	0.1000	28731.69
112	0.3995	-30000.11	146	2.2513	-29999.99	180	1.0435	-29999.97
113	0.1000	26161.56	147	0.1000	3909.67	181	5.2251	-30000.01
114	1.3157	-29999.93	148	0.1000	-26332.90	182	0.1000	-15389.16
115	0.4104	30000.02	149	3.7051	-30000.03	183	0.1000	-12688.31
116	0.1000	16887.60	150	0.4965	-30000.02	184	2.8185	-29999.99
117	0.1000	16305.34	151	0.1000	26043.72	185	0.1000	10736.59
118	0.2331	30000.05	152	1.5729	-29999.94	186	0.1000	-27534.72
119	0.6644	-29999.90	153	0.5302	29999.97	187	4.8746	-30000.03
120	0.7922	-30000.01	154	0.1000	16727.47	188	0.6124	-29999.97
121	0.1000	8675.72	155	0.1000	15483.59	189	0.1000	26804.76
122	3.5178	-30000.02	156	0.3044	29999.97	190	1.7449	-29999.95
123	0.1000	-5481.59	157	0.5050	-29999.90	191	0.6392	29999.95
124	0.1000	-16109.89	158	0.9789	-29999.98	192	0.1000	1228.60
125	1.9165	-29999.99	159	0.1000	9628.93	193	0.9554	29999.96
126	0.1000	-25219.55	160	4.8900	-30000.01	194	1.2867	29999.96
127	0.1000	2879.58	161	0.1000	-11072.92	195	1.3220	-29999.96
128	3.3697	-30000.03	162	0.1000	-16951.18	196	6.4026	-30000.01
129	0.1000	12317.06	163	2.4838	-29999.99	197	0.9962	-30000.01
130	0.4500	-30000.03	164	0.1000	-24691.63	198	2.8014	-29999.99
131	1.2382	-29999.92	165	0.1000	7951.66	199	5.7520	-30000.02
132	0.1000	-10017.48	166	4.5396	-30000.03	200	2.4192	-29999.96
133	0.1000	17077.19	167	0.1000	11555.81			
134	0.1000	16978.96	168	0.5609	-29999.97			
135	0.1000	17032.38	169	1.4104	-29999.94			
136	0.1000	16912.89	170	0.1000	-10000.13			

Table 3.22: Optimum results of the two-hundred-member structure for $\omega = 70$ rad/sec (I)

<table>
<tr><td colspan="9">Two-Hundred-Member Structure (Force Excitation)</td></tr>
<tr><td colspan="3">$\omega = 70\,\text{rad/sec}$</td><td colspan="6">No mass added and No L.P.</td></tr>
<tr><td colspan="3">$A_0 = 0.1\,\text{in}^2$</td><td colspan="6">Modify C.S.A. of all members</td></tr>
<tr><td colspan="3">Displacements (in)</td><td colspan="3">Displacements (in)</td><td colspan="3">Displacements (in)</td></tr>
<tr><td>node</td><td>x-dir</td><td>y-dir</td><td>node</td><td>x-dir</td><td>y-dir</td><td>node</td><td>x-dir</td><td>y-dir</td></tr>
<tr><td>1</td><td>0.0194</td><td>-0.2126</td><td>27</td><td>0.0662</td><td>-0.1580</td><td>53</td><td>0.0327</td><td>-0.0871</td></tr>
<tr><td>2</td><td>0.0358</td><td>-0.1800</td><td>28</td><td>0.0663</td><td>-0.1848</td><td>54</td><td>0.0401</td><td>-0.0792</td></tr>
<tr><td>3</td><td>0.0547</td><td>-0.1960</td><td>29</td><td>0.0016</td><td>-0.1550</td><td>55</td><td>0.0472</td><td>-0.1005</td></tr>
<tr><td>4</td><td>0.0762</td><td>-0.1800</td><td>30</td><td>0.0256</td><td>-0.1224</td><td>56</td><td>0.0473</td><td>-0.1272</td></tr>
<tr><td>5</td><td>0.0960</td><td>-0.2280</td><td>31</td><td>0.0395</td><td>-0.1384</td><td>57</td><td>-0.0161</td><td>-0.0974</td></tr>
<tr><td>6</td><td>0.0343</td><td>-0.1982</td><td>32</td><td>0.0528</td><td>-0.1224</td><td>58</td><td>0.0079</td><td>-0.0648</td></tr>
<tr><td>7</td><td>0.0303</td><td>-0.1791</td><td>33</td><td>0.0768</td><td>-0.1704</td><td>59</td><td>0.0213</td><td>-0.0808</td></tr>
<tr><td>8</td><td>0.0374</td><td>-0.1656</td><td>34</td><td>0.0184</td><td>-0.1406</td><td>60</td><td>0.0336</td><td>-0.0648</td></tr>
<tr><td>9</td><td>0.0444</td><td>-0.1727</td><td>35</td><td>0.0144</td><td>-0.1200</td><td>61</td><td>0.0576</td><td>-0.1128</td></tr>
<tr><td>10</td><td>0.0525</td><td>-0.1816</td><td>36</td><td>0.0213</td><td>-0.1080</td><td>62</td><td>0.0001</td><td>-0.0830</td></tr>
<tr><td>11</td><td>0.0605</td><td>-0.1721</td><td>37</td><td>0.0282</td><td>-0.1160</td><td>63</td><td>-0.0039</td><td>-0.0628</td></tr>
<tr><td>12</td><td>0.0686</td><td>-0.1656</td><td>38</td><td>0.0352</td><td>-0.1240</td><td>64</td><td>0.0020</td><td>-0.0504</td></tr>
<tr><td>13</td><td>0.0766</td><td>-0.1874</td><td>39</td><td>0.0420</td><td>-0.1160</td><td>65</td><td>0.0079</td><td>-0.0558</td></tr>
<tr><td>14</td><td>0.0766</td><td>-0.2136</td><td>40</td><td>0.0495</td><td>-0.1080</td><td>66</td><td>0.0146</td><td>-0.0664</td></tr>
<tr><td>15</td><td>0.0105</td><td>-0.1838</td><td>41</td><td>0.0567</td><td>-0.1292</td><td>67</td><td>0.0212</td><td>-0.0609</td></tr>
<tr><td>16</td><td>0.0345</td><td>-0.1512</td><td>42</td><td>0.0568</td><td>-0.1560</td><td>68</td><td>0.0293</td><td>-0.0504</td></tr>
<tr><td>17</td><td>0.0485</td><td>-0.1672</td><td>43</td><td>-0.0072</td><td>-0.1262</td><td>69</td><td>0.0372</td><td>-0.0714</td></tr>
<tr><td>18</td><td>0.0624</td><td>-0.1512</td><td>44</td><td>0.0168</td><td>-0.0936</td><td>70</td><td>0.0373</td><td>-0.0984</td></tr>
<tr><td>19</td><td>0.0864</td><td>-0.1992</td><td>45</td><td>0.0303</td><td>-0.1096</td><td>71</td><td>-0.0249</td><td>-0.0686</td></tr>
<tr><td>20</td><td>0.0273</td><td>-0.1694</td><td>46</td><td>0.0432</td><td>-0.0936</td><td>72</td><td>-0.0009</td><td>-0.0360</td></tr>
<tr><td>21</td><td>0.0233</td><td>-0.1488</td><td>47</td><td>0.0672</td><td>-0.1416</td><td>73</td><td>0.0000</td><td>-0.0520</td></tr>
<tr><td>22</td><td>0.0303</td><td>-0.1368</td><td>48</td><td>0.0095</td><td>-0.1118</td><td>74</td><td>0.0240</td><td>-0.0360</td></tr>
<tr><td>23</td><td>0.0372</td><td>-0.1448</td><td>49</td><td>0.0055</td><td>-0.0912</td><td>75</td><td>0.0480</td><td>-0.0840</td></tr>
<tr><td>24</td><td>0.0443</td><td>-0.1528</td><td>50</td><td>0.0123</td><td>-0.0792</td><td>76</td><td>0.0000</td><td>0.0000</td></tr>
<tr><td>25</td><td>0.0513</td><td>-0.1447</td><td>51</td><td>0.0191</td><td>-0.0872</td><td>77</td><td>0.0000</td><td>0.0000</td></tr>
<tr><td>26</td><td>0.0589</td><td>-0.1368</td><td>52</td><td>0.0260</td><td>-0.0952</td><td></td><td></td><td></td></tr>
</table>

<table>
<tr><td></td><td>ω_n (rad/sec)</td><td colspan="2" rowspan="2"></td></tr>
<tr><td>1</td><td>94.67</td></tr>
<tr><td>2</td><td>333.48</td><td>Minimum Weight</td><td>7039.61 lb</td></tr>
<tr><td>3</td><td>523.95</td><td>CPU Time</td><td>31.555 sec</td></tr>
</table>

Table 3.23: Optimum results of the two-hundred-member structure for $\omega = 70$ rad/sec (II)

Two-Hundred-Member Structure (Force Excitation)								
$\omega = 70\,\mathrm{rad/sec}$			No mass added and No L.P.					
$A_0 = 0.1\,\mathrm{in}^2$			Modify C.S.A. of all members					
Link	Area (in^2)	Stress (psi)	Link	Area (in^2)	Stress (psi)	Link	Area (in^2)	Stress (psi)
1	0.1000	20576.86	35	0.7097	-29999.99	69	0.1000	-5535.91
2	0.1000	23589.24	36	0.1802	-29999.85	70	1.1200	-30000.01
3	0.1000	26888.69	37	0.1000	24607.62	71	0.1000	4305.26
4	0.1000	24744.34	38	0.5704	-30000.03	72	0.1000	-25945.41
5	0.2118	-30000.05	39	0.1444	29999.79	73	1.6217	-29999.98
6	0.1593	-29999.91	40	0.1000	17526.94	74	0.2879	-29999.77
7	0.1000	4574.56	41	0.1000	17343.39	75	0.1000	26101.89
8	0.3456	-30000.00	42	0.1023	29999.61	76	0.9944	-30000.07
9	0.1000	-241.03	43	0.5352	-30000.10	77	0.2758	29999.89
10	0.1000	-18156.13	44	0.3647	-29999.86	78	0.1000	17355.25
11	0.2279	-29999.98	45	0.1000	8519.14	79	0.1000	16585.52
12	0.1000	-23457.04	46	1.2459	-29999.99	80	0.1625	29999.77
13	0.1000	6336.35	47	0.1000	-5051.65	81	0.6829	-30000.12
14	0.3750	-29999.99	48	0.1000	-15926.51	82	0.5825	-29999.93
15	0.1000	9444.42	49	0.7844	-30000.01	83	0.1000	8606.46
16	0.1282	-29999.83	50	0.1000	-24758.44	84	2.3051	-29999.98
17	0.2357	-30000.07	51	0.1000	3389.50	85	0.1000	-5310.09
18	0.1000	-10060.48	52	1.2855	-29999.98	86	0.1000	-15957.84
19	0.1000	17684.62	53	0.1000	12257.66	87	1.3547	-30000.02
20	0.1000	17591.28	54	0.2401	-29999.72	88	0.1000	-25027.16
21	0.1000	20189.62	55	0.6588	-30000.11	89	0.1000	3132.50
22	0.1000	20084.43	56	0.1000	-10085.17	90	2.2868	-29999.96
23	0.1000	20140.73	57	0.1000	17524.90	91	0.1000	12416.32
24	0.1000	19961.01	58	0.1000	17334.92	92	0.3385	-29999.85
25	0.1000	142.72	59	0.1000	17727.61	93	1.0042	-30000.10
26	0.5463	-30000.02	60	0.1000	17535.39	94	0.1000	-10068.79
27	0.1000	26061.82	61	0.1000	18807.63	95	0.1000	17373.19
28	0.2325	-29999.92	62	0.1000	18428.74	96	0.1000	17144.73
29	0.6803	-30000.00	63	0.1000	241.20	97	0.1000	17416.32
30	0.1000	-16238.61	64	0.8703	-30000.06	98	0.1000	17179.82
31	0.1000	-2482.10	65	0.1000	29840.91	99	0.1000	18606.47
32	0.5624	-29999.99	66	0.4377	-29999.88	100	0.1000	18080.41
33	0.1000	6287.13	67	1.5821	-29999.99	101	0.1000	288.89
34	0.1000	-23730.29	68	0.1000	-15713.65	102	1.0180	-30000.08

Table 3.24: Optimum results of the two-hundred-member structure for $\omega = 70$ rad/sec (III)

Two-Hundred-Member Structure (Force Excitation)								
$\omega = 70\,\mathrm{rad/sec}$			No mass added and No L.P.					
$A_0 = 0.1\,\mathrm{in}^2$			Modify C.S.A. of all members					
Link	Area (in^2)	Stress (psi)	Link	Area (in^2)	Stress (psi)	Link	Area (in^2)	Stress (psi)
103	0.1000	29753.86	137	0.1000	18366.43	171	0.1000	14689.49
104	0.6552	-29999.94	138	0.1000	17759.68	172	0.1000	14645.89
105	2.6423	-29999.98	139	0.1000	295.18	173	0.1000	16707.26
106	0.1000	-15822.69	140	1.0017	-30000.09	174	0.1000	16539.73
107	0.1000	-5662.55	141	0.1000	29656.65	175	0.1000	20287.95
108	1.6908	-30000.01	142	0.8676	-30000.00	176	0.1000	19702.22
109	0.1000	4185.34	143	3.8707	-29999.98	177	0.1000	263.45
110	0.1000	-26297.32	144	0.1000	-16073.43	178	0.8405	-30000.07
111	2.6240	-29999.97	145	0.1000	-5635.38	179	0.1000	28680.80
112	0.3852	-29999.88	146	2.2619	-30000.01	180	1.0483	-30000.03
113	0.1000	25943.77	147	0.1000	3909.08	181	5.2502	-29999.99
114	1.3402	-30000.08	148	0.1000	-26504.17	182	0.1000	-15357.17
115	0.4127	29999.98	149	3.7019	-29999.97	183	0.1000	-12768.08
116	0.1000	16885.88	150	0.4750	-29999.99	184	2.8322	-30000.01
117	0.1000	16126.35	151	0.1000	25828.66	185	0.1000	10791.47
118	0.2211	29999.95	152	1.6170	-30000.07	186	0.1000	-27676.04
119	0.6670	-30000.13	153	0.5333	30000.03	187	4.8595	-29999.97
120	0.7956	-29999.99	154	0.1000	16744.01	188	0.5843	-30000.05
121	0.1000	8703.90	155	0.1000	15340.74	189	0.1000	26622.73
122	3.5332	-29999.98	156	0.2882	30000.06	190	1.8135	-30000.05
123	0.1000	-5453.91	157	0.5064	-30000.12	191	0.6420	30000.06
124	0.1000	-16091.47	158	0.9832	-30000.03	192	0.1000	1158.00
125	1.9256	-30000.02	159	0.1000	9679.90	193	1.0265	30000.03
126	0.1000	-25196.08	160	4.9132	-29999.99	194	1.3374	30000.04
127	0.1000	2764.21	161	0.1000	-11096.94	195	1.3260	-30000.05
128	3.3646	-29999.96	162	0.1000	-16923.70	196	6.4342	-29999.99
129	0.1000	12531.93	163	2.4963	-30000.01	197	0.9418	-30000.01
130	0.4292	-29999.98	164	0.1000	-24667.75	198	2.8759	-30000.01
131	1.2810	-30000.08	165	0.1000	7897.24	199	5.7186	-29999.98
132	0.1000	-10034.82	166	4.5228	-29999.97	200	2.5065	-30000.04
133	0.1000	17175.54	167	0.1000	11738.09			
134	0.1000	16979.81	168	0.5334	-30000.05			
135	0.1000	17079.98	169	1.4778	-30000.06			
136	0.1000	16843.17	170	0.1000	-10000.42			

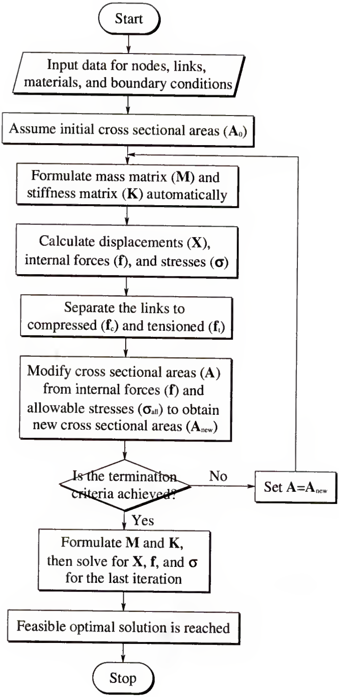
Start
Input data for nodes, links, materials, and boundary conditions
Assume initial cross sectional areas ($\mathbf{A}_0$)
Formulate mass matrix (**M**) and stiffness matrix (**K**) automatically
Calculate displacements (**X**), internal forces (**f**), and stresses ($\boldsymbol{\sigma}$)
Separate the links to compressed ($\mathbf{f}_c$) and tensioned ($\mathbf{f}_t$)
Modify cross sectional areas (**A**) from internal forces (**f**) and allowable stresses ($\boldsymbol{\sigma}_{all}$) to obtain new cross sectional areas ($\mathbf{A}_{new}$)
Is the termination criteria achieved?
No
Set $\mathbf{A}=\mathbf{A}_{new}$
Yes
Formulate **M** and **K**, then solve for **X**, **f**, and $\boldsymbol{\sigma}$ for the last iteration
Feasible optimal solution is reached
Stop

Figure 3.1: Flowchart of solution algorithm by the successive iteration approach

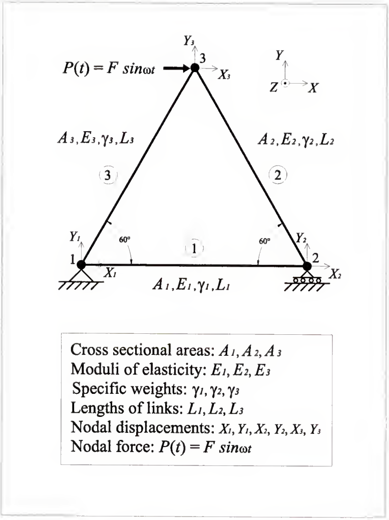
Y_3
3
$P(t) = F\ sin\omega t$
X_3
Y
Z
X
A_3, E_3, γ_3, L_3
A_2, E_2, γ_2, L_2
3
2
Y_1
60°
1
60°
Y_2
1
2
X_1
X_2
A_1, E_1, γ_1, L_1

Cross sectional areas: A_1, A_2, A_3
Moduli of elasticity: E_1, E_2, E_3
Specific weights: $\gamma_1, \gamma_2, \gamma_3$
Lengths of links: L_1, L_2, L_3
Nodal displacements: $X_1, Y_1, X_2, Y_2, X_3, Y_3$
Nodal force: $P(t) = F\ sin\omega t$

Figure 3.2: Simple three-link truss

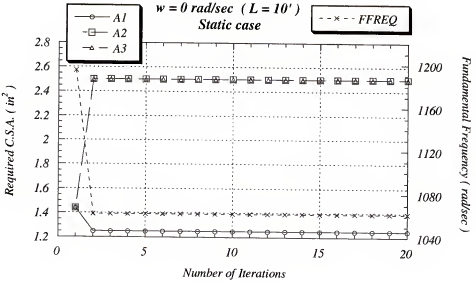

Figure 3.3: Convergent performance for $\omega = 0\,\mathrm{rad/sec}$

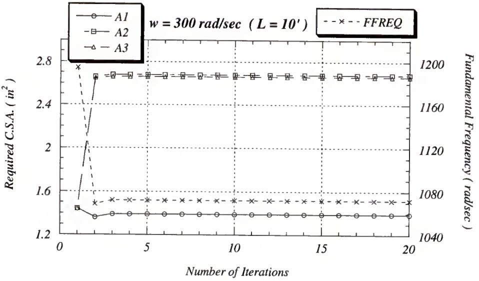

Figure 3.4: Convergent performance for $\omega = 300\,\mathrm{rad/sec}$

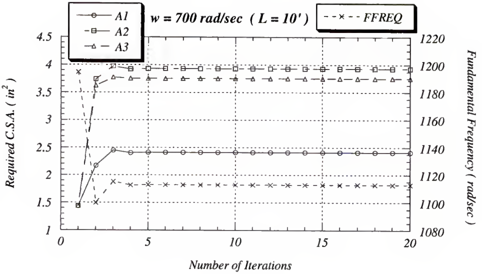

Figure 3.5: Convergent performance for $\omega = 700\,\mathrm{rad/sec}$

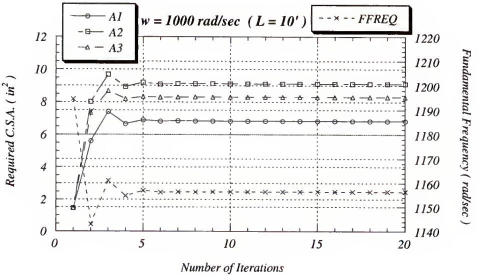

Figure 3.6: Convergent performance for $\omega = 1000\,\mathrm{rad/sec}$

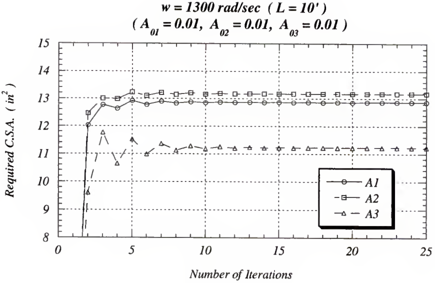

Figure 3.7: Dependency on initial values for arbitrarily chosen cross sectional areas

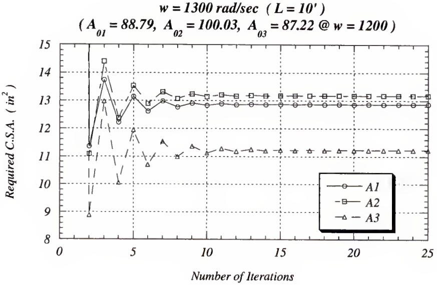

Figure 3.8: Dependency on initial values for cross sectional areas obtained for $\omega = 1200\,\mathrm{rad/sec}$

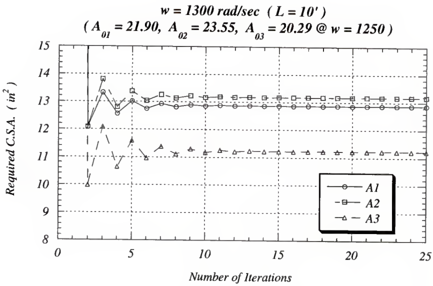

Figure 3.9: Dependency on initial values for cross sectional areas obtained for $\omega =$ 1250 rad/sec

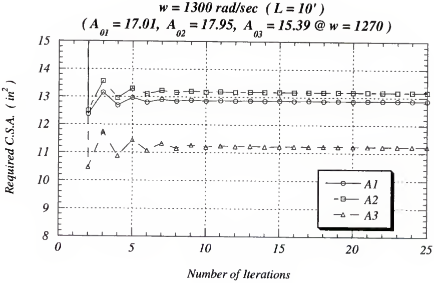

Figure 3.10: Dependency on initial values for cross sectional areas obtained for $\omega =$ 1270 rad/sec

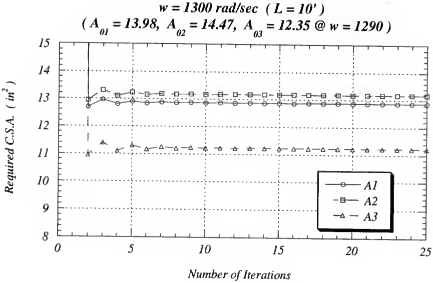

Figure 3.11: Dependency on initial values for cross sectional areas obtained for $\omega =$ 1290 rad/sec

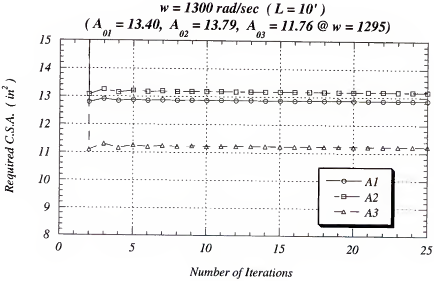

Figure 3.12: Dependency on initial values for cross sectional areas obtained for $\omega =$ 1295 rad/sec

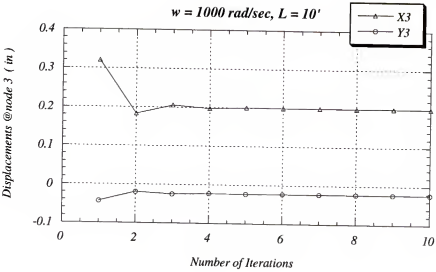

Figure 3.13: Displacements at top node for $\omega = 1000\,\mathrm{rad/sec}$

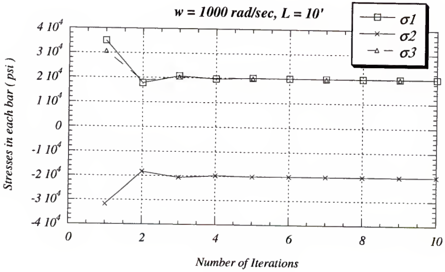

Figure 3.14: Stresses in each link for $\omega = 1000\,\mathrm{rad/sec}$

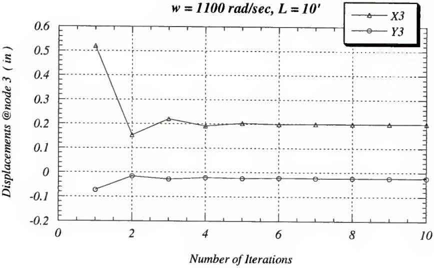

Figure 3.15: Displacements at top node for $\omega = 1100\,\mathrm{rad/sec}$

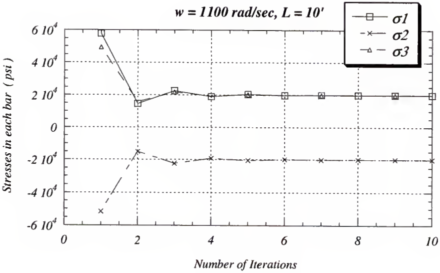

Figure 3.16: Stresses in each link for $\omega = 1100\,\mathrm{rad/sec}$

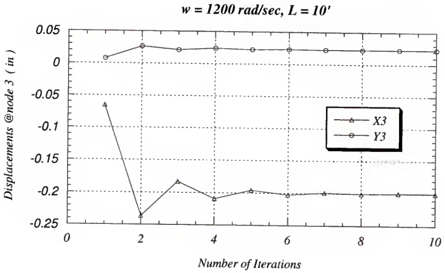

Figure 3.17: Displacements at top node for $\omega = 1200\,\mathrm{rad/sec}$

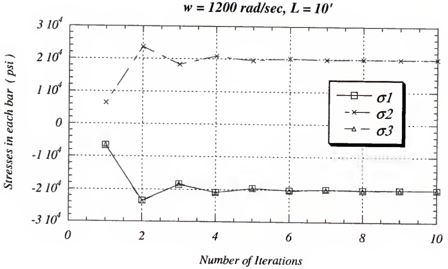

Figure 3.18: Stresses in each link for $\omega = 1200\,\mathrm{rad/sec}$

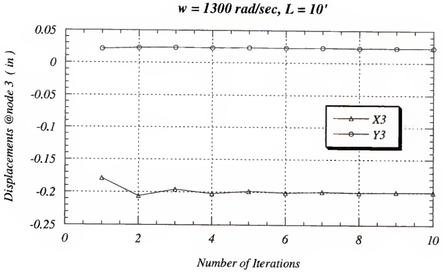

Figure 3.19: Displacements at top node for $\omega = 1300\,\mathrm{rad/sec}$

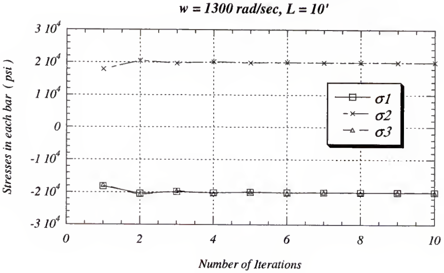

Figure 3.20: Stresses in each link for $\omega = 1300\,\mathrm{rad/sec}$

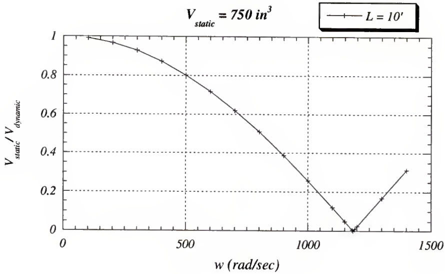

Figure 3.21: Optimum volume ratios of the three-link truss for a wide range of forcing frequencies (I)

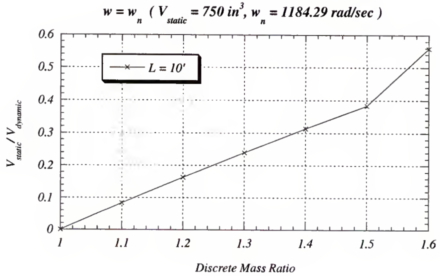

Figure 3.22: Optimum volume ratios vs. discrete values of added mass for resonant situation of the three-link truss

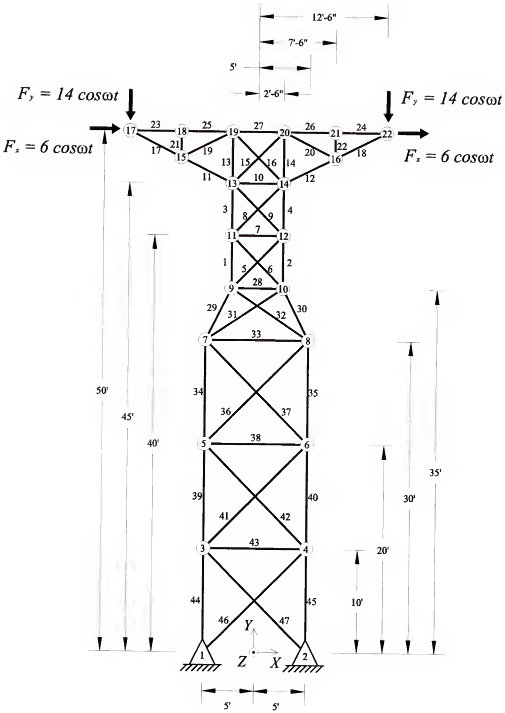

Figure 3.23: Forty-seven-member tower

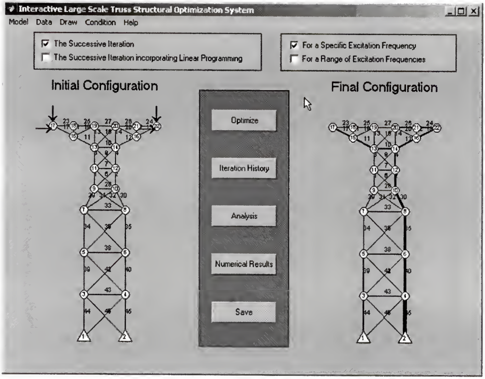

☑ The Successive Iteration
☐ The Successive Iteration incorporating Linear Programming

☑ For a Specific Excitation Frequency
☐ For a Range of Excitation Frequencies

Figure 3.24: Optimum design of forty-seven-member tower for $\omega = 50$ rad/sec

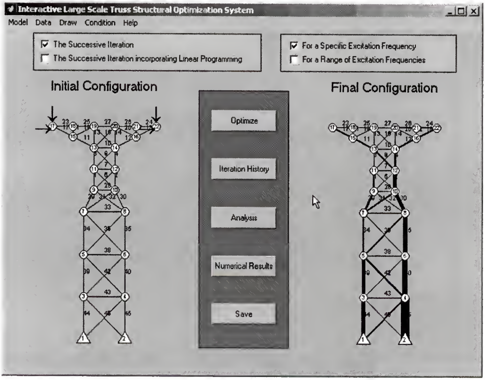

☑ The Successive Iteration
☐ The Successive Iteration incorporating Linear Programming

☑ For a Specific Excitation Frequency
☐ For a Range of Excitation Frequencies

Figure 3.25: Optimum design of forty-seven-member tower for $\omega = 200$ rad/sec

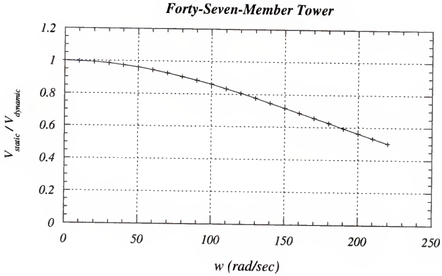

Figure 3.26: Optimum volume ratios of the forty-seven-member tower for a wide range of forcing frequencies (I)

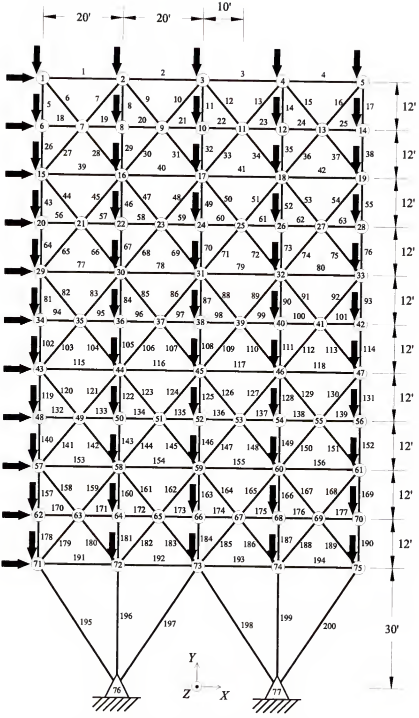

Figure 3.27: Two-hundred-member structure

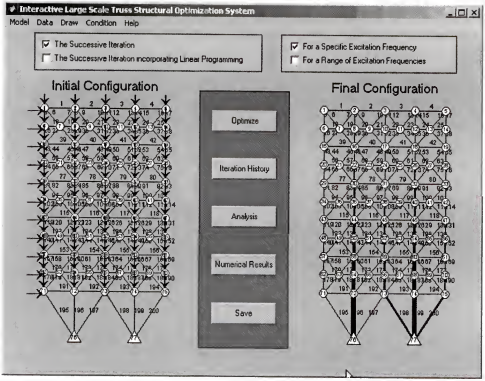

☑ The Successive Iteration

☐ The Successive Iteration incorporating Linear Programming

☑ For a Specific Excitation Frequency

☐ For a Range of Excitation Frequencies

Figure 3.28: Optimum design of two–hundred-member structure for $\omega = 20$ rad/sec

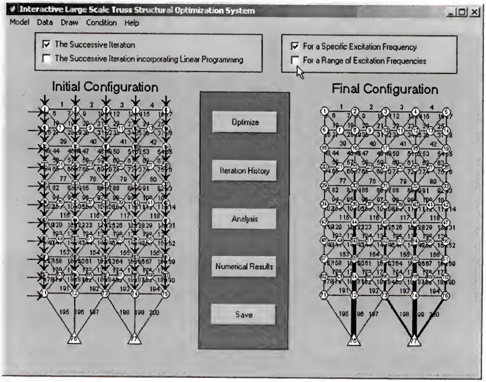

☑ The Successive Iteration

☐ The Successive Iteration incorporating Linear Programming

☑ For a Specific Excitation Frequency

☐ For a Range of Excitation Frequencies

Figure 3.29: Optimum design of two–hundred-member structure for $\omega = 80$ rad/sec

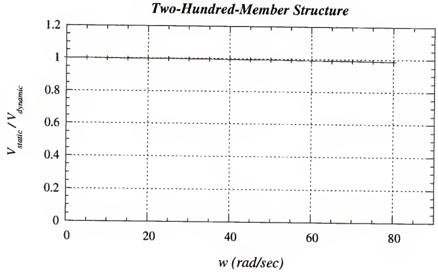

Figure 3.30: Optimum volume ratios of the two-hundred-member structure for a wide range of forcing frequencies (I)

CHAPTER 4
SOLUTION ALGORITHM BY INCORPORATING LINEAR PROGRAMMING

As an extension of the successive iteration approach presented in the previous chapter, an algorithm incorporating linear programming is developed based on the displacement field (or mode shape) obtained by successive iteration. One benefit of this new algorithm is that the oscillatory behavior which occurs at high frequency excitations when using the successive iteration approach alone can be overcome by incorporating linear programing.

4.1 Linear Programming and Simplex Techniques

Linear programming (LP) is a fundamental mathematical programming method used in solving linear optimization problems. The characteristic of the problems is that the objective function and all the constraints are expressed in linear terms of the design parameters. In n-dimensional space, the objective function and constraints are all hypersurfaces, and each hypersurface of the objective function corresponds to some specific value of the objective function. In three-dimensional space, the hypersurfaces reduce to a family of planes, called iso-merit surfaces, and the point where the constant objective hyperplane touches the constraint hypersurface (or hypersurfaces) is the point for the optimal solution; therefore, the optimal solution is expected to occur at a vertex of the design region. Furthermore, the following fundamental theorem of linear programming showing the exclusiveness of the optimal solution finding has been proved by Chvátal [63]:

Theorem 1 *For the linear programming problems of the form*

$$\begin{aligned} &\textit{Maximize} \quad && \mathbf{CX} \\ &\textit{Subject to} \quad && \begin{cases} \mathbf{AX} = \mathbf{b} \\ \mathbf{X}_l \le \mathbf{X} \le \mathbf{X}_u \end{cases} \end{aligned} \tag{4.1}$$

It has the following three properties:

(1) If it has no optimal solution, then it is either infeasible or unbounded.

(2) If it has a feasible solution, then it has a normal basic feasible solution providing A has full row rank.

(3) If it has an optimal solution, than it has a normal basic optimal solution providing A has full row rank.

Before 1940s, optimization techniques on system of equations were essentially heuristics. The first systematic method, called the simplex method, of solving the general linear programming problem was developed by Dantzig [68] in the late 1940s. The simplex method observes that the feasible solution set of such linear programs are convex, which means that the feasible solution set of a linear program of n variables can be expressed as a convex polygon in n-dimensional space. At the same time, the inequality constraints have been transformed into a set of linear equality constraints by introducing a set of non-negative slack variables. The main strategy of the simplex method is that of successive improvements: find a set of feasible solution, then try to proceed to another set of "better" feasible solution. After repeating this process a finite number of times, a guaranteed optimal solution, if it exists, will be eventually reached. In summary, the simplex method uses a systematic process for generating and testing feasible points in order to obtain an optimal solution to a linear program.

However, on account of computational efficiency and numerical accuracy, the search of an optimal solution could take an extended period of time and involve a great deal of computations, especially for large problems involving a very large number of design variables. Hence, many implementations of the simplex method have been developed to address these specific problems. Among those, the revised simplex method, the two-phase simplex method, the dual simplex procedure, and the primal-dual algorithm are popular implementations, and they are discussed by Papadimitriou and Steiglitz [69], Jeter [70], and Chvátal [63]. As for this study, the optimization toolbox in MATLAB has been used. The linear programming algorithm in the optimization toolbox is based on LIPSOL [71], which is a variant of Mehrotra's predictor-corrector algorithm [72], a primal-dual interior-point method. It is so called since both the primal and the dual programs are solved simultaneously. Details can be found in the paper by Zhang [71] and documentation in MATLAB optimization toolbox.

4.2 Topology of the System Matrices

In the current section, the topology of the system matrices will be generated by derivation. The formulation is unique since it is derived by an unconventional manner in contrast with those by common matrix or finite element methods [15, 73]. Although matrix or finite element methods are rather popular and easily implemented in computer program for many problems, they are too cumbersome to carry out the computational implementation of the problem under investigation because the design variables are difficult to be extracted during the process of forming and assembling the system matrices. This situation can be overcome by embracing the proposed procedure described in this section since the design parameters exist in a global manner without assemblage process. Moreover, this procedure is easy to implement in computer codes.

4.2.1 General Cases

One formulation of the governing differential equations introduced in Chapter 2 will be used as a starting point for the reason just mentioned in the last paragraph.

This starting point is from Seireg's approach [62, p.69] and is restated here:

$$M\ddot{x} = \sum F_x = -\left[\sum_{i=1}^{N} l_i^2 k_i\right] x - \left[\sum_{i=1}^{N} l_i m_i k_i\right] y - \left[\sum_{i=1}^{N} l_i n_i k_i\right] z \tag{4.2}$$

$$M\ddot{y} = \sum F_y = -\left[\sum_{i=1}^{N} m_i l_i k_i\right] x - \left[\sum_{i=1}^{N} m_i^2 k_i\right] y - \left[\sum_{i=1}^{N} m_i n_i k_i\right] z \tag{4.3}$$

$$M\ddot{z} = \sum F_z = -\left[\sum_{i=1}^{N} n_i l_i k_i\right] x - \left[\sum_{i=1}^{N} n_i m_i k_i\right] y - \left[\sum_{i=1}^{N} n_i^2 k_i\right] z \tag{4.4}$$

where

$M \equiv$ mass of the node

$x, y, z \equiv$ displacement of the node in x, y, and z directions

$k_i \equiv$ stiffness of the ith link

$l_i,\ m_i, n_i \equiv$ directional *cosine* for the ith link

These equations of motion can be extended to a system of elastically connected nodes by considering relative displacement for x, y, and z in the equations. Simultaneously, the external loads can also be incorporated in the equations. Therefore, the extended version is shown as follows:

$$M_j\ddot{x}_j = -\sum_{i=1}^{N} l_i^2 k_i \left(x_j - x_i\right) - \sum_{i=1}^{N} l_i m_i k_i \left(y_j - y_i\right) - \sum_{i=1}^{N} l_i n_i k_i \left(z_j - z_i\right) + \left(R_j\right)_x \tag{4.5}$$

$$M_j\ddot{y}_j = -\sum_{i=1}^{N} m_i l_i k_i \left(x_j - x_i\right) - \sum_{i=1}^{N} m_i^2 k_i \left(y_j - y_i\right) - \sum_{i=1}^{N} m_i n_i k_i \left(z_j - z_i\right) + \left(R_j\right)_y \tag{4.6}$$

$$M_j\ddot{z}_j = -\sum_{i=1}^{N} n_i l_i k_i \left(x_j - x_i\right) - \sum_{i=1}^{N} n_i m_i k_i \left(y_j - y_i\right) - \sum_{i=1}^{N} n_i^2 k_i \left(z_j - z_i\right) + \left(R_j\right)_z \tag{4.7}$$

where

$M_j \equiv$ mass of the jth node

$x_j, y_j, z_j \equiv$ displacement of the jth node in x, y, and z directions

$(R_j)_x, (R_j)_y, (R_j)_z \equiv$ external force at the jth node in x, y, and z directions

Subsequently, using the proposed model for the truss member described in Chapter 2, that is, $M = 0.40528\,\rho AL$ and $k = AE/L$, the above equations of motion can be rearranged as follows:

$$\sum_{i=1}^{N}\{\left[l_i^2(x_j - x_i) + l_i m_i(y_j - y_i) + l_i n_i(z_j - z_i)\right]\left(\frac{E_i}{L_i}\right) - 0.40528\rho_i L_i \omega^2 x_j\} A_i = (R_j)_x \tag{4.8}$$

$$\sum_{i=1}^{N}\{\left[m_i l_i(x_j - x_i) + m_i^2(y_j - y_i) + m_i n_i(z_j - z_i)\right]\left(\frac{E_i}{L_i}\right) - 0.40528\rho_i L_i \omega^2 y_j\} A_i = (R_j)_y \tag{4.9}$$

$$\sum_{i=1}^{N}\{\left[n_i l_i(x_j - x_i) + n_i m_i(y_j - y_i) + n_i^2(z_j - z_i)\right]\left(\frac{E_i}{L_i}\right) - 0.40528\rho_i L_i \omega^2 z_j\} A_i = (R_j)_z \tag{4.10}$$

where

$\omega \equiv$ forcing frequency

$\rho_i \equiv$ density of the ith link

$A_i \equiv$ cross sectional area of the ith link

$L_i \equiv$ length of the ith link

$E_i \equiv$ modulus of elasticity of the ith link

In two-dimensional space, the equations can be reduced to the following:

$$\sum_{i=1}^{N} \left\{ \left[l_i^2 (x_j - x_i) + l_i m_i (y_j - y_i)\right] \left(\frac{E_i}{L_i}\right) - 0.40528 \rho_i L_i \omega^2 x_j \right\} A_i = (R_j)_x \quad (4.11)$$

$$\sum_{i=1}^{N} \left\{ \left[m_i l_i (x_j - x_i) + m_i^2 (y_j - y_i)\right] \left(\frac{E_i}{L_i}\right) - 0.40528 \rho_i L_i \omega^2 y_j \right\} A_i = (R_j)_y \quad (4.12)$$

This final algebraic form can be recast into a matrix form so that it is convenient for computer handling. To demonstrate this method, we can use the simple three-link truss described in Chapter 3 as an example: Assume A_i is the cross sectional area for the ith link and $(R_j)_x$ and $(R_j)_y$ represent the reaction at the jth node in x and y directions, the topology of the system matrices of the transformed equations can be written as:

$$\begin{bmatrix} \times & \times & \times & -1 & 0 & 0 \\ \times & \times & \times & 0 & -1 & 0 \\ \times & \times & \times & 0 & 0 & 0 \\ \times & \times & \times & 0 & 0 & -1 \\ \times & \times & \times & 0 & 0 & 0 \\ \times & \times & \times & 0 & 0 & 0 \end{bmatrix}_{6\times6} \begin{Bmatrix} A_1 \\ A_2 \\ A_3 \\ (R_1)_x \\ (R_1)_y \\ (R_2)_y \end{Bmatrix}_{6\times1} = \begin{Bmatrix} 0 \\ 0 \\ 0 \\ 0 \\ 50000 \\ 0 \end{Bmatrix}_{6\times1} \quad (4.13)$$

In general, suppose a structure has n links and m nodes, and the external forces in x and y directions at the ith node can be represented by $(F_i)_x$ and $(F_i)_y$ with A_i as the cross sectional area of the ith link. If node 1 and node 2 are chosen to be the structural supports, that is, the support reactions are $(R_1)_x$, $(R_1)_y$, $(R_2)_x$, $(R_2)_y$, then the topology of the system matrices will be cast in a general form:

$$\begin{bmatrix} \mathbf{AA}_{11} & \mathbf{AA}_{12} \\ \mathbf{AA}_{21} & \mathbf{AA}_{22} \end{bmatrix}_{2m\times(n+4)} \begin{Bmatrix} \mathbf{BB}_1 \\ \mathbf{BB}_2 \end{Bmatrix}_{(n+4)\times1} = \begin{Bmatrix} \mathbf{CC}_1 \\ \mathbf{CC}_2 \end{Bmatrix}_{2m\times1} \quad (4.14)$$

where

$$\mathbf{AA}_{11} \equiv \text{some } \ (4 \times n) \ \text{ matrix} \tag{4.15}$$

$$\mathbf{AA}_{21} \equiv \text{some } \ (2m-4) \times n \text{ matrix} \tag{4.16}$$

$$\mathbf{AA}_{12} = -\mathbf{I}_{4\times 4} \tag{4.17}$$

$$\mathbf{AA}_{22} = \mathbf{0}_{(2m-4)\times 4} \tag{4.18}$$

$$\mathbf{BB}_1 = \left\{ \begin{matrix} A_1 \\ \vdots \\ A_n \end{matrix} \right\}_{n\times 1} \tag{4.19}$$

$$\mathbf{BB}_2 = \left\{ \begin{matrix} (R_1)_x \\ (R_1)_y \\ (R_2)_x \\ (R_2)_y \end{matrix} \right\}_{4\times 1} \tag{4.20}$$

$$\mathbf{CC}_1 = \mathbf{0}_{4\times 1} \tag{4.21}$$

$$\mathbf{CC}_2 = \left\{ \begin{matrix} (F_3)_x \\ (F_3)_y \\ \vdots \\ \left(F_{\frac{2m-4}{2}}\right)_x \\ \left(F_{\frac{2m-4}{2}}\right)_y \end{matrix} \right\}_{(2m-4)\times 1} \tag{4.22}$$

By using the notation for the matrix and vectors gives the following form:

$$[\mathbf{\Sigma}]\{\mathcal{A}\} = \{\mathcal{F}\} \tag{4.23}$$

where

$$[\Sigma] = \begin{bmatrix} \mathbf{AA}_{11} & \mathbf{AA}_{12} \\ \mathbf{AA}_{21} & \mathbf{AA}_{22} \end{bmatrix}_{2m\times(n+4)} \tag{4.24}$$

$$\{\mathcal{A}\} = \begin{Bmatrix} \mathbf{BB}_1 \\ \mathbf{BB}_2 \end{Bmatrix}_{(n+4)\times 1} \tag{4.25}$$

$$\{\mathcal{F}\} = \begin{Bmatrix} \mathbf{CC}_1 \\ \mathbf{CC}_2 \end{Bmatrix}_{2m\times 1} \tag{4.26}$$

Since this approach deals with information nodal-wise, the information about every link connected to any node should be given as an input to the computer. The matrix ($[\Sigma]$) is so named since the vector ($\{\mathcal{A}\}$) consists of mostly cross sectional areas and the vector ($\{\mathcal{F}\}$) is a force vector.

In summary, the advantage of adopting the proposed approach is that it deals with information nodal-wise and globally. Therefore, information can be easily input into the computer and handled by the linear programming algorithm. In contrast, the matrix methods handle information elemental-wise and needs to assemble elemental information in order to obtain global information; they are too cumbersome to carry out the computational implementation on the considered optimization problem because the design variables are difficult to be extracted during the process of forming and assembling the system matrices.

4.2.2 Adding Discrete Masses at the Joints

As stated in Chapter 3, another design consideration can improve the performance by adding discrete masses at the nodes.

A three degrees of freedom system is used to illustrate the approach. Suppose $\mathbf{M}^*$ includes the masses of the links, M_i, and extra masses, m_i, where i is equal to 1, 2, and 3. Starting from the following equations:

$$\left(\mathbf{K} - \omega^2 \mathbf{M}^*\right) \mathbf{X} = \mathbf{F} \tag{4.27}$$

where

$$\mathbf{M}^* \equiv \text{body mass} + \text{added mass}$$

In the example of 3 degrees of freedom system:

$$\left(\begin{bmatrix} \times & \times & \times \\ \times & \times & \times \\ \times & \times & \times \end{bmatrix} - \omega^2 \begin{bmatrix} M_1 + m_1 & 0 & 0 \\ 0 & M_2 + m_2 & 0 \\ 0 & 0 & M_3 + m_3 \end{bmatrix} \right) \begin{Bmatrix} x_1 \\ x_2 \\ x_3 \end{Bmatrix} = \begin{Bmatrix} F_1 \\ F_2 \\ F_3 \end{Bmatrix} \tag{4.28}$$

Those added mass terms can be rearranged and moved to the right; therefore,

$$\left(\begin{bmatrix} \times & \times & \times \\ \times & \times & \times \\ \times & \times & \times \end{bmatrix} - \omega^2 \begin{bmatrix} M_1 & 0 & 0 \\ 0 & M_2 & 0 \\ 0 & 0 & M_3 \end{bmatrix} \right) \begin{Bmatrix} x_1 \\ x_2 \\ x_3 \end{Bmatrix} = \begin{Bmatrix} F_1 \\ F_2 \\ F_3 \end{Bmatrix} + \omega^2 \begin{Bmatrix} m_1 x_1 \\ m_2 x_2 \\ m_3 x_3 \end{Bmatrix} \tag{4.29}$$

Finally, the equations can be recast into a similar form to the last section since the left hand side of the equations is invariant; as a result, we reach the following form:

$$[\boldsymbol{\Sigma}] \{\mathcal{A}\} = \{\mathcal{F}^*\} \tag{4.30}$$

where

$$\{\mathcal{F}^*\} \text{ include the added mass}$$

4.3 Linear Program for This Study

According to the last section, our linear program can be formulated as follows:

$$\begin{array}{ll} \text{Find} & \mathbf{A} \\ \text{To Minimize} & W = \sum_{i=1}^{n} \rho_i A_i L_i \\ \text{Subject to} & \left\{ \begin{array}{l} [\Sigma]\{\mathcal{A}\} = \{\mathcal{F}\} \\ (A_i)_{lower} \le A_i \end{array} \right. \end{array} \tag{4.31}$$

$$n = \text{number of links}$$

Since the displacements obtained by the successive iteration approach are known, the design variables are the cross sectional areas and the reaction forces.

Accordingly, the solution algorithm by incorporating linear programming can be described as follows:

(1) Apply the stress constraint in order to reach the fully stressed structure for static loading or low frequency excitation.

(2) Find the displacements ($\mathbf{X}$) for the solution obtained by successive iterations.

(3) Use $\mathbf{X}$ as an input in the linear program to solve for cross the sectional areas ($\mathbf{A}$) at any forcing frequency which minimize the weight.

(4) Check if the stress in any member exceeds the allowable stress.

(5) Use stress constraints in the linear program as needed for any overstressed member.

The flowchart of this solution algorithm is given in Figure 4.1.

4.4 Improvements in Previous Example Problems by Incorporating Linear Programming

As mentioned in Section 3.3, in some problems for the cases of forcing frequencies greater than a certain level, using the successive iteration approach alone seemingly could not find convergent results. In this section, the solution algorithm which incorporates linear programming is examined and indeed provides a remedy for this situation.

For the three-link truss, the optimum volume ratios for a wide range of forcing frequencies by incorporating linear programming are shown in Figure 4.2. Compared with Figure 3.21, it can be seen that the adversely non-convergence situation has been controlled. The non-convergence situation exhibits oscillatory behavior of the weight during iteration when using the successive iteration approach alone. A reasonable explanation is the alternatively increasing and decreasing nature of the stresses ($\boldsymbol{\sigma}$) and cross sectional areas (**A**) during each successive iteration for a specific higher forcing frequency, since the forces (**F**) are invariant. Therefore, from the information given in Figure 4.2, both the first and the second resonances of the structure can be reached using the solution algorithm by incorporating linear programming. The reason behind this success is due to the observation of the displacement field (or mode shape) from the static and lower frequency cases. According to the results of these cases, the displacement field (or mode shape) does not change significantly between zero and the first resonance frequency of the structure. In a similar fashion, the displacement field does not change much between the first resonance and the second resonance of the structure. However, the mode shape does change when frequencies move from the first stage to the second stage. In other words, for frequencies above the first resonance, the mode shape seems to shift to another configuration. The corresponding mode shapes for both stages are shown in Figure 4.3 and Figure 4.4.

By adding discrete masses at the nodes, the adverse situation at resonance can be alleviated. Figure 4.5 illustrates this idea by doubling the joint mass at each node. At the point of resonance for the original structure without adding masses, the volume ratio increases to about 0.7 by adding masses. In other words, the minimum weight of the structure with added mass has been reduced drastically. Therefore, since structures are usually designed for a certain range of frequencies, good designs can be achieved by taking into account this design variable if the resonance of the original structure happens to fall into the design region.

In the case of forty-seven-member tower, the optimum volume ratios for a wide range of forcing frequencies by incorporating linear programming are shown in Figure 4.6. Using the successive iteration approach alone, convergence results can only reach 220 rad/sec as shown in Figure 3.26. By incorporating linear programming, it can be shown that results can be reached for an extended range of frequencies.

For the two-hundred-member structure, the optimum volume ratios for a wide range of forcing frequencies by incorporating linear programming are shown in Figure 4.7. As seen in Figure 3.30, optimum weight of the structure can be obtained up to 80 rad/sec. Figure 4.7 shows the improvement of the performance by incorporating linear programming technique. Results can now be reached up to 240 rad/sec.

In summary it can be seen from the example problems demonstrated in this chapter that whenever the convergent solution can not be found by using the successive iteration approach alone, linear programming technique can be incorporated to remedy this situation up to a certain level of higher frequencies. Therefore, when design for a certain range of frequencies, if a convergence problem occurs for certain higher frequencies, linear programming technique can be applied by using the successive iteration solution for a lower frequency than the one of interest. Accordingly, the design domain can be extended to higher frequencies, which may have convergence problems by using the successive iteration alone. It can not be ascertained that this procedure produces the best possible solution as will be addressed in Chapter 6 when a general recommended algorithm is discussed.

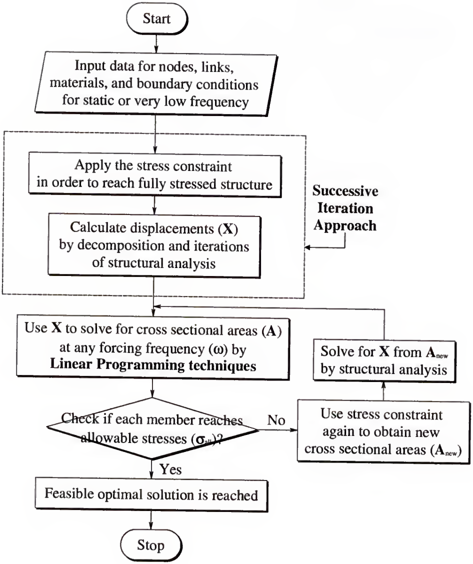
Start
Input data for nodes, links, materials, and boundary conditions for static or very low frequency
Apply the stress constraint in order to reach fully stressed structure
Calculate displacements (X) by decomposition and iterations of structural analysis
Successive Iteration Approach
Use X to solve for cross sectional areas (A) at any forcing frequency (ω) by Linear Programming techniques
Solve for X from A_new by structural analysis
Check if each member reaches allowable stresses (σ_all)?
No
Use stress constraint again to obtain new cross sectional areas (A_new)
Yes
Feasible optimal solution is reached
Stop

Figure 4.1: Flowchart of solution algorithm by incorporating linear programming

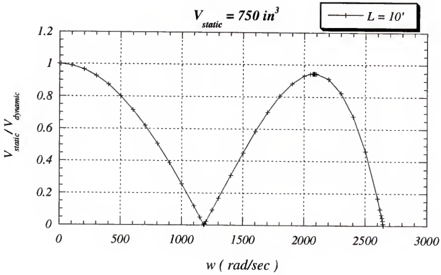

Figure 4.2: Optimum volume ratios of the three-link truss for a wide range of forcing frequencies (II)

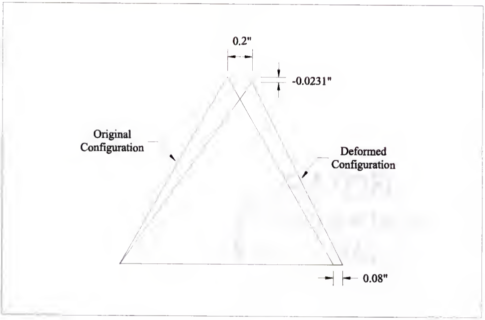

Figure 4.3: The first mode shape of the three-link truss

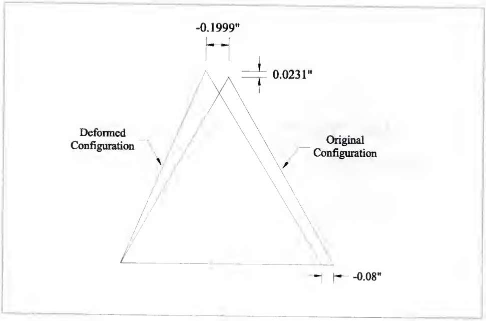

Figure 4.4: The second mode shape of the three-link truss

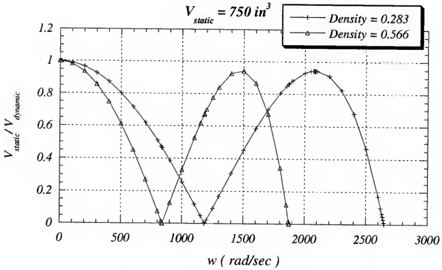

Figure 4.5: Optimum volume ratios of the three-link truss for added mass case

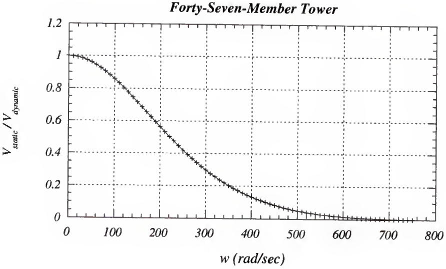

Figure 4.6: Optimum volume ratios of the forty-seven-member tower for a wide range of forcing frequencies (II)

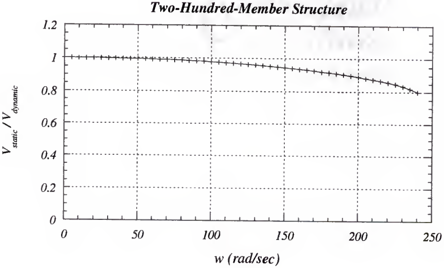

Figure 4.7: Optimum volume ratios of the two-hundred-member structure for a wide range of forcing frequencies (II)

CHAPTER 5
SOLUTION ALGORITHM BY NONLINEAR PROGRAMMING APPROACH

Nonlinear programming (NLP) methods can be used for optimizing both the geometry of the structure and the member sizes. Generally speaking, nonlinear programming problems are more difficult to solve than linear ones. A large number of algorithms have been proposed; however, there is seldom efficient general purpose NLP methods if they exist. In this chapter, one of the NLP methods will be introduced and applied to the example problems. One advantage of using NLP techniques is to generate a local optimum, which can be compared with the results obtained by the successive iteration approach or by incorporating linear programming as previously discussed.

5.1 Nonlinear Programming Techniques

In nonlinear programming (NLP) problems, some or all of the objective functions and constraint functions are not linear. A general NLP problems can be stated as follows:

$$\begin{array}{ll} \text{Find} & \mathbf{x} \\ \text{To minimize} & f(\mathbf{x}) \\ \text{Subject to} & \left\{ \begin{array}{l} \mathbf{g}(\mathbf{x}) \leq \mathbf{0} \\ \mathbf{h}(\mathbf{x}) = \mathbf{0} \end{array} \right. \end{array} \tag{5.1}$$

where

$$\mathbf{x} = (x_1, x_2, \cdots, x_n)^T \tag{5.2}$$

$$\mathbf{g} = (g_1, g_2, \cdots, g_m)^T \tag{5.3}$$

$$\mathbf{h} = (h_1, h_2, \cdots, h_k)^T \tag{5.4}$$

NLP problems can be categorized as unconstraint and constraint problems depending on whether **g** and **h** exist or not. Generally speaking, the optimization techniques can be classified into two different points of view. One is called optimality criteria or indirect approach in which optimality criteria are the conditions a function must fulfil at its optimum point. In this point of view, optimality criteria have to be derived from mathematical considerations. Consequently, all the solutions may need to be investigated to fulfil the optimality criteria that one derived; then, the most economical one from such a set will be selected. A direct derivation of all possible optimal solutions can be difficult if the number of optimality criteria is large and they are highly nonlinear. However, optimality criteria can be used for the iterative redesign of complex structures [74]. The other point of view is called search or direct approach. Starting with an estimate of the optimum design, or initial feasible solution. We try to change our feasible design in a manner that it becomes more and more economical by iterations until it cannot be improved any further. A solution of a NLP problem generally requires an iterative process to set up a direction of search (or a search path) at each major iteration. In this approach, we search the design region for optimum points. Usually, such a solution is a local optimum. If, by chance, the best of all local optima is found, then the global optimum can be reached. The global solution can be found by either some exhaustive search of the feasible set, or by showing the problem to be convex. Both processes can require extensive computations.

Usually, in practice, numerical methods for nonlinear optimization problems are needed since the analytical methods for solving some practical problems are either too awkward or not applicable at all, especially for large-scale problems. An accurate and efficient solution to the problem does not only depend on the size of the problem in terms of the number of design variables and constraints but also on behavior of the objective function and constraints. In constraint optimization, the general purpose is to transform the original problem into an easier subproblem that can then be solved and used as the basis of an iterative procedure. An efficient and currently popular approach is to use the Kuhn-Tucker (KT) equations as necessary conditions for optimality for a constrained optimization problem. If the problem is a convex programming problem, then the KT equations are both necessary and sufficient conditions for a global solution as stated previously. Referring to Equation (5.1), the KT equations can be derived from the Lagrange multiplier method. The Lagrange function (L) for the problem can be defined as

$$L = f\left(\mathbf{x}\right) + \boldsymbol{\lambda}_E^T \mathbf{h}\left(\mathbf{x}\right) + \boldsymbol{\lambda}_I^T \left(\mathbf{g}\left(\mathbf{x}\right) + \mathbf{s}^2\right) \tag{5.5}$$

where

$$\boldsymbol{\lambda}_E = \left(\left(\lambda_E\right)_1, \left(\lambda_E\right)_2, \cdots, \left(\lambda_E\right)_k\right) \tag{5.6}$$

$$\boldsymbol{\lambda}_I = \left(\left(\lambda_I\right)_1, \left(\lambda_I\right)_2, \cdots, \left(\lambda_I\right)_m\right) \tag{5.7}$$

$\boldsymbol{\lambda}_E$ and $\boldsymbol{\lambda}_I$ are Lagrange multipliers

In order to find a stationary point of the Lagrange function (L) for all $\mathbf{x}$ and $\boldsymbol{\lambda}$, the following equations have to be satisfied:

$$\frac{\partial L}{\partial x_j} \equiv \frac{\partial f}{\partial x_j} + \sum_{i=1}^{k} \left(\lambda_E\right)_i^* \frac{\partial h_i}{\partial x_j} + \sum_{i=1}^{m} \left(\lambda_I\right)_i^* \frac{\partial g_i}{\partial x_j} = 0 \tag{5.8}$$

$$\frac{\partial L}{\partial \left(\lambda_E\right)_i} \equiv h_i\left(\mathbf{x}^*\right) = 0 \qquad i = 1, \cdots, k \tag{5.9}$$

$$\frac{\partial L}{\partial \left(\lambda_I\right)_i} \equiv g_i\left(\mathbf{x}^*\right) + s_i^2 = 0 \qquad i = 1, \cdots, m \tag{5.10}$$

$$\frac{\partial L}{\partial s_i} \equiv 2\left(\lambda_I\right)_i^* s_i = 0 \qquad i = 1, \cdots, m \tag{5.11}$$

$$\left(\lambda_I\right)_i^* \geq 0 \qquad i = 1, \cdots, m \tag{5.12}$$

Equation (5.10) ensures that the inequality constraints are satisfied. Equation (5.11) states that either s_i or $(\lambda_I)_i$ is zero, which implies that either the constraint is active, that is $g_i = 0$, or it is inactive, that is $(\lambda_I)_i = 0$, which implies $g_i < 0$. Equation (5.11) is also known as the switching conditions or complementary slackness conditions. Equation (5.8) has a geometrical meaning. To see this, rearranging terms give

$$-\frac{\partial f}{\partial x_j} = \sum_{i=1}^{k} (\lambda_E)_i^* \frac{\partial h_i}{\partial x_j} + \sum_{i=1}^{m} (\lambda_I)_i^* \frac{\partial g_i}{\partial x_j} \tag{5.13}$$

This shows that negative gradient direction (steepest descent direction) for the objective function lies in the subspace spanned by the gradients of the constraints at the stationary point. In other words, $(-\nabla f)$ is a linear combination of the gradients of the constraints $\mathbf{g}$ and $\mathbf{h}$ with Lagrange multipliers $\boldsymbol{\lambda}_E$ and $\boldsymbol{\lambda}_I$ as the scalar parameters of the linear combination. The solution of the KT equations provides the basis for many constrained NLP algorithms. These algorithms attempt to compute directly the Lagrange multipliers. Constrained quasi-Newton methods guarantee superlinear convergence by accumulating second order information regarding the KT equations using a quasi-Newton updating procedure. These methods are commonly referred to as sequential quadratic programming (SQP) methods since a quadratic programming (QP) sub-problem is solved at each major iteration.

5.2 Sequential Quadratic Programming

Sequential quadratic programming (SQP) is a modern and powerful method in solving nonlinear programming problems. Schittowski [75] has tested a large number of problems by implementing a version of SQP and proved that it has superior performance to every other tested method in terms of efficiency, accuracy, and percentage of successful solutions. An overview of SQP can be found in Gill, Murray, and Wright [76], Powell [77], and Schittowski [75]. A general description of the method is stated below.

Most numerical methods for constrained optimization compute change in design by solving an approximate subproblem at each major iteration. This approximation or linearization is obtained by Taylor series expansions for the objective and constraint functions. First, we need to write first order approximation of Taylor series expansion about an estimate at the ith iteration in order to arrive an approximate subproblem. For the objective function, it can be written as

$$f\left(\mathbf{x}^{(i)} + \Delta\mathbf{x}^{(i)}\right) \cong f\left(\mathbf{x}^{(i)}\right) + \nabla f^{T}\left(\mathbf{x}^{(i)}\right)\Delta\mathbf{x}^{(i)} \tag{5.14}$$

and for the inequality and equality constraints, respectively, they can be expanded as

$$g_j\left(\mathbf{x}^{(i)} + \Delta\mathbf{x}^{(i)}\right) \cong g_j\left(\mathbf{x}^{(i)}\right) + \nabla g_j^{T}\left(\mathbf{x}^{(i)}\right)\Delta\mathbf{x}^{(i)} \leq 0 \tag{5.15}$$

$$h_p\left(\mathbf{x}^{(i)} + \Delta x^{(i)}\right) \cong h_p\left(\mathbf{x}^{(i)}\right) + \nabla h_p^{T}\left(\mathbf{x}^{(i)}\right)\Delta\mathbf{x}^{(i)} = 0 \tag{5.16}$$

where

$$j = 1, \cdots, m$$

$$p = 1, \cdots, k$$

Therefore, the linearized subproblem can be written as follows:

$$\begin{array}{ll} \text{Minimize} & \nabla f^{T}\left(\mathbf{x}^{(i)}\right)\Delta\mathbf{x}^{(i)} \\ \text{Subject to} & \left\{ \begin{array}{l} \nabla g_j^{T}\left(\mathbf{x}^{(i)}\right)\Delta\mathbf{x}^{(i)} \leq -g_j\left(\mathbf{x}^{(i)}\right) \\ \nabla h_p^{T}\left(\mathbf{x}^{(i)}\right)\Delta\mathbf{x}^{(i)} = -h_p\left(\mathbf{x}^{(i)}\right) \end{array} \right. \end{array} \tag{5.17}$$

Define $\mathbf{d} = \Delta\mathbf{x}^{(i)}$, the QP subproblem can be stated below:

$$\begin{array}{ll} \text{Minimize} & \nabla f^{T}\left(\mathbf{x}^{(i)}\right)\mathbf{d} + \frac{1}{2}\mathbf{d}^{T}\mathbf{H}^{(i)}\mathbf{d} \\ \text{Subject to} & \left\{ \begin{array}{l} \nabla g_j^{T}\left(\mathbf{x}^{(i)}\right)\mathbf{d} \leq -g_j\left(\mathbf{x}^{(i)}\right) \\ \nabla h_p^{T}\left(\mathbf{x}^{(i)}\right)\mathbf{d} = -\,h_p\left(\mathbf{x}^{(i)}\right) \end{array} \right. \end{array} \tag{5.18}$$

where $\mathbf{H}^{(i)}$ is a positive definite approximation to the Hessian of the Lagrangian function, which can be formulated as

$$L = f(\mathbf{x}) + \boldsymbol{\lambda}_E^T \mathbf{h}(\mathbf{x}) + \boldsymbol{\lambda}_I^T \mathbf{g}(\mathbf{x}) \tag{5.19}$$

$\mathbf{H}^{(i)}$ can be approximated using any of the Quasi-Newton or update methods. This QP subproblem can be solved by any QP algorithm. Many algorithms can be found for solving QP subproblems [76, 78]. The solution of the QP subproblem is used to form a new iteration which can be stated as

$$\mathbf{x}^{(i+1)} = \mathbf{x}^{(i)} + \Delta^{(i)}\mathbf{d}^{(i)} \tag{5.20}$$

where $\Delta^{(i)}$ is a step size which can be obtained by an appropriate line search procedure so that a sufficient minimization in a objective function is reached.

As for this study, the optimization toolbox of MATLAB has been used. In solving nonlinear optimization problems, MATLAB uses its version of implementation for the SQP method. It consists of three main stages:

(1) Updating of the Hessian matrix of the Lagrangian function,

(2) QP problem solution,

(3) Line search and objective function calculation.

In the first stage, Quasi-Newton approximation, which is based on finite-differencing calculated gradient, is calculated to approximate the Hessian. It also uses finite-differencing to approximate the Jacobian of the constraints when linearizing the constraints. In the second stage, to solve the QP subproblem using a combinatorial approach to determine which of the linearized constraints are active in determining the solution. Detail can be found in the documentation of MATLAB optimization toolbox.

5.3 Illustrative Problems

In this section, all the example problems used in Chapter 3 have been tested by NLP approach. The NLP problem can be formulated in the following:

$$
\begin{array}{ll}
\text{Find} & \mathbf{A} \\
\text{To minimize} & W = \sum\limits_{i=1}^{n} \rho_i A_i L_i \\
\text{Subject to} & \left\{ \begin{array}{c} \left(\mathbf{K} - \omega^2 \mathbf{M}\right) \mathbf{X} = \mathbf{F} \\ \boldsymbol{\sigma} \leq \boldsymbol{\sigma}_{allow} \\ \mathbf{A} \geq \mathbf{A}_{lower} \end{array} \right.
\end{array} \tag{5.21}
$$

The strategies used to test the example problems by NLP algorithm are stated as follows:

(1) Use **A** and **X** calculated from the successive iteration (SI) approach or by incorporating LP as initial input to the NLP algorithm.

(2) Use any $\mathbf{A}_0$ and calculate $\mathbf{X}_0$ from the equations of motion (EOM), then input $\mathbf{A}_0$ and $\mathbf{X}_0$ to the NLP algorithm.

(3) Use any arbitrary $\mathbf{A}_0$ and $\mathbf{X}_0$ as initial input to the NLP algorithm.

Afterwards, compare the results calculated from the NLP algorithm with the results obtained from algorithms of previous chapters. In this way, we can compare the performance in terms of accuracy and efficiency among these algorithms.

For the three-link truss case, one of the tested cases is tabulated in Table 5.1. It lists the results of each strategy and of the successive iteration approach for comparison, for $\omega = 500$ rad/sec. For such a simple structure, the minium weight by using the successive iteration approach is 264.9259 lb and the optimal weight by using NLP approach is 264.9258 lb for each different strategy used. The results show good correlation between the results from these approaches even for the most flexible choice of initial guess of strategy (3), although the algorithm usually requires an appropriate starting point. However, the CPU time can be greatly reduced by using the successive iteration approach even for this simple structure.

Table 5.2 to Table 5.9 list all detailed results of the forty-seven-member tower for different frequencies by using NLP approach. Unlike the three-link truss case, it is almost impossible to obtain any feasible solution by using strategy (2) or (3). Only strategy (1) can be found to be useful in finding the optimal results. Hence, for large-scale structures, the optimal solution finding is strongly dependent on the choice of initial guess of the design variables by using the NLP approach. If any appropriate starting point can not be provided, the usefulness of NLP approach will be greatly reduced. Compared with previous results, listed in Table 3.3 to Table 3.12, by using the successive iteration alone, the stresses and displacements obtained by NLP are approximately the same for each frequency case. Even for those low stressed members mentioned in Chapter 3, the stresses are almost of the same order for each case. The optimum weight by using NLP for each case is only slightly improved over the results by using the successive iteration approach alone. However, the CPU time by using NLP with the result of the successive iteration as a starting point, which are approximately six to sixty times of the CPU time by using the successive iteration alone with any arbitrary starting point in these cases, has been greatly extended if NLP is used.

In the case of the two-hundred-member structure, two of the tested results are tabulated in Table 5.10 to Table 5.15 by using NLP approach. As would be expected, only strategy (1) can be found to be useful in finding the optimal solution. Strategies (2) and (3) are both extremely difficult to proceed. For almost all of the tested cases, searching jobs of NLP keep cycling for several hours, no matter how the step size is changed, without any sign of stopping if any arbitrary starting point is selected. For both cases in Table 5.10 to Table 5.15, the stresses and displacements are approximately the same as those of the cases, listed in Table 3.14 to Table 3.24, shown in Chapter 3. The CPU time of using NLP approach with the result of the successive iteration as a starting point are about thirty-two times of that using the successive iteration approach alone with any arbitrary starting point in the tested cases. Furthermore, the optimum weight by using NLP for each case shows little improvement over the results by using the successive iteration approach alone.

To summarize, the most important issues of nonlinear programming approach concerning large-scale problems are the choice of the starting point and execution time. An appropriate initial guess needs to be provided in order to obtain feasible solution; otherwise, searching job for NLP becomes extremely difficult and, for most of the time, unsuccessful. For almost all of the tested cases, searching jobs of NLP keep cycling for several hours, no matter how the step size is changed, without any sign of stopping if any arbitrary starting point is selected. On the other hand, the successive iteration approach can provide a reasonable starting point for NLP. However, the results from both of these approaches are approximately the same in each tested case. As would be expected, the more the variables, the longer the CPU time is. Therefore, for the considered large-scale structures, NLP alone proved to be significantly inferior to the proposed approach. Comparisons between the proposed approach, which is described in Chapter 6, and the NLP approach for the forty-seven-member tower and the two-hundred-member structure are given in Table 5.16 and Table 5.17, respectively.

Table 5.1: NLP results for the three-link truss

	SI	Strategy (1)	Strategy (2)	Strategy (2)	Strategy (2)	Strategy (3)
$\mathbf{A}_0$ (in^2)	2	**A** from SI	0.1	2	5	0.1
$\mathbf{X}_0$ (in)	**	**X** from SI	**X** from EOM	**X** from EOM	**X** from EOM	0
A_1 (in^2)	1.7099	1.7099	1.7099	1.7099	1.7099	1.7099
A_2 (in^2)	3.0784	3.0784	3.0784	3.0784	3.0784	3.0784
A_3 (in^2)	3.0061	3.0061	3.0061	3.0061	3.0061	3.0061
X_2 (in)	0.0800	0.0800	0.0800	0.0800	0.0800	0.0800
X_3 (in)	0.2000	0.2000	0.2000	0.2000	0.2000	0.2000
Y_3 (in)	-0.0231	-0.0231	-0.0231	-0.0231	-0.0231	-0.0231
σ_1 (psi)	20000.00	20000.00	20000.00	20000.00	20000.00	20000.00
σ_2 (psi)	-20000.00	-20000.00	-20000.00	-20000.00	-20000.00	-20000.00
σ_3 (psi)	20000.00	20000.00	20000.00	20000.00	20000.00	20000.00
W (lb)	264.9259	264.9258	264.9258	264.9258	264.9258	264.9258
CPU TIME (sec)	0.02	0.391	1.0410	0.8610	5.0580	1.2320

	Strategy (3)	Strategy (3)	Strategy (3)	Strategy (3)	Strategy (3)	
$\mathbf{A}_0$ (in^2)	2	5	0.1	2	5	
$\mathbf{X}_0$ (in)	0	0	0.001	0.001	0.001	
A_1 (in^2)	1.7099	1.7099	1.7099	1.7099	1.7099	
A_2 (in^2)	3.0784	3.0784	3.0784	3.0784	3.0784	
A_3 (in^2)	3.0061	3.0061	3.0061	3.0061	3.0061	
X_2 (in)	0.0800	0.0800	0.0800	0.0800	0.0800	
X_3 (in)	0.2000	0.2000	0.2000	0.2000	0.2000	
Y_3 (in)	-0.0231	-0.0231	-0.0231	-0.0231	-0.0231	
σ_1 (psi)	20000.00	20000.00	20000.00	20000.00	20000.00	
σ_2 (psi)	-20000.00	-20000.00	-20000.00	-20000.00	-20000.00	
σ_3 (psi)	20000.00	20000.00	20000.00	20000.00	20000.00	
W (lb)	264.9258	264.9258	264.9258	264.9258	264.9258	
CPU TIME (sec)	1.0320	1.4320	3.3040	3.3450	1.6030	

Table 5.2: NLP results of the forty-seven-member tower for $\omega = 0$

<table>
<tr><th colspan="9">Forty-Seven-Member Tower (Force Excitation)</th></tr>
<tr><th colspan="3">$\omega = 0$</th><th colspan="6">No mass added</th></tr>
<tr><th colspan="9">Use results of $\omega = 0$ from SI as input into NLP</th></tr>
<tr><th rowspan="2">Link</th><th rowspan="2">Area
(in^2)</th><th rowspan="2">Stress
(psi)</th><th rowspan="2">Link</th><th rowspan="2">Area
(in^2)</th><th rowspan="2">Stress
(psi)</th><th colspan="3">Displacements (in)</th></tr>
<tr><th>node</th><th>x-dir</th><th>y-dir</th></tr>
<tr><td>1</td><td>0.8979</td><td>20000.00</td><td>26</td><td>1.7000</td><td>20000.00</td><td>1</td><td>0.0000</td><td>0.0000</td></tr>
<tr><td>2</td><td>2.8028</td><td>-15000.00</td><td>27</td><td>1.3728</td><td>20000.00</td><td>2</td><td>0.0000</td><td>0.0000</td></tr>
<tr><td>3</td><td>0.4293</td><td>20000.00</td><td>28</td><td>0.1000</td><td>-15000.00</td><td>3</td><td>0.0200</td><td>0.0080</td></tr>
<tr><td>4</td><td>1.8276</td><td>-15000.00</td><td>29</td><td>0.9934</td><td>20000.00</td><td>4</td><td>0.0220</td><td>-0.0060</td></tr>
<tr><td>5</td><td>0.2858</td><td>20000.00</td><td>30</td><td>3.1476</td><td>-15000.00</td><td>5</td><td>0.0560</td><td>0.0160</td></tr>
<tr><td>6</td><td>0.7503</td><td>-15000.00</td><td>31</td><td>0.9339</td><td>-15000.00</td><td>6</td><td>0.0539</td><td>-0.0120</td></tr>
<tr><td>7</td><td>0.3272</td><td>20000.00</td><td>32</td><td>0.3812</td><td>20000.00</td><td>7</td><td>0.0980</td><td>0.0240</td></tr>
<tr><td>8</td><td>0.1000</td><td>20000.00</td><td>33</td><td>0.1742</td><td>20000.00</td><td>8</td><td>0.1060</td><td>-0.0180</td></tr>
<tr><td>9</td><td>0.9980</td><td>-15000.00</td><td>34</td><td>0.5357</td><td>20000.00</td><td>9</td><td>0.1210</td><td>0.0175</td></tr>
<tr><td>10</td><td>1.5972</td><td>-15000.00</td><td>35</td><td>3.2858</td><td>-15000.00</td><td>10</td><td>0.1180</td><td>-0.0158</td></tr>
<tr><td>11</td><td>2.0870</td><td>-15000.00</td><td>36</td><td>0.7981</td><td>20000.00</td><td>11</td><td>0.1613</td><td>0.0215</td></tr>
<tr><td>12</td><td>2.0870</td><td>-15000.00</td><td>37</td><td>0.1000</td><td>-10088.84</td><td>12</td><td>0.1653</td><td>-0.0188</td></tr>
<tr><td>13</td><td>0.2728</td><td>20000.00</td><td>38</td><td>0.1000</td><td>-5177.67</td><td>13</td><td>0.2155</td><td>0.0255</td></tr>
<tr><td>14</td><td>0.4362</td><td>-15000.00</td><td>39</td><td>1.6384</td><td>20000.00</td><td>14</td><td>0.2125</td><td>-0.0218</td></tr>
<tr><td>15</td><td>0.4627</td><td>20000.00</td><td>40</td><td>3.4154</td><td>-15000.00</td><td>15</td><td>0.2455</td><td>0.0780</td></tr>
<tr><td>16</td><td>0.5145</td><td>-15000.00</td><td>41</td><td>0.1000</td><td>17411.17</td><td>16</td><td>0.2420</td><td>-0.0883</td></tr>
<tr><td>17</td><td>2.0870</td><td>-15000.00</td><td>42</td><td>1.0153</td><td>-15000.00</td><td>17</td><td>0.2618</td><td>0.1030</td></tr>
<tr><td>18</td><td>2.0870</td><td>-15000.00</td><td>43</td><td>0.1000</td><td>5000.00</td><td>18</td><td>0.2658</td><td>0.0780</td></tr>
<tr><td>19</td><td>0.1000</td><td>0.00</td><td>44</td><td>1.7866</td><td>20000.00</td><td>19</td><td>0.2698</td><td>0.0295</td></tr>
<tr><td>20</td><td>0.1000</td><td>0.00</td><td>45</td><td>4.8179</td><td>-15000.00</td><td>20</td><td>0.2738</td><td>-0.0248</td></tr>
<tr><td>21</td><td>0.1000</td><td>0.00</td><td>46</td><td>0.7261</td><td>20000.00</td><td>21</td><td>0.2778</td><td>-0.0883</td></tr>
<tr><td>22</td><td>0.1000</td><td>0.00</td><td>47</td><td>0.1632</td><td>-15000.00</td><td>22</td><td>0.2818</td><td>-0.1753</td></tr>
<tr><td>23</td><td>1.1000</td><td>20000.00</td><td colspan="6"></td></tr>
<tr><td>24</td><td>1.7000</td><td>20000.00</td><td colspan="3">Minimum Weight</td><td colspan="3">1379.51 sec</td></tr>
<tr><td>25</td><td>1.1000</td><td>20000.00</td><td colspan="3">CPU Time</td><td colspan="3">28.421 sec</td></tr>
</table>

Table 5.3: NLP results of the forty-seven-member tower for $\omega = 30$ rad/sec

Forty-Seven-Member Tower (Force Excitation)								
$\omega = 30\,\text{rad/sec}$			No mass added					
Use results of $\omega = 30\,\text{rad/sec}$ from SI as inputs into NLP								
Link	Area (in^2)	Stress (psi)	Link	Area (in^2)	Stress (psi)	Displacements (in)		
						node	x-dir	y-dir
1	0.6900	20000.00	26	1.7030	20000.00	1	0.0000	0.0000
2	3.1458	-15000.00	27	1.1960	20000.00	2	0.0000	0.0000
3	0.4483	19999.99	28	0.1000	-15000.00	3	0.0200	0.0080
4	1.8411	-15000.00	29	1.1514	20000.00	4	0.0220	-0.0060
5	0.6218	20000.00	30	3.0131	-15000.00	5	0.0560	0.0160
6	0.3224	-15000.00	31	1.2239	-15000.00	6	0.0540	-0.0120
7	0.1000	20000.00	32	0.1801	20000.00	7	0.0980	0.0240
8	0.1000	20000.00	33	0.2839	20000.00	8	0.1060	-0.0180
9	1.0157	-15000.00	34	0.5564	20000.00	9	0.1210	0.0175
10	1.8284	-15000.00	35	3.3328	-15000.00	10	0.1180	-0.0158
11	2.0862	-15000.00	36	0.8175	20000.00	11	0.1613	0.0215
12	2.0890	-15000.00	37	0.1000	-10050.28	12	0.1653	-0.0188
13	0.1000	20000.00	38	0.1000	-5100.56	13	0.2155	0.0255
14	0.6799	-15000.00	39	1.6876	20000.00	14	0.2125	-0.0218
15	0.7202	20000.00	40	3.4626	-15000.00	15	0.2455	0.0781
16	0.1875	-15000.00	41	0.1000	17449.72	16	0.2420	-0.0883
17	2.0861	-15000.00	42	1.0428	-15000.00	17	0.2618	0.1030
18	2.0888	-15000.00	43	0.1000	5000.00	18	0.2658	0.0781
19	0.1000	-217.45	44	1.8361	20000.00	19	0.2698	0.0295
20	0.1000	250.15	45	4.9047	-15000.00	20	0.2738	-0.0248
21	0.1000	29.80	46	0.7473	20000.00	21	0.2778	-0.0883
22	0.1000	-51.85	47	0.1637	-15000.00	22	0.2818	-0.1753
23	1.0986	20000.00						
24	1.7022	20000.00	Minimum Weight			1398.72 lb		
25	1.0981	20000.00	CPU Time			43.49 sec		

Table 5.4: NLP results of the forty-seven-member tower for $\omega = 50$ rad/sec

Forty-Seven-Member Tower (Force Excitation)								
$\omega = 50\,\text{rad/sec}$			No mass added					
Use results of $\omega = 50\,\text{rad/sec}$ from SI as inputs into NLP								
Link	Area (in^2)	Stress (psi)	Link	Area (in^2)	Stress (psi)	Displacements (in)		
						node	x-dir	y-dir
1	0.7246	20000.00	26	1.7083	20000.00	1	0.0000	0.0000
2	3.2174	-15000.00	27	1.1888	20000.00	2	0.0000	0.0000
3	0.4824	19999.99	28	0.1000	-15000.00	3	0.0200	0.0080
4	1.8652	-15000.00	29	1.2070	20000.00	4	0.0220	-0.0060
5	0.6483	20000.00	30	3.0756	-15000.00	5	0.0560	0.0160
6	0.3233	-15000.00	31	1.2540	-15000.00	6	0.0540	-0.0120
7	0.1000	20000.00	32	0.1868	20000.00	7	0.0980	0.0240
8	0.1000	20000.00	33	0.2767	19999.99	8	0.1060	-0.0180
9	1.0474	-15000.00	34	0.5935	20000.00	9	0.1210	0.0175
10	1.8298	-15000.00	35	3.4174	-15000.00	10	0.1180	-0.0157
11	2.0847	-15000.00	36	0.8526	20000.00	11	0.1613	0.0215
12	2.0925	-15000.00	37	0.1000	-9979.10	12	0.1653	-0.0187
13	0.1000	20000.00	38	0.1000	-4958.19	13	0.2155	0.0255
14	0.7034	-15000.00	39	1.7762	20000.00	14	0.2125	-0.0217
15	0.7434	20000.00	40	3.5476	-15000.00	15	0.2456	0.0782
16	0.1857	-15000.00	41	0.1000	17520.90	16	0.2421	-0.0884
17	2.0845	-15000.00	42	1.0926	-15000.00	17	0.2618	0.1030
18	2.0920	-15000.00	43	0.1000	5000.00	18	0.2658	0.0782
19	0.1000	-603.84	44	1.9256	20000.00	19	0.2698	0.0295
20	0.1000	696.69	45	5.0615	-15000.00	20	0.2738	-0.0247
21	0.1000	82.67	46	0.7858	20000.00	21	0.2778	-0.0884
22	0.1000	-144.61	47	0.1647	-15000.00	22	0.2818	-0.1752
23	1.0962	20000.00						
24	1.7060	20000.00	Minimum Weight			1433.33 lb		
25	1.0948	20000.00	CPU Time			52.575 sec		

Table 5.5: NLP results of the forty-seven-member tower for $\omega = 80$ rad/sec

Forty-Seven-Member Tower (Force Excitation)								
$\omega = 80\,\text{rad/sec}$			No mass added					
Use results of $\omega = 80\,\text{rad/sec}$ from SI as inputs into NLP								
Link	Area (in^2)	Stress (psi)	Link	Area (in^2)	Stress (psi)	Displacements (in)		
						node	x-dir	y-dir
1	0.8099	20000.00	26	1.7214	20000.00	1	0.0000	0.0000
2	3.3949	-15000.00	27	1.1715	20000.00	2	0.0000	0.0000
3	0.5662	20000.00	28	0.1000	-15000.00	3	0.0200	0.0080
4	1.9243	-15000.00	29	1.3448	20000.00	4	0.0220	-0.0060
5	0.7142	20000.00	30	3.2308	-15000.00	5	0.0560	0.0160
6	0.3257	-15000.00	31	1.3281	-15000.00	6	0.0542	-0.0120
7	0.1000	20000.00	32	0.2027	20000.00	7	0.0980	0.0240
8	0.1000	20000.00	33	0.2584	20000.00	8	0.1060	-0.0180
9	1.1257	-15000.00	34	0.6858	20000.00	9	0.1210	0.0175
10	1.8331	-15000.00	35	3.6297	-15000.00	10	0.1180	-0.0158
11	2.0810	-15000.00	36	0.9416	20000.00	11	0.1613	0.0215
12	2.1012	-15000.00	37	0.1000	-9790.81	12	0.1653	-0.0188
13	0.1000	20000.00	38	0.1000	-4581.62	13	0.2155	0.0255
14	0.7610	-15000.00	39	1.9996	20000.00	14	0.2125	-0.0218
15	0.8005	20000.00	40	3.7608	-15000.00	15	0.2457	0.0784
16	0.1811	-15000.00	41	0.1000	17709.19	16	0.2422	-0.0887
17	2.0807	-15000.00	42	1.2197	-15000.00	17	0.2618	0.1030
18	2.0998	-15000.00	43	0.1000	5000.00	18	0.2658	0.0784
19	0.1000	-1544.76	44	2.1514	20000.00	19	0.2698	0.0295
20	0.1000	1795.11	45	5.4580	-15000.00	20	0.2738	-0.0248
21	0.1000	210.99	46	0.8841	20000.00	21	0.2778	-0.0887
22	0.1000	-373.86	47	0.1673	-15000.00	22	0.2818	-0.1753
23	1.0903	20000.00						
24	1.7155	20000.00	Minimum Weight			1520.21 lb		
25	1.0868	20000.00	CPU Time			29.712 sec		

Table 5.6: NLP results of the forty-seven-member tower for ω = 100 rad/sec

<table>
<tr><td colspan="9">Forty-Seven-Member Tower (Force Excitation)</td></tr>
<tr><td colspan="3">ω = 100 rad/sec</td><td colspan="6">No mass added</td></tr>
<tr><td colspan="9">Use results of ω = 100 rad/sec from SI as inputs into NLP</td></tr>
<tr><td rowspan="2">Link</td><td rowspan="2">Area
(in^2)</td><td rowspan="2">Stress
(psi)</td><td rowspan="2">Link</td><td rowspan="2">Area
(in^2)</td><td rowspan="2">Stress
(psi)</td><td colspan="3">Displacements (in)</td></tr>
<tr><td>node</td><td>x-dir</td><td>y-dir</td></tr>
<tr><td>1</td><td>0.8900</td><td>20000.00</td><td>26</td><td>1.7335</td><td>20000.00</td><td>1</td><td>0.0000</td><td>0.0000</td></tr>
<tr><td>2</td><td>3.5621</td><td>-15000.00</td><td>27</td><td>1.1556</td><td>20000.00</td><td>2</td><td>0.0000</td><td>0.0000</td></tr>
<tr><td>3</td><td>0.6447</td><td>20000.00</td><td>28</td><td>0.1000</td><td>-15000.00</td><td>3</td><td>0.0200</td><td>0.0080</td></tr>
<tr><td>4</td><td>1.9795</td><td>-15000.00</td><td>29</td><td>1.4753</td><td>20000.00</td><td>4</td><td>0.0220</td><td>-0.0060</td></tr>
<tr><td>5</td><td>0.7768</td><td>20000.00</td><td>30</td><td>3.3776</td><td>-15000.00</td><td>5</td><td>0.0560</td><td>0.0160</td></tr>
<tr><td>6</td><td>0.3283</td><td>-15000.00</td><td>31</td><td>1.3976</td><td>-15000.00</td><td>6</td><td>0.0543</td><td>-0.0120</td></tr>
<tr><td>7</td><td>0.1000</td><td>20000.00</td><td>32</td><td>0.2172</td><td>20000.00</td><td>7</td><td>0.0980</td><td>0.0240</td></tr>
<tr><td>8</td><td>0.1000</td><td>20000.00</td><td>33</td><td>0.2403</td><td>20000.00</td><td>8</td><td>0.1060</td><td>-0.0180</td></tr>
<tr><td>9</td><td>1.1995</td><td>-15000.00</td><td>34</td><td>0.7735</td><td>20000.00</td><td>9</td><td>0.1210</td><td>0.0175</td></tr>
<tr><td>10</td><td>1.8360</td><td>-15000.00</td><td>35</td><td>3.8333</td><td>-15000.00</td><td>10</td><td>0.1180</td><td>-0.0158</td></tr>
<tr><td>11</td><td>2.0777</td><td>-15000.00</td><td>36</td><td>1.0282</td><td>20000.00</td><td>11</td><td>0.1613</td><td>0.0215</td></tr>
<tr><td>12</td><td>2.1093</td><td>-15000.00</td><td>37</td><td>0.1000</td><td>-9597.32</td><td>12</td><td>0.1653</td><td>-0.0188</td></tr>
<tr><td>13</td><td>0.1000</td><td>20000.00</td><td>38</td><td>0.1000</td><td>-4194.64</td><td>13</td><td>0.2155</td><td>0.0255</td></tr>
<tr><td>14</td><td>0.8147</td><td>-15000.00</td><td>39</td><td>2.2154</td><td>20000.00</td><td>14</td><td>0.2125</td><td>-0.0218</td></tr>
<tr><td>15</td><td>0.8535</td><td>20000.00</td><td>40</td><td>3.9654</td><td>-15000.00</td><td>15</td><td>0.2458</td><td>0.0786</td></tr>
<tr><td>16</td><td>0.1770</td><td>-15000.00</td><td>41</td><td>0.1000</td><td>17902.68</td><td>16</td><td>0.2424</td><td>-0.0890</td></tr>
<tr><td>17</td><td>2.0771</td><td>-15000.00</td><td>42</td><td>1.3443</td><td>-15000.00</td><td>17</td><td>0.2618</td><td>0.1030</td></tr>
<tr><td>18</td><td>2.1071</td><td>-15000.00</td><td>43</td><td>0.1000</td><td>5000.00</td><td>18</td><td>0.2658</td><td>0.0786</td></tr>
<tr><td>19</td><td>0.1000</td><td>-2412.12</td><td>44</td><td>2.3696</td><td>20000.00</td><td>19</td><td>0.2698</td><td>0.0295</td></tr>
<tr><td>20</td><td>0.1000</td><td>2821.79</td><td>45</td><td>5.8424</td><td>-15000.00</td><td>20</td><td>0.2738</td><td>-0.0248</td></tr>
<tr><td>21</td><td>0.1000</td><td>328.74</td><td>46</td><td>0.9806</td><td>20000.00</td><td>21</td><td>0.2778</td><td>-0.0890</td></tr>
<tr><td>22</td><td>0.1000</td><td>-589.52</td><td>47</td><td>0.1701</td><td>-15000.00</td><td>22</td><td>0.2818</td><td>-0.1753</td></tr>
<tr><td>23</td><td>1.0850</td><td>20000.00</td><td colspan="6"></td></tr>
<tr><td>24</td><td>1.7244</td><td>20000.00</td><td colspan="3">Minimum Weight</td><td colspan="3">1603.68 lb</td></tr>
<tr><td>25</td><td>1.0794</td><td>20000.00</td><td colspan="3">CPU Time</td><td colspan="3">30.574 sec</td></tr>
</table>

Table 5.7: NLP results of the forty-seven-member tower for ω = 140 rad/sec

Forty-Seven-Member Tower (Force Excitation)								
ω = 140 rad/sec			No mass added					
Use results of ω = 140 rad/sec from SI as inputs into NLP								
Link	Area (in^2)	Stress (psi)	Link	Area (in^2)	Stress (psi)	Displacements (in)		
						node	x-dir	y-dir
1	1.1102	20000.00	26	1.7666	20000.00	1	0.0000	0.0000
2	4.0247	-15000.00	27	1.1138	20000.00	2	0.0000	0.0000
3	0.8597	20000.00	28	0.1000	-15000.00	3	0.0200	0.0080
4	2.1291	-15000.00	29	1.8385	20000.00	4	0.0220	-0.0060
5	0.9530	20000.00	30	3.7866	-15000.00	5	0.0560	0.0160
6	0.3370	-15000.00	31	1.5877	-15000.00	6	0.0548	-0.0120
7	0.1000	20000.00	32	0.2548	20000.00	7	0.0980	0.0240
8	0.1000	20000.00	33	0.1865	20000.00	8	0.1060	-0.0180
9	1.4039	-15000.00	34	1.0190	20000.00	9	0.1210	0.0175
10	1.8430	-15000.00	35	4.4140	-15000.00	10	0.1180	-0.0158
11	2.0688	-15000.00	36	1.2811	20000.00	11	0.1613	0.0215
12	2.1314	-15000.00	37	0.1000	-8978.30	12	0.1653	-0.0188
13	0.1000	20000.00	38	0.1000	-2956.61	13	0.2155	0.0255
14	0.9601	-15000.00	39	2.8378	20000.00	14	0.2125	-0.0218
15	0.9971	20000.00	40	4.5492	-15000.00	15	0.2461	0.0792
16	0.1660	-15000.00	41	0.1000	18521.70	16	0.2427	-0.0897
17	2.0678	-15000.00	42	1.7123	-15000.00	17	0.2618	0.1030
18	2.1269	-15000.00	43	0.1000	5000.00	18	0.2658	0.0792
19	0.1000	-4719.61	44	3.0003	20000.00	19	0.2698	0.0295
20	0.1000	5621.39	45	6.9592	-15000.00	20	0.2738	-0.0248
21	0.1000	639.46	46	1.2671	20000.00	21	0.2778	-0.0898
22	0.1000	-1184.24	47	0.1795	-15000.00	22	0.2818	-0.1753
23	1.0707	20000.00						
24	1.7483	20000.00	Minimum Weight			1842.44 lb		
25	1.0600	20000.00	CPU Time			21.001 sec		

Table 5.8: NLP results of the forty-seven-member tower for ω = 190 rad/sec

<table>
<tr><th colspan="9">Forty-Seven-Member Tower (Force Excitation)</th></tr>
<tr><th colspan="3">$\omega = 190\,\text{rad/sec}$</th><th colspan="6">No mass added</th></tr>
<tr><th colspan="9">Use results of $\omega = 190\,\text{rad/sec}$ from SI as inputs into NLP</th></tr>
<tr><th rowspan="2">Link</th><th rowspan="2">Area
(in^2)</th><th rowspan="2">Stress
(psi)</th><th rowspan="2">Link</th><th rowspan="2">Area
(in^2)</th><th rowspan="2">Stress
(psi)</th><th colspan="3">Displacements (in)</th></tr>
<tr><th>node</th><th>x-dir</th><th>y-dir</th></tr>
<tr><td>1</td><td>1.5033</td><td>20000.00</td><td>26</td><td>1.8253</td><td>20000.00</td><td>1</td><td>0.0000</td><td>0.0000</td></tr>
<tr><td>2</td><td>4.8941</td><td>-15000.00</td><td>27</td><td>1.0438</td><td>20000.00</td><td>2</td><td>0.0000</td><td>0.0000</td></tr>
<tr><td>3</td><td>1.2525</td><td>20000.00</td><td>28</td><td>0.1000</td><td>-13552.19</td><td>3</td><td>0.0200</td><td>0.0080</td></tr>
<tr><td>4</td><td>2.3921</td><td>-15000.00</td><td>29</td><td>2.5294</td><td>20000.00</td><td>4</td><td>0.0220</td><td>-0.0060</td></tr>
<tr><td>5</td><td>1.3029</td><td>20000.00</td><td>30</td><td>4.5406</td><td>-15000.00</td><td>5</td><td>0.0560</td><td>0.0160</td></tr>
<tr><td>6</td><td>0.3395</td><td>-15000.00</td><td>31</td><td>1.9523</td><td>-15000.00</td><td>6</td><td>0.0538</td><td>-0.0120</td></tr>
<tr><td>7</td><td>0.1000</td><td>18552.19</td><td>32</td><td>0.2998</td><td>20000.00</td><td>7</td><td>0.0986</td><td>0.0240</td></tr>
<tr><td>8</td><td>0.1000</td><td>19276.10</td><td>33</td><td>0.1000</td><td>18552.19</td><td>8</td><td>0.1060</td><td>-0.0180</td></tr>
<tr><td>9</td><td>1.7872</td><td>-15000.00</td><td>34</td><td>1.4968</td><td>20000.00</td><td>9</td><td>0.1211</td><td>0.0177</td></tr>
<tr><td>10</td><td>1.8489</td><td>-15000.00</td><td>35</td><td>5.5373</td><td>-15000.00</td><td>10</td><td>0.1184</td><td>-0.0155</td></tr>
<tr><td>11</td><td>2.0537</td><td>-15000.00</td><td>36</td><td>1.7818</td><td>20000.00</td><td>11</td><td>0.1617</td><td>0.0217</td></tr>
<tr><td>12</td><td>2.1709</td><td>-15000.00</td><td>37</td><td>0.1000</td><td>-10920.37</td><td>12</td><td>0.1654</td><td>-0.0185</td></tr>
<tr><td>13</td><td>0.1000</td><td>20000.00</td><td>38</td><td>0.1000</td><td>-5392.93</td><td>13</td><td>0.2156</td><td>0.0257</td></tr>
<tr><td>14</td><td>1.2182</td><td>-15000.00</td><td>39</td><td>4.0464</td><td>20000.00</td><td>14</td><td>0.2126</td><td>-0.0215</td></tr>
<tr><td>15</td><td>1.2514</td><td>20000.00</td><td>40</td><td>5.7466</td><td>-15000.00</td><td>15</td><td>0.2467</td><td>0.0804</td></tr>
<tr><td>16</td><td>0.1472</td><td>-15000.00</td><td>41</td><td>0.1778</td><td>17303.53</td><td>16</td><td>0.2435</td><td>-0.0907</td></tr>
<tr><td>17</td><td>2.0520</td><td>-15000.00</td><td>42</td><td>2.4081</td><td>-15000.00</td><td>17</td><td>0.2619</td><td>0.1032</td></tr>
<tr><td>18</td><td>2.1618</td><td>-15000.00</td><td>43</td><td>0.1000</td><td>5000.00</td><td>18</td><td>0.2659</td><td>0.0805</td></tr>
<tr><td>19</td><td>0.1000</td><td>-8680.92</td><td>44</td><td>4.3064</td><td>20000.00</td><td>19</td><td>0.2699</td><td>0.0297</td></tr>
<tr><td>20</td><td>0.1000</td><td>10642.93</td><td>45</td><td>9.1724</td><td>-15000.00</td><td>20</td><td>0.2739</td><td>-0.0245</td></tr>
<tr><td>21</td><td>0.1000</td><td>1165.45</td><td>46</td><td>1.8153</td><td>20000.00</td><td>21</td><td>0.2779</td><td>-0.0909</td></tr>
<tr><td>22</td><td>0.1000</td><td>-2271.68</td><td>47</td><td>0.2757</td><td>-15000.00</td><td>22</td><td>0.2819</td><td>-0.1750</td></tr>
<tr><td>23</td><td>1.0467</td><td>20000.00</td><td colspan="6"></td></tr>
<tr><td>24</td><td>1.7906</td><td>20000.00</td><td colspan="3">Minimum Weight</td><td colspan="3">2314.76 lb</td></tr>
<tr><td>25</td><td>1.0274</td><td>20000.00</td><td colspan="3">CPU Time</td><td colspan="3">177.736 sec</td></tr>
</table>

Table 5.9: NLP results of the forty-seven-member tower for ω = 200 rad/sec

<table>
<tr><th colspan="9">Forty-Seven-Member Tower (Force Excitation)</th></tr>
<tr><th colspan="3">$\omega = 200$ rad/sec</th><th colspan="6">No mass added</th></tr>
<tr><th colspan="9">Use results of $\omega = 200$ rad/sec from SI as inputs into NLP</th></tr>
<tr><th rowspan="2">Link</th><th rowspan="2">Area
(in^2)</th><th rowspan="2">Stress
(psi)</th><th rowspan="2">Link</th><th rowspan="2">Area
(in^2)</th><th rowspan="2">Stress
(psi)</th><th colspan="3">Displacements (in)</th></tr>
<tr><th>node</th><th>x-dir</th><th>y-dir</th></tr>
<tr><td>1</td><td>1.5868</td><td>20000.00</td><td>26</td><td>1.8395</td><td>20000.00</td><td>1</td><td>0.0000</td><td>0.0000</td></tr>
<tr><td>2</td><td>5.1326</td><td>-15000.00</td><td>27</td><td>1.0272</td><td>20000.00</td><td>2</td><td>0.0000</td><td>0.0000</td></tr>
<tr><td>3</td><td>1.3540</td><td>20000.00</td><td>28</td><td>0.1000</td><td>-11025.30</td><td>3</td><td>0.0200</td><td>0.0080</td></tr>
<tr><td>4</td><td>2.4506</td><td>-15000.00</td><td>29</td><td>2.7201</td><td>20000.00</td><td>4</td><td>0.0220</td><td>-0.0060</td></tr>
<tr><td>5</td><td>1.4144</td><td>20000.00</td><td>30</td><td>4.7130</td><td>-15000.00</td><td>5</td><td>0.0560</td><td>0.0160</td></tr>
<tr><td>6</td><td>0.3131</td><td>-15000.00</td><td>31</td><td>2.0729</td><td>-15000.00</td><td>6</td><td>0.0540</td><td>-0.0120</td></tr>
<tr><td>7</td><td>0.1000</td><td>16025.30</td><td>32</td><td>0.2864</td><td>20000.00</td><td>7</td><td>0.0996</td><td>0.0240</td></tr>
<tr><td>8</td><td>0.1000</td><td>18012.65</td><td>33</td><td>0.1000</td><td>16025.30</td><td>8</td><td>0.1060</td><td>-0.0180</td></tr>
<tr><td>9</td><td>1.8912</td><td>-15000.00</td><td>34</td><td>1.6227</td><td>20000.00</td><td>9</td><td>0.1214</td><td>0.0181</td></tr>
<tr><td>10</td><td>1.8444</td><td>-15000.00</td><td>35</td><td>5.8308</td><td>-15000.00</td><td>10</td><td>0.1192</td><td>-0.0152</td></tr>
<tr><td>11</td><td>2.0499</td><td>-15000.00</td><td>36</td><td>1.9158</td><td>20000.00</td><td>11</td><td>0.1624</td><td>0.0221</td></tr>
<tr><td>12</td><td>2.1801</td><td>-15000.00</td><td>37</td><td>0.1000</td><td>-12042.27</td><td>12</td><td>0.1656</td><td>-0.0182</td></tr>
<tr><td>13</td><td>0.1000</td><td>20000.00</td><td>38</td><td>0.1000</td><td>-5109.83</td><td>13</td><td>0.2159</td><td>0.0261</td></tr>
<tr><td>14</td><td>1.2810</td><td>-15000.00</td><td>39</td><td>4.3744</td><td>20000.00</td><td>14</td><td>0.2129</td><td>-0.0212</td></tr>
<tr><td>15</td><td>1.3133</td><td>20000.00</td><td>40</td><td>6.0607</td><td>-15000.00</td><td>15</td><td>0.2471</td><td>0.0810</td></tr>
<tr><td>16</td><td>0.1426</td><td>-15000.00</td><td>41</td><td>0.1924</td><td>17445.08</td><td>16</td><td>0.2439</td><td>-0.0906</td></tr>
<tr><td>17</td><td>2.0482</td><td>-15000.00</td><td>42</td><td>2.6059</td><td>-15000.00</td><td>17</td><td>0.2621</td><td>0.1036</td></tr>
<tr><td>18</td><td>2.1701</td><td>-15000.00</td><td>43</td><td>0.1000</td><td>5000.00</td><td>18</td><td>0.2661</td><td>0.0811</td></tr>
<tr><td>19</td><td>0.1000</td><td>-9638.53</td><td>44</td><td>4.6576</td><td>20000.00</td><td>19</td><td>0.2701</td><td>0.0301</td></tr>
<tr><td>20</td><td>0.1000</td><td>11850.33</td><td>45</td><td>9.7758</td><td>-15000.00</td><td>20</td><td>0.2741</td><td>-0.0242</td></tr>
<tr><td>21</td><td>0.1000</td><td>1293.28</td><td>46</td><td>1.9717</td><td>20000.00</td><td>21</td><td>0.2781</td><td>-0.0909</td></tr>
<tr><td>22</td><td>0.1000</td><td>-2532.41</td><td>47</td><td>0.2989</td><td>-15000.00</td><td>22</td><td>0.2821</td><td>-0.1747</td></tr>
<tr><td>23</td><td>1.0410</td><td>20000.00</td><td colspan="6"></td></tr>
<tr><td>24</td><td>1.8008</td><td>20000.00</td><td colspan="3">Minimum Weight</td><td colspan="3">2441.00 lb</td></tr>
<tr><td>25</td><td>1.0198</td><td>20000.00</td><td colspan="3">CPU Time</td><td colspan="3">41.690 sec</td></tr>
</table>

Table 5.10: NLP results of the two-hundred-member structure for ω = 20 rad/sec (I)

Two-Hundred-Member Structure (Force Excitation)								
ω = 20 rad/sec			No mass added					
Use results of ω = 20 rad/sec from SI as inputs into NLP								
Displacements (in)			Displacements (in)			Displacements (in)		
node	x-dir	y-dir	node	x-dir	y-dir	node	x-dir	y-dir
1	0.0189	-0.2130	27	0.0662	-0.1581	53	0.0325	-0.0872
2	0.0354	-0.1803	28	0.0662	-0.1851	54	0.0398	-0.0793
3	0.0544	-0.1963	29	0.0013	-0.1553	55	0.0470	-0.1005
4	0.0761	-0.1803	30	0.0254	-0.1226	56	0.0470	-0.1274
5	0.0962	-0.2284	31	0.0393	-0.1386	57	-0.0163	-0.0976
6	0.0339	-0.1986	32	0.0529	-0.1226	58	0.0078	-0.0649
7	0.0299	-0.1794	33	0.0769	-0.1707	59	0.0212	-0.0809
8	0.0370	-0.1659	34	0.0181	-0.1409	60	0.0337	-0.0649
9	0.0441	-0.1729	35	0.0141	-0.1202	61	0.0577	-0.1130
10	0.0522	-0.1819	36	0.0210	-0.1082	62	0.0000	-0.0832
11	0.0603	-0.1723	37	0.0279	-0.1161	63	-0.0040	-0.0629
12	0.0684	-0.1659	38	0.0349	-0.1242	64	0.0019	-0.0505
13	0.0765	-0.1875	39	0.0418	-0.1161	65	0.0077	-0.0559
14	0.0765	-0.2140	40	0.0492	-0.1082	66	0.0144	-0.0665
15	0.0101	-0.1842	41	0.0566	-0.1293	67	0.0210	-0.0609
16	0.0342	-0.1515	42	0.0566	-0.1563	68	0.0291	-0.0505
17	0.0483	-0.1675	43	-0.0075	-0.1265	69	0.0371	-0.0714
18	0.0625	-0.1515	44	0.0166	-0.0938	70	0.0371	-0.0986
19	0.0865	-0.1995	45	0.0301	-0.1098	71	-0.0251	-0.0688
20	0.0270	-0.1698	46	0.0433	-0.0938	72	-0.0010	-0.0361
21	0.0230	-0.1490	47	0.0673	-0.1418	73	0.0000	-0.0521
22	0.0300	-0.1370	48	0.0093	-0.1121	74	0.0240	-0.0361
23	0.0369	-0.1450	49	0.0053	-0.0914	75	0.0481	-0.0841
24	0.0440	-0.1531	50	0.0121	-0.0793	76	0.0000	0.0000
25	0.0511	-0.1449	51	0.0189	-0.0873	77	0.0000	0.0000
26	0.0587	-0.1370	52	0.0257	-0.0954			
Minimum Weight			6968.18 lb		CPU Time		902.217 sec	

Table 5.11: NLP results of the two-hundred-member structure for ω = 20 rad/sec (II)

Two-Hundred-Member Structure (Force Excitation)								
$\omega = 20\,\text{rad/sec}$			No mass added					
Use results of $\omega = 20\,\text{rad/sec}$ from SI as inputs into NLP								
Link	Area (in^2)	Stress (psi)	Link	Area (in^2)	Stress (psi)	Link	Area (in^2)	Stress (psi)
1	0.1000	20632.31	35	0.7059	-30050.00	69	0.1000	-5395.24
2	0.1000	23713.00	36	0.1831	-30050.00	70	1.1106	-30050.00
3	0.1000	27045.28	37	0.1000	25071.45	71	0.1000	4392.28
4	0.1000	25134.86	38	0.5654	-30050.00	72	0.1000	-25641.09
5	0.2105	-30050.00	39	0.1433	30050.00	73	1.6122	-30050.00
6	0.1592	-30050.00	40	0.1000	17645.89	74	0.3016	-30050.00
7	0.1000	4551.59	41	0.1000	17759.48	75	0.1000	26511.38
8	0.3438	-30050.00	42	0.1086	30050.00	76	0.9730	-30050.00
9	0.1000	-269.48	43	0.5307	-30050.00	77	0.2728	30050.00
10	0.1000	-18235.78	44	0.3629	-30050.00	78	0.1000	17420.84
11	0.2263	-30050.00	45	0.1000	8504.80	79	0.1000	16964.46
12	0.1000	-23452.88	46	1.2375	-30050.00	80	0.1763	30050.00
13	0.1000	6359.81	47	0.1000	-5105.65	81	0.6764	-30050.00
14	0.3730	-30050.00	48	0.1000	-15980.50	82	0.5777	-30050.00
15	0.1000	9324.34	49	0.7776	-30050.00	83	0.1000	8590.35
16	0.1306	-30050.00	50	0.1000	-24828.19	84	2.2857	-30050.00
17	0.2325	-30050.00	51	0.1000	3601.54	85	0.1000	-5386.78
18	0.1000	-10004.86	52	1.2792	-30050.00	86	0.1000	-16008.40
19	0.1000	17672.78	53	0.1000	11913.21	87	1.3411	-30050.00
20	0.1000	17665.27	54	0.2529	-30050.00	88	0.1000	-25117.74
21	0.1000	20278.20	55	0.6400	-30050.00	89	0.1000	3359.59
22	0.1000	20269.71	56	0.1000	-10006.82	90	2.2819	-30050.00
23	0.1000	20221.44	57	0.1000	17437.62	91	0.1000	12032.84
24	0.1000	20206.88	58	0.1000	17422.38	92	0.3634	-30050.00
25	0.1000	11.52	59	0.1000	17774.63	93	0.9590	-30050.00
26	0.5434	-30050.00	60	0.1000	17759.15	94	0.1000	-10005.49
27	0.1000	26153.58	61	0.1000	18779.77	95	0.1000	17224.30
28	0.2313	-30050.00	62	0.1000	18749.10	96	0.1000	17206.06
29	0.6767	-30050.00	63	0.1000	19.19	97	0.1000	17391.78
30	0.1000	-16204.19	64	0.8637	-30050.00	98	0.1000	17372.81
31	0.1000	-2327.52	65	0.1000	29919.79	99	0.1000	18490.24
32	0.5592	-30050.00	66	0.4343	-30050.00	100	0.1000	18447.63
33	0.1000	6314.47	67	1.5705	-30050.00	101	0.1000	22.59
34	0.1000	-23433.90	68	0.1000	-15713.09	102	1.0093	-30050.00

Table 5.12: NLP results of the two-hundred-member structure for ω = 20 rad/sec (III)

Two-Hundred-Member Structure (Force Excitation)								
ω = 20 rad/sec			No mass added					
Use results of ω = 20 rad/sec from SI as inputs into NLP								
Link	Area (in^2)	Stress (psi)	Link	Area (in^2)	Stress (psi)	Link	Area (in^2)	Stress (psi)
103	0.1000	29834.24	137	0.1000	18189.92	171	0.1000	14622.14
104	0.6486	-30050.00	138	0.1000	18140.69	172	0.1000	14618.82
105	2.6188	-30050.00	139	0.1000	22.63	173	0.1000	16619.03
106	0.1000	-15869.66	140	0.9938	-30050.00	174	0.1000	16605.66
107	0.1000	-5543.28	141	0.1000	29750.85	175	0.1000	20062.63
108	1.6741	-30050.00	142	0.8581	-30050.00	176	0.1000	20014.96
109	0.1000	4227.28	143	3.8320	-30050.00	177	0.1000	19.74
110	0.1000	-26003.20	144	0.1000	-16153.13	178	0.8358	-30050.00
111	2.6150	-30050.00	145	0.1000	-5542.16	179	0.1000	28816.08
112	0.4113	-30050.00	146	2.2375	-30050.00	180	1.0375	-30050.00
113	0.1000	26391.75	147	0.1000	3912.88	181	5.1950	-30050.00
114	1.2920	-30050.00	148	0.1000	-26238.16	182	0.1000	-15444.26
115	0.4075	30050.00	149	3.7025	-30050.00	183	0.1000	-12651.16
116	0.1000	16897.25	150	0.5143	-30050.00	184	2.8010	-30050.00
117	0.1000	16467.98	151	0.1000	26272.74	185	0.1000	10708.46
118	0.2430	30050.00	152	1.5317	-30050.00	186	0.1000	-27465.32
119	0.6609	-30050.00	153	0.5265	30050.00	187	4.8805	-30050.00
120	0.7877	-30050.00	154	0.1000	16726.53	188	0.6358	-30050.00
121	0.1000	8673.74	155	0.1000	15618.63	189	0.1000	27007.70
122	3.4989	-30050.00	156	0.3179	30050.00	190	1.6821	-30050.00
123	0.1000	-5527.84	157	0.5029	-30050.00	191	0.6355	30050.00
124	0.1000	-16154.09	158	0.9734	-30050.00	192	0.1000	1275.09
125	1.9045	-30050.00	159	0.1000	9608.51	193	0.8921	30050.00
126	0.1000	-25289.73	160	4.8619	-30050.00	194	1.2403	30050.00
127	0.1000	2977.79	161	0.1000	-11083.96	195	1.3162	-30050.00
128	3.3694	-30050.00	162	0.1000	-17002.90	196	6.3647	-30050.00
129	0.1000	12151.85	163	2.4680	-30050.00	197	1.0412	-30050.00
130	0.4672	-30050.00	164	0.1000	-24758.75	198	2.7316	-30050.00
131	1.1987	-30050.00	165	0.1000	8011.21	199	5.7724	-30050.00
132	0.1000	-10002.77	166	4.5475	-30050.00	200	2.3392	-30050.00
133	0.1000	17014.85	167	0.1000	11416.89			
134	0.1000	16999.33	168	0.5838	-30050.00			
135	0.1000	17006.88	169	1.3491	-30050.00			
136	0.1000	16987.94	170	0.1000	-10000.01			

Table 5.13: NLP results of the two-hundred-member structure for $\omega = 50$ rad/sec (I)

Two-Hundred-Member Structure (Force Excitation)								
$\omega = 50$ rad/sec			No mass added					
Use results of $\omega = 50$ rad/sec from SI as inputs into NLP								
Displacements (in)			Displacements (in)			Displacements (in)		
node	x-dir	y-dir	node	x-dir	y-dir	node	x-dir	y-dir
1	0.0191	-0.2128	27	0.0662	-0.1580	53	0.0326	-0.0871
2	0.0356	-0.1801	28	0.0662	-0.1849	54	0.0399	-0.0793
3	0.0545	-0.1961	29	0.0015	-0.1552	55	0.0471	-0.1005
4	0.0761	-0.1801	30	0.0255	-0.1225	56	0.0471	-0.1273
5	0.0961	-0.2282	31	0.0394	-0.1385	57	-0.0162	-0.0975
6	0.0341	-0.1984	32	0.0528	-0.1225	58	0.0078	-0.0648
7	0.0301	-0.1792	33	0.0769	-0.1705	59	0.0212	-0.0809
8	0.0372	-0.1657	34	0.0183	-0.1407	60	0.0336	-0.0648
9	0.0442	-0.1727	35	0.0142	-0.1201	61	0.0576	-0.1129
10	0.0523	-0.1817	36	0.0212	-0.1081	62	0.0001	-0.0831
11	0.0604	-0.1722	37	0.0280	-0.1160	63	-0.0039	-0.0629
12	0.0685	-0.1657	38	0.0350	-0.1241	64	0.0019	-0.0504
13	0.0765	-0.1874	39	0.0419	-0.1160	65	0.0078	-0.0559
14	0.0765	-0.2137	40	0.0493	-0.1081	66	0.0145	-0.0664
15	0.0103	-0.1840	41	0.0566	-0.1292	67	0.0211	-0.0609
16	0.0343	-0.1513	42	0.0567	-0.1561	68	0.0292	-0.0504
17	0.0484	-0.1673	43	-0.0073	-0.1263	69	0.0371	-0.0713
18	0.0624	-0.1513	44	0.0167	-0.0937	70	0.0372	-0.0985
19	0.0865	-0.1993	45	0.0302	-0.1097	71	-0.0250	-0.0687
20	0.0271	-0.1696	46	0.0432	-0.0937	72	-0.0010	-0.0360
21	0.0231	-0.1489	47	0.0672	-0.1417	73	0.0000	-0.0520
22	0.0301	-0.1369	48	0.0094	-0.1119	74	0.0240	-0.0360
23	0.0371	-0.1449	49	0.0054	-0.0913	75	0.0480	-0.0841
24	0.0442	-0.1529	50	0.0122	-0.0793	76	0.0000	0.0000
25	0.0512	-0.1448	51	0.0190	-0.0872	77	0.0000	0.0000
26	0.0587	-0.1369	52	0.0258	-0.0953			
Minimum Weight			7002.84 lb		CPU Time		906.063 sec	

Table 5.14: NLP results of the two-hundred-member structure for $\omega = 50$ rad/sec (II)

Two-Hundred-Member Structure (Force Excitation)								
$\omega = 50\,\text{rad/sec}$			No mass added					
Use results of $\omega = 50\,\text{rad/sec}$ from SI as inputs into NLP								
Link	Area (in^2)	Stress (psi)	Link	Area (in^2)	Stress (psi)	Link	Area (in^2)	Stress (psi)
1	0.1000	20605.17	35	0.7078	-30020.00	69	0.1000	-5457.70
2	0.1000	23652.54	36	0.1818	-30020.00	70	1.1153	-30020.00
3	0.1000	26968.52	37	0.1000	24851.62	71	0.1000	4351.68
4	0.1000	24949.85	38	0.5679	-30020.00	72	0.1000	-25774.43
5	0.2112	-30020.00	39	0.1439	30020.00	73	1.6169	-30020.00
6	0.1593	-30020.00	40	0.1000	17591.13	74	0.2953	-30020.00
7	0.1000	4561.30	41	0.1000	17566.38	75	0.1000	26315.20
8	0.3447	-30020.00	42	0.1057	30020.00	76	0.9832	-30020.00
9	0.1000	-254.62	43	0.5329	-30020.00	77	0.2743	30020.00
10	0.1000	-18193.11	44	0.3638	-30020.00	78	0.1000	17390.34
11	0.2271	-30020.00	45	0.1000	8508.48	79	0.1000	16788.60
12	0.1000	-23447.53	46	1.2417	-30020.00	80	0.1699	30020.00
13	0.1000	6348.41	47	0.1000	-5076.63	81	0.6796	-30020.00
14	0.3740	-30020.00	48	0.1000	-15950.88	82	0.5801	-30020.00
15	0.1000	9378.75	49	0.7810	-30020.00	83	0.1000	8594.93
16	0.1295	-30020.00	50	0.1000	-24788.21	84	2.2952	-30020.00
17	0.2341	-30020.00	51	0.1000	3503.89	85	0.1000	-5347.50
18	0.1000	-10030.59	52	1.2823	-30020.00	86	0.1000	-15980.61
19	0.1000	17676.27	53	0.1000	12071.03	87	1.3478	-30020.00
20	0.1000	17629.01	54	0.2470	-30020.00	88	0.1000	-25068.21
21	0.1000	20235.21	55	0.6489	-30020.00	89	0.1000	3254.83
22	0.1000	20181.85	56	0.1000	-10043.00	90	2.2847	-30020.00
23	0.1000	20181.61	57	0.1000	17475.94	91	0.1000	12208.96
24	0.1000	20090.28	58	0.1000	17379.94	92	0.3519	-30020.00
25	0.1000	72.39	59	0.1000	17751.95	93	0.9803	-30020.00
26	0.5449	-30020.00	60	0.1000	17654.62	94	0.1000	-10034.66
27	0.1000	26107.86	61	0.1000	18791.11	95	0.1000	17290.76
28	0.2319	-30020.00	62	0.1000	18598.69	96	0.1000	17175.62
29	0.6785	-30020.00	63	0.1000	121.38	97	0.1000	17401.99
30	0.1000	-16214.81	64	0.8669	-30020.00	98	0.1000	17282.45
31	0.1000	-2398.07	65	0.1000	29877.75	99	0.1000	18542.65
32	0.5609	-30020.00	66	0.4360	-30020.00	100	0.1000	18275.38
33	0.1000	6300.55	67	1.5762	-30020.00	101	0.1000	144.07
34	0.1000	-23564.30	68	0.1000	-15708.34	102	1.0136	-30020.00

Table 5.15: NLP results of the two-hundred-member structure for ω = 50 rad/sec (III)

Two-Hundred-Member Structure (Force Excitation)								
ω = 50 rad/sec			No mass added					
Use results of ω= 50 rad/sec from SI as input into NLP								
Link	Area (in^2)	Stress (psi)	Link	Area (in^2)	Stress (psi)	Link	Area (in^2)	Stress (psi)
103	0.1000	29791.30	137	0.1000	18270.12	171	0.1000	14650.62
104	0.6518	-30020.00	138	0.1000	17961.56	172	0.1000	14629.23
105	2.6303	-30020.00	139	0.1000	145.69	173	0.1000	16657.65
106	0.1000	-15843.19	140	0.9977	-30020.00	174	0.1000	16573.19
107	0.1000	-5595.84	141	0.1000	29701.32	175	0.1000	20164.33
108	1.6823	-30020.00	142	0.8627	-30020.00	176	0.1000	19865.98
109	0.1000	4207.64	143	3.8508	-30020.00	177	0.1000	128.48
110	0.1000	-26131.96	144	0.1000	-16111.84	178	0.8382	-30020.00
111	2.6197	-30020.00	145	0.1000	-5582.78	179	0.1000	28747.69
112	0.3993	-30020.00	146	2.2495	-30020.00	180	1.0427	-30020.00
113	0.1000	26177.28	147	0.1000	3910.93	181	5.2218	-30020.00
114	1.3147	-30020.00	148	0.1000	-26354.21	182	0.1000	-15400.23
115	0.4100	30020.00	149	3.7030	-30020.00	183	0.1000	-12700.75
116	0.1000	16891.35	150	0.4962	-30020.00	184	2.8162	-30020.00
117	0.1000	16309.01	151	0.1000	26059.91	185	0.1000	10744.38
118	0.2329	30020.00	152	1.5717	-30020.00	186	0.1000	-27555.84
119	0.6639	-30020.00	153	0.5298	30020.00	187	4.8718	-30020.00
120	0.7916	-30020.00	154	0.1000	16733.16	188	0.6120	-30020.00
121	0.1000	8684.91	155	0.1000	15488.63	189	0.1000	26822.15
122	3.5156	-30020.00	156	0.3042	30020.00	190	1.7435	-30020.00
123	0.1000	-5490.23	157	0.5046	-30020.00	191	0.6387	30020.00
124	0.1000	-16120.97	158	0.9782	-30020.00	192	0.1000	1223.22
125	1.9149	-30020.00	159	0.1000	9638.54	193	0.9546	30020.00
126	0.1000	-25239.06	160	4.8868	-30020.00	194	1.2856	30020.00
127	0.1000	2879.10	161	0.1000	-11085.33	195	1.3210	-30020.00
128	3.3679	-30020.00	162	0.1000	-16962.24	196	6.3984	-30020.00
129	0.1000	12326.32	163	2.4818	-30020.00	197	0.9955	-30020.00
130	0.4497	-30020.00	164	0.1000	-24709.87	198	2.7992	-30020.00
131	1.2372	-30020.00	165	0.1000	7956.61	199	5.7487	-30020.00
132	0.1000	-10017.50	166	4.5370	-30020.00	200	2.4173	-30020.00
133	0.1000	17086.28	167	0.1000	11564.08			
134	0.1000	16987.98	168	0.5605	-30020.00			
135	0.1000	17039.11	169	1.4092	-30020.00			
136	0.1000	16919.60	170	0.1000	-10000.13			

Table 5.16: Comparisons between the proposed approach and NLP approach for the forty-seven-member tower

Forty-Seven-Member Tower				
Starting Point	CPU Time (sec)		Optimum Weight (lb)	
	Proposed Approach	NLP	Proposed Approach	NLP
(1) ω= 30 rad/sec				
Ai = Any arbitrary number	1.282	No convergence after several hours	1398.81	Not applicable
Ai = Solution from proposed approach		43.49		1398.72
(2) ω= 50 rad/sec				
Ai = Any arbitrary number	1.272	No convergence after several hours	1433.61	Not applicable
Ai = Solution from proposed approach		52.575		1433.33
(3) ω= 80 rad/sec				
Ai = Any arbitrary number	1.221	No convergence after several hours	1521.01	Not applicable
Ai = Solution from proposed approach		29.712		1520.21
(4) ω= 100 rad/sec				
Ai = Any arbitrary number	0.611	No convergence after several hours	1605.06	Not applicable
Ai = Solution from proposed approach		30.574		1603.68
(5) ω= 140 rad/sec				
Ai = Any arbitrary number	3.555	No convergence after several hours	1845.32	Not applicable
Ai = Solution from proposed approach		21.001		1842.44
(6) ω= 190 rad/sec				
Ai = Any arbitrary number	2.975	No convergence after several hours	2320.90	Not applicable
Ai = Solution from proposed approach		177.736		2314.76
(7) ω= 200 rad/sec				
Ai = Any arbitrary number	4.276	No convergence after several hours	2448.34	Not applicable
Ai = Solution from proposed approach		41.690		2441.00

Table 5.17: Comparisons between the proposed approach and NLP approach for the two-hundred-member structure

Two-Hundred-Member Structure				
Starting Point	CPU Time (sec)		Optimum Weight (lb)	
	Proposed Approach	NLP	Proposed Approach	NLP
(1) ω= 20 rad/sec				
Ai = Any arbitrary number	28.962	No convergence after several hours	6979.15	Not applicable
Ai = Solution from proposed approach		902.217		6968.18
(2) ω= 35 rad/sec				
Ai = Any arbitrary number	28.151	No convergence after several hours	6990.17	Not applicable
Ai = Solution from proposed approach		597.630		6989.07
(3) ω= 50 rad/sec				
Ai = Any arbitrary number	27.540	No convergence after several hours	7007.25	Not applicable
Ai = Solution from proposed approach		906.063		7002.84
(4) ω= 60 rad/sec				
Ai = Any arbitrary number	26.398	No convergence after several hours	7022.05	Not applicable
Ai = Solution from proposed approach		596.228		7021.39
(5) ω= 80 rad/sec				
Ai = Any arbitrary number	48.600	No convergence after several hours	7059.96	Not applicable
Ai = Solution from proposed approach		979.990		7055.50

CHAPTER 6
RECOMMENDED APPROACH

A recommended general approach will be presented in this chapter. This approach combines the techniques which are addressed in previous chapters. By using this general approach, "fully stressed" designs can be achieved for a wide range of excitation frequencies. If only a certain small range of excitation frequencies is of interest, which is usually the case, optimum or near optimum designs can be found easily and efficiently by this recommended procedure.

6.1 General Remarks

As mentioned in previous chapters, the optimization problems considered in this study are both nonlinear and large scale. Nonlinear programming (NLP) problems are, in general, much more difficult to solve than linear ones. In addition, efficient general purpose NLP methods are rare for large-scale problems. In Chapter 5, it has been shown that, for the considered large-scale structures, an appropriate starting point has to be provided in order to obtain a feasible solution if the nonlinear programming approach is used to solve the optimization problem directly. If any arbitrary initial guess is used as a starting point, the search becomes extremely difficult. For almost all the tested cases, the search by NLP keeps cycling (no matter how the step size is changed) for several hours without any indication of stopping if any arbitrary starting point is selected. Even when the result obtained from the successive iteration approach with or without incorporating linear programming is used as the starting point for the NLP, the optimum solution is only slightly improved. While the CPU time used to obtain this slight improvement is many times (over thirty times for a two-hundred-member structure, for example) of that used to reach the solution by the successive iteration approach with any arbitrary initial guess. In conclusion, the disadvantages of NLP approach are that it is difficult to select a starting point to converge and very time consuming even when an efficient NLP algorithm and a good starting point are used.

6.2 A General Recommended Approach

In general, the successive iteration approach offers an effective and efficient way of searching for the optimum or near optimum designs of structures. For lower frequencies, an optimum or near optimum solution can always be found expeditiously by using the successive iteration approach alone. In order to speed up the convergence for any excitation frequency, the cross sectional areas obtained for a frequency lower than the frequency of interest can be used as a starting point for the desired frequency. Starting from upper bound (5) or lower bound (0.1) of the cross sectional areas can sometimes make some difference in the solution. As a general rule, large initial cross sectional areas are better for low frequencies, and small initial areas are better for high frequencies. For high frequencies, some oscillation of the weight during the iteration may sometimes occur. This oscillation is the reason that a convergent solution could not be found for some of the frequencies. Linear programming as discussed in Chapter 4 can then be incorporated into the successive iteration approach in order to overcome the convergence problem for these frequencies. Generally speaking, if successive iteration alone converges to a solution at a frequency which is lower than the desired frequency, the calculated displacements can be used as an input to the linear program at the desired frequency in order to achieve a convergent solution. To find out if a better solution is possible, use iteration again by modifying all the cross sectional areas or only the cross sectional areas of the members which have stresses exceeding the allowable values. If the solution improves, linear program can be used again to find if a better solution can be obtained. For structures with small number of links, adding discrete masses at the joints can be used to avoid resonant situation.

If desired, the results from the general approach can be used as a starting point in the NLP algorithm to determine if an improvement can be obtained.

The first step in the recommended approach is to use successive iteration. The search at this step may converge to a solution or may not produce a convergent solution at the desired frequency.

If using the successive iteration alone converges to a solution at the frequency of interest, cross sectional areas of all the links have to be modified during each iteration in order to satisfy the stress constraint. If the modification of the cross sectional areas of the members which have stresses exceed the allowable stresses only is used in every iteration starting from the very beginning of the iteration process for the convergent case, it will give higher weight than the case of modification of all the variables in each iteration since some very low stressed members do not have the chance to reach fully stressed state from the very beginning of the iteration process. Accordingly, all the variables have to be modified from the beginning of the iteration process in order for each member to reach as fully stressed state as possible. In addition, for the convergent case, modification of all variables in every iteration during the iteration process always gives a good solution efficiently. Afterwards, if desired, linear programming can be incorporated with the converged solution as an input at that frequency to ensure that it is the smallest fully stressed weight. For the convergent case, among all the cases tested in the study, linear programming with the converged solution as an input always gives the same result as that of using the successive iteration approach alone at that same frequency.

On the other hand, if using the successive iteration alone does not converge to a solution at a specific frequency, a good solution can still be found by incorporating linear programming. For this situation, the successive iteration is applied at lower frequencies (ten or twenty percent lower than the desired frequency). If a converged solution can be found at a lower frequency, linear programming is then used with the converged solution as an input at the frequency of interest. Subsequently, to explore the possibility of a better result, the solution from the linear programming can be used as input to the successive iteration algorithm by modifying all the areas or the high stressed areas only. Afterwards, if solution improves, use linear programming again at that frequency to determine if a better solution can be obtained. During the searching process, if the best solution at the desired frequency is the result of SI, linear programming is used to ensure that it is a smallest fully stressed weight.

With the general approach, described above, optimum or near optimum, can be achieved for a wide range of excitation frequencies. This approach is very efficient and easy to execute. One drawback, however, is that convergent solutions may not be achieved for some high frequencies in such cases, it can be supplemented by the alternative searching process discussed in the next section. Combined with the alternative process discussed in the next section, the general approach can always be used to find a good convergent solution. Only optimality can be guaranteed if a fully stressed structure is achieved and followed by linear programming to assure that it is the smallest fully stressed weight.

6.3 An Alternative Search Process For Cases Where Convergence Difficulties May Be Encountered

As discussed in the previous section, a general approach is developed for the optimum design of large-scale structures which ensures reaching a convergent solution for a wide range of excitation frequencies. If convergence difficulties occur at certain excitation frequencies (usually very high frequencies), the following search process is developed to obtain a good solution at these frequencies.

It was found that in some cases, using successive iteration alone does not produce a convergent solution. The following search process proved to be useful in such cases. It is observed that the weight calculated by modifying all areas in every iteration is always lower than that obtained by modifying high stressed areas only in every iteration at a certain excitation frequencies. However, at these frequencies, the convergent solution by the modification of all areas in every iteration can not be achieved. In this case, the weight calculated by "modifying all areas" for the first several iterations followed by "modifying high stressed areas only" for the rest of the iterations was found to be helpful in achieving a convergent solution. The steps for the proposed procedure are as follows: First, a test is run at the particular excitation frequency for a certain range of iterations (for example, two hundred iterations) by modifying the cross sectional areas of all members of the structure in every iteration with the objective of forcing each member to be as fully stressed as possible. A typical result of the weight versus number of iterations is shown in Figure 6.1. This test run is only a reference for the following steps. Second, at the same frequency, the process is to "modify the areas of all members" up to a certain number of iterations, then this is followed by "modifying the high stressed areas only" for the remaining iterations until a convergent result occurs. The first stage of "modifying all areas" in this process is to ensure that every member of the structure would be as fully stressed as possible. The second stage of "modifying high stressed areas only" in the process reduces the number of variables in such a way that a convergent solution can be achieved. A convergent feasible solution can always be found. Third, the second step is repeated until the best convergent feasible result is obtained at this frequency.

Since trying to repeat for all the cases in the weight versus number of iterations results is tedious (for example, if the test run in the first step has two-hundred iterations, the second step needs to be done two-hundred times), the following suggestions can be considered. For all the tested cases in the second step, at a particular frequency, it was observed that the calculated weight by using the proposed process is always higher than that in the weight versus number of iteration results at that particular number of iteration. For this reason, it is reasonable to consider valley points as reference searching points in order to reduce the number of search trials. It is also observed that a convergent feasible solution usually occurs if the second stage is applied at shallow or flat valleys rather than pointed valleys with sharp rise on both sides in the volume versus number of iterations results. Therefore, only valleys that have a reasonable width should be considered, and the pointed valleys with sharp rise on both sides should be ignored. By the proposed process, the best results from "flat valleys" along the entire spectrum of iterations should be used in the second stage in order to find convergent solutions.

In summary, the search process can be stated as follows:

(1) At the frequency of interest, if using the general approach described in the previous section cannot produce an acceptable solution, continue with the following steps (This usually occurs at high excitation frequencies where several natural modes exist in close proximity).

(2) A test is run at the desired frequency for a certain large number of iterations (for example, two hundred iterations) by modifying the cross sectional areas of all members of the structure in every iteration with the objective of forcing each member to be as fully stressed as possible. This test run is only a reference for the following steps.

(3) From results of the volume versus number of iterations obtained from step (2), consider the shallow or flat valleys rather than pointed valleys with sharp rise on both sides. The proposed process is to "modify the areas of all members" up to a certain number of iterations (for example, modify all areas from the first to an iteration located at shallow or flat valleys) using an arbitrary starting point, then continue by "modifying the high stressed areas only" until a convergent result occurs. The convergent solution found is always feasible.

(4) Go to the next location on the flat valleys of the volume versus number of iterations results obtained from step (2). If the weight at this location is

higher than the calculated weight obtained from step (3), repeat step (4). If not, go to step (3).

(5) Continue step (4) for all the possible points located at the shallow or flat valleys until the best among the calculated convergent feasible solutions is obtained.

(6) The best feasible solution from step (5) is then used as the input into the linear programming algorithm at this frequency in order to obtain the smallest fully stressed weight at this particular frequency.

Using this alternative search process, a convergent solution can always be achieved. The result can then be optimized at that frequency and extended to higher frequencies beyond it by linear programming. This alternative process is understandably more time consuming than the general approach, but it is still orders of magnitude faster than using NLP directly where an optimum solution is not guaranteed. It should be noted that this process is only a supplement to the general approach discussed in the previous section to be considered when a convergent solution at the higher frequencies is not achieved.

6.4 Numerical Illustration of the Proposed Approach

The two-hundred-member structure with the applied loads described in Chapter 3 is used as an illustration of the proposed general approach.

Figure 6.2 to Figure 6.11 represent a set of possible good solutions at different excitation frequencies by using the proposed approach. In these figures, "SI only" stands for the result obtained by using the successive iteration approach only either by modifying all cross sectional areas for convergent case or by the optional technique described in the previous section for non-convergent case. "From 40 SI & LP" stands for the result obtained by using the successive iteration approach alone at frequency of 40 rad/sec to produce a convergent solution, then by incorporating linear programming to reach a fully stressed structure at the desired frequency. Best solutions chosen from these individual frequencies are redrawn in the Figure 6.12. Compared with Figure 4.7, the design domain is extended from 240 rad/sec to 500 rad/sec. If higher frequency solution is still needed, the alternative searching process described in the previous section can be used. Table 6.1 and Figure 6.13 represent the first five natural frequencies of the best solutions shown in Figure 6.12 calculated at the different excitation frequencies. It can be seen that the first two natural frequencies are well separated and they are approximately constants. By contrast, the next two natural frequencies are relatively close to each other and this appears to be one of the reasons for the non-convergence problems which occurred near these frequencies when implementing the successive iteration approach.

Table 6.1: Natural frequencies at different excitation frequencies (rad/sec)

ω	$(\omega_n)_1$	$(\omega_n)_2$	$(\omega_n)_3$	$(\omega_n)_4$	$(\omega_n)_5$
0	95.1227	334.5651	524.7992	554.1452	686.5192
50	94.9273	334.0703	524.4254	551.4006	685.3539
100	93.9422	332.9543	524.3308	543.0610	683.7913
150	80.7119	314.0745	467.2705	514.7712	650.0895
200	102.4350	312.9407	476.8897	558.0160	669.1651
250	79.1410	310.2122	460.0183	501.3473	637.0627
300	94.6391	339.0859	544.9048	582.1925	685.0239
350	94.9508	326.3078	538.6167	578.4932	689.4687
400	97.5652	330.0092	505.4074	604.9812	673.6318
450	87.6456	326.4350	503.1300	641.7588	682.5435
500	105.0072	333.1884	525.2015	640.9199	668.0461

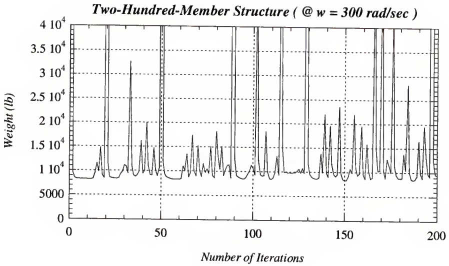

Figure 6.1: A typical non-convergence case of iteration history at a specific excitation frequency

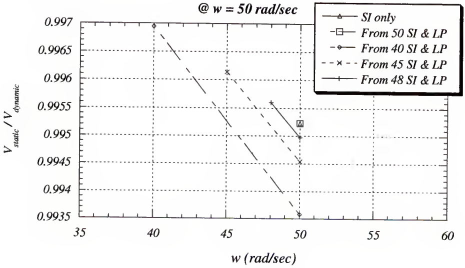

Figure 6.2: Candidates of optimum volume ratio for $\omega = 50\,\mathrm{rad/sec}$

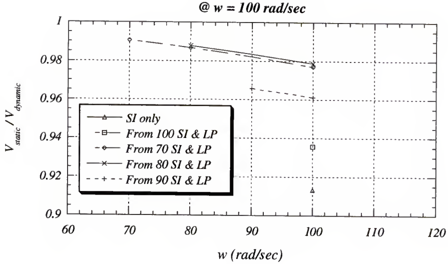

Figure 6.3: Candidates of optimum volume ratio for $\omega = 100\,\mathrm{rad/sec}$

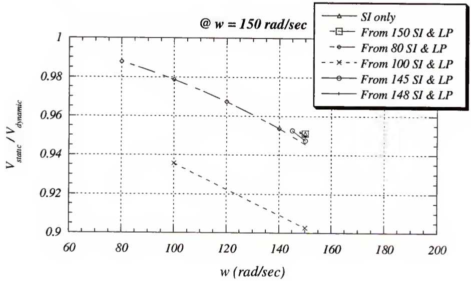

Figure 6.4: Candidates of optimum volume ratio for $\omega = 150\,\mathrm{rad/sec}$

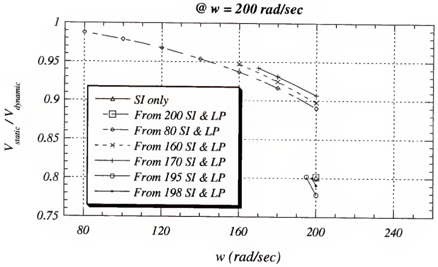

Figure 6.5: Candidates of optimum volume ratio for $\omega = 200\,\mathrm{rad/sec}$

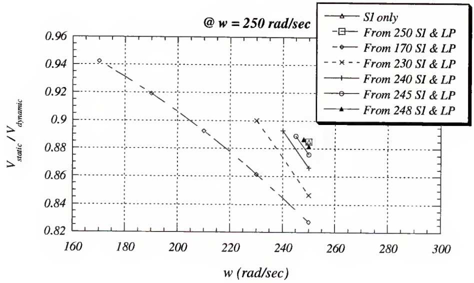

Figure 6.6: Candidates of optimum volume ratio for $\omega = 250\,\mathrm{rad/sec}$

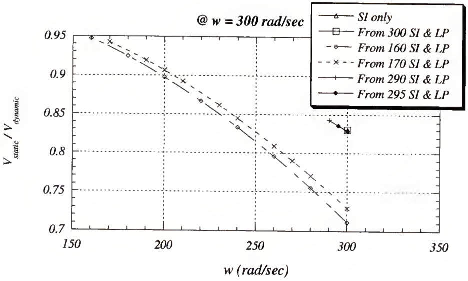

Figure 6.7: Candidates of optimum volume ratio for $\omega = 300\,\mathrm{rad/sec}$

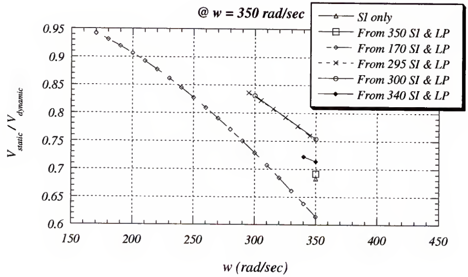

Figure 6.8: Candidates of optimum volume ratio for $\omega = 350\,\mathrm{rad/sec}$

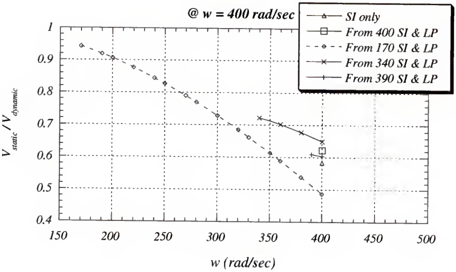

Figure 6.9: Candidates of optimum volume ratio for $\omega = 400\,\mathrm{rad/sec}$

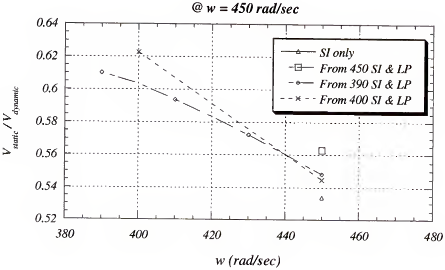

Figure 6.10: Candidates of optimum volume ratio for $\omega = 450\,\mathrm{rad/sec}$

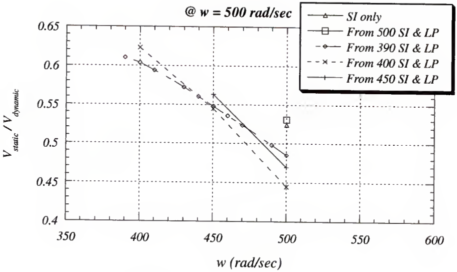

Figure 6.11: Candidates of optimum volume ratio for $\omega = 500\,\mathrm{rad/sec}$

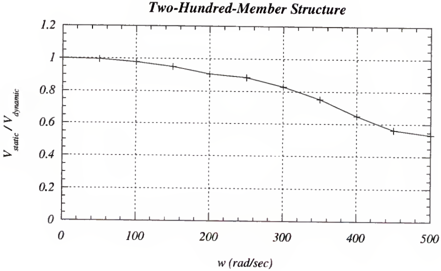

Figure 6.12: Optimum volume ratios of the two-hundred-member structure for a wide range of forcing frequencies (III)

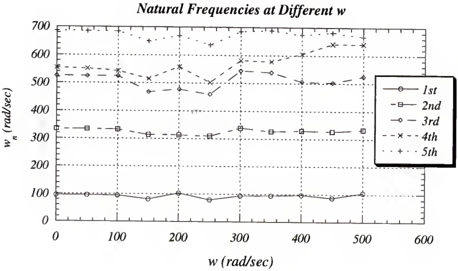

Figure 6.13: Natural frequencies of the optimized structure at different excitation frequencies

CHAPTER 7
SOME OBSERVATIONS ON THE EFFECT OF THE NUMBER OF LINKS AND THE LOADING CONDITIONS

It is observed in the course of this investigation that it is not possible to converge to a design with a reasonable weight at the resonant frequency for the three-link truss by the general approach except by adding extra masses at the joints. However, this was not the case for the two-hundred-member structure with the applied loads at the locations described in Chapter 3. At the resonant frequency, a "fully stressed" design with reasonable weight can be obtained by the general approach. This chapter gives an explanation for these observations.

The natural frequency (ω_n) is not sensitive to the link area for a small number of links since the system is essentially a well defined discrete parameter system where both mass and stiffness are proportional to the link areas. For a one link structure, it is not affected at all by the area. For the three-link truss, the results given in Figure 7.1, show that the inverse of the dynamic magnification factor $(1 - (\omega/\omega_n)^2)$ gives a close indication of the weight change of the fully stressed design determined by using the successive iteration approach. This is to be expected since the natural frequency of this small structure is not sensitive to the link area, and the only way to change the mass distribution (and in turn to achieve a finite weight of the structure at resonance) is to add mass at the joints.

As the number of links increases and the forces are applied at many locations, the problem approaches that of a continuous system and the mass and stiffness distribution can have a significant effect on the mode shapes and the modal response to excitations at given locations. If most of the mass is at or close to the excitation, this will isolate the rest of the structure from the full effect of the disturbance. This can be seen in Figure 7.2 to Figure 7.7. If the forces are confined to few locations, then the design is less sensitive to the mass distribution. The more the excitation forces are distributed, the more sensitive the design is to the mass distribution.

It can be seen that the "fully stressed" designs for both the forty-seven-member tower and the two-hundred-member structure have very high weights at the resonant frequency when the load is applied at two locations only. On the other hand if the load is applied at many locations (as in the case of the two-hundred-member structure with loads at most of the nodes) it is possible to achieve reasonable weight values even at resonance. This can be readily seen in Figure 7.6, Figure 7.7, and Figure 6.12. The latter figure shows that good finite weight designs can be achieved over a range of frequencies covering the first three natural modes when the force excitations are widely distributed at numerous joints. By contrast, when the loads are applied at two joints only, a finite volume for the same structure can not be achieved in the vicinity of the second natural frequency ($\omega_n \approx 360$ rad/sec) as shown in Figure 7.7.

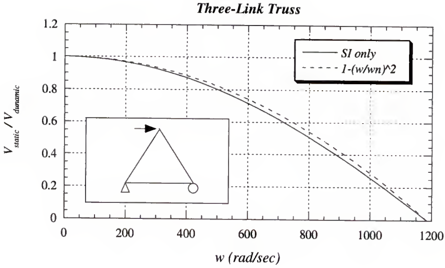

Figure 7.1: Three-link truss

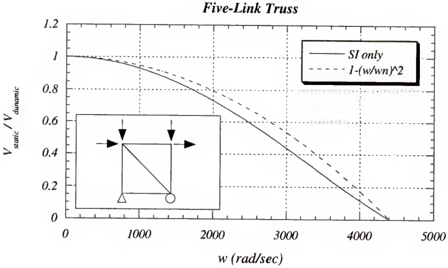

Figure 7.2: Five-link truss

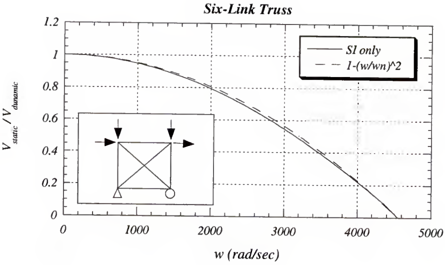

Figure 7.3: Six-link truss

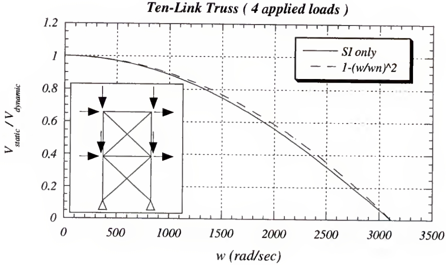

Figure 7.4: Ten-link truss (four-loads)

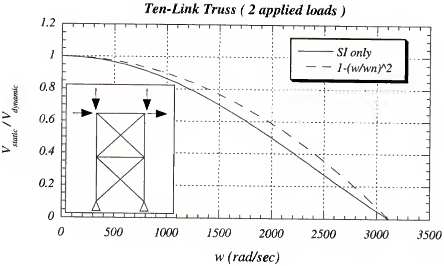

Figure 7.5: Ten-link truss (two loads)

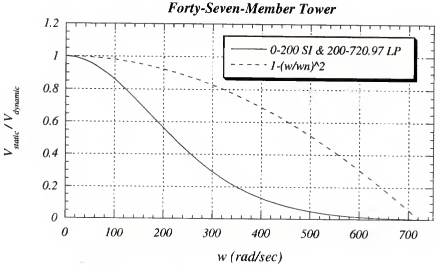

Figure 7.6: Forty-seven-member tower

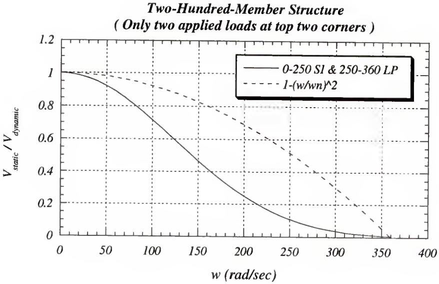

Figure 7.7: Two-hundred-member structure

CHAPTER 8
DYNAMIC RESPONSE ANALYSIS

In this chapter, one of the commonly used implicit time integration methods, so called constant average acceleration method (or Trapezoidal rule), will be considered. The purpose is to use this method as an analysis tool for the interactive program which will be described in the next chapter.

8.1 Introduction

Dynamic response analysis, also called time-history analysis or transient response analysis, is the study of how a structure responds to any kind of time-dependent loading. The methods for dynamic response analysis can be divided into two categories: modal methods (or mode superposition methods) and direct integration methods (or step-by-step methods).

In modal approach, several methods have been proposed and are commonly used [79–81]. To name a few, mode superposition methods, superposition of Ritz vectors [82] are commonly used. Modal methods are effective because of the properties of orthogonality and linear independence that the eigenvectors possess. Generally speaking, in mode superposition methods, the eigenvalues (or natural frequencies) and eigenvectors (or mode shapes) can be found by solving the eigenproblems of the free vibration problems of the system of interest. Afterwards, the mode shape matrix which consists of mode shape vectors serves to transform the generalized normal coordinates to the geometric coordinates due to the property of linear independence. Finally, the property of orthogonality of the normal modes is used to uncouple the equations of motion of the system. Therefore, a number of single degree of freedom systems can be solved independently since the system has been uncoupled. The dynamic response of the structure can be obtained by solving independently for the response of each modal coordinate; then the displacements of the original system are obtained by superposition of the response in each mode. Accordingly, this approach can also be called mode displacement superposition method. A useful variant of the mode superposition method is called the mode acceleration method in which only the inertial and viscous terms are used in modal transformation [81]. Ritz vectors can also serve as a basis instead of the eigenvectors. The approach is called superposition of Ritz vectors. However, Ritz vectors do not have all of the desirable properties of eigenvectors but are much more efficient to compute than mode superposition methods. Most of the computational expense in the mode superposition methods occurs in solving the eigenproblems, especially for large-scale systems. Modal reduction, or sometimes called condensation, can be employed to reduce the size of the basis, which reduces the computational expense. Many methods exist and continue to be proposed in the literature [79, 80]. There is an accuracy concern about the reduced basis approximation since the response depends on the number of modes included in the modal analysis. Even in structural dynamics problems, such as earthquake loading, only the lower frequencies and modes are used as reduced basis approximation; since only lower modes are significantly excited, some error will be introduced into the analysis.

In contrast to the modal methods, direct integration methods do not require any transformation of the basis. In other words, the coupled governing ordinary differential equations of motion are integrated directly without any preliminary uncoupling by modes [83]. In direct integration methods, the problem is solved by integrating the system of ordinary differential equations directly based on the appropriate finite difference approximation using a numerical step-by-step procedure. Basically, there are two general classes of algorithms for the time integration in the step-by-step methods:

explicit and implicit. In the explicit integration approaches, the response history is divided into a sequence of time steps. During each step, the response is updated by using the information, displacements and their time derivatives, from previous time steps. Explicit algorithms involve no matrix inversion if mass and damping matrices are diagonal; therefore, there is no need to solve any algebraic equations. They are simple in structure and easy in implementation and require only modest core storage in treating very large problems. However, explicit algorithms are only conditionally stable, so they usually need a very small time step size to ensure numerical stability, and a very large number of time steps may be required. A popular scheme of the explicit algorithm is the central difference method. In the implicit integration approaches, updating of the displacements requires information about the time derivatives of the current displacements, which are unknown. In contrast to explicit algorithms, most of the useful implicit algorithms are unconditionally stable and have no restriction on the time step size other than as required for accuracy. But, they require the solution of algebraic equations in every time step, which leads to large computer memory storage and considerably more computational cost per time step. In addition, implicit methods are more difficult than explicit methods to implement. In practice, the choice of maximum time step size in implicit methods depends on accuracy considerations. Constant average acceleration method, Houbolt method, and Wilson-θ method are three of the many commonly used implicit methods. Explicit methods are considered to be suitable for short-duration problems, such as impact or shock wave problems, since a large amount of time steps is not needed. Implicit methods are preferable for long-duration problems, such as harmonically loaded systems, since they are more efficient than explicit methods. For the purpose of efficiency, the constant average acceleration method (or the trapezoidal rule) is chosen for use in this study, for it is unconditionally stable thus allowing rather large time step sizes to be used. Computing time can be greatly reduced, although the problems studied are large scaled. Detailed discussion of all of the direct integration methods mentioned in this introduction can be found in Bathe [80] and Hughes [2].

8.2 The Constant Average Acceleration Method-An Implicit Algorithm

The constant average acceleration method (or the trapezoidal rule) is a special case of Newmark family of methods, although Newmark [84] originally proposed the constant average acceleration method. The Newmark methods can be given by

$$\mathbf{X}_{n+1} = \mathbf{X}_n + \Delta t\dot{\mathbf{X}}_n + \frac{\Delta t^2}{2}[(1-2\beta)\ddot{\mathbf{X}}_n + 2\beta\ddot{\mathbf{X}}_{n+1}] \tag{8.1}$$

$$\dot{\mathbf{X}}_{n+1} = \dot{\mathbf{X}}_n + \Delta t[(1-\gamma)\ddot{\mathbf{X}}_n + \gamma\ddot{\mathbf{X}}_{n+1}] \tag{8.2}$$

where β and γ are numbers chosen by the analyst in order to control accuracy and stability. If $\beta = 0$, the methods are explicit; otherwise, if $\beta > 0$, the methods are implicit in nature. It can be shown [85] that this algorithm is guaranteed stable if $2\beta \geq \gamma \geq 1/2$.

A popular unconditionally stable implicit method is the constant average acceleration method (or the trapezoidal rule) by choosing $\gamma = 1/2$ and $\beta = 1/4$. The method is so called since it is based on the assumption that the acceleration along each coordinate of the system remains constant over the small time interval Δt, and its value is the average of those at the beginning and the end of the interval. It can be shown by the following, when $\gamma = 1/2$ and $\beta = 1/4$ in the Newmark methods,

$$\mathbf{X}_{n+1} = \mathbf{X}_n + \Delta t\dot{\mathbf{X}}_n + \frac{\Delta t^2}{4}(\ddot{\mathbf{X}}_n + \ddot{\mathbf{X}}_{n+1}) \tag{8.3}$$

$$\dot{\mathbf{X}}_{n+1} = \dot{\mathbf{X}}_n + \frac{\Delta t}{2}(\ddot{\mathbf{X}}_n + \ddot{\mathbf{X}}_{n+1}) \tag{8.4}$$

They can be solved for $\ddot{\mathbf{X}}_{n+1}$ and $\dot{\mathbf{X}}_{n+1}$ to give

$$\ddot{\mathbf{X}}_{n+1} = -\ddot{\mathbf{X}}_n + \frac{4}{(\Delta t)^2}(\mathbf{X}_{n+1} - \mathbf{X}_n - \Delta t\dot{\mathbf{X}}_n) \tag{8.5}$$

$$\dot{\mathbf{X}}_{n+1} = -\dot{\mathbf{X}}_n + \frac{2}{\Delta t}(\mathbf{X}_{n+1} - \mathbf{X}_n) \tag{8.6}$$

These are the relationships between the response parameters at time $n\Delta t$ and $(n+1)\Delta t$. These relationships can be combined with the equations of motion at time $(n+1)\Delta t$ in the following:

$$\mathbf{M}\ddot{\mathbf{X}}_{n+1} + \mathbf{C}\dot{\mathbf{X}}_{n+1} + \mathbf{K}\mathbf{X}_{n+1} = \mathbf{F}_{n+1} \tag{8.7}$$

to give

$$\mathbf{A}\mathbf{X}_{n+1} = \mathbf{B} \tag{8.8}$$

where

$$\mathbf{A} = \frac{4}{(\Delta t)^2}\mathbf{M} + \frac{2}{\Delta t}\mathbf{C} + \mathbf{K} \tag{8.9}$$

$$\mathbf{B} = \mathbf{F}_{n+1} + \mathbf{M}(\frac{4}{(\Delta t)^2}\mathbf{X}_n + \frac{4}{\Delta t}\dot{\mathbf{X}}_n + \ddot{\mathbf{X}}_n) + \mathbf{C}(\frac{2}{\Delta t}\mathbf{X}_n + \dot{\mathbf{X}}_n) \tag{8.10}$$

As seen from the above relations, $\mathbf{X}_{n+1}$can be solved by Equation (8.8). Then, the resulting value is substituted into Equation (8.5) and Equation (8.6), respectively, to obtain $\ddot{\mathbf{X}}_{n+1}$ and $\dot{\mathbf{X}}_{n+1}$. It will be noted that the solution for $\mathbf{X}_{n+1}$ requires factorization of $\mathbf{K}$. It can also be noted that the initial values of displacements, velocities, and accelerations at time $n\Delta t$ are needed for the solution to begin with. Since this method is unconditionally stable, it is numerically stable for any time step size used. Nonetheless, the choice of the time step size should be based on accuracy considerations. For a second-order accurate time integration method, such as trapezoidal rule, it is shown [80] that the time step size should be less or equal to $T/20$, in which $T = 2\pi/\omega$ and $\omega = 4\omega_u$ where ω_u is the frequency of the loading, to give a very good accuracy for modes that participate dynamically in the response.

A computational procedure by using the constant average acceleration method can be listed as follows:

(1) Formulate the mass matrix (**M**), damping matrix (**C**), and stiffness matrix (**K**) for a specific optimum design.

(2) Set initial conditions for displacements $(\mathbf{X}_0)$ and velocities $(\dot{\mathbf{X}}_0)$.

(3) Calculate the initial acceleration $(\ddot{\mathbf{X}}_0)$ by the equations of motion at the beginning of the time history $\ddot{\mathbf{X}}_0 = \mathbf{M}^{-1}\left(\mathbf{F}_0 - \mathbf{C}\dot{\mathbf{X}}_0 - \mathbf{K}\mathbf{X}_0\right)$.

(4) Solve displacements $(\mathbf{X}_{n+1})$ for the time step $n+1$ by Equation (8.8) to Equation (8.10).

(5) Update velocities $(\dot{\mathbf{X}}_{n+1})$ and accelerations $(\ddot{\mathbf{X}}_{n+1})$ for the time step $n+1$ by Equation (8.5) and Equation (8.6).

(6) Repeat from procedure (4) for the next time step $n = n+1$ until the desired number of time step is reached.

CHAPTER 9
INTERACTIVE PROCEDURE

An interactive program combining the proposed algorithms described in previous chapters with an interactive model creation facility via graphical user interfaces (GUIs) has been developed during this study for interactive optimum design and analysis of large-scale structures with static or dynamic loadings.

9.1 Introduction

A good design of large-scale structures usually requires a combination of algorithmic decisions and subjective judgement from the designer. Besides, an intricate computer program should allow the user to concentrate on the more creative aspects of design. Providing an environment for interaction between the designer and the automated optimization and analysis programs can be an important consideration for developing efficient and effective tools for design and analysis.

A graphical user interface (GUI) is a user interface, which is a method of communication between a user and a computer or computer program, incorporating different graphical objects into a complete interactive tool. It provides an intuitive means through which the user can communicate with the computer without programming commands. Accordingly, a GUI is a commonly used medium for development of interactive programs. MATLAB provides a set of structured event driven components that can be easily programmed to create any kinds of useful graphical user interfaces.

For the purpose of this study, a GUI program has been developed for optimum design and analysis of large-scale structures with static or dynamic loadings under MATLAB programming environment. In addition to the main GUI program, an interactive model creation program is developed for efficient creation and modification of the original model for design and analysis according to the input of designer.

9.2 The Interactive Program

The program is named "Interactive Large-Scale Truss Structural Optimization System." The program has been developed to combine the successive iteration (SI) algorithm, the SI algorithm incorporating linear programming (LP), nonlinear programming (NLP) algorithm, and constant average acceleration methods, with an interactive model creation facility via graphical user interface (GUI) for interactive optimum design and analysis of large-scale truss structures with dynamic (currently harmonically excited and impulsive) loadings, although static loadings can be applied as well. It can automatically formulate the dynamic equilibrium equations with compatibility of joint displacements. The optimization criterion is the minimum weight of the truss subject to the specified constraints (currently stress constraint only). With the interactive graphic model creation program, users are allowed to add, delete or modify the nodal coordinates, truss members, support and excitation nodal locations, and interactively input materials property information. The optimization algorithm rapidly evaluates the effect of these changes on improving the design merit and guides the user towards further modifications which can be potentially beneficial. The design can be made at a specific excitation frequency or for a range of excitation frequencies. After the optimum design is determined, the structures can be analyzed as needed (for example, stress level of a certain member, and displacement of a certain node) in time domain at a specific excitation frequency. The main optimization process is based on the SI algorithm or the SI algorithm incorporating LP. The NLP algorithm can be only used as a checking process since it is very time consuming even though the starting point input in the program is the solution from the SI algorithm. The main analysis process is based on the constant average acceleration method which is derived from the popular Newmark family of methods. Although the example problem given is a 2-D problem, the program is readily applicable for 3-D structural problems.

The process of the interactive program can be divided into three stages: model generation, optimum design, and analysis.

The first stage, as shown in the main windows of Figure 9.1, is to generate a new model for design and analysis either by "interactively creating model" or using an "external input file." If "interactively creating model" is preferred, the structural model creation program which has been developed in this study and illustrated in Figure 9.2, can be used to interactively input geometric data (such as selection and modification of nodal points, members, support and excitation nodes, as shown in Figure 9.3) and material information (such as specific weight, modulus of elasticity, and allowable tensile and compressive stress, as shown in Figure 9.4). At each step of model generation, a detailed instruction shown in the window can be followed. If the selection of information is not satisfied at any step of the model generation, users can always redraw and re-select the information as they wish. After all the selections are completed, the new generated model can be drawn and saved as a data file, as shown in Figure 9.5. An automatically generated input data sheet, as shown in another window of Figure 9.6, can be used to check for correctness at this point if needed. If error is found, users can modify it by reconstructing the model. The completed initial structural model can then be automatically loaded into the main window, as shown in Figure 9.7. An alternative model creation method is to load an external input data file from the main window as is conventionally done if a formatted external data file is provided in advance.

The second stage is the main design stage of optimization. Algorithmic decision can be made between the SI approach and the SI approach incorporating LP. Optimization can also be performed for a specific excitation frequency or a range of excitation frequencies all at once. If optimization for a specific frequency is preferred, numerical results (such as stress in each member, displacements at each node, natural frequencies, optimum weight, and CPU time) can be listed on a table as shown in Figure 9.8. If the results are not satisfactory, the optimization can always be re-performed easily and rapidly. If the results are satisfactory, the relative area distribution can be drawn as shown in Figure 9.9. The iteration history can also be drawn as shown in Figure 9.10 when encountering a non-convergent case at that frequency. If optimization for a range of excitation frequencies is preferred, a plot of the volume ratio verses frequency will be shown automatically after the optimization process is completed, as shown in Figure 9.11. NLP can be performed at a specific excitation frequency if needed.

The final stage is the analysis stage which is performed at a specific excitation frequency. From the final configuration of the main window (Figure 9.9), some with members with large areas are observed. For these members, the time history of the stress level can be examined. Also the time response of any high stressed member can also be examined. Furthermore, the time history responses of any node can be examined if needed as shown in Figure 9.12 for an example of 20 rad/sec excitation frequency. The movement of the dynamically loaded truss can also be displayed using the results of the time history analysis. One example of the forty-seven-member tower under harmonic loading is shown in Figure 9.13. In order to see the movement of the tower, the displacements are amplified since the design algorithm is based on the assumption of small displacement.

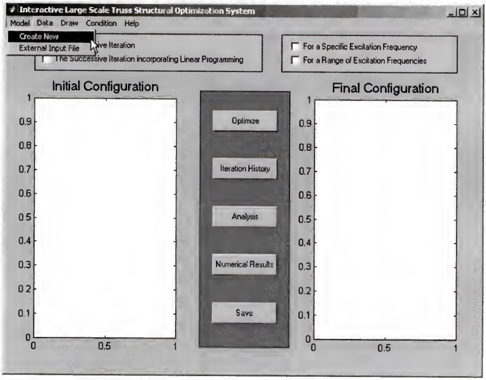
Interactive Large Scale Truss Structural Optimization System
Model Data Draw Condition Help
Create New
External Input File
...ive Iteration
The Successive Iteration incorporating Linear Programming
☐ For a Specific Excitation Frequency
☐ For a Range of Excitation Frequencies
Initial Configuration
Final Configuration
Optimize
Iteration History
Analysis
Numerical Results
Save
0 0.1 0.2 0.3 0.4 0.5 0.6 0.7 0.8 0.9 1
0 0.5 1

Figure 9.1: Main window of the interactive program

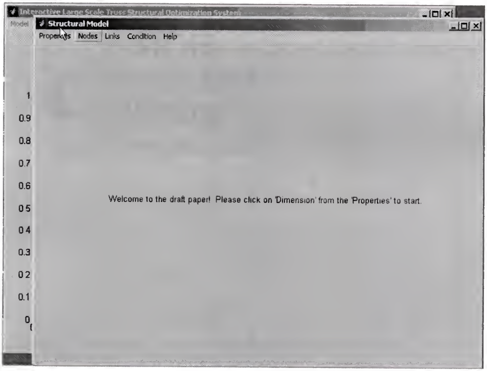
Interactive Large Scale Truss Structural Optimization System
Model
Structural Model
Properties Nodes Links Condition Help
0 0.1 0.2 0.3 0.4 0.5 0.6 0.7 0.8 0.9 1

Welcome to the draft paper! Please click on 'Dimension' from the 'Properties' to start.

Figure 9.2: The structural model creation program

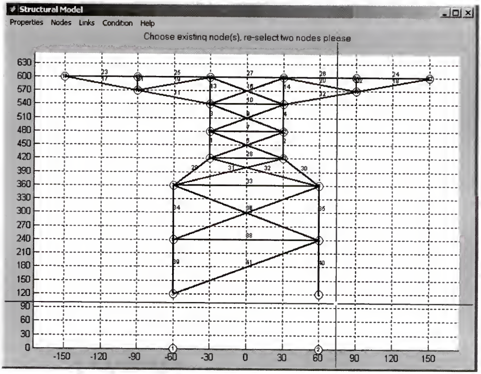

Choose existinq node(s), re-select two nodes please

Figure 9.3: Interactive input of geometric information through the structural model creation program

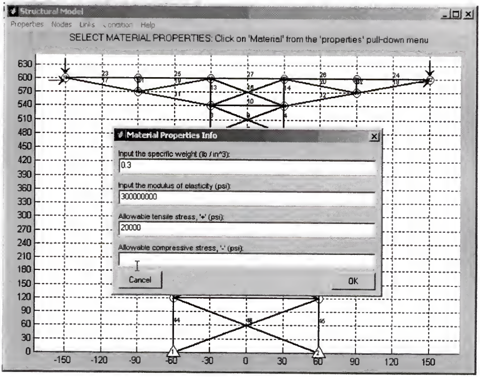

SELECT MATERIAL PROPERTIES: Click on 'Material' from the 'properties' pull-down menu

Input the specific weight (lb / in^3): 0.3

Input the modulus of elasticity (psi): 300000000

Allowable tensile stress, '+' (psi): 20000

Allowable compressive stress, '-' (psi):

Figure 9.4: Interactive input of material information through the structural model creation program

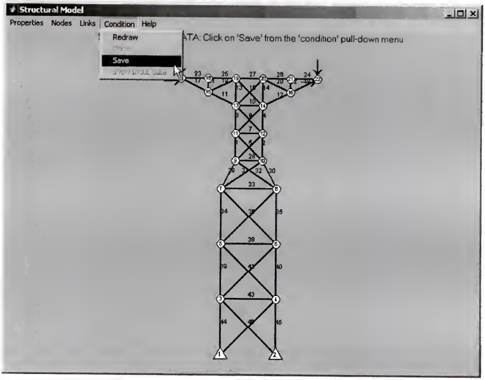

ATA: Click on 'Save' from the 'condition' pull-down menu

Figure 9.5: A new generated structural model through the structural model creation program

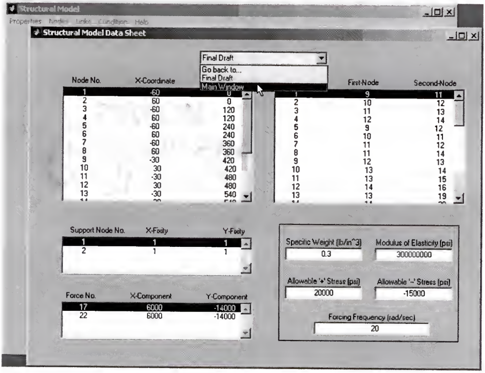

Node No.	X-Coordinate	
1	-60	0
2	60	0
3	-60	120
4	60	120
5	-60	240
6	60	240
7	-60	360
8	60	360
9	-30	420
10	30	420
11	-30	480
12	30	480
13	-30	540

	First-Node	Second-Node
1	9	11
2	10	12
3	11	13
4	12	14
5	9	12
6	10	11
7	11	12
8	11	14
9	12	13
10	13	14
11	13	15
12	14	16
13	13	19

Support Node No.	X-Fixity	Y-Fixity
1	1	1
2	1	1

Force No.	X-Component	Y-Component
17	6000	-14000
22	6000	-14000

Specific Weight (lb/in^3): 0.3

Modulus of Elasticity (psi): 300000000

Allowable '+' Stress (psi): 20000

Allowable '-' Stress (psi): -15000

Forcing Frequency (rad/sec): 20

Figure 9.6: Automatically generated input data sheet through the structural model creation program

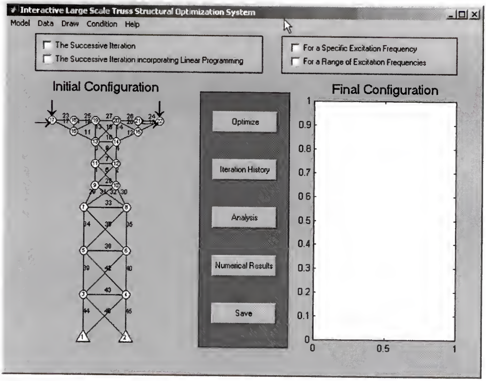

☐ The Successive Iteration
☐ The Successive Iteration incorporating Linear Programming

☐ For a Specific Excitation Frequency
☐ For a Range of Excitation Frequencies

Figure 9.7: Automatically loaded structural model into the main window

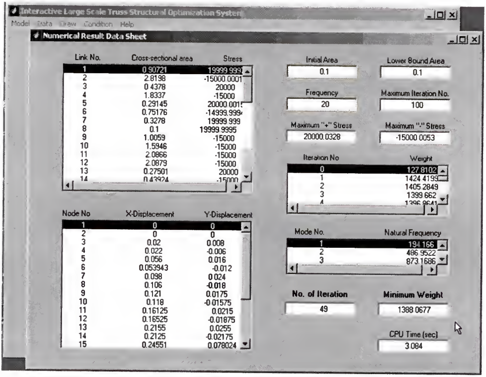

Interactive Large Scale Truss Structural Optimization System
Model
Data
Draw
Condition
Help
Numerical Result Data Sheet

Link No.	Cross-sectional area	Stress
1	0.90721	19999.999
2	2.8198	-15000.0001
3	0.4378	20000
4	1.8337	-15000
5	0.29145	20000.001
6	0.75176	-14999.999
7	0.3278	19999.999
8	0.1	19999.9995
9	1.0059	-15000
10	1.5946	-15000
11	2.0866	-15000
12	2.0879	-15000
13	0.27501	20000
14	0.43924	-15000

Node No	X-Displacement	Y-Displacement
1	0	0
2	0	0
3	0.02	0.008
4	0.022	-0.006
5	0.056	0.016
6	0.053943	-0.012
7	0.098	0.024
8	0.106	-0.018
9	0.121	0.0175
10	0.118	-0.01575
11	0.16125	0.0215
12	0.16525	-0.01875
13	0.2155	0.0255
14	0.2125	-0.02175
15	0.24551	0.078024

Initial Area: 0.1
Lower Bound Area: 0.1
Frequency: 20
Maximum Iteration No.: 100
Maximum "+" Stress: 20000.0328
Maximum "-" Stress: -15000.0053

Iteration No	Weight
0	127.8102
1	1424.4199
2	1405.2849
3	1399.662
4	1396.9641

Mode No.	Natural Frequency
1	194.166
2	486.9522
3	873.1686

No. of Iteration: 49
Minimum Weight: 1388.0677
CPU Time (sec): 3.084

Figure 9.8: Numerical result data sheet for optimum design

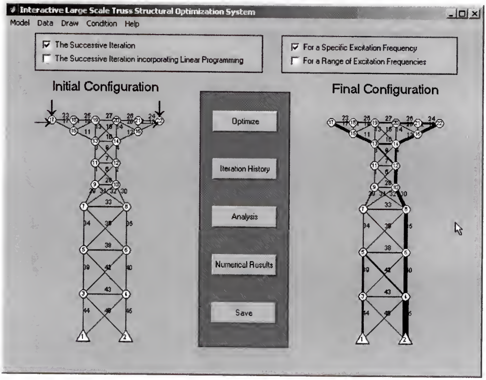

☑ The Successive Iteration
☐ The Successive Iteration incorporating Linear Programming

☑ For a Specific Excitation Frequency
☐ For a Range of Excitation Frequencies

Figure 9.9: The relative area distribution drawn in the main window

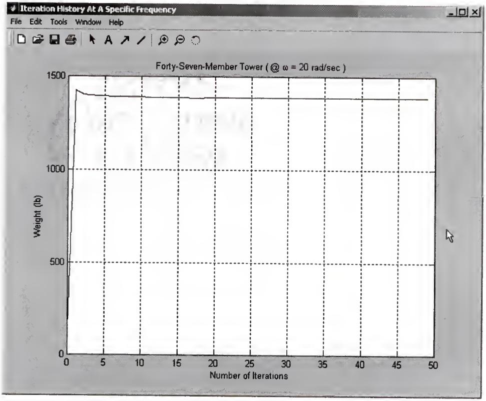

Figure 9.10: Iteration history at a specific excitation frequency

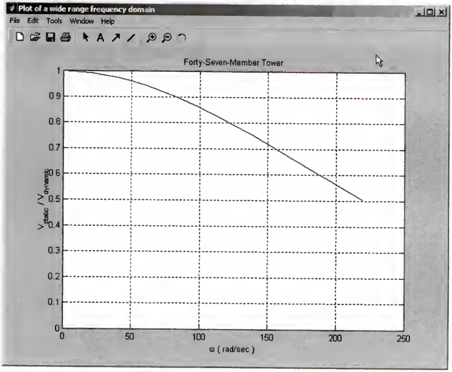

Figure 9.11: A plot of optimum volume ratio for a range of frequencies

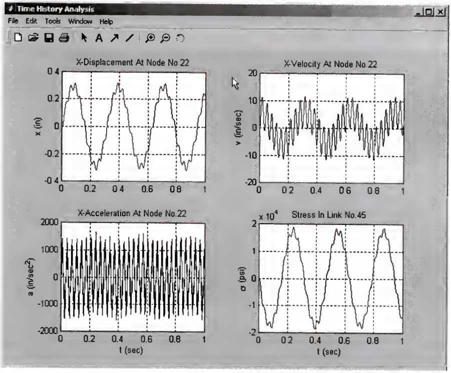

Figure 9.12: Sample results for the time history analysis

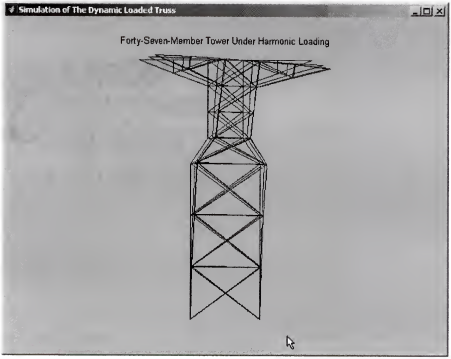
Simulation of The Dynamic Loaded Truss
Forty-Seven-Member Tower Under Harmonic Loading

Figure 9.13: Display of the movement of the forty-seven-member tower under harmonic loading

CHAPTER 10
SUMMARY, CONCLUSION, AND RECOMMENDATIONS

10.1 Summary

In this study, a general procedure for the optimum design of large-scale truss structures subjected to harmonic excitations has been developed. The study reported can be summarized in the following:

(1) A new equivalent mass model of the truss member is developed as described in Chapter 2. The proposed equivalent discrete mass model is obtained by using a scaling factor, which is calculated either from theoretical continuous model or numerical discrete lumped or consistent mass model, in order to derive an equivalent mass matrix for the first mode axial response of each truss member.

(2) In Chapter 3, a two level decomposition and successive iteration (SI) approach are presented in order to overcome the difficulties of solving the nonlinear optimization directly by means of nonlinear programming. The illustrative example problems show excellent success with respect to this issue and they are solved very efficiently. For a forty-seven-member tower, the CPU time, by using Pentium II 333 MH_z personal computer, is approximately 0.065 second per iteration; and it, by using SI approach, usually needs very few numbers of iterations to reach an optimum solution, depending on accuracy needed (one of the tested problem for the forty-seven-member tower, for example, when $\omega = 80\,\mathrm{rad/sec}$, the CPU time is 1.221 seconds). For a two-hundred-member

structure, when $\omega = 50\,\mathrm{rad/sec}$, the CPU time is 27.540 seconds. The program used is implemented in both Fortran language and MATLAB environment and it is designed for a 3-D model. Therefore, the actual CPU time of a 2-D version should be even shorter than those given here.

(3) For some of the excitation frequencies, using the successive iteration approach alone can not find convergent results. This situation can be well remedied by incorporating the linear programming (LP) approach which is presented in Chapter 4. The reason behind this success is due to the observation of the displacement field (or mode shape) from lower frequency results obtained by using the successive iteration alone. According to the results, the displacement field (or mode shape) does not change significantly for each individual mode; therefore, the displacements can be used as an input to the linear program in order to solve for the optimum volume. A new formulation based on Seireg's approach [62] for the system matrices has also been developed. It is unique since it is derived in an unconventional manner in contrast to formulations derived by common matrix or finite element methods. Although matrix or finite element methods are useful for some problems, they are too cumbersome for computational implementation of the problem under investigation because the design variables are difficult to be extracted during the process of forming the element matrices and assembling the global system matrices. In the proposed procedure the design parameters exist in a global manner. Moreover, this procedure is easy to implement in computer codes.

(4) Nonlinear programming (NLP) results are also calculated in Chapter 5 for comparison. It shows that, for large-scale structures, choosing a starting point is critical in finding an optimum solution. For all the tested cases, the search with NLP was found to cycle for several hours, no matter how the step size is changed, without any sign of stopping if any arbitrary starting

point is chosen. However, if the results from the SI approach are used as a starting point for the NLP, an optimum solution can be obtained by NLP, but the CPU time is always much longer than that of the SI approach with any arbitrary starting point. For the forty-seven-member tower, one tested example, when $\omega = 200\,\text{rad/sec}$, the CPU time by NLP with the results from SI as input is 41.690 seconds. For two-hundred-member structure, when $\omega = 50\,\text{rad/sec}$, the CPU time by NLP with results from SI as input is 906.063 seconds. In both cases the NLP solution was not significantly different from that obtained by SI.

(5) A recommended general approach combines the advantages of both the SI approach and the SI approach incorporating LP has been developed as stated in Chapter 6. Another searching process is also proposed as an alternative when the proposed approach fails to produce a convergent solution. This situation may occur at high excitation frequencies where several natural modes exist in close proximity to the excitation frequency. Using this alternative procedure, an optimum or near optimum solution can always be reached in such situations.

(6) Some observations on the effect of the number of links and the loading condition is presented in Chapter 7. An explanation is given for the reason why an optimum solution with reasonable weight can not be reached at resonance for a small structure or a large structure with applied loads at few locations.

(7) In Chapter 9, an interactive program combining the proposed algorithms described in this study with an interactive model creation facility via graphical user interfaces (GUIs) has been developed as an aid for optimum design. One of the implicit methods, constant average acceleration method (or Trapezoidal rule), is used as a time domain analysis tool which can be used

in conjunction with the interactive program. This method is discussed in Chapter 8.

(8) The procedure is extended to deal with the design of structures subjected to harmonic base excitation and impulsive loading. The results are given in Appendix B and Appendix C, respectively.

(9) It should be noted that since the lengths of the members are known beforehand, buckling is taken into consideration in selecting the allowable stress in compression for the different links.

10.2 Conclusion

The following can be concluded from the reported study.

(1) Using the proposed general procedure described in Chapter 6, an optimum or near optimum solution can always be reached for very large-scale truss structures under harmonic excitations at any frequency.

(2) It has been shown in this study that, for large-scale structures, using NLP directly to solve the considered nonlinear optimization problem is significantly inferior to the proposed approach. Using the proposed approach with any arbitrary starting point converges extremely fast to an optimum or near optimum solution. With any arbitrary starting point, NLP was found not converge to a solution for the large structures even when allowed to search for hours. Even when using the results obtained from the proposed approach as a starting point, the NLP converges very slowly to a slightly improved optimum solution; even the stresses and displacements obtained by NLP are approximately the same as those obtained by the proposed approach.

10.3 Recommendations

The followings are some recommendations for future studies.

(1) Experimental investigations using a scale model of the structure should be undertaken to confirm the theoretical findings.

(2) Harmonic disturbance at different frequencies and phase relations needs to be studied.

(3) Loading conditions can be extended to include general loading functions, random disturbances, and some typical earthquake disturbances.

(4) Shape synthesis by deleting or combining links would be an interesting extension of the reported study.

(5) The optimum design procedure should be extended to incorporate any nodal displacement constraints imposed on the structures.

APPENDIX A
FORMULATION OF A CONSISTENT MASS MATRIX

The governing equations of motion can be derived by the requirement of equivalence of the work of external forces to the internal energy which can be shown as follows:

$$\int_V \delta\mathbf{u}^T\mathbf{F}dV + \int_S \delta\mathbf{u}^T\boldsymbol{\Phi}dS + \sum_{i=1}^{n}\delta\mathbf{u}_i^T\mathbf{p}_i$$
$$= \int_V \left(\delta\boldsymbol{\epsilon}^T\boldsymbol{\sigma} + \delta\mathbf{u}^T\rho\ddot{\mathbf{u}} + \delta\mathbf{u}^T c\dot{\mathbf{u}}\right) dV \tag{A.1}$$

where $\delta\mathbf{u}$ are virtual displacements, $\delta\boldsymbol{\epsilon}$ are virtual strains, $\mathbf{F}$ are body forces, $\boldsymbol{\Phi}$ are surface tractions, $\mathbf{p}_i$ are concentrated loads, $\boldsymbol{\sigma}$ are stresses, $\rho\ddot{\mathbf{u}}$ are inertia forces, and $c\dot{\mathbf{u}}$ are damping forces. Displacement field ($\mathbf{u}$) can be expressed as

$$\mathbf{u} = \mathbf{N}\mathbf{d} \tag{A.2}$$

where $\mathbf{N}$ are shape functions and are functions of space only, and $\mathbf{d}$ are nodal degrees of freedom and are functions of time only. Strains can be expressed as

$$\boldsymbol{\epsilon} = \mathbf{B}\mathbf{d} \tag{A.3}$$

where $\mathbf{B} = \boldsymbol{\partial}\mathbf{N}$ is the strain-displacement matrix and $\boldsymbol{\partial}$ represents a space differential operator matrix. The governing equations of motion, for linear elastic materials, can be obtained by substituting Equation (A.2) and Equation (A.3) into Equation (A.1) so that

$$\mathbf{m}\ddot{\mathbf{d}} + \mathbf{c}\dot{\mathbf{d}} + \mathbf{k}\mathbf{d} = \mathbf{f} \tag{A.4}$$

where

$$\mathbf{m} = \int_V \rho \mathbf{N}^T \mathbf{N} dV \tag{A.5}$$

$$\mathbf{c} = \int_V c \mathbf{N}^T \mathbf{N} dV \tag{A.6}$$

$$\mathbf{k} = \int_V \mathbf{B}^T \mathbf{E} \mathbf{B} dV \tag{A.7}$$

$$\mathbf{f} = \int_V \mathbf{N}^T \mathbf{F} dV + \int_S \mathbf{N}^T \mathbf{\Phi} dS + \sum_{i=1}^{n} \mathbf{p}_i \tag{A.8}$$

where **E** is the modulus of elasticity matrix. This process is commonly called semidiscretization since the partial differential equations implicitly exist in Equation (A.1) has been transformed into a system of ordinary differential equations of Equation (A.4) by discretizing only in space domain.

By assuming the model to be linear interpolation of displacements for a uniform prismatic bar, referring to Figure 2.3, the shape functions are

$$\mathbf{N} = \left(1 - \frac{x}{L}, \frac{x}{L}\right) \tag{A.9}$$

Hence, the stiffness matrix ($\mathbf{k}$) for a uniform prismatic bar of length (L) , cross sectional area (A), and modulus of elasticity (E) can be obtained mathematically by finding **B** matrix first and substituting **B** matrix into Equation (A.7) as follows:

$$\mathbf{B} = \boldsymbol{\partial} \mathbf{N} = \frac{d}{dx}\left(1 - \frac{x}{L}, \frac{x}{L}\right) = \left(-\frac{1}{L}, \frac{1}{L}\right) \tag{A.10}$$

$$\mathbf{k} = \int_V \mathbf{B}^T \mathbf{E} \mathbf{B} dV = \int_0^L E \left(-\frac{1}{L}, \frac{1}{L}\right)^T \left(-\frac{1}{L}, \frac{1}{L}\right) A dx \tag{A.11}$$

Therefore, as expected, the stiffness matrix can be shown as

$$\mathbf{k} = \frac{AE}{L} \begin{bmatrix} 1 & -1 \\ -1 & 1 \end{bmatrix} \tag{A.12}$$

Using the same shape function, the consistent mass matrix ($\mathbf{m}$) for a uniform prismatic bar of length (L) and cross sectional area (A) can be derived by substituting

Equation (A.9) into Equation (A.5) as follows:

$$\mathbf{m} = \int_V \rho \mathbf{N}^T \mathbf{N} dV = \int_0^L \rho \left(1 - \frac{x}{L}, \frac{x}{L}\right)^T \left(1 - \frac{x}{L}, \frac{x}{L}\right) A dx \tag{A.13}$$

Finally, the consistent mass matrix becomes

$$\mathbf{m} = \frac{\rho A L}{6} \begin{bmatrix} 2 & 1 \\ 1 & 2 \end{bmatrix} \tag{A.14}$$

To transform the stiffness matrix ($\mathbf{k}$) and the consistent mass matrix ($\mathbf{m}$) from local coordinates ($\mathbf{d}_l$) to global coordinates ($\mathbf{d}_g$), referring to the coordinate systems in Figure A.1, consider the strain energy (U) and the kinetic energy (T) as follows:

$$U = \frac{1}{2} \mathbf{d}_l^T \mathbf{k}_l \mathbf{d}_l \tag{A.15}$$

$$T = \frac{1}{2} \dot{\mathbf{d}}_l^T \mathbf{m}_l \dot{\mathbf{d}}_l \tag{A.16}$$

where

$$\mathbf{d}_l = (x_1, y_1, x_2, y_2) \tag{A.17}$$

$$\mathbf{k}_l = \frac{AE}{L} \begin{bmatrix} 1 & 0 & -1 & 0 \\ 0 & 0 & 0 & 0 \\ -1 & 0 & 1 & 0 \\ 0 & 0 & 0 & 0 \end{bmatrix} \tag{A.18}$$

$$\mathbf{m}_l = \frac{\rho A L}{6} \begin{bmatrix} 2 & 0 & 1 & 0 \\ 0 & 0 & 0 & 0 \\ 1 & 0 & 2 & 0 \\ 0 & 0 & 0 & 0 \end{bmatrix} \tag{A.19}$$

The coordinate transformation between local and global coordinates is

$$\mathbf{d}_l = \mathbf{T} \mathbf{d}_g \tag{A.20}$$

where

$$\mathbf{d}_g = \left(\underline{\mathrm{x}}_1, \underline{\mathrm{y}}_1, \underline{\mathrm{x}}_2, \underline{\mathrm{y}}_2\right) \tag{A.21}$$

$$\mathbf{T}= \begin{bmatrix} c & s & 0 & 0 \\ -s & c & 0 & 0 \\ 0 & 0 & c & s \\ 0 & 0 & -s & c \end{bmatrix} \tag{A.22}$$

$$c \equiv \cos\theta \tag{A.23}$$

$$s \equiv \sin\theta \tag{A.24}$$

In order to represent both the stiffness matrix $(\mathbf{k})$ and the consistent mass matrix $(\mathbf{m})$ in terms of global coordinates, substitute Equation (A.20) into Equation (A.15) and Equation (A.16) such that

$$U = \frac{1}{2}\mathbf{d}_g^T\mathbf{k}_g\mathbf{d}_g \tag{A.25}$$

$$T = \frac{1}{2}\dot{\mathbf{d}}_g^T\mathbf{m}_g\dot{\mathbf{d}}_g \tag{A.26}$$

where

$$\mathbf{k}_g = \mathbf{T}^T\mathbf{k}_l\mathbf{T} \tag{A.27}$$

$$\mathbf{m}_g = \mathbf{T}^T\mathbf{m}_l\mathbf{T} \tag{A.28}$$

Therefore, the stiffness matrix (**k**) and the consistent mass matrix (**m**) in terms of global coordinates can be obtained as

$$\mathbf{k} = \mathbf{k}_g = \mathbf{T}^T \mathbf{k}_l \mathbf{T} = \frac{AE}{L} \begin{bmatrix} c^2 & cs & -c^2 & -cs \\ cs & s^2 & -cs & -s^2 \\ -c^2 & -cs & c^2 & cs \\ -cs & -s^2 & cs & s^2 \end{bmatrix} \tag{A.29}$$

$$\mathbf{m} = \mathbf{m}_g = \mathbf{T}^T \mathbf{m}_l \mathbf{T} = \frac{\rho AL}{6} \begin{bmatrix} 2c^2 & 2cs & c^2 & cs \\ 2cs & 2s^2 & cs & s^2 \\ c^2 & cs & 2c^2 & 2cs \\ cs & s^2 & 2cs & 2s^2 \end{bmatrix} \tag{A.30}$$

Equation (A.29) and Equation (A.30) can be extended for a three-dimensional version in a similar manner.

To illustrate the comparison between the proposed discrete mass model and the consistent mass model by using the proposed approach, using both the three-link truss and the forty-seven-member tower as examples, the results for $\omega = 300\,\text{rad/sec}$ and $\omega = 100\,\text{rad/sec}$, respectively, are shown in Table A.1 to Table A.5. It can be shown that both results show essentially the same link stress values and the same nodal displacements for the discrete and consistent mass models. Although the optimum weight is a little lower for the consistent mass model, the CPU time is a little shorter for the discrete mass model. Using the consistent mass matrix, similar convergence problems to the discrete mass matrix occur for some of the higher frequencies as described in Chapter 3 by using the successive iteration method alone. These problems were easily overcome by using the linear programming (LP) with the discrete mass formulation. However, the LP formulation is too cumbersome to implement computationally by using the consistent mass model as described in Chapter 4. In addition, for the dynamic response analysis by direct integration methods, using the discrete mass model involves no matrix inversion for the explicit methods. This is extremely efficient for large scale systems under impact since matrix inversion can be very expensive computationally for such systems.

Table A.1: Optimum results of the three-link truss for both the discrete mass model and consistent mass model

Three-Link Truss (Force Excitation, $\omega=$ 300 rad/sec)					
Discrete Mass Model					
Link	Area (in^2)	Stress (psi)	Displacements (in)		
			node	x-dir	y-dir
1	1.3937	20000.00	1	0.0000	0.0000
2	2.6829	-20000.00	2	0.0800	0.0000
3	2.6600	20000.00	3	0.2000	-0.0231
CPU Time (sec)		0.05	Min. Weight (lb)		228.97
Consistent Mass Model					
Link	Area (in^2)	Stress (psi)	Displacements (in)		
			node	x-dir	y-dir
1	1.3041	20000.00	1	0.0000	0.0000
2	2.5470	-20000.00	2	0.0800	0.0000
3	2.5267	20000.00	3	0.2000	-0.0231
CPU Time (sec)		0.08	Min. Weight (lb)		216.77

Table A.2: Comparison of optimum results for the three-link truss between the discrete mass model and consistent mass model

Three-Link Truss (Force Excitation, $\omega=$ 300 rad/sec)			
	Discrete Mass Model	Consistent Mass Model	Ratio
Optimum Weight (lb)	228.97	216.77	0.9467
CPU Time (sec)	0.050	0.080	1.600

Table A.3: Optimum results of the forty-seven-member tower by using the discrete mass model

Forty-Seven-Member Tower (Force Excitation, Discrete Mass Model)								
ω= 100 rad/sec			No mass added and No L.P.					
$A_0 = 0.1\,\text{in}^2$			Modify C.S.A. of all members					
Link	Area (in^2)	Stress (psi)	Link	Area (in^2)	Stress (psi)	Displacements (in)		
						node	x-dir	y-dir
1	1.1342	19999.99	26	1.7335	20000.00	1	0.0000	0.0000
2	3.2430	-15000.00	27	1.3824	20000.00	2	0.0000	0.0000
3	0.6125	20000.00	28	0.1000	-14999.93	3	0.0200	0.0080
4	2.0266	-15000.00	29	1.3434	20000.00	4	0.0220	-0.0060
5	0.4362	20000.01	30	3.5611	-15000.00	5	0.0560	0.0160
6	0.7847	-14999.99	31	1.1084	-15000.00	6	0.0543	-0.0120
7	0.3062	19999.99	32	0.4358	19999.99	7	0.0980	0.0240
8	0.1482	19999.99	33	0.1197	19999.92	8	0.1060	-0.0180
9	1.1361	-15000.00	34	0.7757	19999.98	9	0.1210	0.0175
10	1.5750	-15000.00	35	3.8367	-15000.00	10	0.1180	-0.0158
11	2.0777	-15000.00	36	1.0292	20000.01	11	0.1613	0.0215
12	2.1093	-15000.00	37	0.1000	-9597.34	12	0.1653	-0.0188
13	0.3298	20000.00	38	0.1000	-4194.54	13	0.2155	0.0255
14	0.5103	-15000.00	39	2.2190	20000.02	14	0.2125	-0.0218
15	0.5309	20000.00	40	3.9688	-14999.99	15	0.2458	0.0786
16	0.6097	-15000.00	41	0.1000	17904.57	16	0.2424	-0.0890
17	2.0771	-15000.00	42	1.3456	-15000.04	17	0.2618	0.1030
18	2.1071	-15000.00	43	0.1000	5003.57	18	0.2658	0.0786
19	0.1000	-2412.12	44	2.3733	19999.92	19	0.2698	0.0295
20	0.1000	2821.79	45	5.8477	-15000.03	20	0.2738	-0.0248
21	0.1000	328.74	46	0.9816	20000.25	21	0.2778	-0.0890
22	0.1000	-589.52	47	0.1702	-14998.52	22	0.2818	-0.1752
23	1.0850	20000.00						
24	1.7244	20000.00						
25	1.0794	20000.00						
CPU Time		2.594 sec	Minimum Weight			1605.06 lb		

Table A.4: Optimum results of the forty-seven-member tower by using the consistent mass model

Forty-Seven-Member Tower (Force Excitation, Consistent Mass Model)								
ω= 100 rad/sec			No mass added and No L.P.					
$A_0 = 0.1\,\text{in}^2$			Modify C.S.A. of all members					
Link	Area (in^2)	Stress (psi)	Link	Area (in^2)	Stress (psi)	Displacements (in)		
						node	x-dir	y-dir
1	1.0487	20000.00	26	1.7166	20000.00	1	0.0000	0.0000
2	3.0932	-15000.00	27	1.3774	20000.00	2	0.0000	0.0000
3	0.5456	20000.00	28	0.1000	-14999.97	3	0.0200	0.0080
4	1.9028	-15000.00	29	1.2344	20000.00	4	0.0220	-0.0060
5	0.3996	20000.01	30	3.4324	-15000.00	5	0.0560	0.0160
6	0.7857	-15000.00	31	1.0506	-15000.00	6	0.0539	-0.0120
7	0.3282	19999.99	32	0.4119	20000.00	7	0.0980	0.0240
8	0.1227	20000.00	33	0.1366	19999.97	8	0.1060	-0.0180
9	1.1463	-15000.00	34	0.7049	19999.99	9	0.1210	0.0175
10	1.5567	-15000.00	35	3.6704	-15000.00	10	0.1180	-0.0158
11	2.1071	-15000.00	36	0.9555	20000.01	11	0.1613	0.0215
12	2.0681	-15000.00	37	0.1000	-10071.35	12	0.1653	-0.0188
13	0.2964	20000.00	38	0.1000	-5142.64	13	0.2155	0.0255
14	0.4671	-15000.00	39	2.0340	20000.01	14	0.2125	-0.0218
15	0.4961	20000.00	40	3.8029	-15000.00	15	0.2455	0.0780
16	0.5601	-15000.00	41	0.1000	17429.47	16	0.2420	-0.0883
17	2.0938	-15000.00	42	1.2294	-15000.02	17	0.2618	0.1030
18	2.0807	-15000.00	43	0.1000	5001.52	18	0.2658	0.0780
19	0.1000	-86.59	44	2.1831	19999.97	19	0.2698	0.0295
20	0.1000	89.63	45	5.5116	-15000.01	20	0.2738	-0.0248
21	0.1000	9.09	46	0.8879	20000.11	21	0.2778	-0.0883
22	0.1000	-10.28	47	0.1636	-14999.38	22	0.2818	-0.1752
23	1.0966	20000.00						
24	1.7056	20000.00						
25	1.0899	20000.00						
CPU Time		2.784 sec	Minimum Weight			1530.16 lb		

Table A.5: Comparison of optimum results for the forty-seven-member tower between the discrete mass model and consistent mass model

Forty-Seven-Member Tower (Force Excitation, ω= 100 rad/sec)			
	Discrete Mass Model	Consistent Mass Model	Ratio
Optimum Weight (lb)	1605.06	1530.16	0.9533
CPU Time (sec)	2.594	2.784	1.073

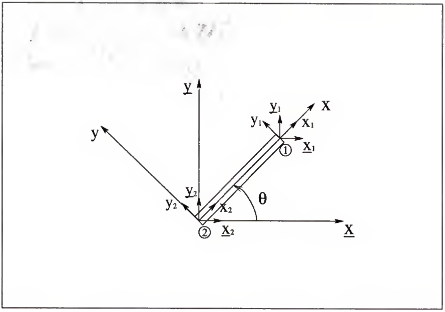

Figure A.1: Coordinate transformation

APPENDIX B
BASE EXCITATION

The formulation of the equations of motion of the structure under ground excitation is presented and some numerical illustrations using the two-hundred-member structure are also given.

The equations of motion of the undamped dynamic system under base excitation can be represented as

$$\mathbf{M}\ddot{\mathbf{X}}^{t} + \mathbf{K}\mathbf{X} = \mathbf{0} \tag{B.1}$$

where

$\mathbf{X}^t \equiv$ total displacement vector relative to some fixed reference axis

$\mathbf{X} \equiv$ relative displacement vector to the support

The relation among the displacements can be expressed as

$$\mathbf{X}^t = \mathbf{X} + \mathbf{X}_g \tag{B.2}$$

where

$$\mathbf{X}_g \equiv \text{support displacement vector}$$

Equation (B.1) can be expressed in terms of total displacements by using Equation (B.2) as follows:

$$\mathbf{M}\ddot{\mathbf{X}}^{t} + \mathbf{K}\mathbf{X}^t = \mathbf{K}\mathbf{X}_g \tag{B.3}$$

It can also be expressed in terms of relative displacements by substituting Equation (B.2) into Equation (B.1) to obtain

$$\mathbf{M}\ddot{\mathbf{X}} + \mathbf{K}\mathbf{X} = -\mathbf{M}\ddot{\mathbf{X}}_g \tag{B.4}$$

The use of Equation (B.3) or Equation (B.4) depends on whether the ground displacements or accelerations are provided. In this study, Equation (B.3) is used since base excitation is prescribed as displacement functions. The term $\mathbf{KX}_g$ in Equation (B.3) can be treated as an effective force term. Therefore, the solution algorithm remains the same as that described in previous chapters.

The case of the two-hundred-member structure is used as an example with a horizontal sinusoidal base excitation with amplitude of one inch applied to the support of the structure. The original vertical nodal external forces as seen in the force excitation cases in previous chapters are used to guide the selection of the equivalent masses at all the same nodes. The result of static case is shown in Table B.1 to Table B.3. Table B.4 to Table B.12 gives the results of minimum weight, CPU time, cross sectional area and stress in each link, and the displacements in x and y directions of each node for several different base excitation frequencies. It is shown that the allowable stresses have been reached for most of the members with the exception of some low stressed members. It is also observed that the optimum weight increases rapidly as the frequency increases. This situation is explained in Figure B.1 and Figure B.2. The segment between $\omega = 10\,\text{rad/sec}$ and $30\,\text{rad/sec}$ of the Figure B.2 shows that the rapid increase in volume shown in Figure B.1 is primarily due to the increase in the inertial loading which is proportional to ω^2. Figure B.3 represents optimum volume ratios of the two-hundred-member structure under base excitation for a wide range of frequencies.

Table B.1: Optimum results of the two-hundred-member structure for static case (I)

Two-Hundred-Member Structure (Base Excitation)	
$\omega = 0\,\mathrm{rad/sec}$ (Static case)	(10000/386.4) of equivalent force mass added and No L.P.
A_0 from static case result $(A)_{\omega=0}$	10000 vertical force at joints and Modify C.S.A. of all members

Displacements (in)			Displacements (in)			Displacements (in)		
node	x-dir	y-dir	node	x-dir	y-dir	node	x-dir	y-dir
1	-0.0480	-0.2216	27	0.0287	-0.1539	53	0.0085	-0.0868
2	-0.0240	-0.1800	28	0.0287	-0.1784	54	0.0169	-0.0792
3	0.0000	-0.1960	29	-0.0442	-0.1640	55	0.0253	-0.0967
4	0.0240	-0.1800	30	-0.0202	-0.1224	56	0.0253	-0.1208
5	0.0480	-0.2216	31	0.0000	-0.1384	57	-0.0403	-0.1064
6	-0.0304	-0.2072	32	0.0202	-0.1224	58	-0.0163	-0.0648
7	-0.0304	-0.1825	33	0.0442	-0.1640	59	0.0000	-0.0808
8	-0.0205	-0.1656	34	-0.0270	-0.1496	60	0.0163	-0.0648
9	-0.0107	-0.1732	35	-0.0270	-0.1253	61	0.0403	-0.1064
10	0.0000	-0.1816	36	-0.0181	-0.1080	62	-0.0236	-0.0920
11	0.0107	-0.1732	37	-0.0092	-0.1156	63	-0.0236	-0.0681
12	0.0205	-0.1656	38	0.0000	-0.1240	64	-0.0157	-0.0504
13	0.0304	-0.1825	39	0.0092	-0.1156	65	-0.0078	-0.0580
14	0.0304	-0.2072	40	0.0181	-0.1080	66	0.0000	-0.0664
15	-0.0461	-0.1928	41	0.0270	-0.1253	67	0.0078	-0.0580
16	-0.0221	-0.1512	42	0.0270	-0.1496	68	0.0157	-0.0504
17	0.0000	-0.1672	43	-0.0422	-0.1352	69	0.0236	-0.0681
18	0.0221	-0.1512	44	-0.0182	-0.0936	70	0.0236	-0.0920
19	0.0461	-0.1928	45	0.0000	-0.1096	71	-0.0384	-0.0776
20	-0.0287	-0.1784	46	0.0182	-0.0936	72	-0.0144	-0.0360
21	-0.0287	-0.1539	47	0.0422	-0.1352	73	0.0000	-0.0520
22	-0.0193	-0.1368	48	-0.0253	-0.1208	74	0.0144	-0.0360
23	-0.0100	-0.1444	49	-0.0253	-0.0967	75	0.0384	-0.0776
24	0.0000	-0.1528	50	-0.0169	-0.0792	76	0.0000	0.0000
25	0.0100	-0.1444	51	-0.0085	-0.0868	77	0.0000	0.0000
26	0.0193	-0.1368	52	0.0000	-0.0952			

	ω_n(rad/sec)		
1	16.218		
2	225.498	Minimum Weight	6964.49 lb
3	345.336	CPU Time	67.878 sec

Table B.2: Optimum results of the two-hundred-member structure for static case (II)

<table>
<tr><th colspan="9">Two-Hundred-Member Structure (Base Excitation)</th></tr>
<tr><th colspan="3">$\omega = 0\,\mathrm{rad/sec}$
(Static case)</th><th colspan="6">(10000/386.4) of equivalent force
mass added and No L.P.</th></tr>
<tr><th colspan="3">A_0 from static case
result $(A)_{\omega=0}$</th><th colspan="6">10000 vertical force at joints
and Modify C.S.A. of all members</th></tr>
<tr><th>Link</th><th>Area (in^2)</th><th>Stress (psi)</th><th>Link</th><th>Area (in^2)</th><th>Stress (psi)</th><th>Link</th><th>Area (in^2)</th><th>Stress (psi)</th></tr>
<tr><td>1</td><td>0.1112</td><td>30000.39</td><td>35</td><td>0.7047</td><td>-30000.00</td><td>69</td><td>0.1000</td><td>2837.53</td></tr>
<tr><td>2</td><td>0.1204</td><td>30000.36</td><td>36</td><td>0.2377</td><td>-30000.28</td><td>70</td><td>1.1363</td><td>-29999.99</td></tr>
<tr><td>3</td><td>0.1204</td><td>30000.36</td><td>37</td><td>0.1000</td><td>28778.57</td><td>71</td><td>0.1000</td><td>2837.53</td></tr>
<tr><td>4</td><td>0.1112</td><td>30000.39</td><td>38</td><td>0.5332</td><td>-29999.90</td><td>72</td><td>0.1000</td><td>-16606.27</td></tr>
<tr><td>5</td><td>0.1999</td><td>-29999.74</td><td>39</td><td>0.1986</td><td>30000.15</td><td>73</td><td>1.6295</td><td>-30000.03</td></tr>
<tr><td>6</td><td>0.1737</td><td>-30000.39</td><td>40</td><td>0.1000</td><td>27601.93</td><td>74</td><td>0.4669</td><td>-30000.09</td></tr>
<tr><td>7</td><td>0.1000</td><td>9583.42</td><td>41</td><td>0.1000</td><td>27601.93</td><td>75</td><td>0.1000</td><td>28307.87</td></tr>
<tr><td>8</td><td>0.3714</td><td>-30000.00</td><td>42</td><td>0.1986</td><td>30000.15</td><td>76</td><td>0.8142</td><td>-29999.90</td></tr>
<tr><td>9</td><td>0.1000</td><td>5271.02</td><td>43</td><td>0.4809</td><td>-29999.83</td><td>77</td><td>0.3311</td><td>30000.03</td></tr>
<tr><td>10</td><td>0.1000</td><td>-17073.35</td><td>44</td><td>0.4061</td><td>-30000.11</td><td>78</td><td>0.1000</td><td>25202.38</td></tr>
<tr><td>11</td><td>0.2459</td><td>-29999.98</td><td>45</td><td>0.1000</td><td>10053.25</td><td>79</td><td>0.1000</td><td>25202.38</td></tr>
<tr><td>12</td><td>0.1000</td><td>-17073.35</td><td>46</td><td>1.2962</td><td>-30000.04</td><td>80</td><td>0.3311</td><td>30000.03</td></tr>
<tr><td>13</td><td>0.1000</td><td>5271.02</td><td>47</td><td>0.1000</td><td>4049.14</td><td>81</td><td>0.6053</td><td>-29999.85</td></tr>
<tr><td>14</td><td>0.3714</td><td>-30000.00</td><td>48</td><td>0.1000</td><td>-17817.88</td><td>82</td><td>0.6115</td><td>-30000.02</td></tr>
<tr><td>15</td><td>0.1000</td><td>9583.42</td><td>49</td><td>0.8030</td><td>-29999.99</td><td>83</td><td>0.1000</td><td>10523.51</td></tr>
<tr><td>16</td><td>0.1737</td><td>-30000.39</td><td>50</td><td>0.1000</td><td>-17817.88</td><td>84</td><td>2.3983</td><td>-30000.03</td></tr>
<tr><td>17</td><td>0.1999</td><td>-29999.74</td><td>51</td><td>0.1000</td><td>4049.14</td><td>85</td><td>0.1000</td><td>2826.74</td></tr>
<tr><td>18</td><td>0.1000</td><td>0.00</td><td>52</td><td>1.2962</td><td>-30000.04</td><td>86</td><td>0.1000</td><td>-18562.55</td></tr>
<tr><td>19</td><td>0.1000</td><td>24576.86</td><td>53</td><td>0.1000</td><td>10053.25</td><td>87</td><td>1.3600</td><td>-29999.99</td></tr>
<tr><td>20</td><td>0.1000</td><td>24576.86</td><td>54</td><td>0.4061</td><td>-30000.11</td><td>88</td><td>0.1000</td><td>-18562.55</td></tr>
<tr><td>21</td><td>0.1000</td><td>26740.00</td><td>55</td><td>0.4809</td><td>-29999.83</td><td>89</td><td>0.1000</td><td>2826.74</td></tr>
<tr><td>22</td><td>0.1000</td><td>26740.00</td><td>56</td><td>0.1000</td><td>0.00</td><td>90</td><td>2.3983</td><td>-30000.03</td></tr>
<tr><td>23</td><td>0.1000</td><td>24576.86</td><td>57</td><td>0.1000</td><td>23372.64</td><td>91</td><td>0.1000</td><td>10523.51</td></tr>
<tr><td>24</td><td>0.1000</td><td>24576.86</td><td>58</td><td>0.1000</td><td>23372.64</td><td>92</td><td>0.6115</td><td>-30000.02</td></tr>
<tr><td>25</td><td>0.1000</td><td>0.00</td><td>59</td><td>0.1000</td><td>24923.95</td><td>93</td><td>0.6053</td><td>-29999.85</td></tr>
<tr><td>26</td><td>0.5332</td><td>-29999.90</td><td>60</td><td>0.1000</td><td>24923.95</td><td>94</td><td>0.1000</td><td>0.00</td></tr>
<tr><td>27</td><td>0.1000</td><td>28778.57</td><td>61</td><td>0.1000</td><td>23372.64</td><td>95</td><td>0.1000</td><td>22168.03</td></tr>
<tr><td>28</td><td>0.2377</td><td>-30000.28</td><td>62</td><td>0.1000</td><td>23372.64</td><td>96</td><td>0.1000</td><td>22168.03</td></tr>
<tr><td>29</td><td>0.7047</td><td>-30000.00</td><td>63</td><td>0.1000</td><td>0.00</td><td>97</td><td>0.1000</td><td>23107.30</td></tr>
<tr><td>30</td><td>0.1000</td><td>-15383.89</td><td>64</td><td>0.8142</td><td>-29999.90</td><td>98</td><td>0.1000</td><td>23107.30</td></tr>
<tr><td>31</td><td>0.1000</td><td>3581.56</td><td>65</td><td>0.1000</td><td>28307.87</td><td>99</td><td>0.1000</td><td>22168.03</td></tr>
<tr><td>32</td><td>0.5792</td><td>-29999.99</td><td>66</td><td>0.4669</td><td>-30000.09</td><td>100</td><td>0.1000</td><td>22168.03</td></tr>
<tr><td>33</td><td>0.1000</td><td>3581.56</td><td>67</td><td>1.6295</td><td>-30000.03</td><td>101</td><td>0.1000</td><td>0.00</td></tr>
<tr><td>34</td><td>0.1000</td><td>-15383.89</td><td>68</td><td>0.1000</td><td>-16606.27</td><td>102</td><td>0.9386</td><td>-29999.90</td></tr>
</table>

Table B.3: Optimum results of the two-hundred-member structure for static case (III)

Two-Hundred-Member Structure (Base Excitation)								
$\omega=0$ rad/sec (Static case)			(10000/386.4) of equivalent force mass added and No L.P.					
A_0 from static case result $(A)_{\omega=0}$			10000 vertical force at joints and Modify C.S.A. of all members					
Link	Area (in^2)	Stress (psi)	Link	Area (in^2)	Stress (psi)	Link	Area (in^2)	Stress (psi)
103	0.1000	27837.30	137	0.1000	20963.21	171	0.1000	19758.24
104	0.6692	-30000.02	138	0.1000	20963.21	172	0.1000	19758.24
105	2.7316	-30000.03	139	0.1000	0.00	173	0.1000	19473.11
106	0.1000	-17828.95	140	0.9271	-29999.92	174	0.1000	19473.11
107	0.1000	2093.14	141	0.1000	27366.73	175	0.1000	19758.24
108	1.6934	-29999.99	142	0.8446	-29999.98	176	0.1000	19758.24
109	0.1000	2093.14	143	3.9903	-30000.02	177	0.1000	0.00
110	0.1000	-17828.95	144	0.1000	-19051.83	178	0.8003	-29999.94
111	2.7316	-30000.03	145	0.1000	1348.56	179	0.1000	26896.13
112	0.6692	-30000.02	146	2.2504	-30000.00	180	0.9930	-29999.96
113	0.1000	27837.30	147	0.1000	1348.56	181	5.3849	-30000.01
114	0.9386	-29999.90	148	0.1000	-19051.83	182	0.1000	-20274.83
115	0.4463	29999.98	149	3.9903	-30000.02	183	0.1000	603.87
116	0.1000	22802.27	150	0.8446	-29999.98	184	2.8075	-30000.00
117	0.1000	22802.27	151	0.1000	27366.73	185	0.1000	603.87
118	0.4463	29999.98	152	0.9271	-29999.92	186	0.1000	-20274.83
119	0.5937	-29999.87	153	0.5444	29999.96	187	5.3849	-30000.01
120	0.7900	-29999.98	154	0.1000	20401.80	188	0.9930	-29999.96
121	0.1000	10993.94	155	0.1000	20401.80	189	0.1000	26896.13
122	3.6570	-30000.03	156	0.5444	29999.96	190	0.8003	-29999.94
123	0.1000	1604.05	157	0.4670	-29999.90	191	0.6525	29999.95
124	0.1000	-19307.31	158	0.9416	-29999.96	192	0.1000	18001.08
125	1.9171	-29999.99	159	0.1000	11464.45	193	0.1000	18001.08
126	0.1000	-19307.31	160	5.0516	-30000.02	194	0.6525	29999.95
127	0.1000	1604.05	161	0.1000	381.18	195	1.2797	-29999.96
128	3.6570	-30000.03	162	0.1000	-20052.14	196	6.5330	-30000.01
129	0.1000	10993.94	163	2.4742	-30000.00	197	1.8855	-30000.00
130	0.7900	-29999.98	164	0.1000	-20052.14	198	1.8855	-30000.00
131	0.5937	-29999.87	165	0.1000	381.18	199	6.5330	-30000.01
132	0.1000	0.00	166	5.0516	-30000.02	200	1.2797	-29999.96
133	0.1000	20963.21	167	0.1000	11464.45			
134	0.1000	20963.21	168	0.9416	-29999.96			
135	0.1000	21290.32	169	0.4670	-29999.90			
136	0.1000	21290.32	170	0.1000	0.00			

Table B.4: Optimum results of the two-hundred-member structure under base excitation for $\omega = 5$ rad/sec (I)

Two-Hundred-Member Structure (Base Excitation)	
ω= 5 rad/sec	(10000/386.4) of equivalent force mass added and No L.P.
$A_0$from static case result $(A)_{\omega=0}$	10000 vertical force at joints and Modify C.S.A. of all members

Displacements (in)			Displacements (in)			Displacements (in)		
node	x-dir	y-dir	node	x-dir	y-dir	node	x-dir	y-dir
1	1.2959	-0.1415	27	1.2816	-0.1702	53	1.1373	-0.0737
2	1.3136	-0.1473	28	1.2850	-0.2079	54	1.1485	-0.0792
3	1.3338	-0.1683	29	1.1734	-0.0867	55	1.1566	-0.1127
4	1.3578	-0.1800	30	1.1974	-0.0968	56	1.1597	-0.1503
5	1.3818	-0.2511	31	1.2187	-0.1107	57	1.0569	-0.0489
6	1.2872	-0.1271	32	1.2427	-0.1224	58	1.0707	-0.0477
7	1.2838	-0.1274	33	1.2621	-0.1935	59	1.0947	-0.0547
8	1.2941	-0.1353	34	1.1573	-0.0765	60	1.1187	-0.0648
9	1.3011	-0.1442	35	1.1543	-0.0782	61	1.1376	-0.1359
10	1.3131	-0.1539	36	1.1663	-0.0845	62	1.0539	-0.0403
11	1.3218	-0.1597	37	1.1768	-0.0895	63	1.0512	-0.0357
12	1.3331	-0.1656	38	1.1888	-0.0964	64	1.0577	-0.0373
13	1.3410	-0.1981	39	1.1997	-0.1021	65	1.0614	-0.0310
14	1.3444	-0.2367	40	1.2109	-0.1080	66	1.0710	-0.0419
15	1.2369	-0.1127	41	1.2189	-0.1414	67	1.0778	-0.0444
16	1.2609	-0.1221	42	1.2221	-0.1791	68	1.0888	-0.0504
17	1.2807	-0.1395	43	1.1088	-0.0647	69	1.0969	-0.0849
18	1.3047	-0.1512	44	1.1326	-0.0719	70	1.0998	-0.1215
19	1.3251	-0.2223	45	1.1566	-0.0820	71	1.0208	-0.0293
20	1.2239	-0.1001	46	1.1806	-0.0936	72	1.0399	-0.0267
21	1.2207	-0.1018	47	1.1993	-0.1647	73	1.0346	-0.0289
22	1.2325	-0.1097	48	1.0952	-0.0582	74	1.0586	-0.0360
23	1.2410	-0.1165	49	1.0924	-0.0540	75	1.0826	-0.1071
24	1.2530	-0.1251	50	1.1044	-0.0599	76	1.0000	0.0000
25	1.2625	-0.1303	51	1.1145	-0.0626	77	1.0000	0.0000
26	1.2737	-0.1368	52	1.1265	-0.0684			

	ω_n(rad/sec)		
1	16.735		
2	44.166	Minimum Weight	8203.43 lb
3	46.864	CPU Time	102.187 sec

Table B.5: Optimum results of the two-hundred-member structure under base excitation for $\omega = 5$ rad/sec (II)

Two-Hundred-Member Structure (Base Excitation)								
ω= 5 rad/sec			(10000/386.4) of equivalent force mass added and No L.P.					
$A_0$from static case result $(A)_{\omega=0}$			10000 vertical force at joints and Modify C.S.A. of all members					
Link	Area (in^2)	Stress (psi)	Link	Area (in^2)	Stress (psi)	Link	Area (in^2)	Stress (psi)
1	0.1112	22117.45	35	0.7177	-30000.00	69	0.1184	-29999.98
2	0.1204	25362.31	36	0.2377	-20568.01	70	1.2013	-30000.01
3	0.1302	30000.00	37	0.1000	13497.61	71	0.1000	20867.33
4	0.1160	30000.00	38	0.5738	-30000.00	72	0.2093	-29999.92
5	0.2044	-30000.00	39	0.2138	30000.04	73	1.6316	-30000.00
6	0.1737	-29662.84	40	0.1000	24761.05	74	0.4669	-18851.74
7	0.1000	5999.27	41	0.1145	29999.97	75	0.1000	8601.82
8	0.3714	-24995.08	42	0.1986	25494.94	76	1.0126	-30000.00
9	0.1000	-16581.99	43	0.4809	-26224.75	77	0.3311	29940.91
10	0.1000	3933.63	44	0.4846	-30000.03	78	0.1000	26610.42
11	0.2885	-30000.00	45	0.1000	16165.10	79	0.1985	29999.94
12	0.1000	-22872.22	46	1.2962	-25864.66	80	0.3311	24259.71
13	0.1000	12053.29	47	0.1000	-27303.15	81	0.6053	-21410.89
14	0.3808	-30000.00	48	0.1000	12358.36	82	0.7069	-29999.97
15	0.1000	4972.76	49	0.8652	-30000.02	83	0.1000	21221.85
16	0.1737	-23234.37	50	0.1980	-29999.92	84	2.3983	-25651.85
17	0.2354	-30000.00	51	0.1000	17504.70	85	0.2429	-30000.19
18	0.1000	-8339.33	52	1.2962	-29980.30	86	0.1000	16853.15
19	0.1000	25764.31	53	0.1000	-289.55	87	1.3600	-29845.23
20	0.1000	17374.09	54	0.4061	-19486.09	88	0.3446	-29999.91
21	0.1008	30000.01	55	0.6748	-30000.00	89	0.1000	18969.88
22	0.1000	21738.27	56	0.1000	-7936.74	90	2.4000	-29999.99
23	0.1000	28284.86	57	0.1000	29358.10	91	0.1000	-925.36
24	0.1000	19641.74	58	0.1000	21343.22	92	0.6115	-19825.01
25	0.1000	8711.29	59	0.1062	30000.02	93	1.0177	-30000.01
26	0.5405	-30000.00	60	0.1000	23735.49	94	0.1000	-7508.15
27	0.1088	30000.01	61	0.1000	28029.10	95	0.1129	29999.99
28	0.2606	-30000.00	62	0.1000	19745.99	96	0.1000	26249.20
29	0.7047	-27486.93	63	0.1000	8337.99	97	0.1166	30000.03
30	0.1000	13996.09	64	0.8142	-27850.07	98	0.1000	27242.79
31	0.1000	-26645.83	65	0.1510	30000.00	99	0.1000	27948.40
32	0.6251	-30000.00	66	0.5818	-30000.02	100	0.1000	20045.14
33	0.1000	17173.16	67	1.6295	-26754.36	101	0.1000	7939.14
34	0.1000	-27993.61	68	0.1000	20588.83	102	0.9386	-24514.05

Table B.6: Optimum results of the two-hundred-member structure under base excitation for $\omega = 5$ rad/sec (III)

Two-Hundred-Member Structure (Base Excitation)								
ω= 5 rad/sec			(10000/386.4) of equivalent force mass added and No L.P.					
$A_0$from static case result $(A)_{\omega=0}$			10000 vertical force at joints and Modify C.S.A. of all members					
Link	Area (in^2)	Stress (psi)	Link	Area (in^2)	Stress (psi)	Link	Area (in^2)	Stress (psi)
103	0.1785	29999.99	137	0.1000	27881.50	171	0.1000	16180.43
104	0.8147	-29999.98	138	0.1000	20353.26	172	0.1000	9217.52
105	2.7316	-26202.65	139	0.1000	7539.44	173	0.1000	24021.49
106	0.1000	23678.89	140	0.9271	-19479.39	174	0.1000	17030.04
107	0.2656	-30000.18	141	0.1673	30000.00	175	0.1000	27486.51
108	1.6934	-29912.71	142	1.0110	-30000.01	176	0.1000	20313.16
109	0.1000	19533.32	143	3.9903	-25513.15	177	0.1000	7153.35
110	0.3465	-29999.90	144	0.1000	26457.72	178	0.8003	-22893.49
111	2.7357	-29999.99	145	0.3833	-29999.55	179	0.1000	23296.15
112	0.6692	-19525.31	146	2.2504	-28538.32	180	0.9930	-22705.68
113	0.1000	8506.37	147	0.1000	20434.95	181	5.3849	-22122.76
114	1.3549	-30000.00	148	0.5503	-30000.28	182	0.1000	16622.74
115	0.4463	29751.00	149	4.0550	-29999.99	183	1.0976	-30000.14
116	0.1169	29999.19	150	0.8446	-20045.59	184	2.8075	-27107.02
117	0.2722	29999.91	151	0.1000	8928.80	185	0.1000	25098.93
118	0.4463	23381.74	152	1.5986	-30000.01	186	0.7144	-29999.77
119	0.5937	-13509.48	153	0.5444	17230.93	187	5.6299	-30000.01
120	0.9075	-30000.00	154	0.2746	30000.35	188	0.9930	-20946.58
121	0.1000	19174.77	155	0.4123	30000.24	189	0.1000	12643.54
122	3.6570	-25093.44	156	0.5444	23568.70	190	1.7416	-30000.01
123	0.3596	-29999.53	157	0.4670	-17764.91	191	0.6525	23821.97
124	0.1000	19334.27	158	0.9416	-22034.27	192	0.1000	-6556.73
125	1.9171	-28260.91	159	0.1000	5296.12	193	1.3975	29999.94
126	0.5482	-30000.28	160	5.0516	-21598.11	194	1.3601	30000.01
127	0.1000	19815.38	161	1.0589	-30000.14	195	1.2797	-24936.27
128	3.7199	-29999.99	162	0.1000	5032.52	196	6.5330	-22224.21
129	0.1000	-1052.45	163	2.4742	-26706.20	197	1.8855	-3359.88
130	0.7900	-20166.46	164	0.6871	-29999.76	198	4.1752	-30000.01
131	1.2620	-30000.01	165	0.1000	16912.60	199	7.0454	-29999.99
132	0.1000	-7104.75	166	5.2954	-30000.01	200	2.4577	-30000.01
133	0.1086	30000.02	167	0.1000	2394.10			
134	0.1000	25345.66	168	0.9416	-21001.99			
135	0.1148	29999.99	169	1.4057	-30000.02			
136	0.1000	27109.56	170	0.1000	-6834.10			

Table B.7: Optimum results of the two-hundred-member structure under base excitation for $\omega = 15$ rad/sec (I)

Two-Hundred-Member Structure (Base Excitation)								
ω= 15 rad/sec			(10000/386.4) of equivalent force mass added and No L.P.					
$A_0$from static case result $(A)_{\omega=0}$			10000 vertical force at joints and Modify C.S.A. of all members					
Displacements (in)			Displacements (in)			Displacements (in)		
node	x-dir	y-dir	node	x-dir	y-dir	node	x-dir	y-dir
1	1.9316	0.2241	27	1.6540	-0.1796	53	1.2772	-0.0368
2	1.9264	0.0998	28	1.6660	-0.2368	54	1.2892	-0.0792
3	1.9315	-0.0216	29	1.5539	0.1972	55	1.3012	-0.1304
4	1.9472	-0.1494	30	1.5300	0.1007	56	1.3132	-0.1792
5	1.9712	-0.2800	31	1.5365	-0.0075	57	1.2379	0.1437
6	1.8399	0.2146	32	1.5494	-0.1168	58	1.2143	0.0648
7	1.8279	0.1621	33	1.5734	-0.2224	59	1.2038	0.0000
8	1.8399	0.0971	34	1.4686	0.1828	60	1.2143	-0.0648
9	1.8279	0.0421	35	1.4566	0.1375	61	1.2362	-0.1648
10	1.8399	-0.0236	36	1.4511	0.0920	62	1.1769	0.1293
11	1.8334	-0.0789	37	1.4391	0.0493	63	1.1649	0.0865
12	1.8454	-0.1417	38	1.4511	-0.0049	64	1.1529	0.0504
13	1.8562	-0.2008	39	1.4481	-0.0568	65	1.1409	0.0280
14	1.8682	-0.2656	40	1.4601	-0.1054	66	1.1529	-0.0009
15	1.7304	0.2189	41	1.4721	-0.1568	67	1.1409	-0.0280
16	1.7266	0.1021	42	1.4841	-0.2080	68	1.1529	-0.0504
17	1.7287	-0.0161	43	1.3853	0.1725	69	1.1649	-0.0974
18	1.7424	-0.1303	44	1.3656	0.0861	70	1.1769	-0.1504
19	1.7664	-0.2512	45	1.3506	0.0000	71	1.1260	0.1149
20	1.6412	0.2045	46	1.3746	-0.0936	72	1.1020	0.0360
21	1.6292	0.1589	47	1.3986	-0.1936	73	1.0780	0.0000
22	1.6395	0.0998	48	1.3114	0.1581	74	1.1020	-0.0360
23	1.6275	0.0439	49	1.2994	0.1169	75	1.1260	-0.1360
24	1.6395	-0.0136	50	1.2892	0.0744	76	1.0000	0.0000
25	1.6378	-0.0675	51	1.2772	0.0368	77	1.0000	0.0000
26	1.6498	-0.1245	52	1.2892	-0.0012			

	ω_n(rad/sec)		
1	32.199		
2	60.292	Minimum Weight	27445.10 lb
3	69.585	CPU Time	56.421 sec

Table B.8: Optimum results of the two-hundred-member structure under base excitation for ω = 15 rad/sec (II)

Two-Hundred-Member Structure (Base Excitation)								
ω= 15 rad/sec			(10000/386.4) of equivalent force mass added and No L.P.					
$A_0$from static case result $(A)_{\omega=0}$			10000 vertical force at joints and Modify C.S.A. of all members					
Link	Area (in^2)	Stress (psi)	Link	Area (in^2)	Stress (psi)	Link	Area (in^2)	Stress (psi)
1	0.1112	-6453.41	35	0.7047	-23767.60	69	2.2017	-29999.93
2	0.1204	6292.21	36	0.3322	30000.01	70	1.1363	-12629.98
3	0.1204	19654.77	37	0.7973	-30000.00	71	1.0736	30000.03
4	0.3080	30000.00	38	0.8633	-30000.00	72	1.8676	-30000.08
5	0.1999	19853.08	39	0.1986	-4802.14	73	1.6295	-16133.55
6	0.5493	-30000.00	40	0.1000	2664.23	74	0.5976	29999.98
7	0.1000	24400.71	41	0.1000	17123.47	75	2.1717	-29999.99
8	0.3714	5660.61	42	0.6211	30000.01	76	2.5205	-30000.00
9	0.5812	-30000.01	43	0.7050	29999.82	77	0.3311	-29850.87
10	0.1000	27833.81	44	0.9908	-29999.94	78	0.1000	8123.45
11	0.2459	4306.88	45	0.2571	30000.36	79	0.1000	16060.41
12	0.5781	-29999.98	46	1.2962	4871.29	80	1.4008	30000.02
13	0.3678	29999.99	47	1.7770	-29999.92	81	0.9700	29999.98
14	0.3714	-15945.90	48	0.7426	29999.97	82	0.6115	-26253.45
15	0.5827	-30000.00	49	0.8030	-5320.41	83	0.4737	30000.00
16	0.1737	20333.02	50	1.5748	-30000.09	84	2.3983	18023.16
17	0.4783	-30000.00	51	0.7811	30000.02	85	3.0331	-29999.98
18	0.3577	-30000.00	52	1.2962	-12004.99	86	0.9615	30000.06
19	0.1925	29999.26	53	1.9413	-29999.99	87	1.3600	-5388.41
20	0.1654	-30000.86	54	0.4061	27164.15	88	2.8302	-29999.94
21	0.3036	30000.02	55	2.1408	-30000.00	89	2.3200	29999.98
22	0.1000	-16273.91	56	0.3195	-30000.00	90	2.3983	-23667.23
23	0.4497	30000.00	57	0.1000	25727.14	91	2.7321	-30000.09
24	0.1000	27187.46	58	0.2341	-30000.01	92	0.6115	23116.50
25	0.3636	30000.00	59	0.3056	29999.97	93	4.9283	-29999.98
26	0.5332	-8965.78	60	0.1000	-4151.45	94	0.2861	-30000.00
27	0.5127	29999.80	61	0.3570	30000.01	95	0.1000	-13753.07
28	0.9805	-29999.88	62	0.1000	10519.41	96	0.3300	-29999.99
29	0.7047	-10403.03	63	0.3260	30000.00	97	0.2583	30000.01
30	0.4605	30000.25	64	0.8142	15162.75	98	0.1000	-7480.43
31	0.9488	-30000.13	65	0.5756	30000.16	99	0.5544	29999.65
32	0.5792	-15674.24	66	1.3089	-29999.95	100	0.2683	29999.27
33	0.7632	29999.99	67	1.6295	-1903.62	101	0.2930	30000.00
34	0.9736	-29999.99	68	1.1675	29999.98	102	0.9386	21487.01

Table B.9: Optimum results of the two-hundred-member structure under base excitation for $\omega = 15$ rad/sec (III)

Two-Hundred-Member Structure (Base Excitation)								
ω= 15 rad/sec			(10000/386.4) of equivalent force mass added and No L.P.					
$A_0$from static case result $(A)_{\omega=0}$			10000 vertical force at joints and Modify C.S.A. of all members					
Link	Area (in^2)	Stress (psi)	Link	Area (in^2)	Stress (psi)	Link	Area (in^2)	Stress (psi)
103	0.6627	30000.00	137	0.9657	30000.09	171	0.3120	-30000.01
104	0.7239	-30000.08	138	0.7082	30000.12	172	0.5425	-30000.00
105	2.7316	12360.90	139	0.2621	30000.00	173	0.1258	29999.99
106	1.4255	30000.04	140	0.9757	29999.98	174	0.1000	-29999.88
107	3.4969	-29999.99	141	0.5993	30000.04	175	0.5521	30000.00
108	1.6934	-10250.14	142	0.8446	-23106.56	176	0.3140	30000.00
109	2.7778	29999.93	143	3.9903	19963.32	177	0.2353	30000.00
110	3.2884	-29999.90	144	3.7046	29999.95	178	0.9312	30000.00
111	2.7316	-24666.94	145	2.9692	-30000.03	179	0.1000	4898.90
112	0.6692	22129.28	146	2.2504	-2401.20	180	0.9930	-2341.21
113	2.7552	-30000.14	147	5.3025	30000.00	181	8.4663	29999.97
114	5.3027	-29999.99	148	6.2636	-30000.01	182	5.6565	30000.00
115	0.4463	-24525.58	149	8.1926	-29999.94	183	5.9578	-29999.97
116	0.1000	-18740.06	150	0.8446	8361.17	184	2.8075	-1894.39
117	1.2413	30000.04	151	0.1000	-24315.01	185	8.0851	30000.01
118	1.6716	30000.13	152	8.6083	-30000.03	186	4.1829	-30000.02
119	1.2782	29999.98	153	0.5444	-29512.66	187	19.3005	-29999.98
120	0.7900	-19597.19	154	0.1000	-13199.82	188	0.9930	-11098.31
121	0.4646	30000.05	155	0.1000	13199.96	189	0.1000	7590.36
122	3.6570	24397.50	156	0.5444	27335.03	190	9.1646	-30000.03
123	2.5809	-30000.03	157	1.2394	30000.00	191	0.6531	-30000.00
124	3.3161	29999.95	158	0.9416	-4499.35	192	4.5580	-30000.00
125	1.9171	2401.05	159	0.1000	23980.44	193	9.2558	30000.03
126	5.4219	-30000.00	160	8.7896	29999.97	194	6.5602	30000.03
127	4.4612	29999.99	161	5.4276	-29999.97	195	1.2797	17833.44
128	7.8435	-29999.94	162	5.1261	30000.00	196	12.4265	29999.98
129	0.4282	-30000.17	163	2.4742	1894.32	197	21.4715	30000.01
130	0.7900	22130.41	164	3.6645	-30000.02	198	20.1211	-30000.00
131	8.2392	-30000.03	165	7.5670	30000.01	199	23.1377	-29999.99
132	0.2556	-30000.00	166	18.9567	-29999.98	200	11.4263	-30000.03
133	0.1000	-25469.62	167	0.1000	-10540.97			
134	0.3384	-30000.01	168	0.9416	-9774.81			
135	0.1520	29999.99	169	8.8012	-30000.03			
136	0.1000	-29999.87	170	0.2293	-30000.00			

Table B.10: Optimum results of the two-hundred-member structure under base excitation for $\omega = 30$ rad/sec (I)

Two-Hundred-Member Structure (Base Excitation)								
ω= 30 rad/sec			(10000/386.4) of equivalent force mass added and No L.P.					
$A_0$from static case result $(A)_{\omega=0}$			10000 vertical force at joints and Modify C.S.A. of all members					
Displacements (in)			Displacements (in)			Displacements (in)		
node	x-dir	y-dir	node	x-dir	y-dir	node	x-dir	y-dir
1	1.9919	0.2744	27	1.6540	-0.1796	53	1.2772	-0.0368
2	1.9679	0.1344	28	1.6660	-0.2368	54	1.2892	-0.0792
3	1.9574	0.0000	29	1.5734	0.2224	55	1.3012	-0.1304
4	1.9679	-0.1344	30	1.5494	0.1168	56	1.3132	-0.1792
5	1.9919	-0.2800	31	1.5455	0.0000	57	1.2383	0.1648
6	1.8786	0.2600	32	1.5494	-0.1168	58	1.2143	0.0648
7	1.8666	0.1944	33	1.5734	-0.2224	59	1.2038	0.0000
8	1.8647	0.1236	34	1.4841	0.2080	60	1.2143	-0.0648
9	1.8527	0.0628	35	1.4721	0.1568	61	1.2383	-0.1648
10	1.8647	-0.0059	36	1.4601	0.1037	62	1.1769	0.1504
11	1.8527	-0.0628	37	1.4481	0.0568	63	1.1649	0.0966
12	1.8647	-0.1326	38	1.4601	-0.0016	64	1.1529	0.0504
13	1.8666	-0.1944	39	1.4481	-0.0568	65	1.1409	0.0280
14	1.8786	-0.2656	40	1.4601	-0.1056	66	1.1529	-0.0009
15	1.7692	0.2512	41	1.4721	-0.1568	67	1.1409	-0.0280
16	1.7514	0.1228	42	1.4841	-0.2080	68	1.1529	-0.0504
17	1.7481	0.0000	43	1.3986	0.1936	69	1.1649	-0.0966
18	1.7514	-0.1228	44	1.3746	0.0936	70	1.1769	-0.1504
19	1.7692	-0.2512	45	1.3506	0.0000	71	1.1260	0.1360
20	1.6660	0.2368	46	1.3746	-0.0936	72	1.1020	0.0360
21	1.6540	0.1796	47	1.3986	-0.1936	73	1.0780	0.0000
22	1.6588	0.1183	48	1.3132	0.1792	74	1.1020	-0.0360
23	1.6468	0.0600	49	1.3012	0.1304	75	1.1260	-0.1360
24	1.6588	-0.0025	50	1.2892	0.0792	76	1.0000	0.0000
25	1.6468	-0.0600	51	1.2772	0.0368	77	1.0000	0.0000
26	1.6588	-0.1216	52	1.2892	-0.0012			

	ω_n(rad/sec)		
1	68.167		
2	82.930	Minimum Weight	109270.32 lb
3	110.649	CPU Time	38.465 sec

Table B.11: Optimum results of the two-hundred-member structure under base excitation for $\omega = 30$ rad/sec (II)

Two-Hundred-Member Structure (Base Excitation)								
ω= 30 rad/sec			(10000/386.4) of equivalent force mass added and No L.P.					
$A_0$from static case result $(A)_{\omega=0}$			10000 vertical force at joints and Modify C.S.A. of all members					
Link	Area (in^2)	Stress (psi)	Link	Area (in^2)	Stress (psi)	Link	Area (in^2)	Stress (psi)
1	1.0750	-29999.97	35	0.7047	-20515.80	69	4.5860	-30000.01
2	0.1204	-13199.97	36	1.2858	30000.00	70	1.1363	-5186.61
3	0.1204	13200.00	37	3.7295	-30000.00	71	3.9177	30000.00
4	1.4693	30000.00	38	1.1954	-30000.00	72	7.3281	-29999.99
5	0.4566	30000.09	39	0.1986	-22199.93	73	1.6295	-9930.26
6	0.7494	-30000.07	40	0.1000	-4200.08	74	6.8503	30000.00
7	1.6776	29999.99	41	0.1000	4199.96	75	6.4549	-30000.00
8	0.3714	22432.86	42	0.1986	22200.07	76	9.5185	-30000.00
9	2.3354	-29999.99	43	6.0590	30000.00	77	3.7646	-30000.00
10	0.9950	30000.00	44	4.8058	-29999.99	78	0.1000	-4799.99
11	0.2459	12286.50	45	3.2464	30000.00	79	0.1000	4800.01
12	1.5600	-30000.00	46	1.2962	9432.15	80	5.1383	30000.00
13	2.0609	30000.00	47	3.4858	-30000.02	81	9.4683	30000.00
14	0.3714	-3650.80	48	4.7643	30000.00	82	0.6115	-23114.81
15	2.5738	-30000.00	49	0.8030	5186.74	83	8.3539	30000.00
16	0.1737	23114.86	50	5.3694	-29999.99	84	2.3983	27209.08
17	0.6548	-30000.00	51	1.9616	29999.99	85	11.3140	-30000.00
18	1.4639	-30000.00	52	1.2962	-2569.84	86	4.4807	29999.99
19	0.1000	-4800.19	53	5.3213	-30000.00	87	1.3600	3287.09
20	1.4695	-30000.00	54	5.7265	30000.00	88	6.0327	-30000.01
21	0.3501	30000.01	55	8.9953	-30000.00	89	12.4671	30000.00
22	1.1025	-30000.00	56	1.3214	-30000.00	90	2.3983	-23301.58
23	1.4695	30000.00	57	0.1000	12000.11	91	11.7864	-30000.00
24	0.1000	4799.90	58	1.2565	-30000.00	92	0.6115	23114.67
25	1.4660	30000.00	59	0.1000	29999.79	93	15.3574	-30000.00
26	0.5332	18332.80	60	1.1943	-30000.00	94	1.1898	-30000.00
27	2.8300	29999.99	61	1.2565	30000.00	95	1.2048	-29999.98
28	1.8984	-30000.03	62	0.1000	-11999.86	96	2.3535	-29999.99
29	0.7047	1733.92	63	1.3354	30000.00	97	1.0411	30000.00
30	2.4427	30000.00	64	5.9134	30000.00	98	0.1000	-29999.82
31	3.7817	-29999.99	65	4.3549	30000.00	99	2.3928	30000.01
32	0.5792	-12286.51	66	5.9068	-30000.00	100	1.2440	30000.02
33	4.1001	30000.00	67	1.6295	3067.77	101	1.2136	30000.00
34	3.6010	-30000.00	68	5.8671	30000.00	102	9.3017	30000.00

Table B.12: Optimum results of the two-hundred-member structure under base excitation for $\omega = 30$ rad/sec (III)

Two-Hundred-Member Structure (Base Excitation)								
ω= 30 rad/sec			(10000/386.4) of equivalent force mass added and No L.P.					
$A_0$from static case result $(A)_{\omega=0}$			10000 vertical force at joints and Modify C.S.A. of all members					
Link	Area (in^2)	Stress (psi)	Link	Area (in^2)	Stress (psi)	Link	Area (in^2)	Stress (psi)
103	8.3831	30000.00	137	2.6174	29999.96	171	1.0540	-30000.00
104	0.6692	-22131.06	138	1.5617	29999.93	172	2.1331	-30000.00
105	2.7316	21124.32	139	1.1091	30000.00	173	0.1000	29999.98
106	7.2085	29999.99	140	15.8316	30000.01	174	0.8040	-30000.00
107	14.0369	-30000.00	141	0.1000	22130.65	175	2.1644	30000.00
108	1.6934	-3287.22	142	0.8446	-8361.29	176	1.0890	30000.00
109	14.4920	30000.00	143	18.9756	29999.98	177	0.9963	30000.00
110	8.0628	-30000.01	144	25.7478	30000.01	178	15.2737	30000.01
111	2.7316	-25031.68	145	18.8261	-30000.00	179	0.1000	-8545.61
112	0.6692	22131.26	146	2.2504	-2406.00	180	0.9930	10142.94
113	11.8179	-29999.99	147	11.2699	30000.00	181	60.7725	30000.00
114	15.8608	-30000.00	148	26.7930	-29999.99	182	13.6133	30000.00
115	6.1648	-30000.00	149	15.0349	-30000.01	183	31.5296	-30000.01
116	1.3981	-29999.96	150	0.8446	8360.29	184	2.8075	-1897.40
117	9.4313	30000.01	151	0.1000	-22131.42	185	33.2266	30000.00
118	8.4079	30000.00	152	26.3736	-30000.00	186	22.6478	-30000.00
119	16.0183	30000.01	153	1.2355	-30000.00	187	59.8071	-30000.00
120	0.7900	-22130.43	154	0.1000	-13200.02	188	0.9930	-10143.06
121	0.4201	30000.40	155	0.1000	13199.99	189	0.1000	8545.46
122	19.2432	29999.98	156	1.2701	30000.00	190	27.1581	-30000.00
123	16.5794	-29999.99	157	15.4842	30000.01	191	11.0094	-30000.01
124	23.4942	30000.00	158	0.9416	8545.60	192	20.8043	-30000.00
125	1.9171	2406.04	159	0.1000	11496.42	193	35.1593	30000.00
126	23.9148	-30000.00	160	61.0587	30000.00	194	19.4882	30000.00
127	8.3975	30000.01	161	29.6573	-30000.01	195	18.0751	30000.01
128	14.6367	-30000.01	162	11.7357	30000.00	196	71.1974	30000.00
129	0.4201	-29999.78	163	2.4742	1897.41	197	89.9382	30000.00
130	0.7900	22131.55	164	20.1644	-30000.00	198	88.9854	-30000.00
131	25.8889	-30000.00	165	30.7499	30000.00	199	77.8422	-30000.00
132	1.0747	-30000.00	166	59.4267	-30000.00	200	33.1746	-30000.00
133	1.5271	-30000.14	167	0.1000	-11496.28			
134	2.5969	-30000.08	168	0.9416	-8545.46			
135	0.1000	29999.94	169	26.6975	-30000.00			
136	0.9092	-30000.00	170	0.9614	-30000.00			

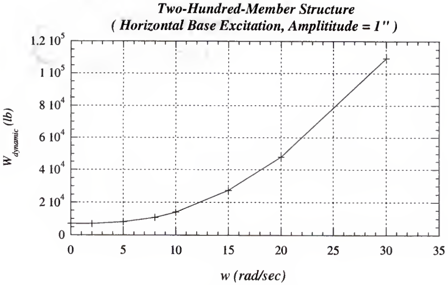

Figure B.1: Optimum weights of the two-hundred-member structure under base excitation for a range of frequencies

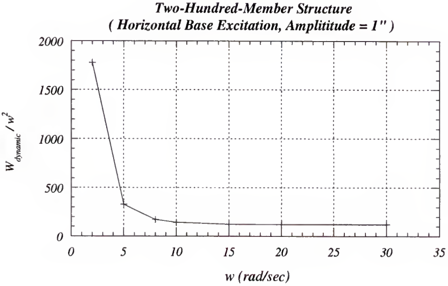

Figure B.2: Ratios of the optimum weight to frequency square of the two-hundred-member structure under base excitation for a range of frequencies

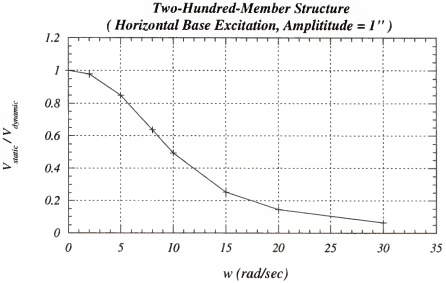

Figure B.3: Optimum volume ratios of the two-hundred-member structure under base excitation for a range of frequencies

APPENDIX C
IMPULSIVE LOADING

A modal superposition method with the successive iteration approach is presented in order to optimize the design of structures subjected to an impulse. The Duhamel integration can then be used for any general forcing function.

A general undamped dynamic system can be represented by

$$\mathbf{M}\ddot{\mathbf{X}} + \mathbf{K}\mathbf{X} = \mathbf{F} \tag{C.1}$$

This coupled system can be uncoupled into normal modes as briefly described in Chapter 8. The eigenvalues (or natural frequencies) and eigenvectors (or mode shapes) can be calculated first by solving the eigenproblems of the free vibration problems as follows:

$$\mathbf{K}\boldsymbol{\phi}_i = \omega_i^2 \mathbf{M}\boldsymbol{\phi}_i \tag{C.2}$$

where

$$i = 1, 2, \cdots, n$$

$$n \equiv \text{number of degrees of freedom}$$

The mode shape matrix $(\boldsymbol{\Phi})$ which consists of mode shape vectors $(\boldsymbol{\phi}_i)$ as its columns then serves to transform the generalized coordinate vector $(\mathbf{Y})$, which consists of normal coordinates of the structure, to the geometric coordinate vector $(\mathbf{X})$ as

$$\mathbf{X} = \boldsymbol{\Phi}\mathbf{Y} \tag{C.3}$$

where

$$\mathbf{\Phi}= [\boldsymbol{\phi}_1, \boldsymbol{\phi}_2, \cdots, \boldsymbol{\phi}_n] \tag{C.4}$$

$$\mathbf{X}= (x_1,x_2, \cdots, x_n)^T \tag{C.5}$$

$$\mathbf{Y}= (y_1, y_2, \cdots, y_n)^T \tag{C.6}$$

This relation is on account of the property of linear independence that the eigenvectors possess. Substitute Equation (C.3) into Equation (C.1) to get

$$\mathbf{M\Phi\ddot{Y}} + \mathbf{K\Phi Y} = \mathbf{F} \tag{C.7}$$

Premultiply Equation (C.7) by the transpose of the mode shape matrix ($\mathbf{\Phi}$) and take advantage of the property of the orthogonality of the normal modes which can be described as

$$\boldsymbol{\phi}_i^T\mathbf{M}\boldsymbol{\phi}_j = \begin{cases} m_i & \text{if } i = j \\ 0 & \text{if } i \neq j \end{cases} \tag{C.8}$$

$$\boldsymbol{\phi}_i^T\mathbf{K}\boldsymbol{\phi}_j = \begin{cases} k_i & \text{if } i = j \\ 0 & \text{if } i \neq j \end{cases} \tag{C.9}$$

Equation (C.7) becomes an uncoupled system of the form

$$m_i\ddot{y}_i + k_i y_i = f_i \tag{C.10}$$

where

$$m_i = \boldsymbol{\phi}_i^T\mathbf{M}\boldsymbol{\phi}_i \tag{C.11}$$

$$k_i = \boldsymbol{\phi}_i^T\mathbf{K}\boldsymbol{\phi}_i \tag{C.12}$$

$$f_i = \boldsymbol{\phi}_i^T\mathbf{F} \tag{C.13}$$

$$i = 1, 2, \cdots, n$$

In addition, Equation (C.2) is multiplied on both sides by $\boldsymbol{\phi}_i^T$ to get

$$k_i = \omega_i^2 m_i \tag{C.14}$$

If the calculated eigenvectors are normalized in such a way that Equation (C.8) becomes

$$\bar{\boldsymbol{\phi}}_i^T \mathbf{M} \bar{\boldsymbol{\phi}}_j = \begin{cases} 1 & \text{if } i = j \\ 0 & \text{if } i \neq j \end{cases} \tag{C.15}$$

where

$$\bar{\boldsymbol{\phi}}_i \equiv \text{ the } i\text{th normalized eigenvector}$$

then Equation (C.9) and Equation (C.14) become

$$\bar{\boldsymbol{\phi}}_i^T \mathbf{K} \bar{\boldsymbol{\phi}}_j = \begin{cases} \lambda_i & \text{if } i = j \\ 0 & \text{if } i \neq j \end{cases} \tag{C.16}$$

$$\lambda_i = \omega_i^2 \tag{C.17}$$

Accordingly, the uncoupled system will have the form of

$$\ddot{\eta}_i + \lambda_i \eta_i = \bar{f}_i \tag{C.18}$$

where

$$\lambda_i = \omega_i^2 = \bar{\boldsymbol{\phi}}_i^T \mathbf{K} \bar{\boldsymbol{\phi}}_i \tag{C.19}$$

$$\bar{f}_i = \bar{\boldsymbol{\phi}}_i^T \mathbf{F} \tag{C.20}$$

$$i = 1, 2, \cdots, n$$

This procedure can be used to obtain an independent single-degree-of-freedom (SDOF) equation for each mode of vibration of the undamped structure. Thus, the use of the normal coordinates serves to transform a coupled system of n geometric-coordinate equations to an uncoupled system of n independent normal-coordinate equations.

After the transformation, the response of each modal coordinate can be solved separately and then superposed by Equation (C.3) to obtain the response in the original geometric coordinates.

To solve an independent SDOF equation for each mode of vibration of the structure, a convolution (or Duhamel) integral

$$y_i(t) = \frac{1}{m_i \omega_i} \int_0^t f_i(\tau) \sin \omega_i (t - \tau)\, d\tau, \ t \geq 0 \tag{C.21}$$

can be used to solve a general forcing loading problem. For impulse ($\mathbf{I}$) loading problem, using Equation (C.21), the amplitude of the response can be represented by

$$Y_i = \frac{\boldsymbol{\phi}_i^T \mathbf{I}}{m_i \omega_i} \tag{C.22}$$

$\mathbf{I}$ is an impulse vector including impulse at one location only. For example, if a unit impulse is applied in the direction of the first degree of freedom of the system, $\mathbf{I} = (1, 0, 0, \cdots, 0)^T$. If the impulse is applied at more than one location, the phase relations should be considered.

The successive iteration approach combining the modal superposition method can be applied to optimize an impulsive loading problem. A solution algorithm is developed and stated as follows:

(1) Assume initial cross sectional areas ($\mathbf{A}_0$).

(2) Formulate the mass matrix ($\mathbf{M}$) and stiffness matrix ($\mathbf{K}$) automatically by displacement (or stiffness) method.

(3) Calculate eigenvalues (ω_k^2) and eigenvectors ($\boldsymbol{\phi}_k$ or ϕ_{ik}) of the system in Equation (C.2).

(4) Find the generalized or modal mass by Equation (C.11). If discrete mass model is used, Equation (C.8) can be simplified as

$$M_k = \sum_{i=1}^{n} m_i \phi_{ik}^2 \tag{C.23}$$

(5) Find the modal coordinates by Equation (C.22) or

$$Y_k = \frac{I\phi_{ik}}{M_k\omega_k} \tag{C.24}$$

(6) Superpose the modal coordinates by using Equation (C.3) or

$$x_i = \sum_{k=1}^{n} Y_k\phi_{ik} \tag{C.25}$$

to obtain the original geometric coordinates.

(7) Calculate the internal forces ($\mathbf{f}$) and stresses ($\boldsymbol{\sigma}$).

(8) Find new cross sectional areas ($\mathbf{A}$) from the internal forces ($\mathbf{f}$), allowable stresses ($\boldsymbol{\sigma}_{allow}$), and buckling critical stresses ($\boldsymbol{\sigma}_b$).

(9) Repeat from step (1) until convergence.

The forty-seven-member tower is selected as an example to illustrate the impulsive loading problem. The impulse is applied at top left corner (node 17). For large-scale systems, solving the eigenproblem could be a time consuming work. Therefore, modal reduction can be used to reduce the computational expenses. For this reason, the results of a series of tests using different numbers of modes is shown in Table C.1 to Table C.3 and Figure C.1 to Figure C.3. Figure C.4 shows relative cross sectional area distribution for links other than links 23 and 25 since the cross sectional areas of links 23 and 25 are considerably higher than those of the other links. As would be expected, the more the numbers of modes are involved, the more accurate the results are. However, the CPU time is still reasonably short if all forty modes are used in the superposition. Therefore, for this example, all modes were used for most accurate results. It shows reasonably that the link 23 requires larger cross sectional area than that of other links since the impulse is applied at node 17. This suggests that a mass should be added at node 17 as a filter instead of using larger cross sectional area for the link 23. Table C.4 to Table C.6 tabulate the optimum results of some other tested cases. It is shown that the allowable stresses have been reached for most of the members.

Table C.1: Five modes approximation for the forty-seven-member tower under impulsive loading (I)

Forty-Seven-Member Tower (Impulsive loading)								
Impulse = 100 lb-sec			No mass added and No L.P.					
A_0= 0.1 in^2		Use first 5 terms			Modify C.S.A. of all members			
Link	Area (in^2)	Stress (psi)	Link	Area (in^2)	Stress (psi)	Displacements (in)		
						node	x-dir	y-dir
1	21.6447	20000.00	26	0.1000	16082.65	1	0.0000	0.0000
2	25.2581	-15000.00	27	6.3682	-15000.00	2	0.0000	0.0000
3	18.3935	20000.00	28	0.1554	20000.00	3	0.0200	0.0080
4	11.3314	-15000.00	29	26.6016	20000.00	4	0.0220	-0.0060
5	7.8186	20000.00	30	19.0855	-15000.00	5	0.0480	0.0160
6	1.2144	-15000.00	31	13.5863	-15000.00	6	0.0560	-0.0120
7	0.1708	-15000.00	32	10.1618	20000.00	7	0.0760	0.0240
8	1.6313	20000.00	33	0.3011	-15000.00	8	0.0700	-0.0180
9	10.7198	-15000.00	34	20.4791	20000.00	9	0.0885	0.0227
10	0.1554	20000.00	35	3.4756	-15000.00	10	0.0925	-0.0105
11	3.2466	20000.00	36	5.1104	-15000.00	11	0.1357	0.0267
12	0.1000	-14190.26	37	0.1694	19999.99	12	0.1327	-0.0135
13	2.2700	20000.00	38	0.2282	19999.99	13	0.1830	0.0307
14	9.1253	-15000.00	39	19.3356	20000.00	14	0.1870	-0.0165
15	9.8531	20000.00	40	3.0168	-15000.00	15	0.2140	0.1027
16	1.2771	-15000.00	41	0.1328	19999.99	16	0.2141	-0.0779
17	1.8111	20000.00	42	0.1000	-5000.00	17	0.2502	0.1852
18	0.1000	-10168.13	43	0.1000	4999.99	18	0.2472	0.1047
19	2.5884	-15000.00	44	20.1563	20000.00	19	0.2442	0.0347
20	0.1000	8221.52	45	2.9878	-15000.00	20	0.2412	-0.0195
21	0.6376	20000.00	46	0.1501	19999.99	21	0.2445	-0.0781
22	0.1000	-2163.09	47	0.1310	-15000.00	22	0.2469	-0.1486
23	2.6695	-15000.00						
24	0.1000	12375.03						
25	3.3213	-15000.00						

	ω_n (rad/sec)		
1	80.914		
2	389.428	Minimum Weight	7321.30 lb
3	520.235	CPU Time	43.573 sec

Table C.2: Fifteen modes approximation for the forty-seven-member tower under impulsive loading (I)

Forty-Seven-Member Tower (Impulsive loading)								
Impulse = 100 lb-sec			No mass added and No L.P.					
A_0= 0.1 in^2	Use first 15 terms			Modify C.S.A. of all members				
Link	Area (in^2)	Stress (psi)	Link	Area (in^2)	Stress (psi)	Displacements (in)		
						node	x-dir	y-dir
1	7.0758	20000.00	26	0.1000	3385.08	1	0.0000	0.0000
2	7.9303	-15000.00	27	6.7902	-15000.00	2	0.0000	0.0000
3	7.8937	20000.00	28	0.1463	20000.00	3	0.0200	0.0080
4	9.1049	-15000.00	29	5.9634	20000.00	4	0.0202	-0.0060
5	0.1000	10777.47	30	4.9025	-15000.00	5	0.0542	0.0160
6	0.1000	-3462.57	31	3.9185	-15000.00	6	0.0544	-0.0120
7	0.1000	-10370.21	32	1.3062	20000.00	7	0.1015	0.0240
8	0.1636	20000.00	33	0.2385	-15000.00	8	0.0955	-0.0180
9	0.1000	-12685.10	34	3.2681	20000.00	9	0.1140	0.0227
10	5.7222	20000.00	35	3.0865	-15000.00	10	0.1180	-0.0105
11	10.9322	20000.00	36	0.1000	9172.89	11	0.1567	0.0267
12	0.1925	20000.00	37	0.1000	-13925.77	12	0.1546	-0.0135
13	0.5475	20000.00	38	0.1000	494.24	13	0.2039	0.0307
14	4.3631	-15000.00	39	3.0394	20000.00	14	0.2079	-0.0165
15	5.8916	20000.00	40	3.1189	-15000.00	15	0.2305	0.0940
16	10.0646	-15000.00	41	0.1000	17987.41	16	0.2364	-0.0635
17	20.6310	20000.00	42	0.1106	-15000.00	17	0.2712	0.1852
18	0.1000	-1520.39	43	0.1000	480.58	18	0.2682	0.0925
19	11.8016	20000.00	44	2.9871	20000.00	19	0.2652	0.0347
20	0.2822	-15000.00	45	3.2697	-15000.00	20	0.2622	-0.0195
21	7.6519	-15000.00	46	0.1000	17740.29	21	0.2628	-0.0625
22	0.1000	10283.90	47	0.1469	-15000.00	22	0.2635	-0.1184
23	27.6960	-15000.00						
24	0.1000	3208.67						
25	29.0470	-15000.00						

	ω_n (rad/sec)		
1	66.940		
2	308.156	Minimum Weight	4404.31 lb
3	451.563	CPU Time	24.165 sec

Table C.3: All modes (forty) expansion for the forty-seven-member tower under impulsive loading (I)

Forty-Seven-Member Tower (Impulsive loading)								
Impulse = 100 lb-sec			No mass added and No L.P.					
A_0= 0.1 in^2	Use first 40 terms			Modify C.S.A. of all members				
Link	Area (in^2)	Stress (psi)	Link	Area (in^2)	Stress (psi)	Displacements (in)		
						node	x-dir	y-dir
1	4.2274	20000.01	26	0.1000	-7288.63	1	0.0000	0.0000
2	5.1403	-15000.00	27	3.1944	-14999.99	2	0.0000	0.0000
3	4.0482	19999.97	28	0.1002	20000.06	3	0.0200	0.0080
4	5.1769	-15000.02	29	3.6819	20000.00	4	0.0206	-0.0060
5	0.1198	19999.79	30	4.1575	-15000.01	5	0.0546	0.0160
6	0.1000	-14997.69	31	2.3269	-14999.99	6	0.0560	-0.0120
7	0.1000	-14995.88	32	1.7833	20000.01	7	0.1040	0.0240
8	0.2363	20000.72	33	0.1918	-15000.03	8	0.0980	-0.0180
9	0.1028	-14998.72	34	2.3750	20000.00	9	0.1165	0.0228
10	1.9506	19999.94	35	2.3324	-15000.01	10	0.1205	-0.0105
11	3.5128	19999.99	36	0.1000	11704.57	11	0.1637	0.0268
12	0.1000	5092.52	37	0.1674	-15000.01	12	0.1607	-0.0135
13	0.8911	20000.01	38	0.1000	3409.14	13	0.2110	0.0308
14	1.8909	-14999.99	39	2.4659	20000.00	14	0.2150	-0.0165
15	2.3009	19999.99	40	2.5114	-15000.01	15	0.2376	0.0940
16	5.1194	-15000.00	41	0.1178	20000.04	16	0.2427	-0.0694
17	5.7711	20000.00	42	0.1244	-14999.96	17	0.2782	0.1852
18	0.1000	2702.82	43	0.1000	1591.03	18	0.2752	0.0925
19	3.7465	20000.00	44	2.6396	20000.00	19	0.2722	0.0348
20	0.1000	-6455.46	45	2.6630	-15000.00	20	0.2692	-0.0195
21	3.2615	-15000.00	46	0.1000	18295.52	21	0.2678	-0.0692
22	0.1000	1496.34	47	0.1850	-15000.01	22	0.2669	-0.1164
23	87.9634	-15000.00						
24	0.1000	-4438.56						
25	17.7019	-15000.00						

	ω_n (rad/sec)		
1	71.522		
2	263.174	Minimum Weight	3773.42 lb
3	478.669	CPU Time	97.240 sec

Table C.4: Forty-seven-member tower under Impulse = 50 lb-sec

Forty-Seven-Member Tower (Impulsive loading)								
Impulse = 50 lb-sec			No mass added and No L.P.					
A_0= 0.1 in^2		Use first 40 terms			Modify C.S.A. of all members			
Link	Area (in^2)	Stress (psi)	Link	Area (in^2)	Stress (psi)	Displacements (in)		
						node	x-dir	y-dir
1	2.1315	20000.00	26	0.1000	-7148.62	1	0.0000	0.0000
2	2.5810	-15000.00	27	1.6724	-15000.00	2	0.0000	0.0000
3	2.0725	20000.00	28	0.1000	17451.69	3	0.0161	0.0080
4	2.5896	-15000.00	29	1.8765	20000.00	4	0.0155	-0.0060
5	0.1000	11507.96	30	2.0384	-15000.00	5	0.0445	0.0160
6	0.1000	-3468.90	31	1.2204	-15000.00	6	0.0447	-0.0120
7	0.1000	-6373.58	32	0.8629	20000.00	7	0.0886	0.0240
8	0.1000	19177.66	33	0.1000	-12451.69	8	0.0836	-0.0180
9	0.1000	-9864.45	34	1.1878	20000.00	9	0.1019	0.0224
10	1.0106	20000.00	35	1.1594	-15000.00	10	0.1054	-0.0109
11	1.7964	20000.00	36	0.1000	6427.40	11	0.1440	0.0264
12	0.1000	4894.38	37	0.1000	-9891.10	12	0.1427	-0.0139
13	0.4571	20000.00	38	0.1000	524.30	13	0.1909	0.0304
14	0.9537	-15000.00	39	1.2339	20000.00	14	0.1949	-0.0169
15	1.1691	20000.00	40	1.2336	-15000.00	15	0.2175	0.0936
16	2.5818	-15000.00	41	0.1000	10766.08	16	0.2226	-0.0698
17	2.9133	20000.00	42	0.1000	-8714.74	17	0.2582	0.1849
18	0.1000	2620.01	43	0.1000	-1421.61	18	0.2552	0.0921
19	1.8616	20000.00	44	1.3044	20000.00	19	0.2522	0.0344
20	0.1000	-6289.41	45	1.3206	-15000.00	20	0.2492	-0.0199
21	1.6184	-15000.00	46	0.1000	11888.04	21	0.2477	-0.0697
22	0.1000	1448.56	47	0.1000	-10098.85	22	0.2469	-0.1170
23	44.0375	-15000.00						
24	0.1000	-4338.79						
25	8.9456	-15000.00						

	ω_n (rad/sec)		
1	79.143		
2	278.768	Minimum Weight	1918.30 lb
3	552.132	CPU Time	80.606 sec

Table C.5: Forty-seven-member tower under Impulse = 80 lb-sec

Forty-Seven-Member Tower (Impulsive loading)								
Impulse = 80 lb-sec			No mass added and No L.P.					
A_0= 0.1 in^2		Use first 40 terms			Modify C.S.A. of all members			
Link	Area (in^2)	Stress (psi)	Link	Area (in^2)	Stress (psi)	Displacements (in)		
						node	x-dir	y-dir
1	3.3865	20000.00	26	0.1000	-7259.20	1	0.0000	0.0000
2	4.1061	-15000.00	27	2.5811	-15000.00	2	0.0000	0.0000
3	3.2519	20000.00	28	0.1000	20000.00	3	0.0200	0.0080
4	4.1357	-15000.00	29	2.9569	20000.00	4	0.0199	-0.0060
5	0.1000	18294.02	30	3.3032	-15000.00	5	0.0539	0.0160
6	0.1000	-11281.30	31	1.8831	-15000.00	6	0.0546	-0.0120
7	0.1000	-10974.58	32	1.4108	20000.00	7	0.1026	0.0240
8	0.1805	20000.00	33	0.1525	-15000.00	8	0.0966	-0.0180
9	0.1000	-12987.29	34	1.8949	20000.00	9	0.1151	0.0227
10	1.5732	20000.00	35	1.8663	-15000.00	10	0.1191	-0.0105
11	2.8230	20000.00	36	0.1000	10875.42	11	0.1608	0.0267
12	0.1000	5052.85	37	0.1216	-15000.00	12	0.1586	-0.0135
13	0.7163	20000.00	38	0.1000	1750.84	13	0.2081	0.0307
14	1.5123	-15000.00	39	1.9745	20000.00	14	0.2121	-0.0165
15	1.8443	20000.00	40	1.9985	-15000.00	15	0.2347	0.0940
16	4.1009	-15000.00	41	0.1000	18214.63	16	0.2398	-0.0694
17	4.6253	20000.00	42	0.1025	-15000.00	17	0.2753	0.1852
18	0.1000	2686.56	43	0.1000	-321.57	18	0.2723	0.0925
19	2.9930	20000.00	44	2.1016	20000.00	19	0.2693	0.0347
20	0.1000	-6420.40	45	2.1349	-15000.00	20	0.2663	-0.0195
21	2.6048	-15000.00	46	0.1000	17339.22	21	0.2649	-0.0692
22	0.1000	1486.46	47	0.1295	-15000.00	22	0.2640	-0.1165
23	70.3881	-15000.00						
24	0.1000	-4418.26						
25	14.1912	-15000.00						

	ω_n (rad/sec)		
1	72.441		
2	264.838	Minimum Weight	3026.22 lb
3	493.487	CPU Time	67.377 sec

Table C.6: Forty-seven-member tower under Impulse = 150 lb-sec

Forty-Seven-Member Tower (Impulsive loading)								
Impulse = 150 lb-sec			No mass added and No L.P.					
A_0= 0.1 in^2		Use first 40 terms			Modify C.S.A. of all members			
Link	Area (in^2)	Stress (psi)	Link	Area (in^2)	Stress (psi)	Displacements (in)		
						node	x-dir	y-dir
1	6.3277	20000.00	26	0.1000	-7319.55	1	0.0000	0.0000
2	7.7362	-15000.00	27	4.7557	-15000.00	2	0.0000	0.0000
3	6.1167	20000.00	28	0.1000	20000.00	3	0.0200	0.0080
4	7.7225	-15000.00	29	5.4971	20000.00	4	0.0207	-0.0060
5	0.1931	20000.00	30	6.2794	-15000.00	5	0.0547	0.0160
6	0.1328	-15000.00	31	3.4456	-15000.00	6	0.0560	-0.0120
7	0.1000	-15000.00	32	2.7097	20000.00	7	0.1040	0.0240
8	0.2846	20000.00	33	0.2760	-15000.00	8	0.0980	-0.0180
9	0.2366	-15000.00	34	3.5837	20000.00	9	0.1165	0.0227
10	2.9649	20000.00	35	3.4826	-15000.00	10	0.1205	-0.0105
11	5.2668	20000.00	36	0.1000	11566.38	11	0.1638	0.0267
12	0.1000	5127.89	37	0.2976	-15000.00	12	0.1608	-0.0135
13	1.3306	20000.00	38	0.1000	3132.76	13	0.2110	0.0307
14	2.8572	-15000.00	39	3.6665	20000.00	14	0.2150	-0.0165
15	3.4645	20000.00	40	3.8306	-15000.00	15	0.2376	0.0940
16	7.6707	-15000.00	41	0.2273	20000.00	16	0.2427	-0.0693
17	8.6563	20000.00	42	0.1244	-15000.00	17	0.2783	0.1852
18	0.1000	2717.08	43	0.1000	1867.25	18	0.2753	0.0925
19	5.6254	20000.00	44	3.9971	20000.00	19	0.2723	0.0347
20	0.1000	-6490.77	45	3.9715	-15000.00	20	0.2693	-0.0195
21	4.8957	-15000.00	46	0.1000	18433.63	21	0.2678	-0.0692
22	0.1000	1505.72	47	0.3417	-15000.00	22	0.2669	-0.1164
23	131.9221	-15000.00						
24	0.1000	-4458.31						
25	26.5127	-15000.00						

	ω_n (rad/sec)		
1	71.486		
2	261.156	Minimum Weight	5650.72 lb
3	478.073	CPU Time	156.425 sec

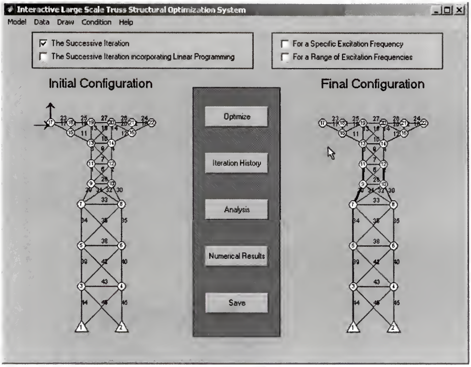

☑ The Successive Iteration
☐ The Successive Iteration incorporating Linear Programming
☐ For a Specific Excitation Frequency
☐ For a Range of Excitation Frequencies

Figure C.1: Five modes approximation for the forty-seven-member tower under impulsive loading (II)

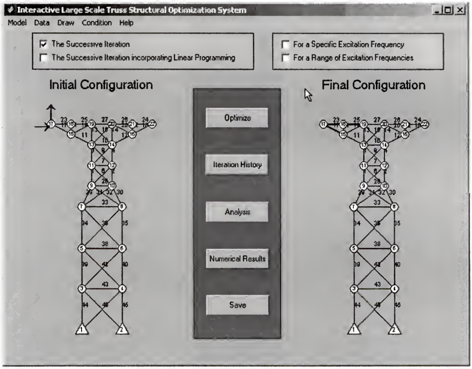

☑ The Successive Iteration
☐ The Successive Iteration incorporating Linear Programming
☐ For a Specific Excitation Frequency
☐ For a Range of Excitation Frequencies

Figure C.2: Fifteen modes approximation for the forty-seven-member tower under impulsive loading (II)

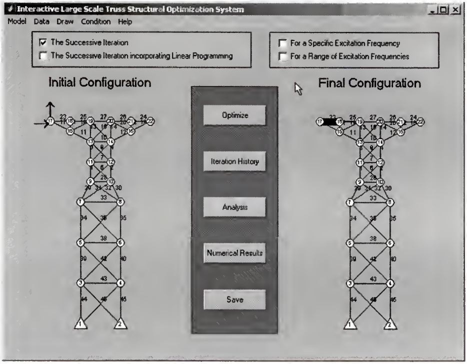

☑ The Successive Iteration
☐ The Successive Iteration incorporating Linear Programming
☐ For a Specific Excitation Frequency
☐ For a Range of Excitation Frequencies

Figure C.3: All modes (forty) expansion for the forty-seven-member tower under impulsive loading (II)

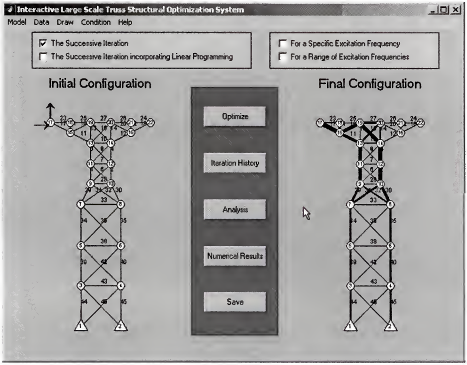

☑ The Successive Iteration
☐ The Successive Iteration incorporating Linear Programming
☐ For a Specific Excitation Frequency
☐ For a Range of Excitation Frequencies

Figure C.4: All modes (forty) expansion for the forty-seven-member tower under impulsive loading (The areas of links 23 and 25 not represented in order to show all other elements to scale) (II)

REFERENCES

[1] Archer, J. S., "Consistent Mass Matrix for Distributed Mass Systems," *Journal of the Structural Division, Proceedings of the American Society of Civil Engineers*, Vol. 89, No. ST4, August 1963, pp. 161–178.

[2] Hughes, T. J. R., *The Finite Element Method*, Prentice-Hall, Englewood Cliffs, NJ, 1987.

[3] Haug, E. J. and Pan, W., "Optimal Inertia Lumping from Modal Mass Matrices for Structural Dynamics," *Computer Methods in Applied Mechanics and Engineering*, Vol. 163, 1998, pp. 171–191.

[4] Wasiutynski, Z. and Brandt, A., "The Present State of Knowledge in the Field of Optimum Design of Structures," *Applied Mechanics Reviews*, Vol. 16, No. 5, May 1963, pp. 341–350.

[5] Sheu, C. Y. and Prager, W., "Recent Developments in Optimal Structural Design," *Applied Mechanics Reviews*, Vol. 21, No. 10, October 1968, pp. 985–992.

[6] Seireg, A., "A Survey of Optimization of Mechanical Design," *Journal of Engineering for Industry*, Vol. 94, No. 2, 1972, pp. 495–499.

[7] Belegundu, A. D. and Arora, J. S., "A Study of Mathematical Programming Methods for Structural Optimization, Part I: Theory," *International Journal for Numerical Methods in Engineering*, Vol. 21, 1985, pp. 1583–1599.

[8] Belegundu, A. D. and Arora, J. S., "A Study of Mathematical Programming Methods for Structural Optimization, Part II: Numerical Results," *International Journal for Numerical Methods in Engineering*, Vol. 21, 1985, pp. 1601–1623.

[9] Papalambros, P. Y., "Optimal Design of Mechanical Engineering Systems," *Transactions of the ASME, Special 50th Anniversary Design Issue*, Vol. 117, June 1995, pp. 55–62.

[10] Sobieszczanski-Sobieski, J., "Optimization by Decomposition in Structural and Multidisciplinary Applications," *Optimization of Large Structural Systems, Vol. I*, edited by G. I. N. Rozvany, Kluwer Academic Publishers, Dordrecht, The Netherlands, 1993, pp. 193–233.

[11] Khorshid, E., *A Procedure for the Design of Large-Scale Mechanical Systems by Decomposition*, Ph.D. Dissertation, University of Wisconsin, Madison, WI, 1998.

[12] Aguilar, R. J., "An Application of Dynamic Programming to Structural Optimization," *Engineering Research Bulletin*, No. 91, The Division of Engineering Research, Louisiana State University and Agricultural and Mechanical College, Baton Rouge, LA, 1967, pp. 1–21.

[13] Palmer, A. C., "Optimal Structure Design by Dynamic Programming," *Journal of the Structural Division, Proceedings of the American Society of Civil Engineers*, Vol. 94, No. ST8, August 1968, pp. 1887–1906.

[14] Palmer, A. C. and Sheppard, D. J., "Optimizing the Shape of Pin-Jointed Structures," *Proceedings of the Institution of Civil Engineers*, Vol. 47, November 1970, pp. 363–376.

[15] Kirsch, U., *Optimal Structural Design*, McGraw Hill Book Company, New York, 1981.

[16] Datta, T. K. and Sarcar, P., "Elastic Minimum Weight Design by Dynamic Programming," *Journal of Structural Engineering*, Vol. 15, No. 3, October 1988, pp. 95–99.

[17] Hino, J., Hashimoto, S., and Yoshimura, T., "Optimum Design for Beams with Discrete and Continuous Variables," *Nippon Kikai Gakkai Ronbunshu C-Hen*, Vol. 57, No. 538, June 1991, pp. 2005–2010.

[18] Shankar, N. and Hajela, P., "Heuristics Driven Strategies for Near-optimal Structural Topology Development," Artificial Intelligence and Structural Engineering Second International Conference on the Application of Artificial Intelligence to Civil and Structural Engineering, Civil-Comp Limited, Edinburgh, Scotland, 1991, pp. 219–226.

[19] Barthelemy, J.-F. M., "Engineering Design Applications of Multilevel Optimization Methods," *Computer Aided Optimum Design of Structures: Application*, edited by D. Brebbia and S. Hernandez, Spring-Verlag, NASA-Langley Research Center, Hamptpon, VA, 1989, pp. 113–122.

[20] Sobieszczanski-Sobieski, J., James, B. B., and Dovi, A. R., "Structural Optimization by Multilevel Decomposition," *AIAA Journal*, Vol. 23, No. 11, 1985, pp. 1775–1782.

[21] Thareja, R. R. and Haftka, R. T., "Efficient Single-Level Solution of Hierarchical Problems in Structural Optimization," *AIAA Journal*, Vol. 28, No. 3, March 1990, pp. 506–514.

[22] Schmit, L. A. and Mehrinfar, M., "Multilevel Optimum Design of Structures with Fiber-Composite Stiffened-Panel Components," *AIAA Journal*, Vol. 20, No. 1, January 1982, pp. 138–147.

[23] Kirsch, U., "Multilevel Approach to Optimum Structural Design," *Journal of the Structural Division, Proceedings of the American Society of Civil Engineers*, Vol. 101, No. ST4, April 1975, pp. 957–974.

[24] Kirsch, U., "Multilevel Optimal Design of Reinforced Concrete Structures," *Engineering Optimization*, Vol. 6, 1983, pp. 207–212.

[25] Kirsch, U., "An Improved Multilevel Structured Synthesis Method," *Journal of Structural Mechanics*, Vol. 13, No. 2, 1985, pp. 123–144.

[26] Haftka, R. T., "An Improved Computational Approach for Multilevel Optimum Design," *Journal of Structural Mechanics*, Vol. 12, No. 2, 1984, pp. 245–261.

[27] Rozvany, G. I. N., *Structural Design via Optimality Criteria*, Kluwer Academic Publishers, Dordrecht, The Netherlands, 1989.

[28] Rozvany, G. I. N., *Optimization of Large Structural Systems*, Kluwer Academic Publishers, Dordrecht, The Netherlands, 1993.

[29] Haftka, R. T. and Gürdal, Z., *Elements of Structural Optimization*, Kluwer Academic Publishers, Dordrecht, The Netherlands, 3rd ed., 1992.

[30] Icerman, L. J., "Optimal Structural Design for Given Dynamic Deflection," *International Journal of Solids and Structures*, Vol. 5, 1969, pp. 473–490.

[31] Fox, R. L. and Kapoor, M. P., "Structural Optimization in the Dynamics Response Regime: A Computational Approach," *AIAA Journal*, Vol. 8, No. 10, October 1970, pp. 1798–1804.

[32] Mróz, Z., "Optimal Design of Elastic Structures Subjected to Dynamic, Harmonically-Varying Loads," *Zeitschrift für Angewandte Mathematik and Mechanik*, Vol. 50, No. 5, May 1970, pp. 303–309.

[33] McCart, B. R., Haug, E. J., and Streeter, T. D., "Optimal Design of Structures with Constraints on Natural Frequency," *AIAA Journal*, Vol. 8, No. 6, June 1970, pp. 1012–1019.

[34] Rubin, C. P., "Minimum Weight Design of Complex Structures Subjected to a Frequency Constraint," *AIAA Journal*, Vol. 8, No. 5, May 1970, pp. 923–927.

[35] Pierson, B. L., "A Survey of Optimal Structural Design under Dynamic Constraints," *International Journal for Numerical Methods in Engineering*, Vol. 4, 1972, pp. 491–499.

[36] Levy, H. J., *Minimum Weight Design under Dynamic Loading*, Ph.D. Dissertation, New York University, New York, April 1972.

[37] Cassis, J. H. and Schmit, L. A., "Optimum Structural Design with Dynamic Constraints," *Journal of the Structural Division, Proceedings of the American Society of Civil Engineers*, Vol. 102, No. ST10, October 1976, pp. 2053–2071.

[38] Feng, T.-T., Arora, J. S., and Haug, Jr., E. J., "Optimal Structural Design under Dynamic Loads," *International Journal for Numerical Methods in Engineering*, Vol. 11, 1977, pp. 39–52.

[39] Hsieh, C. C. and Arora, J. S., "Structural Design Sensitivity Analysis with General Boundary Conditions: Static Problem," *International Journal for Numerical Methods in Engineering*, Vol. 20, 1984, pp. 1661–1670.

[40] Hsieh, C. C. and Arora, J. S., "Structural Design Sensitivity Analysis with General Boundary Conditions: Dynamic Problem," *International Journal for Numerical Methods in Engineering*, Vol. 21, 1985, pp. 267–283.

[41] Zacharopoulos, A., Willmert, K. D., and Khan, M. R., "An Optimality Criterion Method for Structures with Stress, Displacement and Frequency Constraints," *Computers and Structures*, Vol. 19, No. 4, 1984, pp. 621–629.

[42] Kramer, G. J. E. and Grierson, D. E., "Computer Automated Design of Structures under Dynamic Loads," *Computers and Structures*, Vol. 32, No. 2, 1989, pp. 313–325.

[43] Truman, K. and Petruska, D., "Optimum Design of Dynamically Excited Structural Systems Using Time History Analysis," *Computer Aided Optimum Design of Structures*, 2nd International Conference on Computer Aided Optimum Design of Structures, June 1991, pp. 198–207.

[44] Chahande, A. I. and Arora, J. S., "Optimization of Large Structures Subjected to Dynamic Loads with the Multiplier Method," *International Journal for Numerical Methods in Engineering*, Vol. 37, 1994, pp. 413–430.

[45] Bensalem, A., Sibbald, A., and Fairfield, C. A., "The Use of Dynamic Characteristics for The Optimal Design of Arches," *Computers and Structures*, Vol. 68, 1998, pp. 461–472.

[46] Dutta, A. and Ramakrishnan, C. V., "Accurate Computation of Design Sensitivities for Structures under Transient Dynamic Loads Using Time Marching Scheme," *Internation Journal for Numerical Methods in Engineering*, Vol. 41, 1998, pp. 977–999.

[47] Min, S., Kikuchi, N., Park, Y. C., Kim, S., and Chang, S., "Optimal Topology Design of Structures under Dynamic Loads," *Structural Optimization*, Vol. 17, No. 2, 1999, pp. 208–218.

[48] Tong, W. H. and Liu, G. R., "An Optimization Procedure for Truss Structures with Discrete Design Variables and Dynamic Constraints," *Computers and Structures*, Vol. 79, 2001, pp. 155–162.

[49] Bhatti, M. A. and Pister, K. S., "A Dual Criteria Approach for Optimal Design of Earthquake-Resistant Structural Systems," *Earthquake Engineering and Structural Dynamics*, Vol. 9, 1981, pp. 557–572.

[50] Balling, R. J., Pister, K. S., and Ciampi, V., "Optimal Seismic-Resistant Design of A Planar Steel Frame," *Earthquake Engineering and Structural Dynamics*, Vol. 11, 1983, pp. 541–556.

[51] Cheng, F. Y. and Truman, K. Z., "Optimization Algorithm of 3-D Building Systems for Static and Seismic Loading," *Modeling and Simulation in Engineering*, Vol. 3, 1983, pp. 315–326.

[52] Cheng, F. Y. and Juang, D. S., "Assessment of Various Code Provisions Based on Optimum Design of Steel Structures," *Earthquake Engineering and Structural Dynamics*, Vol. 16, 1988, pp. 45–61.

[53] Cheng, F. Y. and Juang, D. S., "Recursive Optimization for Seismic Steel Frames," *Journal of Structural Engineering*, Vol. 115, No. 2, February 1989, pp. 445–466.

[54] Truman, K. Z. and Cheng, F. Y., "Optimum Assessment of Irregular Three-Dimensional Seismic Buildings," *Journal of Structural Engineering*, Vol. 116, No. 12, December 1990, pp. 3324–3337.

[55] Schmidt, L. C., "Fully-Stressed Design of Elastic Redundant Trusses under Alternative Load Systems," *Australian Journal of Applied Science*, Vol. 9, 1958, pp. 337–348.

[56] Razani, R., "Behavior of Fully Stressed Design of Structures and Its Relationship to Minimum-Weight Design," *AIAA Journal*, Vol. 3, No. 12, 1965, pp. 2262–2268.

[57] Kicher, T. P., "Optimum Design-Minimum Weight versus Fully Stressed," *Journal of the Structural Division, Proceedings of the American Society of Civil Engineers*, Vol. 92, No. ST6, December 1966, pp. 265–279.

[58] Dayaratnam, P. and Patnaik, S., "Feasibility of Full Stress Design," *AIAA Journal*, Vol. 7, No. 4, April 1969, pp. 773–774.

[59] Gallagher, R. H. and Zienkiewicz, O. C., *Optimum Structural Design*, John Wiley and Sons, London, 1973.

[60] Levy, H. J. and Wolf, B. M., "Fully Stressed Dynamically Loaded Structures," *The Design Engineering Division of the ASME for Presentation at the Winter*

Annual Meeting, New York, ASME Paper 74-WA/DE-19, November 17-22 1974, pp. 1–11.

[61] Mathias, D. W. and Röhrle, M., "Optimal Structural Design of Dynamically Excited Systems Using the Finite-Element-Method," *ICAS Proceedings 1978 11th Congress of the International Council of the Aeronautical Sciences*, Vol. 1, September 10-16 1978, pp. 582–589.

[62] Seireg, A., *Mechanical Systems Analysis*, International Textbook Company, Scranton, PA, 1969.

[63] Chvátal, V., *Linear Programming*, W. H. Freeman and Company, New York, 1983.

[64] Johnson, D. and Brotton, D. M., "Optimum Elastic Design of Redundant Trusses," *Journal of the Structural Division, Proceedings of the American Society of Civil Engineers*, Vol. 95, No. ST12, December 1969, pp. 2589–2610.

[65] Vanderplaats, G. N. and Moses, F., "Automated Design of Trusses for Optimum Geometry," *Journal of the Structural Division, Proceedings of the American Society of Civil Engineers*, Vol. 98, No. ST3, March 1972, pp. 671–690.

[66] Venkayya, V. B., Khot, N. S., and Reddy, V. S., "Optimization of Structures Based on the Study of Energy Distribution," Presented at the 2nd Conference on Matrix Methods in Structural Mechanics, AFFDL-TR-68-150, Air Force Flight Dynamic Laboratory, Wright-Patterson Air Force Base, Ohio, October 1968.

[67] Haug, E. J. and Arora, J. S., *Applied Optimal Design*, John Wiley and Sons, New York, 1979.

[68] Dantzig, G. B., *Linear Programming and Extensions*, Princeton University Press, Princeton, NJ, 1963.

[69] Papadimitriou, C. H. and Steiglitz, K., *Combinatorial Optimization*, Prentice-Hall, Englewood Cliffs, NJ, 1982.

[70] Jeter, M. W., *Mathematical Programming*, Marcel Dekker, Inc., New York, 1986.

[71] Zhang, Y., "Solving Large-Scale Linear Programs by Interior-Point Methods under the MATLAB Environment," Department of Mathematics and Statisitcs, University of Maryland, Technical Report TR96-01, Baltimore, MD, July 1995.

[72] Mehrotra, S., "On the Implementation of a Primal-Dual Interior Point Method," *SIAM Journal on Optimization*, Vol. 2, 1992, pp. 575–601.

[73] Przemieniecki, J. S., *Theory of Matrix Structural Analysis*, McGraw-Hill Book Company, New York, 1968.

[74] Venkayya, V. B., "Structural Optimization: A Review and Some Recommendations," *International Journal for Numerical Methods in Engineering*, Vol. 13, 1978, pp. 203–228.

[75] Schittowski, K., "NLQPL: A FORTRAN-Subroutine Solving Constrained Nonlinear Programming Problems," *Annals of Operations Research*, Vol. 5, 1985, pp. 485–500.

[76] Gill, P. E., Murray, W., and Wright, M. H., *Practical Optimization*, Academic Press, London, 1981.

[77] Powell, M. J. D., "Variable Metric Methods for Constrained Optimization," *Mathematical Programming: The State of the Art*, edited by A. Bachem, M. Grotschel, and B. Korte, Springer Verlag, New York, 1983, pp. 288–311.

[78] Luenberger, D. G., *Linear and Nonlinear Programming*, Addison-Wesley, Reading, MA, 1984.

[79] Clough, R. W. and Penzien, J., *Dynamics of Structures*, McGraw-Hill, Inc., New York, 2nd ed., 1993.

[80] Bathe, K.-J., *Finite Element Procedures in Engineering Analysis*, Prentice-Hall, Inc., Englewood Cliffs, NJ, 1982.

[81] Craig, Jr., R. R., *Structural Dynamics*, John Wiley and Sons, New York, 1981.

[82] Wilson, E. L., Yuan, M. Y., and Dickens, J. M., "Dynamic Analysis by Direct Superposition of Ritz Vectors," *Earthquake Engineering and Structural Dynamics*, Vol. 10, No. 6, 1982, pp. 813–821.

[83] Belytschko, T., "Transient Analysis," *Structural Mechanics Computer Program*, edited by W. Pilkey, K. Saczalski, and H. Schaeffer, University Press of Virginia, 1974, pp. 255–276.

[84] Newmark, N. M., "A Method of Computation for Structural Dynamics," *Journal of Engineering Mechanics Division, Proceedings of ASCE*, Vol. 85, No. EM3, 1959, pp. 67–94.

[85] Belytschko, T. and Hughes, T. J. R., editors, *Computational Methods for Transient Analysis*, North Holland, Amsterdam, 1983.

BIOGRAPHICAL SKETCH

Chao-Wei Hsiao was born in Taipei, Taiwan, in 1965. He received his Bachelor of Science degree in civil and hydraulic engineering from Chung-Yuan University in 1987. From 1987 to 1989, Chao-Wei served as a military police officer in the Chinese army in Taiwan for his mandatory duty. Before coming to America, he worked in CTCI coporation, an engineering consultant company in Taiwan, as an assistant engineer for oil tank structural and foundation design. From September 1990 to December 1991, he earned his Master of Science degree in civil engineering and engineering mechanics from Columbia University. From 1992 to 1998, Chao-Wei received another Master of Science degree in engineering mechanics while studying in the Ph.D. program at the Department of Engineering Mechanics and Astronautics at the University of Wisconsin-Madison. In 1994 he passed the Ph.D. qualifying examination and was appointed as a teaching assistant to instruct several undergraduate courses including statics, dynamics, and mechanics of materials since 1995. Having great interest in Dr. Ali Seireg's work and the versatile atmosphere of the University of Florida, he transfered his Ph.D. study to the Department of Mechanical Engineering at the University of Florida and has been working on his research for the doctoral degree under the supervision of Dr. Ali Seireg since August 1998.

I certify that I have read this study and that in my opinion it conforms to acceptable standards of scholarly presentation and is fully adequate, in scope and quality, as a dissertation for the degree of Doctor of Philosophy.

Ali Seireg

Ali A. Seireg, Chairman
Ebaugh Professor of
Mechanical Engineering

I certify that I have read this study and that in my opinion it conforms to acceptable standards of scholarly presentation and is fully adequate, in scope and quality, as a dissertation for the degree of Doctor of Philosophy.

Joseph Duffy
Graduate Research Professor of
Mechanical Engineering

I certify that I have read this study and that in my opinion it conforms to acceptable standards of scholarly presentation and is fully adequate, in scope and quality, as a dissertation for the degree of Doctor of Philosophy.

Carl D. Crane III
Professor of Mechanical
Engineering

I certify that I have read this study and that in my opinion it conforms to acceptable standards of scholarly presentation and is fully adequate, in scope and quality, as a dissertation for the degree of Doctor of Philosophy.

John K. Schueller

John K. Schueller
Associate Professor of
Mechanical Engineering

I certify that I have read this study and that in my opinion it conforms to acceptable standards of scholarly presentation and is fully adequate, in scope and quality, as a dissertation for the degree of Doctor of Philosophy.

J. Hammer

Jacob Hammer
Professor of Electrical and Computer
Engineering

This dissertation was submitted to the Graduate Faculty of the College of Engineering and to the Graduate School and was accepted as partial fulfillment of the requirements for the degree of Doctor of Philosophy.

May 2001

M. Jack Ohanian
Dean, College of Engineering

Winfred M. Phillips
Dean, Graduate School